E-ISSN : 2149-9330

TURKISH JOURNAL OF OBSTETRICS AND GYNECOLOGY

March 2026 Volume: 23 Issue: 1 www.tjoddergisi.org

TURKISH SOCIETY OF OBSTETRICS AND GYNECOLOGY

galenos yayınevi

TURKISH JOURNAL OF OBSTETRICS AND GYNECOLOGY

TURKISH JOURNAL OF OBSTETRICS AND GYNECOLOGY

TURKISH JOURNAL OF OBSTETRICS AND GYNECOLOGY

Please refer to the journal's webpage **(https://tjoddergisi.org/)** for "Aims and Scope", "Instructions to Authors" and "Peer-Review and Ethics".

The editorial and publication process of the Turkish Journal of Obstetrics and Gynecology are shaped in accordance with the guidelines of ICMJE, WAME, CSE, COPE, EASE, and NISO. The journal is in conformity with the Principles of Transparency and Best Practice in Scholarly Publishing.

Turkish Journal of Obstetrics and Gynecology is indexed in **PubMed, PubMed Central (PMC), Web of Science-Emerging Sources Citation Index (ESCI), Tübitak/Ulakbim Turkish Medical Database, EBSCO, Embase, Scopus, ProQuest, British Library, Gale, CINAHL, Turk Medline, J-Gate, IdealOnline, CNKI, Hinari, GOALI, ARDI, OARE, AGORA** and **Turkiye Citation Index**.

The journal is published electronically.

Owner: İsmail Mete İtil on behalf of the Turkish Society of Obstetrics and Gynecology

Responsible Manager: Ercan Yılmaz

Contact
Çetin Emeç Bulvarı Hürriyet Caddesi Harbiye Mahallesi 1/13 Öveçler, Ankara, Türkiye
Phone: +90 312 481 06 06 Fax: +90 312 481 28 28 E-mail: editor@tjod.org

Reviewing the articles' conformity to the publishing standards of the Journal, typesetting, reviewing and editing the manuscripts and abstracts in English and publishing process are realized by Galenos.

Publisher Contact
Address: Molla Gürani Mah. Kaçamak Sk. No: 21/1 34093 İstanbul, Türkiye
Phone: +90 (530) 177 30 97 / +90 (539) 307 32 03 **E-mail:** info@galenos.com.tr/yayin@galenos.com.tr **Web:** www.galenos.com.tr
Publisher Certificate Number:14521
Online Publication Date: March 2026 **E-ISSN:** 2149-9330
International scientific journal published quarterly.

TURKISH JOURNAL OF OBSTETRICS AND GYNECOLOGY

CONTENTS

Clinical Investigations

Review

TURKISH JOURNAL OF OBSTETRICS AND GYNECOLOGY

LETTER FROM THE PRESIDENT

Dear TJOD Family,

With the March issue, the first issue of 2026, we are pleased to once again be before you with scientifically strong publications that contribute to the current literature. I would like to congratulate our editors and reviewers who devoted significant effort to the careful selection, evaluation, and preparation of the many national and international submissions included in this issue, and I extend my gratitude to the scientists who submitted their valuable work to our journal.

As the Turkish Society of Obstetrics and Gynecology, we continue our preparations with great dedication and intensive effort for the 23rd National Gynecology and Obstetrics Congress, which we will hold on May 13-17, 2026. We anticipate broad participation, and I would like to invite all our colleagues to our congress.

As I always emphasize, the Turkish Society of Obstetrics and Gynecology is far more than an association; it is an organization that provides the strongest and most immediate response to the professional challenges our physicians face. In recent months, a public statement we issued on behalf of a colleague who had been sentenced to pay record-level compensation following the birth of a baby diagnosed with Down syndrome created a significant nationwide impact. Ultimately, the decision of the local court was overturned by the Court of Cassation in favor of the physician.

Believing in the strength of unity, and by standing hand in hand with our branches, members, and colleagues, we will continue our efforts to achieve the highest standards in every field through the ever-growing strength of our association. I wish you a healthy, happy, and successful year in 2026.

Best Regards
Ismail Mete Itil, Prof. MD
President of TJOD

TURKISH JOURNAL OF OBSTETRICS AND GYNECOLOGY

EDITORIAL

Dear Colleagues,

We are once again together with you through the March 2026 issue of TJOG, the scientific publication of the Turkish Society of Obstetrics and Gynecology. During the preparation of this issue, we experienced a demanding three-month period together with our editorial board, section editors, and reviewers. Our journal receives intense interest from both national and international platforms. This clearly demonstrates the distinguished position of our journal and indicates that, in the coming years, it will become an indispensable cornerstone of prestigious scientific indexes.

In recent years, our journal has achieved a significant breakthrough and has become a preferred journal for the publication of studies conducted by national and international scientists. We would like to share with our esteemed colleagues that our dedicated efforts will continue, and we look forward to meeting you again in the June issue, the second issue of 2026.

Ercan Yilmaz, Prof. MD
Fatih Sendag, Prof. MD

Clinical Investigation / Araştırma

DOI: 10.4274/tjod.galenos.2025.95515

Turk J Obstet Gynecol 2026;23(1):1-7

Evaluating midpregnancy Gas6 levels as predictive value for gestational diabetes and birth outcomes

Gebeliğin ortasında Gas6 düzeylerinin gebelik diyabeti ve doğum sonuçları için öngörü değeri olarak değerlendirilmesi

Yeşim Cıvıl Ürkmez[1], Neşet Gümüşburun[2], Sebati Sinan Ürkmez[3], Samettin Çelik[4], Kübra Şahin[5]

[1]*University of Health Sciences Türkiye, Samsun Training and Research Hospital, Clinic of Medical Biochemistry, Samsun, Türkiye*
[2]*İstanbul Aydın University Faculty of Medicine, Department of Obstetrics and Gynecology, İstanbul, Türkiye*
[3]*Ondokuz Mayıs University Faculty of Medicine, Department of Medical Biochemistry, Samsun, Türkiye*
[4]*Samsun University Faculty of Medicine, Department of Obstetrics and Gynecology, Samsun, Türkiye*
[5]*Samsun Provincial Health Directorate, Samsun, Türkiye*

Abstract

Objective: This study investigated the relationship between maternal serum growth arrest-specific 6 (Gas6) levels measured in the second trimester of pregnancy and the development of gestational diabetes mellitus (GDM); it also evaluated the possible links between this biomarker and maternal and neonatal outcomes.

Materials and Methods: A total of 173 pregnant women were included in this prospective study (89 diagnosed with GDM, 84 healthy controls). Gas6 levels were measured using the ELISA method from blood samples taken during routine screening in the second trimester. The relationships between Gas6 levels and body mass index (BMI), oral glucose tolerance test results, and neonatal data were statistically analysed.

Results: Gas6 levels were significantly higher in the GDM group ($p<0.001$). A strong positive correlation was found between Gas6 and maternal BMI ($r=0.774$), and a moderate positive correlation between Gas6 and oral glucose tolerance test 1-hour glucose level ($r=0.577$). Additionally, high Gas6 levels were found to be statistically significant in association with increased birth weight and intensive care requirements.

Conclusion: Increased Gas6 levels in the second trimester may be a potential biomarker for early prediction of GDM risk and perinatal complications.

Keywords: Gas6, gestational diabetes mellitus, second trimester, biomarker

Öz

Amaç: Bu çalışma, gebeliğin ikinci trimesterinde ölçülen maternal serum büyüme durdurma-spesifik 6 (Gas6) düzeyleri ile gebelik diyabeti gelişimi arasındaki ilişkiyi araştırmış; ayrıca bu biyobelirteç ile maternal ve neonatal sonuçlar arasındaki olası bağlantıları değerlendirmiştir.

Gereç ve Yöntemler: Bu prospektif çalışmaya toplam 173 hamile kadın dahil edildi [89'u gestasyonel diabetes mellitus (GDM) tanısı almış, 84'ü sağlıklı kontrol grubu]. Gas6 düzeyleri, ikinci trimesterde rutin tarama sırasında alınan kan örneklerinden ELISA yöntemi kullanılarak ölçüldü. Gas 6 düzeyleri ile vücut kitle indeksi, oral glukoz tolerans testi sonuçları ve yenidoğan verileri arasındaki ilişkiler istatistiksel olarak analiz edildi.

Bulgular: Gas6 düzeyleri gestasyonel diyabet grubunda anlamlı olarak daha yüksekti ($p<0,001$). Gas6 ile anne vücut kitle indeksi arasında güçlü bir pozitif korelasyon ($r=0,774$) ve Gas 6 ile oral glukoz tolerans testi 1 saatlik glukoz düzeyi arasında orta derecede pozitif bir korelasyon ($r=0,577$) bulundu. Ek olarak, yüksek Gas6 düzeylerinin doğum ağırlığının artması ve yoğun bakım gereksinimi ile istatistiksel olarak anlamlı bir şekilde ilişkili olduğu bulundu. Çalışmamızda GDM grubunda ortalama yaş 30,8±4,9 yıl iken, kontrol grubunda ise 31,3±5,4 yıldı.

Sonuç: İkinci trimesterde artan Gas6 düzeyleri, gestasyonel diyabet riski ve perinatal komplikasyonların erken tahmini için potansiyel bir biyomarker olabilir.

Anahtar Kelimeler: Gas6, gestasyonel diabetes mellitus, ikinci trimester, biyobelirteç

Corresponding Author/Sorumlu Yazar: Asst. Prof. Neşet Gümüşburun,
İstanbul Aydın University Faculty of Medicine, Department of Obstetrics and Gynecology, İstanbul, Türkiye
E-mail: gumusburun@outlook.com **ORCID ID:** orcid.org/0000-0003-4746-5414

Received/Geliş Tarihi: 14.08.2025 **Accepted/Kabul Tarihi:** 22.10.2025 **Epub:** 27.10.2025 **Publication Date/Yayınlanma Tarihi:** 05.03.2026

Cite this article as: Cıvıl Ürkmez Y, Gümüşburun N, Ürkmez SS, Çelik S, Şahin K. Evaluating midpregnancy Gas6 levels as predictive value for gestational diabetes and birth outcomes. Turk J Obstet Gynecol. 2026;23(1):1-7

Introduction

Gestational diabetes mellitus (GDM) is an important metabolic disorder characterised by hyperglycaemia that develops during pregnancy and usually disappears after delivery[1]. GDM can cause complications that threaten both maternal and foetal health, including pre-eclampsia, foetal macrosomia, increased caesarean section rates, neonatal hypoglycaemia, and neonatal intensive care unit (NICU) requirements[2]. GDM diagnosis is usually made using a 75-gram oral glucose tolerance test (OGTT) administered between the 24th and 28th weeks of pregnancy[3]. However, due to certain limitations regarding applicability of this test and patient compliance, we need to identify alternative biomarkers with high sensitivity and specificity that are easy to apply for the diagnosis of GDM.

Growth arrest-specific 6 (Gas6) protein is a multifunctional glycoprotein synthesised in a vitamin K-dependent manner, and exhibits its biological effects primarily through the Axl, Mer, and Tyro3 receptor tyrosine kinases. At the cellular level, it plays key roles in proliferation, suppression of apoptosis, regulation of inflammatory processes, and cell survival[4]. The Gas6/TAM receptor axis is particularly important in the vascular system, where it plays a critical role in platelet activation, endothelial stability, and modulation of immune responses[5,6]. The biological effects of this molecule have made it a potential target not only in terms of basic cell biology, but also in the pathophysiology of many diseases.

Recent studies have shown that the Gas6 protein undergoes significant changes in diseases associated with insulin resistance, such as diabetes, obesity and metabolic syndrome[7,8]. It has been shown that dysfunction develops in endothelial cells via Axl in hyperglycaemic environments, suggesting vascular effects of the Gas6-Axl signalling pathway[9]. In addition, Gas6 levels were found to be associated with increased systemic inflammation. This condition was also linked to type 2 diabetes and its complications[10]. However, it is noteworthy that Gas6 levels may vary in individuals with type 2 diabetes depending on genetic differences, inflammatory processes, and vascular complications[10,11].

Considering the role of Gas6 in the pathophysiology of diabetes, it is thought that similar mechanisms may also be influential in the development of gestational diabetes. However, the number of studies evaluating Gas6 levels during pregnancy and establishing its relationship with GDM is quite limited. This deficiency indicates that the potential role of Gas6 in the diagnosis and prediction of GDM has not yet been sufficiently elucidated. The aim of this study is to evaluate the relationship between maternal serum Gas6 levels measured in the second trimester of pregnancy (between 15 and 20 weeks) and the development of GDM, and to elucidate the potential of this biomarker in predicting perinatal outcomes.

Materials and Methods

This study was designed as a prospective, observational study and was conducted at the Gynaecology and Obstetrics Clinic of University of Health Sciences Türkiye, Samsun Training and Research Hospital between November 2023 and May 2024. Prior to the study, approval was obtained from the Samsun University Faculty of Medicine Non-Interventional Clinical Research Ethics Committee (protocol no: SUKAEK-2023/20/1, date: 01.11.2023). All participants were provided with detailed information about the study and their written consent was obtained. The study was conducted in accordance with the ethical principles of the Helsinki Declaration. Pregnant women who applied for the triple screening test between the 15th and 20th weeks of pregnancy and underwent the OGTT between the 24th and 28th weeks were included in the study. Subsequently, the births of these pregnant women took place at the same hospital. As a result, two groups were formed: those diagnosed with GDM (patients) and healthy pregnant women (controls).

The study included healthy pregnant women aged 18-45 years with a single pregnancy, diagnosed with GDM or without systemic disease, while those with multiple pregnancies, foetal structural anomalies, pre-pregnancy hypertension, renal failure, pre-gestational diabetes and chronic disease, and those under 18 or over 45 years of age were excluded.

Gas6 levels were measured from blood samples taken from pregnant women included in the study during the triple screening test between the 15th and 20th weeks of pregnancy. Subsequently, a standard 75-gram (g) OGTT was administered between the 24th and 28th weeks, and the glucose values at 0, 1, and 2 hours were recorded. Additionally, maternal body mass index (BMI), gestational age, gravida, parity, mode of delivery, newborn birth weight, Apgar scores (at 1 and 5 minutes), the need for neonatal intubation, the presence of meconium, and admission to the NICU were monitored postpartum and evaluated as part of the analysis.

GDM diagnosis was made based on the results of a 75 g OGTT performed between the 24th and 28th weeks of pregnancy. During the test, fasting, 1-hour, and 2-hour serum glucose levels were evaluated using the following threshold values: ≥92 mg/dL, ≥180 mg/dL, and ≥153 mg/dL, respectively. If any of these threshold values were exceeded, a diagnosis of GDM was made in accordance with the recommendations of the International Association of Diabetes and Pregnancy Study Groups[12].

Blood Sampling and Analysis Method

In the second trimester, additional serum samples taken during the triple screening test were collected in yellow-capped tubes in the biochemistry laboratory and then centrifuged at 4000 × g for 10 minutes to separate the serum fraction. The serum samples obtained were stored at -80 °C until the day of analysis.

Gas6 levels were measured using a double antibody sandwich method with a human Gas6 ELISA kit, branded BT Lab Bioassay Technology Laboratory (Cat No. E3257Hu, Shanghai, China). Measurements were performed at 450 nm wavelength using a TECAN brand microtiter reader. The sensitivity limit of the test was 0.13 ng/mL, and the dynamic range was 0.3-90 ng/mL. Values were recorded in ng/mL. Samples exceeding the measurement range were reanalysed after dilution when necessary.

Statistical Analysis

Statistical analyses were performed using SPSS 25.0 software. The distribution of numerical variables was evaluated using the Kolmogorov-Smirnov test, and appropriate tests were selected in accordance with the normality assumption. Parameters showing a normal distribution were expressed as mean ± standard deviation; those not normally distributed were expressed as median (minimum-maximum). For intergroup comparisons, the independent samples t-test was used for normally distributed data, the Mann-Whitney U test for non-normally distributed data, and the chi-square test for categorical data. The relationship between Gas6 levels and maternal BMI, OGTT results, birth weight, and other parameters was evaluated using Spearman's correlation analysis. The diagnostic accuracy of Gas6 levels in GDM diagnosis was analysed using the receiver operating characteristic (ROC) curve. The area under the curve (AUC), cut-off value, sensitivity, specificity, and positive and negative predictive values were calculated. A significance level of $p<0.05$ was accepted for all statistical tests. A post-hoc power analysis (G*Power 3.1.9.7) for a two-tailed independentsamples t-test based on the observed GAS6 means and standard deviations yielded a pooled standard deviation of 18.61 and an effect size of Cohen's d=1.89. At $\alpha=0.05$, the achieved power (1-β) was >0.999, indicating a highly powered study.

Results

A total of 198 pregnant women were initially assessed for eligibility in the study, and 25 were excluded based on predefined criteria (Figure 1). The inclusion and exclusion process of the study population is summarised in Figure 1. Ultimately, a total of 173 pregnant women were evaluated in this study; 89 of them were diagnosed with GDM, and 84 formed the healthy control group. Data on the demographic, clinical, and laboratory characteristics of the participants are presented in Table 1. No significant differences were found between the groups in terms of maternal age (p=0.521), gestational age (p=0.658), gravida (p=0.412), and parity (p=0.119).

The maternal BMI was significantly higher in the GDM group (GDM: 31.9±6.1; control: 25.4±5.6; p<0.001). Neonatal birth weight was measured as 3903.9±395.7 grams in the GDM group and 3518.8±416.6 grams in the control group. The difference between the two groups was found to be statistically significant (p<0.001).

Fasting blood glucose levels were 102.2±21.9 mg/dL in the GDM group and 86.1±5.6 mg/dL in the control group (p<0.001). The 1-hour glucose value in the OGTT was 204.3±36.6 mg/dL in the GDM group and 157.2±22.4 mg/dL in the control group (p<0.001). The 2-hour glucose value in the OGTT was 164.1±49.8 mg/dL in the GDM group and 129.0±16.3 mg/dL in the control group; significant differences were found in both parameters (p<0.001).

The Apgar scores of newborns in the GDM group were also lower than those in the control group. The 1-minute Apgar score was 8.3±1.0 in the GDM group and 8.7±0.7 in the control group (p<0.001); the 5-minute Apgar score was 9.2±1.1 and 9.7±0.8, respectively (p<0.001).

Maternal serum Gas6 levels were significantly higher in the GDM group (GDM: 53.0±21.6 ng/mL; control: 17.8±14.8 ng/mL; p<0.001).

According to the results of correlation analysis, a strong positive correlation was found between serum Gas6 levels and maternal BMI (r=0.774; p<0.001). There was a moderate correlation between OGTT 1-hour glucose value and maternal BMI (r=0.577; p<0.001), OGTT 2-hour glucose value (r=0.451; p=0.001), fasting blood sugar (r=0.414; p<0.001) and

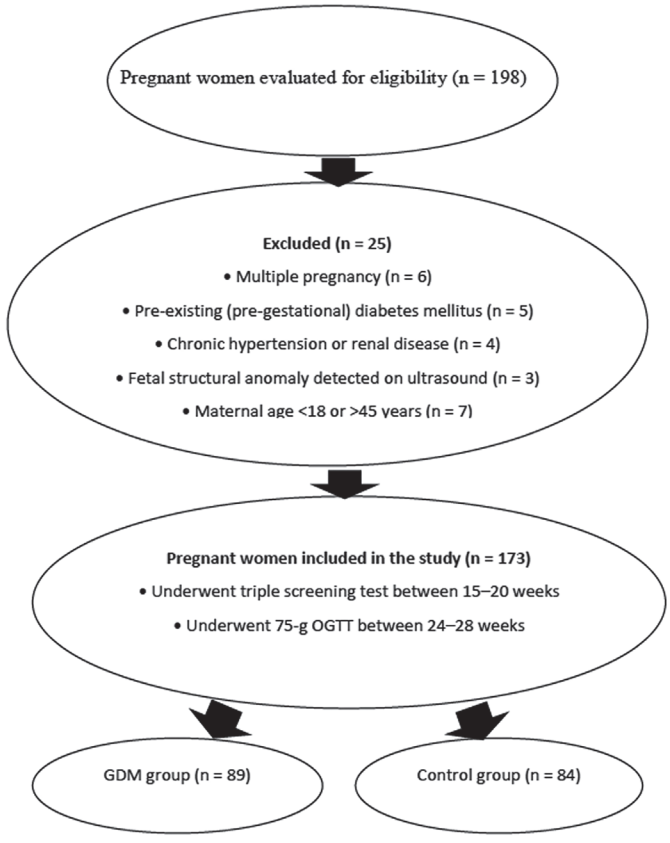

Figure 1. Flowchart of study population selection

GDM: Gestational diabetes mellitus

Table 1. Demographic, laboratory, and clinical data of patients

	Presence of gestational diabetes				p-valueβ
	Yes (n=89)		No (n=84)		
	Mean ± SD	Median (min-max)	Mean ± SD	Median (min-max)	
Maternal age (years)	30.8±4.9	31.0 (20-43)	31.3±5.4	31.0 (20-43)	0.521
Neonatal birth weight (g)	3903.9±395.7	3890.0 (3000-5100)	3518.8±416.6	3450.0 (2700-4500)	**<0.001**
Maternal BMI	31.9±6.1	30.0 (21-44)	25.4±5.6	24.0 (19-42)	**<0.001**
Gestational age (weeks)	37.8±1.5	38.0 (35-40)	37.9±1.4	38.0 (35-40)	0.658
Gravida	2.5±1.4	2.0 (1-6)	2.3±1.4	2.0 (1-7)	0.412
Parity	1.2±1.0	1.0 (0-4)	0.9±1.1	1.0 (0-4)	0.119
Fasting blood glucose (mg/dL)	102.2±21.9	98.0 (74.3-176.1)	86.1±5.6	89.8 (72.9-91.0)	**<0.001**
OGTT 1 (1-hour glucose tolerance Test) (mg/dL)	204.3±36.6	199.1 (126.4-339.4)	157.2±22.4	165.4 (101.6-179.0)	**<0.001**
OGTT 2 (2-hour glucose tolerance test) (mg/dL)	164.1±49.8	156.6 (84.1-378.8)	129.0±16.3	132.2 (58.7-155.2)	**<0.001**
Apgar score (1st minute)	8.3±1.0	9.0 (5-9)	8.7±0.7	9.0 (6-9)	**<0.001**
Apgar score (5th minute)	9.2±1.1	10.0 (7-10)	9.7±0.8	10.0 (7-10)	**<0.001**
Gas 6 level (ng/mL)	53.0±21.6	43.5 (25.5-98.0)	17.8±14.8	14.9 (0.2-82.0)	**<0.001**

* t-test, β: Mann-Whitney U test, BMI: Body mass index, OGTT: Oral Glucose tolerance test, Gas6: Growth arrest–specific 6 protein, SD: Standard deviation, min: Minimum, max: Maximum

Table 2. Distribution between groups according to obstetric and neonatal outcomes and associated Gas6 levels

	Presence of gestational diabetes				p-value*
	Yes (n=89)		No (n=84)		
	n	%	n	%	
Mode of delivery					
Normal delivery	40	44.9	70	83.3	**<0.001**
Cesarean section	49	55.1	14	16.7	
Presence of meconium					
Yes	11	12.4	5	6	0.234
No	78	87.6	79	94	
Neonatal intubation status					
Yes	16	18	9	10.7	0.254
No	73	82	75	89.3	
Admission to neonatal intensive care unit					
Yes	29	32.6	10	11.9	**0.002**
No	60	67.4	74	88.1	

*: Chi-square test, NICU: Neonatal intensive care unit, GAS6: Growth arrest–specific 6 protein

birth weight (r=0.398; p<0.001). In addition, obstetric and neonatal outcomes were compared between the groups, and these results are summarised in Table 2.

The results of the ROC analysis performed to evaluate diagnostic performance are summarized in Figure 1 and Table 3. Gas6 levels were found to be highly predictive of GDM diagnosis, with an AUC value of 0.94 (95% confidence interval: 0.90-0.98; p<0.001). The optimal cut-off value was determined to be 30.0 ng/mL, with a sensitivity of 94.4%, specificity of 85.7%, positive predictive value of 87.6%, and negative predictive value of 85.7% at this point.

Discussion

This study revealed that maternal serum Gas6 levels measured in the second trimester are strongly associated with GDM. Our findings show that Gas6 levels are significantly increased in individuals diagnosed with GDM, and also correlate with maternal BMI, OGTT results, birth weight, and neonatal outcomes.

Gas6 is a vitamin K-dependent glycoprotein that interacts with Tyro3, Axl, Mer receptors and plays a role in cell proliferation, suppression of apoptosis, modulation of inflammation, and regulation of thrombosis[13]. Zhai et al.[14] linked the Axl-Gas6 axis to metabolic disorders, reporting that plasma levels increase in conditions such as type 2 diabetes, obesity, and hypertension. Insulin resistance, inflammation

and vascular dysfunction are known to play a prominent role in the pathophysiology of gestational diabetes[15]. In this context, Gas6's effects of both activating the immune response and regulating the cellular stress response through anti-apoptotic mechanisms make its association with GDM plausible. In line with these findings, the data obtained in our study also suggest that Gas6 levels may be associated with metabolic and inflammatory processes related to gestational diabetes and provide a meaningful parallel with the existing literature.

In a previous study, Varsamis et al.[15] showed that Gas6 levels were significantly higher in patients with type 2 diabetes compared to the control group, and that this increase was associated with BMI and glycemic control. Similarly, in a study conducted by Lee et al.[9], it was reported that Axl receptor expression increased in a hyperglycaemic environment and was associated with endothelial dysfunction and impaired insulin signalling. In our study, the positive correlation between Gas6 levels and both BMI and OGTT 1- and 2-hour glucose levels supports the notion that this biomarker reflects glucose intolerance[16].

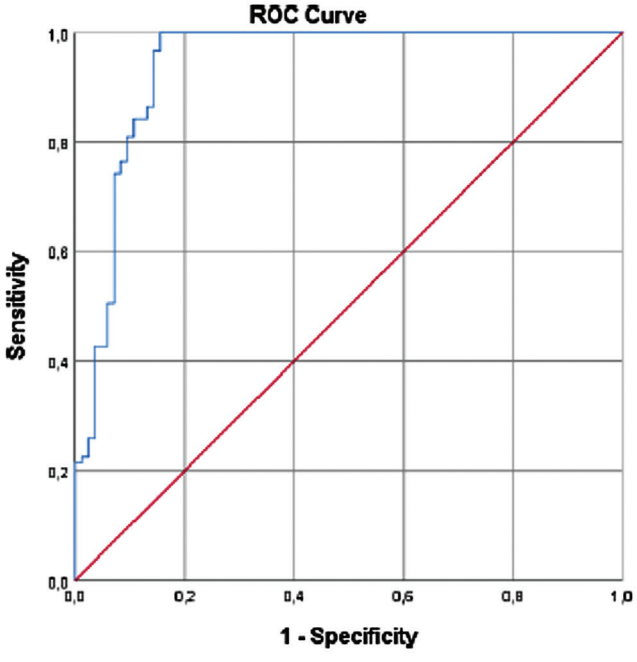

Figure 2. ROC curve for the diagnosis of gestational diabetes mellitus based on serum Gas6 levels

GAS6: Growth arrest–specific 6 protein, ROC: Receiver operating characteristic

One of the notable findings in our study is that Gas6 levels are associated with neonatal birth weight, Apgar scores, and NICU admission rates. In pregnancies with gestational diabetes, macrosomia, respiratory distress at birth, and high NICU admission rates are known to occur[17,18]. In the literature, it has been reported that placental growth factors and maternal metabolism play a decisive role in foetal macrosomia[19,20]. In particular, insulin-like growth factors and hormones such as placental lactogen regulate placental development and foetal growth; changes in these factors increase the risk of macrosomia. Kabaran[21] also showed that maternal nutrition, obesity, and diabetes contribute to the development of foetal macrosomia by affecting placental growth factors. Considering the effects of Gas6 on placental immunity and functions, this biomarker may be considered clinically significant not only for maternal but also for foetal outcomes. Indeed, in our study, the positive correlation found between maternal BMI and fetal birth weight in the GDM group with high Gas6 levels, indicates that Gas6 may be associated with both maternal weight gain and fetal growth processes. However, this relationship may not be causal, as increases in Gas6 levels may reflect maternal weight gain or metabolic changes associated with GDM, or they may arise secondarily to developing fetal macrosomia. Further mechanistic studies are needed to clarify this distinction. Additionally, the relationship observed in our study between high Gas6 levels and caesarean delivery may be relevant to clinical intervention decisions aimed at preventing obstetric complications that may develop due to GDM.

Similar results have been obtained in other studies on the potential use of Gas6 as a biomarker. For example, in an animal model by Schott et al.[22], Gas6 deficiency was reported to improve glucose tolerance, whereas overexpression caused insulin resistance. This situation shows that Gas6 levels increase in parallel with metabolic stress and play an active role in pathophysiological processes. Our findings confirmed the literature that high Gas6 levels are associated with glucose intolerance.

However, there are conflicting findings in the literature regarding the relationship between Gas6 levels and insulin resistance, and glucose metabolism. Some studies have reported that low Gas6 levels are more common in individuals with type 2 diabetes, showing a positive correlation with insulin sensitivity and a negative correlation with inflammation[7,23,24]. However, it was also noted that certain genetic variants and Gas6 levels in obese individuals may be positively associated with insulin resistance[23,25,26]. In our

Table 3. Cut-off values for Growth arrest–specific 6 protein protein in the diagnosis of gestational diabetes mellitus

Cut-off value	Sensitivity (%)	Specificity (%)	Positive predictive value (%)	Negative predictive value (%)
25.0	100.0	84.5	87.3	84.5
30.0	94.4	85.7	87.6	85.7

study, the significantly higher serum Gas6 levels measured in the second trimester in individuals diagnosed with GDM, and those with obesity, support the existing literature reporting a positive association between Gas6 and insulin resistance and metabolic dysfunction. The conflicting findings in this area are likely due to clinical heterogeneity among patient populations, differences in the sensitivity of the ELISA kits used, timing of biomarker measurements, and genetic variations.

The AUC value of 0.94 obtained in our study demonstrates that Gas6 has a very high predictive power in the diagnosis of GDM. The sensitivity and specificity rates of 94.4% and 85.7%, respectively, obtained with a cut-off value of 30.0 ng/mL are clinically significant. While this level of performance may not replace the current OGTT test, it has the potential to serve as a non-invasive and rapid alternative for preliminary screening. Clinically, integrating Gas6 levels into routine screening programmes could enable earlier diagnosis and timely intervention, particularly in high-risk pregnancies. Early diagnosis of GDM will significantly contribute to the prevention of maternal and neonatal complications through dietary adjustments, exercise programmes, and pharmacological treatment, if necessary.

Gas6 has been considered a biomarker of interest not only in metabolic processes but also in obstetric pathologies in recent years. Dai et al.[27] showed that low Gas6 expression in decidual stromal cells in individuals with recurrent pregnancy loss is associated with a decrease in M2 macrophages responsible for immune tolerance. This situation suggests that immune imbalance in early pregnancy loss may be related to Gas6 deficiency. Another notable role of Gas6 is its relationship with preeclampsia. Studies conducted in this context have reported that excessive activation of the Gas6/Axl pathway is associated with symptoms such as trophoblast invasion disorder, oxidative stress, proteinuria, and hypertension, while Axl inhibitors have been shown to reduce these effects[28-31]. In addition, Sang et al.[32] found a correlation between increased Gas6 expression in preeclamptic placentas and blood pressure. In parallel with these findings, it was observed that Axl inhibitors alleviated preeclampsia-like symptoms in experimental models, bringing the potential of this pathway for treatment to the fore. Finally, it was found that Gas6 levels were elevated in intrauterine growth restriction (IUGR) cases and that this may be related to placental inflammation[33]. When evaluated in light of these data, Gas6 is a multifaceted biomarker that may play a role in the diagnosis and treatment not only of gestational diabetes but also of obstetric complications such as preeclampsia, early pregnancy loss, and IUGR, and thus appears to warrant further investigation.

The most important strengths of this study are its prospective design, the correlation of serum samples taken in the second trimester with birth outcomes, and the analysis of a large sample size. In addition, the objective evaluation of Gas6 levels using ROC analysis enabled the diagnostic power of the biomarker to be demonstrated. However, the fact that the study was conducted at a single centre may limit its general validity.

Study Limitations

Furthermore, preanalytical variables and the follow-up period not covering the early stages of pregnancy are among the potential limitations. In addition, this study evaluated only serum Gas6 levels without including mechanistic biomarkers such as oxidative stress, or inflammatory markers, which may limit the understanding of the underlying pathophysiology. Furthermore, the lack of immunohistochemical comparison of placental Gas6 expression is another limitation that could have provided insight into tissue-level mechanisms. Future studies incorporating both systemic and placental analyses may better clarify the mechanistic role of Gas6 in the development of GDM. Validating the findings in the early stages of pregnancy using multicentre designs and long-term follow-ups in the postpartum period will help clarify the diagnostic and prognostic value of Gas6.

Conclusion

This study showed that maternal Gas6 levels measured in the second trimester were significantly associated with gestational diabetes and related adverse perinatal outcomes. The correlation of Gas6 with BMI and OGTT results in particular supports the possibility that this biomarker may be an early indicator of metabolic dysfunction. In clinical practice, Gas6 measurement can be considered as an auxiliary tool in GDM risk classification. Using this measurement can potentially lead to improved outcomes for foeto-maternal health. However, further multicentre and longitudinal studies are needed to establish the prognostic and diagnostic value of Gas6 on a more solid foundation. Gas6 is a strong candidate biomarker for GDM, offering the opportunity for early intervention.

Ethics

Ethics Committee Approval: Ethical approval was obtained from the Samsun University Faculty of Medicine Non-Interventional Clinical Research Ethics Committee (protocol no: SUKAEK-2023/20/1, date: 01.11.2023).

Informed Consent: All participants were provided with detailed information about the study and their written consent was obtained.

Footnotes

Authorship Contributions

Surgical and Medical Practices: Y.C.Ü., S.S.Ü., K.Ş., Concept: N.G., S.Ç., Design: N.G., S.Ç., Data Collection or Processing: Y.C.Ü., S.S.Ü., K.Ş., Analysis or Interpretation: Y.C.Ü., S.S.Ü., K.Ş., Literature Search: N.G., Writing: N.G., S.Ç.

Conflict of Interest: No conflict of interest was declared by the authors.

Financial Disclosure: The authors declared that this study received no financial support.

References

1. McIntyre HD, Catalano P, Zhang C, Desoye G, Mathiesen ER, Damm P. Gestational diabetes mellitus. Nat Rev Dis Primers. 2019;5:47.
2. Sweeting A, Wong J, Murphy HR, Ross GP. A clinical update on gestational diabetes mellitus. Endocr Rev. 2022;43:763-93.
3. Albairmani RA, Basheer BM, Macky MM, Al Syouti T, AlZubaidy H, Elfaki E, et al. Management of diabetes in pregnancy: a review of clinical guidelines and practices. Cureus. 2025;17:e79334.
4. Fernández-Fernández L, Bellido-Mart´n L, de Frutos PG. Growth arrest-specific gene 6 (GAS6). Thromb Haemost. 2008;100:604-10.
5. Rothlin CV, Carrera-Silva EA, Bosurgi L, Ghosh S. TAM receptor signaling in immune homeostasis. Annu Rev Immunol. 2015;33355-91.
6. Law LA, Graham DK, Di Paola J, Branchford BR. GAS6/TAM pathway signaling in hemostasis and thrombosis. Front Med (Lausanne). 2018;5:137.
7. Kuo F-C, Hung Y-J, Shieh Y-S, Hsieh C-H, Hsiao F-C, Lee C-H. The levels of plasma growth arrest-specific protein 6 is associated with insulin sensitivity and inflammation in women. Diabetes Res Clin Pract. 2014;103:304-9.
8. Hsiao F-C, Lin Y-F, Hsieh P-S, Chu N-F, Chen Y-DI, Shieh Y-S, et al. Effect of GAS6 and AXL gene polymorphisms on adiposity, systemic inflammation, and insulin resistance in adolescents. Int J Endocrinol. 2014;2014:674069.
9. Lee C-H, Shieh Y-S, Hsiao F-C, Kuo F-C, Lin C-Y, Hsieh C-H, et al. High glucose induces human endothelial dysfunction through an Axl-dependent mechanism. Diabetes Res Clin Pract. 2016;1:S77.
10. Lee C-H, Chu N-F, Shieh Y-S, Hung Y-J. The growth arrest-specific 6 (Gas6) gene polymorphism c. 834+ 7G> a is associated with type 2 diabetes. Diabetes Res Clin Pract. 2012;95:201-6.
11. Fan H, Han J, Chen L, Feng B, Sun X, Shi B. Association between plasma growth arrest-specific protein 6 and carotid atherosclerosis in type 2 diabetes mellitus. Nutr Metab Cardiovasc Dis. 2022;32:1917-23.
12. Scheuer CM, Jensen DM, McIntyre HD, Ringholm L, Mathiesen ER, Nielsen CPK, et al. Applying WHO2013 diagnostic criteria for gestational diabetes mellitus reveals currently untreated women at increased risk. Acta Diabetol. 2023;60:1663-73.
13. Rizzi M, Tonello S, D'Onghia D, Sainaghi PP. Gas6/TAM axis involvement in modulating inflammation and fibrosis in COVID-19 patients. Int J Mol Sci. 2023;24:951.
14. Zhai X, Pu D, Wang R, Zhang J, Lin Y, Wang Y, et al. Gas6/AXL pathway: immunological landscape and therapeutic potential. Front Oncol. 2023;13:1121130.
15. Varsamis NA, Christou GA, Kiortsis DN. A critical review of the effects of vitamin K on glucose and lipid homeostasis: its potential role in the prevention and management of type 2 diabetes. Hormones (Athens). 2021;20:415-22.
16. Wu G, Ma Z, Cheng Y, Hu W, Deng C, Jiang S, et al. Targeting Gas6/TAM in cancer cells and tumor microenvironment. Mol Cancer. 2018;17:20.
17. Kc K, Shakya S, Zhang H. Gestational diabetes mellitus and macrosomia: a literature review. Ann Nutr Metab. 2015;66(Suppl 2):14-20.
18. Šegregur J, Buković D, Milinović D, Orešković S, Pavelić J, Župić T, et al. Fetal macrosomia in pregnant women with gestational diabetes. Coll Antropol. 2009;33:1121-7.
19. Forbes K, Westwood M. Maternal growth factor regulation of human placental development and fetal growth. J Endocrinol. 2010;207:1-16.
20. Sibiak R, Jankowski M, Gutaj P, Mozdziak P, Kempisty B, Wender-Ożegowska E. Placental lactogen as a marker of maternal obesity, diabetes, and fetal growth abnormalities: current knowledge and clinical perspectives. J Clin Med. 2020;9:1142.
21. Kabaran S. Maternal nutritional factors, fetal macrosomia and increased risk of childhood obesity: effects of excess placental transfer of maternal glucose and fatty acids. Current Nutrition & Food Science. 2023;19:145-57.
22. Schott C, Germain A, Lacombe J, Pata M, Faubert D, Boulais J, et al. GAS6 and AXL promote insulin resistance by rewiring insulin signaling and increasing insulin receptor trafficking to endosomes. Diabetes. 2024;73:1648-61.
23. Dihingia A, Kalita J, Manna P. Implication of a novel Gla-containing protein, Gas6 in the pathogenesis of insulin resistance, impaired glucose homeostasis, and inflammation: a review. Diabetes Res Clin Pract. 2017;128:74-82.
24. Hung Y-J, Lee C-H, Chu N-F, Shieh Y-S. Plasma protein growth arrest–specific 6 levels are associated with altered glucose tolerance, inflammation, and endothelial dysfunction. Diabetes Care. 2010;33:1840-4.
25. Hsieh C-H, Chung R-H, Lee W-J, Lin M-W, Chuang L-M, Quertermous T, et al. Effect of common genetic variants of growth arrest-specific 6 gene on insulin resistance, obesity and type 2 diabetes in an Asian population. PLoS One. 2015;10:e0135681.
26. Hsiao F-C, Lin Y-F, Hsieh P-S, Chu N-F, Shieh Y-S, Hsieh C-H, et al. Circulating growth arrest-specific 6 protein is associated with adiposity, systemic inflammation, and insulin resistance among overweight and obese adolescents. J Clin Endocrinol Metab. 2013;98:E267-74.
27. Dai J-C, Yang J-Y, Chang R-Q, Liang Y, Hu X-Y, Li H, et al. GAS6-mediated dialogue between decidual stromal cells and macrophages is essential for early pregnancy maintenance by inducing M2-like polarization and cell proliferation of decidual macrophages. Mol Hum Reprod. 2022;28:gaac006.
28. Dunaway TM, Lewis JB, Hirschi KM, Mejia CA, Mejia JF, Hall PD, et al. Activation of AXL receptor via Gas6 induces preeclampsia in rats. The FASEB Journal. 2017;31:978.17.
29. Curtis K, Clarke D, Hanegan M, Stapley B, Wendt R, Beckett N, et al. Lung inflammation is associated with preeclampsia development in the rat. Cells. 2022;11:1884.
30. Hall PD, Caskey B, Hirschi KM, Reynolds PR, Arroyo JA. Gas6/AXL modulates increased inflammatory cytokines during preeclampsia in rats. The FASEB Journal. 2018;32:817.5.
31. Jackson M, Gibson TM, Frank E, Hill G, Davidson B, Reynolds PR, et al. Transcriptomic insights into Gas6-induced placental dysfunction: gene targets for preeclampsia therapy. Cells. 2025;14:278.
32. Sang H, Ma Y, Zhu X, Wang L, He M. Expression of Gas6 in placenta and decidua tissues and its relationship with the pathogenesis of preeclampsia. Zhonghua Fu Chan Ke Za Zhi. 2015;50:441-5.
33. Lindqvist PG, Balogh I, Dahlbäck B. Umbilical cord plasma levels of growth-arrest specific protein 6 in intrauterine growth restriction. Acta Obstet Gynecol Scand. 2010;89:22-6.

Clinical Investigation / Araştırma

DOI: 10.4274/tjod.galenos.2025.28235

Turk J Obstet Gynecol 2026;23(1):8-33

Maternal and neonatal outcomes in placenta accreta spectrum: Influence of antenatal diagnosis and surgical strategy

Plasenta akreta spektrumunda maternal ve neonatal sonuçlar: Antenatal tanı ve cerrahi stratejinin etkisi

Lumayat Orujova[1], Rauf Melekoğlu[1], Ercan Yılmaz[1], Halis Özdemir[2], Şeyma Yaşar[3]

[1]İnönü University Faculty of Medicine, Department of Obstetrics and Gynecology, Malatya, Türkiye

[2]KTO Karatay University Faculty of Medicine, Department of Obstetrics and Gynecology, Konya, Türkiye

[3]İnönü University Faculty of Medicine, Department of Biostatistics and Medical Informatics, Malatya, Türkiye

Abstract

Objective: This study aimed to evaluate the influence of antenatal diagnosis and surgical management strategies on maternal and neonatal outcomes in placenta accreta spectrum (PAS) disorders, emphasizing risk factors, timing of delivery, and operative approaches.

Materials and Methods: A retrospective cohort analysis was conducted on 210 women with histopathologically confirmed PAS managed at İnönü University Faculty of Medicine between January 2014 and March 2024. Demographic data, antenatal findings, delivery type, and surgical details were compared between elective and emergency procedures, as well as between uterus-preserving surgery and peripartum hysterectomy. Uterus-preserving surgery refers to conservative techniques that aim to avoid peripartum hysterectomy while controlling hemorrhage.

Results: Of the total cohort, 66.7% underwent elective surgery, whereas 33.3% required emergency intervention. Emergency deliveries occurred earlier (mean 32.1 vs. 36.0 weeks, p<0.001) and were associated with higher blood loss (799 vs. 511 mL, p<0.001), increased perinatal mortality (20% vs. 1.4%, p<0.001), and greater neonatal morbidity, mainly respiratory distress syndrome (47% vs. 14%, p<0.001). Hysterectomy was required in 45.2% of patients, primarily with placenta percreta (60% vs. 23.5%, p<0.001). Anterior placental location (89.5%) strongly correlated with complete invasion (77.7%) and bladder involvement (27.7%, p=0.038). Bladder injuries were more common in elective cases, while ureteral injuries occurred more often in emergencies (p=0.024). Preoperative hematocrit independently predicted hysterectomy risk (odds ratio: 1.092, p=0.034).

Conclusion: Antenatal diagnosis and well-planned elective management significantly improve maternal and neonatal outcomes in PAS. Individualized surgical planning based on invasion depth and maternal condition remains essential to reduce morbidity and mortality.

Keywords: Intraoperative complications, placenta accreta, pregnancy outcome, prenatal diagnosis

Öz

Amaç: Bu çalışma, plasenta akreta spektrumu (PAS) olgularında antenatal tanı ve cerrahi yönetim stratejilerinin maternal ve neonatal sonuçlar üzerindeki etkisini; risk faktörleri, doğum zamanı ve cerrahi yaklaşımlar açısından değerlendirmeyi amaçladı.

Gereç ve Yöntemler: Ocak 2014-Mart 2024 tarihleri arasında İnönü Üniversitesi Tıp Fakültesi'nde yönetilen ve histopatolojik olarak doğrulanan 210 PAS olgusu retrospektif olarak incelendi. Demografik veriler, antenatal bulgular, doğum şekli ve cerrahi özellikler; elektif ve acil girişimler ile uterus koruyucu cerrahi ve peripartum histerektomi grupları arasında karşılaştırıldı. Uterus koruyucu cerrahi, peripartum histerektomiden kaçınarak kanamayı kontrol etmeyi hedefleyen konservatif yaklaşımlar olarak tanımlandı.

PRECIS: Timely antenatal diagnosis and elective management markedly reduce maternal morbidity and perinatal mortality in placenta accreta spectrum, underscoring the importance of planned multidisciplinary prenatal care.

Corresponding Author/Sorumlu Yazar: Rauf Melekoğlu MD,
İnönü University Faculty of Medicine, Department of Obstetrics and Gynecology, Malatya, Türkiye
E-mail: rauf.melekoglu@inonu.edu.tr **ORCID ID:** orcid.org/0000-0001-7113-6691

Received/Geliş Tarihi: 24.08.2025 **Accepted/Kabul Tarihi:** 01.11.2025 **Epub:** 22.01.2026 **Publication Date/Yayınlanma Tarihi:** 05.03.2026

Cite this article as: Orujova L, Melekoğlu R, Yılmaz E, Özdemir H, Yaşar Ş. Maternal and neonatal outcomes in placenta accreta spectrum: influence of antenatal diagnosis and surgical strategy. Turk J Obstet Gynecol. 2026;23(1):8-33

Bulgular: Olguların %66,7'si elektif, %33,3'ü acil koşullarda opere edildi. Acil doğumlar daha erken haftalarda gerçekleşti (32,1 vs. 36,0 hafta, p<0,001) ve daha fazla kan kaybı (799 vs. 511 mL, p<0,001), artmış perinatal mortalite (%20 vs. %1,4, p<0,001) ve neonatal respiratuvar distres (%47 vs. %14, p<0,001) ile ilişkiliydi. Histerektomi oranı %45,2 olup, en sık plasenta perkreta olgularında görüldü (%60 vs. %23,5, p<0,001). Anterior plasenta yerleşimi tam invazyon (%77,7) ve mesane tutulumu (%27,7, p=0,038) ile ilişkiliydi. Preoperatif hematokrit düzeyi histerektomi gereksinimini bağımsız olarak öngördü (risk oranı: 1,092, p=0,034).

Sonuç: Antenatal tanı ve planlı elektif yönetim, PAS olgularında maternal ve neonatal sonuçları belirgin biçimde iyileştirir. İnvazyon derecesi ve maternal duruma göre bireyselleştirilmiş cerrahi planlama, morbidite ve mortaliteyi azaltmada temel öneme sahiptir.

Anahtar Kelimeler: İntraoperatif komplikasyonlar, plasenta akreta, gebelik sonuçları, prenatal tanı

Introduction

Placenta accreta spectrum (PAS) disorders were historically attributed to abnormal trophoblastic invasion. However, current understanding indicates that they arise primarily from uterine scarring and defective decidualization, which lead to a distorted uteroplacental interface and aberrant fibrinoid deposition rather than true villous invasiveness[1]. It is associated with substantial maternal morbidity and mortality, primarily due to massive hemorrhage, increased transfusion requirements, multi-organ injury and, in severe cases, maternal death. The global incidence of PAS has risen markedly over recent decades, a trend largely attributed to the parallel increase in cesarean delivery rates[2]. While planned preterm cesarean hysterectomy without attempts at placental removal remains the most widely accepted standard management, this approach entails irreversible loss of fertility and significant psychological impact for many women. Consequently, alternative uterus-preserving surgical techniques have been explored in selected cases[3].

The pathogenesis of PAS is intrinsically linked to defective decidualization of the endometrium, most commonly occurring at sites of previous uterine scarring from cesarean sections, myomectomies, or other surgical interventions. This defective decidualization results in failure of normal placental separation after delivery, leading to massive hemorrhage that often necessitates emergency hysterectomy[4]. Therefore, accurate antenatal diagnosis is critical for optimizing outcomes. Ultrasound, particularly with the adjunct of color Doppler imaging, remains the primary diagnostic modality, offering high sensitivity and specificity when performed by experienced operators[5]. Magnetic resonance imaging (MRI) is valuable in cases with posterior placental implantation or suspected lateral extension[6]. Key sonographic signs—such as placental lacunae, myometrial thinning, and loss of the hypoechoic retroplacental zone—alongside subplacental hypervascularity on Doppler imaging, provide essential diagnostic clues. The identification of risk factors, including a history of cesarean section, placenta previa, prior uterine surgery, advanced maternal age, and multiparity, further refines clinical suspicion[7].

The clinical implications of PAS extend beyond immediate maternal risks to encompass significant neonatal morbidity. Preterm delivery, whether iatrogenic or spontaneous, is a near-universal consequence, with studies demonstrating that elective delivery at 34-36 weeks in specialized centers optimizes outcomes by balancing fetal maturity against the risk of emergent hemorrhage[8]. However, the ideal timing of delivery remains controversial, with some institutions advocating for earlier delivery to mitigate maternal risks while others prioritize fetal lung maturity[9]. Furthermore, the choice between cesarean hysterectomy and uterus-preserving approaches such as segmental uterine resection or local resection with reconstruction continues to be debated, with each strategy carrying distinct risks and benefits that must be carefully weighed against patient characteristics such as desire for future fertility, and the depth of placental invasion. While hysterectomy minimizes the risk of catastrophic hemorrhage, it carries higher rates of bladder injury and loss of fertility. Uterus-preserving techniques, when feasible, may reduce morbidity and preserve reproductive potential, but require meticulous planning and intraoperative assessment[10].

Despite advances in our understanding of PAS, critical knowledge gaps persist. The long-term outcomes of different management strategies, particularly novel techniques such as segmental uterine resection and multidisciplinary team approaches, remain understudied. Additionally, there are limited data on how antenatal risk factors—including placental location, number of prior cesareans, and biochemical markers—may be leveraged to predict invasion severity and guide individualized treatment plans[11]. This study seeks to address these gaps through a comprehensive analysis of maternal and neonatal outcomes in PAS cases managed at a high-volume tertiary center over a ten-year period. By examining the interplay between antenatal risk stratification, surgical management choices, and clinical outcomes, we aim to contribute evidence-based insights that can inform practice guidelines and improve care for this high-risk population.

Materials and Methods

This retrospective cohort study was conducted at the Department of Obstetrics and Gynecology, İnönü University Faculty of Medicine, after obtaining approval from the Institutional Non-Interventional Clinical Research Ethics Committee (approval date: 02.04.2024; approval number: 2024/5875). The study population comprised all pregnant women diagnosed with PAS and managed at our tertiary care center between January 1, 2014, and December 31, 2023. The diagnosis of PAS was confirmed either intraoperatively, based on direct visualization of abnormal placental adherence and invasion, or postoperatively through histopathological

examination of specimens obtained after cesarean hysterectomy or uterus-preserving procedures.

Eligible participants were women aged between 18 and 48 years who delivered at our hospital and had a confirmed diagnosis of PAS. Exclusion criteria included multiple gestations and cases with incomplete clinical or follow-up data, such as insufficient antenatal visits or missing surgical records.

Data were obtained from the hospital's electronic medical records and recorded into a standardized Excel database specifically designed for this study. Collected variables included maternal demographic and obstetric characteristics [age, gravidity, parity, body mass index (BMI), smoking status, history of previous cesarean deliveries, and history of other gynecological surgeries], comorbid conditions, and obstetric complications. Information regarding gestational age at diagnosis and delivery, diagnostic modality (ultrasound and/or MRI), antenatal corticosteroid administration, and indication for delivery was also documented.

Surgical data included the type of uterine incision, its relationship to placental location, the operative management strategy (cesarean hysterectomy versus uterus-preserving surgery), the anatomical location of the placenta, and the degree of placental invasion (placenta accreta, increta, or percreta). Intraoperative parameters, such as estimated blood loss, number of blood products transfused, and perioperative complications (including bladder and ureteral injuries), were recorded. Preoperative and postoperative laboratory results, specifically hemoglobin and hematocrit levels, were reviewed to evaluate perioperative hematologic changes. Neonatal outcomes included birth weight, 1- and 5-minute Apgar scores, need for neonatal intensive care unit (NICU) admission, and neonatal morbidity and mortality data.

Sample Size and Power Justification

Because this was a retrospective cohort including all eligible PAS cases managed over a 10-year period, no a priori sample size calculation was performed. The final cohort (n=210) provided >80% post hoc statistical power (α=0.05), based on observed effect sizes for perinatal mortality and intraoperative blood loss to detect clinically relevant differences in maternal and neonatal outcomes between elective and emergency delivery groups.

Statistical Analysis

Statistical analyses were performed using IBM SPSS Statistics for Windows, Version 26.0 (IBM Corp., Armonk, NY, USA). Continuous variables were assessed for normality using the Kolmogorov-Smirnov test and expressed as mean ± standard deviation for normally distributed data or median (minimum-maximum) for non-normally distributed data. Categorical variables were presented as frequencies and percentages. For between-group comparisons, the Independent Samples t-test was applied to normally distributed continuous variables, while the Mann-Whitney U test was used for non-normally distributed variables. Associations between categorical variables were analyzed using Pearson's chi-square test, Yates' continuity correction, or Fisher's exact test, as appropriate. To evaluate risk factors associated with adverse maternal and neonatal outcomes, univariate logistic regression analyses were performed to calculate odds ratios (ORs) and 95% confidence intervals (CIs). Variables with a p-value <0.10 in univariate analysis were subsequently included in a multivariate logistic regression model to identify independent predictors. Multicollinearity was evaluated prior to model entry, and model fit was confirmed using the Hosmer-Lemeshow test. A two-tailed p-value <0.05 was considered statistically significant for all analyses.

Results

Table 1 summarizes the demographic, obstetric, maternal, intraoperative, and neonatal characteristics of 210 women diagnosed with PAS. Continuous variables are presented as mean ± standard deviation and median (minimum-maximum), while categorical variables are expressed as counts and percentages.

Study Population Characteristics

A total of 210 women diagnosed with PAS were included in the study. Of these, 140 (66.7%) underwent planned

Table 1. Baseline demographic, obstetric, maternal, and neonatal characteristics of the study population

Variable	Category	Statistics*
Maternal characteristics		
Age (years)		32.50±5.20; 32 (19-45)
BMI (kg/m^2)		27.80±3.90; 27 (20-9)
Smoking	Yes	35 (16.70)
	No	175 (83.30)
IVF pregnancy	Yes	22 (10.50)
	No	188 (89.50)
Previous gynecological surgery	Yes	28 (13.30)
	No	182 (86.70)
Obstetric history		
Gravida		3.20±1.50; 3 (1-8)
Parity		1.80±1.20; 2 (0-6)
Previous cesarean section	0	40 (19.00)
	1	95 (45.20)
	≥2	75 (35.80)
Gestational age at diagnosis (weeks)		26.37±5.62; 24 (17-39)
Gestational age at delivery (weeks)		34.71±3.54; 36 (20-39)

Table 1. Continued

Variable	Category	Statistics*
Other obstetric complications	No	150 (71.43)
	Gestational diabetes	26 (12.38)
	Pregestational diabetes	4 (1.90)
	Gestational hypertension	4 (1.90)
	Chronic hypertension	1 (0.48)
	Preeclampsia	5 (2.38)
	Intrauterine growth restriction	12 (5.71)
	Others	8 (3.80)
Diagnostic method	Ultrasound diagnosis	43 (20.47)
	Ultrasound+Doppler	166 (79.04)
	Ultrasound+MRI	1 (0.48)
Antenatal steroid use	No	70 (33.33)
	Complete course	88 (41.90)
	Incomplete course	24 (11.43)
	Not indicated	28 (13.33)
Indication for delivery	Elective-related to accreta	135 (64.29)
	Elective - not related to accreta	5 (2.38)
	Emergency - related to accreta	44 (20.95)
	Emergency - unrelated to accreta	26 (12.38)
Intrapartum evaluation	Planned hysterectomy	97 (46.19)
	Conservative procedure	87 (41.43)
	Failed conservative procedure followed by immediate hysterectomy	23 (10.95)
	Failed conservative management followed by delayed hysterectomy	3 (1.43)
Intraoperative findings		
Intraoperative blood loss (mL)		1650±620; 1600 (600-4200)
Erythrocyte suspension transfusion (units)		2.46±1.92; 2 (0-10)
Fresh frozen plasma transfusion (units)		0.89±1.17; 0 (0-5)
Cryoprecipitate transfusion (units)		0.22±0.56; 0 (0-3)
Platelet transfusion (units)		0.23±0.7; 0 (0-4)
Conservative management	Hysterectomy	95 (45.24)
	Preventive surgery	115 (54.76)
Compression sutures	No	207 (98.57)
	Yes	3 (1.43)
Type of placental invasion	Accreta	68 (32.38)
	Increta	58 (27.62)
	Percreta	84 (40)
Placental location	Anterior low	25 (11.90)
	Posterior low	22 (10.48)
	Central over the internal os	163 (77.62)
Degree of placental invasion	Focal	58 (27.62)
	Complete	152 (72.38)
Type of cesarean incision	Low transverse	44 (20.95)
	High transverse	87 (41.43)
	Classic	57 (27.14)
	Vertical	22 (10.48)
Relation of incision to placenta	Incision through placenta	6 (2.86)
	Incision away from placenta	204 (97.14)
Preoperative ultrasound	No	12 (5.71)
	Yes	198 (94.29)
Placental organ invasion	No	152 (72.38)
	Bladder invasion	53 (25.24)
	Parametrial invasion	5 (2.38)
Intraoperative complication	No	159 (75.71)
	Unintentional cystotomy	45 (21.43)
	Ureteric injury	4 (1.90)
	Bowel injury	2 (0.95)

Table 1. Continued

Variable	Category	Statistics*
Maternal outcomes		
Maternal ICU stay (days)		0.86±1.48; 0 (0-6)
Hospital stay (days)		5.52±3.06; 5 (1-21)
Postpartum hemoglobin (g/L)		9.13±1.47; 9.1 (4.3-12.9)
Postpartum hematocrit (g/L)		27.77±4.3; 28.25 (14.5-37.1)
Maternal ICU	Yes	71 (33.81)
	No	139 (66.19)
Maternal mortality	Yes	1 (0.48)
	No	209 (99.52)
Neonatal outcomes		
Neonatal weight (g)		2624.85±704.02; 2780 (350-4025)
1-min APGAR score		7.01±1.45; 7 (0-9)
5-min APGAR score		8.75±1.66; 9 (0-10)
Neonatal ICU stay (days)		3.67±6.2; 0 (0-36)
Neonatal respiratory distress syndrome		0.25±0.43; 0 (0-1)
Intrauterine ex	No	206 (98.10)
	Yes	4 (1.90)
Perinatal death	No	194 (92.38)
	Yes	16 (7.62)
Neonatal ICU requirement	No	106 (50.48)
	Yes	104 (49.52)
Neonatal respiratory support requirement	No	115 (54.76)
	Yes	95 (45.24)
Neonatal intracranial hemorrhage	No	193 (91.90)
	Yes	17 (8.10)
Neonatal hypoxic ischemic encephalopathy	No	200 (95.24)
	Yes	10 (4.76)

*: Continuous variables are presented as mean ± standard deviation and median (minimum–maximum), while categorical variables are expressed as counts and percentages. BMI: Body mass index, ICU: Intensive care unit, MRI: Magnetic resonance imaging, IVF: In vitro fertilization

surgery, while 70 (33.3%) required emergency intervention. Emergency procedures were primarily performed due to PAS-related hemorrhage in 44 cases (62.9%), while the remaining 26 patients (37.1%) required urgent surgery for other obstetric indications. In the planned group, 135 deliveries were performed due to PAS and 5 for other obstetric reasons. The demographic profile revealed a mean maternal age of 33.81±4.85 years, with patients demonstrating an average gravidity of 4.30±1.49 and parity of 2.83±1.22. The study population had a mean BMI of 30.60±4.05 kg/m^2, consistent with the known association between obesity and PAS risk. Notably, the average number of prior cesarean deliveries was 2.09±0.98, underscoring the well-established link between uterine scarring and abnormal placentation.

Diagnostic and Clinical Parameters

The mean gestational age at PAS diagnosis was 26.37±5.62 weeks, with definitive management occurring at a mean of 34.71±3.54 weeks. Diagnostic modalities included grayscale ultrasound alone (20.47%), combined grayscale and color Doppler ultrasound (79.04%), and MRI confirmation (0.48%). Preoperative hemoglobin and hematocrit levels averaged 11.23±1.33 g/dL and 34.21±3.63%, respectively, with significant interindividual variability reflecting the spectrum of disease severity.

Comparative Analysis of Delivery Timing

The analysis revealed striking differences between planned and emergency deliveries. Emergency cases were delivered significantly earlier (mean gestational age: 32.13±4.57 weeks) compared to planned deliveries, (36.01±1.86 weeks, $p < 0.001$), resulting in substantial neonatal consequences. This four-week disparity in gestational age had profound clinical implications, particularly for neonatal outcomes. Intraoperative blood loss was markedly higher in emergency cases (799.29±414.28 mL) versus planned deliveries (511.43±311.49 mL, $p<0.001$), though transfusion requirements did not differ significantly between groups ($p>0.05$). Emergency deliveries were associated with higher rates of intraoperative complications, increased NICU admission, higher need for respiratory support, and elevated perinatal mortality compared with elective procedures (Figure 1). Maternal intensive care unit (ICU) admission rates trended higher in emergency deliveries, though this difference did not reach statistical significance (Table 2).

Surgical Management Outcomes

The surgical approach varied significantly based on clinical presentation and intraoperative findings. A Sankey diagram (Figure 2) illustrates the distribution of PAS patients according to timing of surgery (emergency vs. elective), surgical procedure (hysterectomy vs. preventive surgery), and placental location (anterior vs. posterior). Among 210 women, 70 underwent emergency surgery and 140 elective

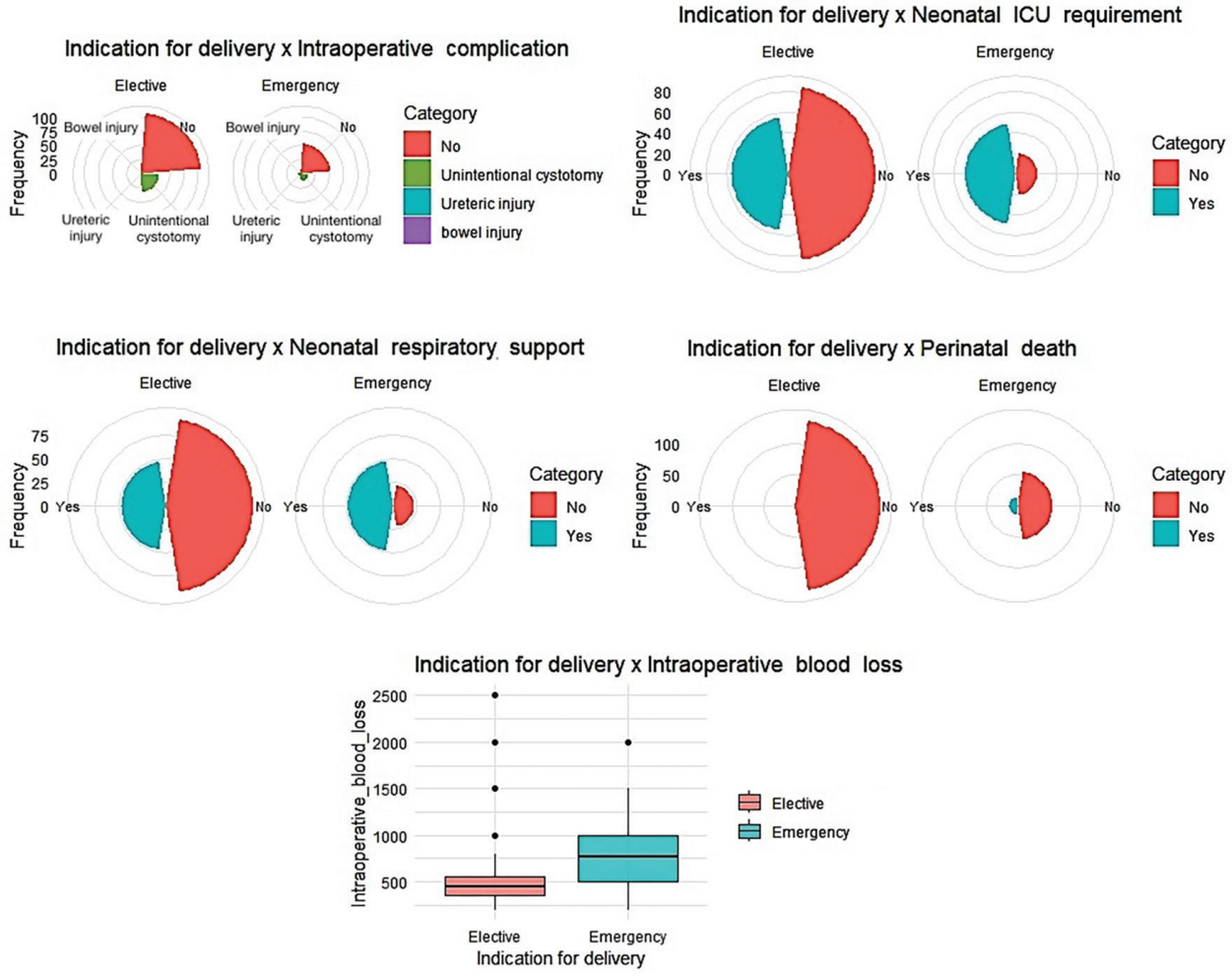

Figure 1. Distribution of maternal and neonatal outcomes by elective and emergency delivery indications

ICU: Intensive care unit

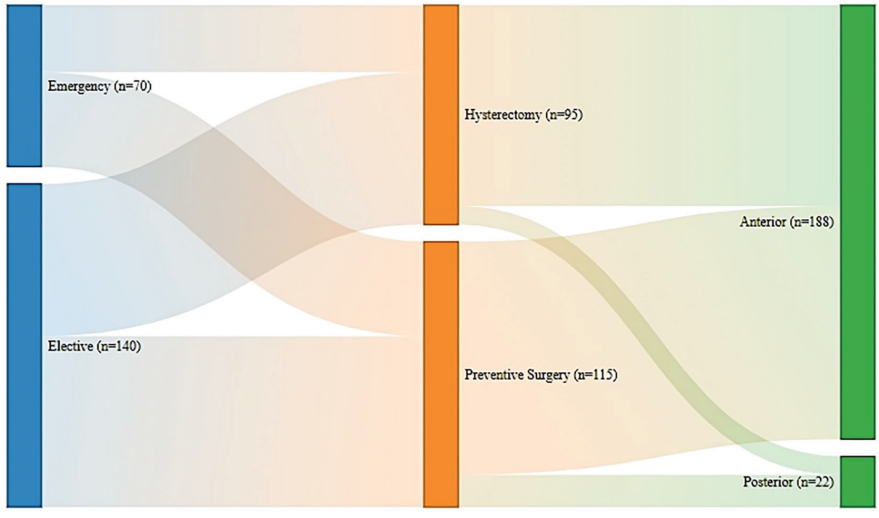

Figure 2. Sankey diagram illustrating the distribution of placenta accreta spectrum patients according to surgical timing (emergency vs. elective), surgical approach (hysterectomy vs. preventive surgery), and placental location (anterior vs. posterior)

Table 2. Comparison of maternal, obstetric, and neonatal characteristics according to elective and emergency indications for cesarean delivery

Variable	Category	Indication for delivery		p-value
		Elective (n=140)	Emergency (n=70)	
		Statistics	Statistics	
Age (year)		33.84±4.7; 34 (22-45)	33.77±5.16; 34 (19-45)	0.947
Gravida		4.28±1.49; 4 (1-10)	4.33±1.5; 4 (2-12)	0.887
Parity		2.83±1.22; 3 (0-6)	2.83±1.23; 3 (0-8)	0.902
BMI (kg/m²)		30.46±4.17; 30 (19-42)	30.86±3.8; 30 (24-42)	0.567
Number of previous cesarean sections		2.06±0.99; 2 (0-5)	2.16±0.94; 2 (0-5)	0.559
Gestational age at diagnosis (weeks)		26.78±5.7; 26 (17-39)	25.56±5.41; 24 (20-38)	0.126
Gestational age at delivery (weeks)		36.01±1.86; 36 (22-39)	32.13±4.57; 34 (20-38)	**<0.001**
Preoperative hemoglobin (g/L)		11.35±1.13; 11.3 (8.1-14)	10.98±1.64; 11.05 (7.1-14.4)	0.174
Preoperative hematocrit (g/L)		34.59±3.18; 34.55 (25.6-44)	33.45±4.31; 33.75 (23.5-46)	0.077
Intraoperative blood loss (cc)		511.43±311.49; 450 (200-2500)	799.29±414.28; 775 (200-2000)	**<0.001**
Erythrocyte transfusion (units)		2.42±1.88; 2 (0-10)	2.54±2.01; 3 (0-10)	0.300
Maternal ICU stay duration (days)		0.76±1.46; 0 (0-6)	1.04±1.52; 0 (0-6)	0.090
Hospital stay duration (days)		5.36±2.92; 5 (1-21)	5.84±3.32; 5 (2-20)	0.198
Postpartum hemoglobin (g/L)		9.21±1.33; 9.2 (4.3-12)	8.96±1.72; 8.8 (4.6-12.9)	0.224
Postpartum hematocrit (g/L)		27.9±3.91; 28.4 (14.5-34.8)	27.53±5.02; 28.1 (14.9-37.1)	0.585
Perioperative tranexamic acid use (vials)		0.4±1.2; 0 (0-4)	0.11±0.67; 0 (0-4)	0.067
Neonatal birth weight (g)		2863.32±455.17; 2880 (450-4025)	2147.91±858.94; 2425 (350-3390)	**<0.001**
1-minute APGAR score		7.35±1.22; 8 (0-9)	6.33±1.63; 6 (0-9)	**<0.001**
5-minute APGAR score		9.11±1.36; 9 (0-10)	8.01±1.94; 8 (0-10)	**<0.001**
Neonatal ICU stay duration		2.13±4.22; 0 (0-35)	6.74±8.14; 3 (0-36)	**<0.001**
Neonatal respiratory distress syndrome		0.14±0.34; 0 (0-1)	0.47±0.5; 0 (0-1)	**<0.001**
Smoking	No	121 (86.4)	59 (84.3)	0.676
	Yes	19 (13.6)	11 (15.7)	
IVF pregnancy	No	137 (97.9)	68 (97.1)	0.749
	Yes	3 (2.1)	2 (2.9)	
Diagnostic method	Ultrasound diagnosis	30 (21.4)	13 (18.5)	0.820
	Ultrasound + Doppler	109 (77.9)	57 (81.4)	
	Ultrasound, confirme by MRI	1 (0.7)	0 (0)	

Table 2. Continued

Variable	Category	Indication for delivery		p-value
		Elective (n=140)	Emergency (n=70)	
		Statistics	Statistics	
Antenatal steroid use	No	51 (36.4)	19 (27.1)	**<0.001**
	Complete course	55 (39.3)	33 (47.1)	
	Incomplete course	7 (5)	17 (24.3)	
	Not indicated	27 (19.2)	1 (1.4)	
Intrapartum assessment	Planned hysterectomy	67 (47.9)	30 (42.9)	0.099
	Conservative procedure	58 (41.4)	29 (41.4)	
	Failed conservative procedure followed by immediate hysterectomy	15 (10.7)	8 (11.4)	
	Failed conservative management followed by delayed hysterectomy	0 (0)	3 (4.3)	
Conservative management	No	66 (47.1)	29 (41.4)	0.432
	Yes	74 (52.9)	41 (58.6)	
Compression suture types	No	137 (97.9)	70 (100)	0.217
	Yes	3 (2.1)	0 (0)	
Type of placental invasion	Accreta	50 (35.7)	18 (25.7)	0.209
	Increta	34 (24.3)	24 (34.3)	
	Percreta	56 (40)	28 (40)	
Placental location	Anterior low	16 (11.4)	9 (12.9)	0.948
	Posterior low	15 (10.7)	7 (10)	
	Central over the internal os	109 (77.9)	54 (77.1)	
Degree of placental invasion	Focal	40 (28.6)	18 (25.7)	0.662
	Complete	100 (71.4)	52 (74.3)	
Cesarean incision type	Low transverse	31 (22.1)	13 (18.6)	0.566
	High transverse	55 (39.3)	32 (45.7)	
	Classic	41 (29.3)	16 (22.9)	
	vertical	13 (9.3)	9 (12.9)	
Relation of incision to placenta	Incision through placenta	3 (2.1)	3 (4.3)	0.380
	Incision away from placenta	137 (97.9)	67 (95.7)	

Table 2. Continued

Variable	Category	Indication for delivery		p-value
		Elective (n=140)	Emergency (n=70)	
		Statistics	Statistics	
Preoperative ultrasound	No	7 (5)	5 (7.1)	0.528
	Yes	133 (95)	65 (92.9)	
Organ invasion by placenta	No	107 (76.4)	45 (64.3)	0.177
	Bladder invasion	30 (21.4)	23 (32.9)	
	Parametrial invasion	3 (2.1)	2 (2.9)	
Intraoperative complications	No	106 (75.7)	53 (75.7)	**0.024**
	Unintentional cystotomy	32 (22.9)	13 (18.6)	
	Ureteric injury	0 (0)	4 (5.7)	
	Bowel injury	2 (1.4)	0 (0)	
Maternal ICU admission	No	98 (70)	41 (58.6)	0.098
	Yes	42 (30)	29 (41.4)	
Maternal mortality	No	139 (99.3)	70 (100)	0.478
	Yes	1 (0.7)	0 (0)	
Intrauterine fetal death	No	138 (98.6)	68 (97.1)	0.475
	Yes	2 (1.4)	2 (2.9)	
Perinatal death	No	138 (98.6)	56 (80)	**<0.001**
	Yes	2 (1.4)	14 (20)	
Neonatal ICU requirement	No	85 (60.7)	21 (30)	**<0.001**
	Yes	55 (39.3)	49 (70)	
Need for neonatal respiratory support	No	93 (66.4)	22 (31.4)	**<0.001**
	Yes	47 (33.6)	48 (68.6)	
Neonatal intracranial hemorrhage	No	136 (97.1)	57 (81.4)	**<0.001**
	Yes	4 (2.9)	13 (18.6)	
Neonatal hypoxic-ischemic encephalopathy	No	137 (97.9)	63 (90)	**0.012**
	Yes	3 (2.1)	7 (10)	

BMI: Body mass index, IVF: In vitro fertilization, ICU: Intensive care unit. Statistically significant p values are indicated in bold

surgery. Of these, 95 (45.2%) underwent hysterectomy and 115 (54.8%) underwent preventive surgery. Placental involvement was predominantly anterior (n=188, 89.5%), with only 22 cases (10.5%) demonstrating posterior invasion.

Anterior placental location was strongly associated with complete invasion and bladder involvement, whereas posterior placentas were mainly characterized by focal invasion and minimal organ involvement (Figure 3). The surgical approach varied significantly based on clinical presentation and intraoperative findings. Anterior placental location was observed in 188 patients (89.5%) and posterior location in 22 patients (10.5%). With respect to invasion type, 68 patients (32.4%) had placenta accreta, 58 (27.6%) had increta, and 84 (40.0%) had percreta. Complete invasion was more common (72.4%) than focal invasion (27.6%). Hysterectomy was performed in 95 cases (45.24%), while uterine-preserving techniques were attempted in 115 patients (54.76%). Among the conservative management group, 23 cases (20%) required conversion to hysterectomy intraoperatively due to uncontrolled hemorrhage, and 3 (2.6%) underwent delayed hysterectomy during the postoperative period. The hysterectomy group demonstrated higher rates of complete placental invasion (92.6% vs. 55.7%,

p<0.001) and placenta percreta (60% vs. 23.5%, p<0.001). Surgical approach also differed significantly, with upper transverse incisions predominating in uterine-preserving cases (65.2%) versus classical incisions in hysterectomies (56.8%, p<0.001) (Table 3). In addition, the number of previous cesarean sections and the rate of perinatal death were higher in the hysterectomy group (Figure 4).

When comparing planned and emergency deliveries, there was no significant difference in preoperative or postoperative hemoglobin and hematocrit levels or in transfusion requirements. However, intraoperative blood loss was significantly higher in the emergency group (799.3±414.3 mL vs. 511.4±311.5 mL; p<0.001).

Neonatal Outcomes

The neonatal consequences of PAS were particularly pronounced in emergency deliveries. Infants born under emergent conditions had significantly lower birth weights (2147.91±858.94 g vs. 2863.32±455.17 g, p<0.001), reflecting their earlier gestational age at delivery. Apgar scores were markedly reduced in the emergency group at both 1-minute (6.33±1.63 vs. 7.35±1.22, p<0.001) and 5-minute assessments (8.01±1.94 vs. 9.11±1.36, p<0.001). NICU admission duration was nearly three times longer for neonates delivered emergently (6.74±8.14 days vs. 2.13±4.22 days, p<0.001). The emergency group also demonstrated higher rates of respiratory distress syndrome (RDS) (47%

Table 3. Comparison of maternal, obstetric, and neonatal characteristics between hysterectomy and conservative surgery

Variables	Category	Conservative management		p-value
		Hysterectomy	Conservative surgery	
		Statistics	Statistics	
Age (year)		35.07±4.14; 35 (25-45)	32.77±5.15; 33 (19-45)	**<0.001**
Gravida		4.59±1.65; 4 (2-12)	4.05±1.31; 4 (1-9)	**0.024**
Parity		3.08±1.31; 3 (1-8)	2.62±1.1; 3 (0-6)	**0.012**
BMI (kg/m²)		30.9±4.14; 30 (22-42)	30.35±3.98; 30 (19-39)	0.37
Number of previous cesarean sections		2.27±0.93; 2 (0-5)	1.94±0.99; 2 (0-5)	**0.013**
Gestational age at diagnosis (weeks)		26.22±5.18; 24 (17-38)	26.5±5.98; 24 (19-39)	0.544
Gestational age at delivery (weeks)		34.71±3; 36 (21-38)	34.72±3.95; 36 (20-39)	0.091
Preoperative hemoglobin (g/L)		11.19±1.21; 11.2 (7.4-14.2)	11.26±1.43; 11.4 (7.1-14.4)	0.397
Preoperative hematocrit (g/L)		34.14±3.28; 33.7 (25.4-46)	34.26±3.9; 34.3 (23.5-44)	0.406
Intraoperative blood loss (cc)		561.05±333.52; 500 (200-2000)	645.65±401.4; 500 (200-2500)	0.055
Erythrocyte transfusion (units)		2.47±1.74; 2 (0-10)	2.45±2.07; 2 (0-10)	0.869
Maternal ICU stay duration (days)		0.74±1.45; 0 (0-6)	0.96±1.5; 0 (0-6)	0.168
Hospital stay duration (days)		5.73±3.43; 5 (1-21)	5.35±2.72; 5 (2-20)	0.522
Postpartum hemoglobin (g/L)		9.12±1.23; 9.1 (5.3-12)	9.14±1.65; 9.2 (4.3-12.9)	0.828
Postpartum hematocrit (g/L)		27.76±3.83; 28.4 (14.5-36.1)	27.78±4.68; 28.2 (14.9-37.1)	0.856
Perioperative tranexamic acid use (vials)		0.17±0.81; 0 (0-4)	0.42±1.23; 0 (0-4)	0.091
Neonatal birth weight (g)		2633.93±624.71; 2780 (350-3890)	2617.36±766; 2790 (480-4025)	0.526
1-minute APGAR score		7.03±1.64; 8 (0-9)	6.99±1.28; 7 (3-9)	0.379
5-minute APGAR score		8.63±1.92; 9 (0-10)	8.84±1.41; 9 (4-10)	0.503
Neonatal ICU stay duration		3.98±6.57; 0 (0-35)	3.41±5.89; 0 (0-36)	0.697
Neonatal respiratory distress syndrome		0.25±0.44; 0 (0-1)	0.24±0.43; 0 (0-1)	0.878
Smoking	No	77 (81.1)	103 (89.6)	0.079
	Yes	18 (18.9)	12 (10.4)	

Table 3. Continued

Variables	Category	Conservative management		p-value
		Hysterectomy	Conservative surgery	
		Statistics	Statistics	
Indication for delivery	Elective	66 (69.5)	74 (64.3)	0.433
	Emergency	29 (30.5)	41 (35.7)	
Intrapartum assessment	Planned hysterectomy	93 (97.9)	4 (3.5)	**<0.001**
	Conservative procedure	2 (2.1)	85 (73.9)	
	Failed conservative procedure followed by immediate hysterectomy	0 (0)	23 (20)	
	Failed conservative management followed by delayed hysterectomy	0 (0)	3 (2.6)	
Compression suture types	No	95 (100)	112 (97.4)	0.113
	Yes	0 (0)	3 (2.6)	
Type of placental invasion	Accreta	15 (15.8)	53 (46.1)	**<0.001**
	Increta	23 (24.2)	35 (30.4)	
	Percreta	57 (60)	27 (23.5)	
Placental location	Anterior low	13 (13.7)	12 (10.4)	0.559
	Posterior low	8 (8.4)	14 (12.2)	
	Central over the internal os	74 (77.9)	89 (77.4)	
Degree of placental invasion	Focal	7 (7.4)	51 (44.3)	**<0.001**
	Complete	88 (92.6)	64 (55.7)	
Cesarean incision type	Low transverse	10 (10.5)	34 (29.6)	**<0.001**
	High transverse	12 (12.6)	75 (65.2)	
	Classic	54 (56.8)	3 (2.6)	
	Vertical	19 (20)	3 (2.6)	
Relation of incision to placenta	Incision through placenta	4 (4.2)	2 (1.7)	0.285
	Incision away from placenta	91 (95.8)	113 (98.3)	
Preoperative ultrasound	No	3 (3.2)	9 (7.8)	0.147
	Yes	92 (96.8)	106 (92.2)	
Organ invasion by placenta	No	64 (67.4)	88 (76.5)	0.321
	Bladder invasion	28 (29.5)	25 (21.7)	
	Parametrial invasion	3 (3.2)	2 (1.7)	

Table 3. Continued

Variables	Category	Conservative management		p-value
		Hysterectomy	Conservative surgery	
		Statistics	Statistics	
Intraoperative complications	No	65 (68.4)	94 (81.7)	0.068
	Unintentional cystotomy	28 (29.5)	17 (14.8)	
	Ureteric injury	1 (1.1)	3 (2.6)	
	Bowel injury	1 (1.1)	1 (0.9)	
Maternal ICU admission	No	66 (69.5)	73 (63.5)	0.361
	Yes	29 (30.5)	42 (36.5)	
Maternal mortality	No	94 (98.9)	115 (100)	0.27
	Yes	1 (1.1)	0 (0)	
Intrauterine fetal death	No	91 (95.8)	115 (100)	**0.026**
	Yes	4 (4.2)	0 (0)	
Perinatal death	No	92 (96.8)	102 (88.7)	**0.027**
	Yes	3 (3.2)	13 (11.3)	
Neonatal ICU requirement	No	48 (50.5)	58 (50.4)	0.989
	Yes	47 (49.5)	57 (49.6)	
Need for neonatal respiratory support	No	51 (53.7)	64 (55.7)	0.775
	Yes	44 (46.3)	51 (44.3)	
Neonatal intracranial hemorrhage	No	90 (94.7)	103 (89.6)	0.171
	Yes	5 (5.3)	12 (10.4)	
Neonatal hypoxic-ischemic encephalopathy	No	93 (97.9)	107 (93)	0.100
	Yes	2 (2.1)	8 (7)	

BMI: Body mass index, ICU: Intensive care unit. Statistically significant p values are indicated in bold

vs. 14%, p<0.001), intracranial hemorrhage (18.6% vs. 2.9%, p<0.001), and hypoxic-ischemic encephalopathy (10% vs. 2.1%, p =0.012). Most alarmingly, perinatal mortality was fourteen times higher in emergency deliveries (20% vs. 1.4%, p<0.001).

Placental Characteristics and Associated Morbidity

The study provided a detailed analysis of placental morphology and its clinical implications. Anterior placental location predominated (89.52%), with these cases demonstrating higher rates of complete invasion (77.7% vs. 27.3% in posterior placentas, p<0.001) and bladder involvement (27.7% vs. 4.5%, p=0.038). Posterior placentas were more likely to show focal invasion (72.7%) and were found in patients with significantly lower BMI (28.95±3.81 vs. 30.79±4.04, p=0.015) (Table 4). Surgical complications varied by placental location, with ureteral injury occurring exclusively in emergency cases (5.7% vs. 0%, p=0.024), while bladder injuries were more common in planned deliveries (22.9% vs. 18.6%, p=0.024).

Antenatal Management

Antenatal steroid administration showed significant variation between groups. Complete courses were more frequently administered in planned deliveries (39.3% vs. 24.3%, p<0.001), while incomplete dosing was more common in emergency cases (24.3% vs. 5%). This disparity in prenatal preparation likely contributed to the observed differences in neonatal outcomes.

Predictive Modeling

In the univariate logistic regression analysis evaluating factors associated with the mode of delivery, variables including maternal age, gravida, parity, BMI, smoking status, and number of previous cesarean sections were not significantly associated with delivery type (p>0.05) (Table 5).

Conversely, lower preoperative hematocrit was identified as a significant predictor of emergency delivery (OR: 1.092; 95% CI: 1.007-1.185; p=0.034), while preoperative hemoglobin level showed a borderline association (OR: 1.234; 95%

CI: 0.992-1.534; p=0.059). In the multivariable model, preoperative hematocrit remained an independent predictor of emergency delivery after adjustment for BMI, number of prior cesarean sections, and placental location, supporting its potential clinical value as an early marker of adverse delivery timing.

Furthermore, in a separate multivariable analysis adjusting for maternal diabetes, hypertension, parity, and gestational age, emergency delivery continued to be independently associated with increased risk of neonatal RDS (adjusted OR: 2.7, 95% CI: 1.4-5.2) and perinatal death (adjusted OR: 3.8, 95% CI: 1.1-8.6), confirming the robustness of the observed associations.

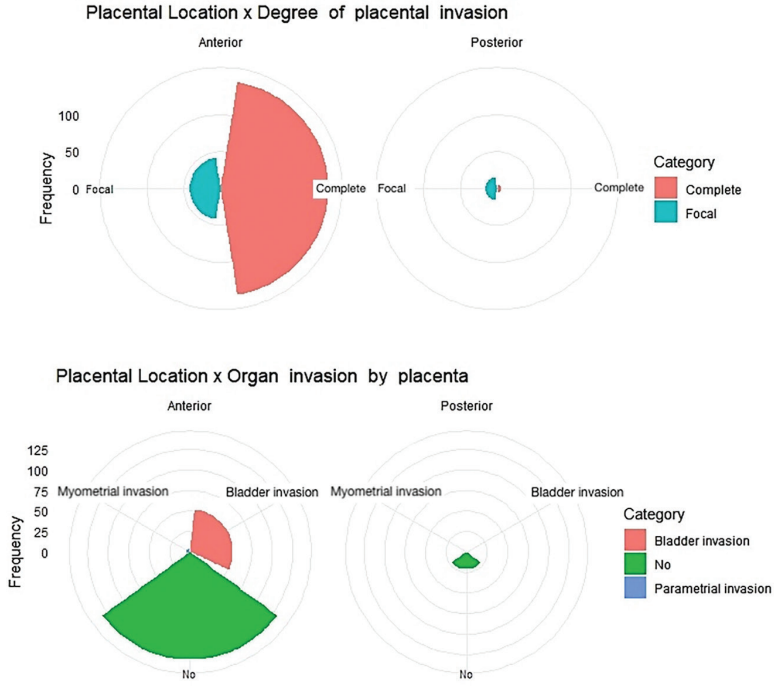

Figure 3. Placental invasion characteristics according to placental location (anterior vs. posterior)

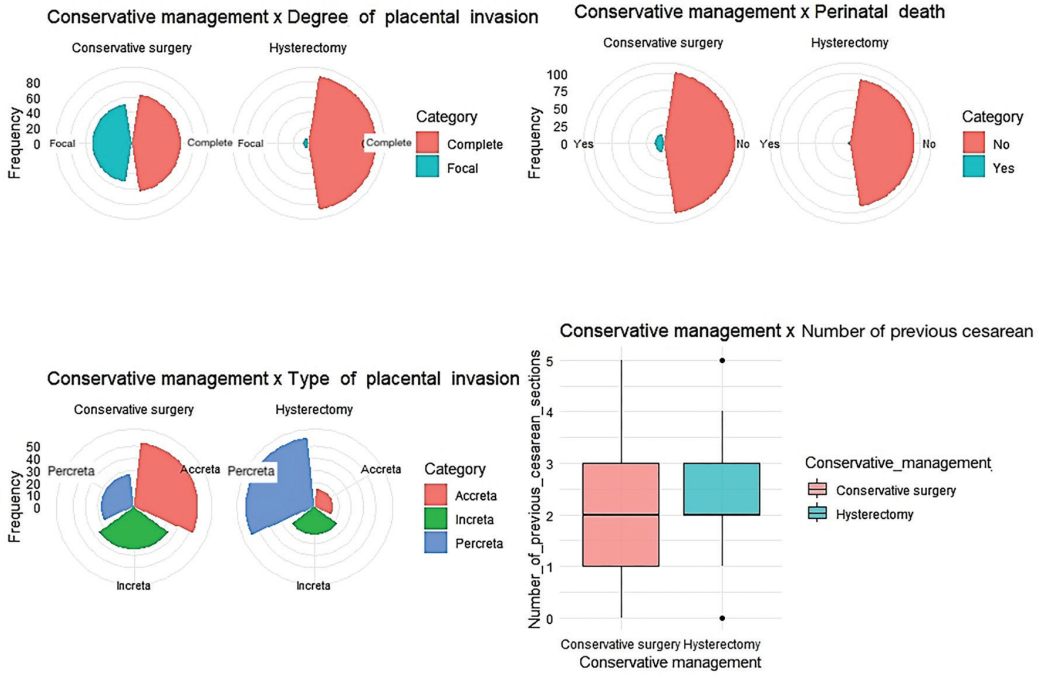

Figure 4. Clinical and obstetric characteristics according to management approach (conservative surgery vs. hysterectomy)

Table 4. Comparison of maternal, obstetric, and neonatal characteristics according to placental location (anterior vs. posterior)

Variables	Category	Placental location		p-value
		Anterior	Posterior	
		Statistics	Statistics	
Age (year)		33.7±4.81; 34 (19-45)	34.82±5.22; 35 (26-43)	0.345
Gravida		4.35±1.5; 4 (1-12)	3.86±1.42; 4 (2-7)	0.113
Parity		2.88±1.22; 3 (0-8)	2.41±1.18; 2 (1-5)	0.053
BMI (kg/m^2)		30.79±4.04; 30 (19-42)	28.95±3.81; 28 (24-41)	**0.015**
Number of previous cesarean sections		2.11±0.98; 2 (0-5)	1.95±0.95; 2 (1-5)	0.286
Gestational age at diagnosis (weeks)		25.88±5.41; 24 (17-38)	30.55±5.77; 31.5 (19-39)	**0.001**
Gestational age at delivery (weeks)		34.55±3.68; 36 (20-39)	36.14±1.49; 36 (33-39)	**0.027**
Preoperative hemoglobin (g/L)		11.21±1.36; 11.2 (7.1-14.4)	11.41±1.1; 11.4 (8.7-14)	0.544
Preoperative hematocrit (g/L)		34.09±3.64; 34.1 (23.5-46)	35.18±3.44; 34.85 (30-44)	0.324
Intraoperative blood loss (cc)		612.77±385.56; 500 (200-2500)	561.36±253.04; 500 (200-1100)	0.947
Erythrocyte transfusion (units)		2.44±1.88; 2 (0-10)	2.68±2.3; 2 (0-10)	0.827
Maternal ICU stay duration (days)		0.82±1.45; 0 (0-6)	1.14±1.75; 0 (0-6)	0.543
Hospital stay duration (days)		5.41±2.98; 5 (1-20)	6.41±3.65; 5.5 (3-21)	**0.045**
Postpartum hemoglobin (g/L)		9.15±1.47; 9.2 (4.3-12.9)	8.95±1.54; 8.75 (6.2-12)	0.345
Postpartum hematocrit (g/L)		27.84±4.31; 28.35 (14.5-37.1)	27.24±4.32; 26.15 (20.4-36.1)	0.354
Perioperative tranexamic acid use (vials)		0.28±1.02; 0 (0-4)	0.55±1.41; 0 (0-4)	0.262
Neonatal birth weight (g)		2591.51±710.08; 2780 (350-3600)	2909.77±589.85; 2800 (1610-4025)	0.182
1-minute APGAR score		6.97±1.5; 7 (0-9)	7.32±0.89; 8 (5-8)	0.449
5-minute APGAR score		8.68±1.72; 9 (0-10)	9.36±0.73; 9.5 (8-10)	0.072
Neonatal ICU stay duration		3.66±6.29; 0.5 (0-36)	3.73±5.53; 0 (0-19)	0.992
Neonatal respiratory distress syndrome		0.24±0.43; 0 (0-1)	0.27±0.46; 0 (0-1)	0.774
Smoking	No	159 (84.57%)	21 (95.45%)	0.168
	Yes	29 (15.43%)	1 (4.55%)	
Diagnostic method	Ultrasound diagnosis	36 (19.14%)	7 (31.81%)	**<0.001**
	Ultrasound + Doppler	152 (80.85%)	14 (63.64%)	
	Ultrasound, confirme by MRI	0 (0.00%)	1 (4.55%)	
Indication for delivery	Elective	125 (66.49%)	15 (68.18%)	0.873
	Emergency	63 (33.51%)	7 (31.82%)	

Table 4. Continued

Variables	Category	Placental location		p-value
		Anterior	Posterior	
		Statistics	Statistics	
Intrapartum assessment	Planned hysterectomy	89 (47.34%)	8 (36.36%)	0.264
	Conservative procedure	78 (41.49%)	9 (40.91%)	
	Failed conservative procedure followed by immediate hysterectomy	18 (9.57%)	5 (22.73%)	
	Failed conservative management followed by delayed hysterectomy	3 (1.60%)	0 (0.00%)	
Conservative management	Hysterectomy	87 (46.28%)	8 (36.36%)	0.377
	Conservative surgery	101 (53.72%)	14 (63.64%)	
Compression suture types	No	187 (99.47%)	20 (90.91%)	**0.001**
	Yes	1 (0.53%)	2 (9.09%)	
Degree of placental invasion	Focal	42 (22.34%)	16 (72.73%)	**<0.001**
	Complete	146 (77.66%)	6 (27.27%)	
Cesarean incision type	Low transverse	29 (15.43%)	15 (68.18%)	**<0.001**
	High transverse	85 (45.21%)	2 (9.09%)	
	Classic	54 (28.72%)	3 (13.64%)	
	Vertical	20 (10.64%)	2 (9.09%)	
Relation of incision to placenta	Incision through placenta	5 (2.66%)	1 (4.55%)	0.615
	Incision away from placenta	183 (97.34%)	21 (95.45%)	
Preoperative ultrasound	No	8 (4.26%)	4 (18.18%)	**0.008**
	Yes	180 (95.74%)	18 (81.82%)	
Organ invasion by placenta	No	131 (69.68%)	21 (95.45%)	**0.038**
	Bladder invasion	52 (27.66%)	1 (4.55%)	
	Parametrial invasion	5 (2.66%)	0 (0.00%)	
Intraoperative complications	No	138 (73.40%)	21 (95.45%)	0.155
	Unintentional cystotomy	44 (23.40%)	1 (4.55%)	
	Ureteric injury	4 (2.13%)	0 (0.00%)	
	Bowel injury	2 (1.06%)	0 (0.00%)	

Table 4. Continued

Variables	Category	Placental location		p-value
		Anterior	Posterior	
		Statistics	Statistics	
Maternal ICU admission	No	124 (65.96%)	15 (68.18%)	0.835
	Yes	64 (34.04%)	7 (31.82%)	
Maternal mortality	No	187 (99.47%)	22 (100.00%)	0.732
	Yes	1 (0.53%)	0 (0.00%)	
Intrauterine fetal death	No	184 (97.87%)	22 (100.00%)	0.490
	Yes	4 (2.13%)	0 (0.00%)	
Perinatal death	No	172 (91.49%)	22 (100.00%)	0.155
	Yes	16 (8.51%)	0 (0.00%)	
Neonatal ICU requirement	No	94 (50.00%)	12 (54.55%)	0.687
	Yes	94 (50.00%)	10 (45.45%)	
Need for neonatal respiratory support	No	103 (54.79%)	12 (54.55%)	0.983
	Yes	85 (45.21%)	10 (45.45%)	
Neonatal intracranial hemorrhage	No	172 (91.49%)	21 (95.45%)	0.519
	Yes	16 (8.51%)	1 (4.55%)	
Neonatal hypoxic-ischemic encephalopathy	No	179 (95.21%)	21 (95.45%)	0.960
	Yes	9 (4.79%)	1 (4.55%)	

BMI: Body mass index, ICU: Intensive care unit. Statistically significant p values are indicated in bold

Table 5. Univariate logistic regression analysis for predictors of elective versus emergency cesarean section

Variables	Odds ratio	p-value	95% CI for EXP(B)	
			Lower	Upper
Age	1.003	0.928	0.945	1.064
Constant	1.823	0.561		
Gravida	0.978	0.819	0.807	1.184
Constant	2.202	0.077		
Parity	1.000	1.000	0.790	1.265
Constant	2.000	0.061		
BMI	0.976	0.505	0.909	1.048
Constant	4.189	0.202		
Smoking	0.842	0.676	0.376	1.884
Constant	1.882	**0.002**		
Number of previous cesarean sections	0.900	0.484	0.671	1.208
Constant	2.496	**0.009**		
Gestational age at delivery (weeks)	1.662	**<0.001**	1.372	2.013
Constant	0.000	**<0.001**		
Preoperative hemoglobin (g/L)	1.234	**0.059**	0.992	1.534
Constant	0.191	0.183		

Table 5. Continued

Variables	Odds ratio	p-value	95% CI for EXP(B)	
			Lower	Upper
Preoperative hematocrit (g/L)	1.092	**0.034**	1.007	1.185
Constant	0.099	0.103		
Intraoperative blood loss (cc)	0.998	**<0.001**	0.997	0.999
Constant	8.571	**<0.001**		
Erythrocyte transfusion (units)	0.968	0.666	0.835	1.122
Constant	2.169	**0.001**		
Maternal ICU stay duration (days)	0.884	0.201	0.733	1.067
Constant	2.233	<0.001		
Hospital stay duration (days)	0.951	0.282	0.868	1.042
Constant	2.644	**0.001**		
Neonatal ICU stay duration (days)	0.874	**<0.001**	0.823	0.928
Constant	3.344	**<0.001**		
Neonatal respiratory distress syndrome	0.176	**<0.001**	0.090	0.345
Constant	3.270	**<0.001**		

BMI: Body mass index, CI: Confidence interval, ICU: Intensive care unit. Statistically significant p values are indicated in bold

Table 6. Pearson correlation coefficients and p-values between clinical and neonatal variables in emergency and elective cesarean groups

			Gravida	Parity	BMI	Number of previous cesarean sections	Gestational age at delivery	Intraoperative blood loss	Erythrocyte transfusion	Maternal ICU stay duration	Hospital stay duration	Neonatal ICU stay duration	Neonatal respiratory distress syndrome
Emergency	Age	Pearson correlation	0.244	0.321	0.221	0.270	0.140	-0.056	-0.206	-0.043	-0.098	-0.043	-0.120
		p-value	**0.042**	**0.007**	0.066	**0.024**	0.247	0.643	0.088	0.723	0.421	0.723	0.323
	Gravida	Pearson correlation		0.881	0.262	0.516	-0.068	-0.145	-0.113	-0.146	-0.164	0.130	0.157
		p-value		**<0.001**	**0.029**	**<0.001**	0.578	0.230	0.353	0.227	0.175	0.282	0.195
	Parite	Pearson correlation			0.302	0.700	-0.045	-0.123	-0.097	-0.159	-0.188	0.070	0.062
		p-value			**0.011**	**<0.001**	0.711	0.311	0.426	0.187	0.119	0.567	0.608
	BMI	Pearson correlation				0.039	-0.009	-0.028	-0.035	-0.145	-0.064	0.010	0.210
		p-value				0.746	0.940	0.821	0.777	0.231	0.596	0.936	0.081
	Number of previous cesarean sections	Pearson correlation					-0.106	0.127	0.153	0.026	0.013	0.157	0.055
		p-value					0.384	0.297	0.206	0.833	0.917	0.196	0.648
	Gestational age at delivery	Pearson correlation						-0.039	-0.134	-0.151	-0.017	-0.385	-0.582
		p-value						0.746	0.269	0.211	0.890	**0.001**	**<0.001**
	Intraoperative blood loss	Pearson correlation							0.880	0.692	0.405	0.142	0.141
		p-value							**<0.001**	**<0.001**	**<0.001**	0.242	0.245
	Erythrocyte transfusion	Pearson correlation								0.723	0.486	0.116	0.202
		p-value								**<0.001**	**<0.001**	0.340	0.094
	Maternal ICU stay duration	Pearson correlation									0.618	0.080	0.201
		p-value									**<0.001**	0.513	0.095
	Hospital stay duration	Pearson correlation										0.041	0.097
		p-value										0.737	0.423
	Neonatal ICU stay duration	Pearson correlation											0.547
		p-value											**<0.001**

Table 6. Continued

			Gravida	Parity	BMI	Number of previous cesarean sections	Gestational age at delivery	Intraoperative blood loss	Erythrocyte transfusion	Maternal ICU stay duration	Hospital stay duration	Neonatal ICU stay duration	Neonatal respiratory distress syndrome
Elective	Age	Pearson correlation	0.215	0.206	0.261	0.196	-0.065	-0.006	0.205	0.137	0.180	0.086	0.098
		p-value	**0.011**	**0.014**	**0.002**	**0.020**	0.448	0.943	**0.015**	0.106	**0.034**	0.313	0.247
	Gravida	Pearson correlation		0.830	0.176	0.551	0.033	-0.096	-0.088	-0.112	-0.016	0.167	0.108
		p-value		**<0.001**	**0.037**	**<0.001**	0.700	0.260	0.300	0.189	0.848	**0.049**	0.204
	Parity	Pearson correlation			0.224	0.676	0.051	-0.084	-0.065	-0.132	-0.083	0.041	0.039
		p-value			**0.008**	**<0.001**	0.549	0.326	0.443	0.121	0.327	0.634	0.650
	BMI	Pearson correlation				0.167	0.099	-0.176	-0.056	-0.063	-0.012	-0.126	-0.089
		p-value				**0.049**	0.243	**0.037**	0.509	0.456	0.889	0.138	0.294
	Number of previous cesarean sections	Pearson correlation					0.004	-0.033	0.106	0.014	-0.039	-0.087	0.040
		p-value					0.966	0.695	0.212	0.867	0.645	0.304	0.637
	Gestational age at delivery	Pearson correlation						-0.103	0.016	0.027	-0.063	-0.149	-0.170
		p-value						0.226	0.855	0.751	0.463	0.078	**0.045**
	Intraoperative blood loss	Pearson correlation							0.591	0.360	0.230	0.067	0.093
		p-value							**<0.001**	**<0.001**	**0.006**	0.429	0.275
	Erythrocyte transfusion	Pearson correlation								0.640	0.525	0.039	0.167
		p-value								**<0.001**	**<0.001**	0.644	**0.049**
	Maternal ICU stay duration	Pearson correlation									0.613	0.124	0.308
		p-value									**<0.001**	0.143	**<0.001**
	Hospital stay duration	Pearson correlation										0.336	0.439
		p-value										**<0.001**	**<0.001**
	Neonatal ICU stay duration	Pearson correlation											0.628
		p-value											**<0.001**

BMI: Body mass index, ICU: Intensive care unit. Statistically significant p values are indicated in bold

Correlational Analysis

Table 6 summarizes the significant correlations observed in the emergency and elective cesarean section groups. In the emergency cesarean section group, maternal age was positively correlated with gravida (r=0.244; p=0.042), parity (r=0.321; p=0.007), and the number of previous cesarean deliveries (r=0.270; p=0.024). Increasing gestational age at delivery was negatively correlated with NICU stay duration (r=-0.385; p=0.001) and the presence of neonatal RDS (r=-0.582; p<0.001). Intraoperative blood loss was strongly correlated with erythrocyte transfusion requirement (r=0.880; p<0.001) and maternal ICU stay duration (r=0.692; p<0.001). In the elective cesarean section group, maternal age showed significant positive correlations with gravida (r=0.215; p=0.011), parity (r=0.206; p=0.014), BMI (r=0.261; p=0.002), and the number of previous cesarean deliveries (r=0.196; p=0.020). Intraoperative blood loss was positively correlated with erythrocyte transfusion (r=0.591; p<0.001) and maternal ICU stay duration (r=0.360; p<0.001). On the other hand, in the hysterectomy group, maternal age showed a positive correlation with gravida (r=0.285, p=0.005), parity (r=0.232, p=0.024), and the number of previous cesarean sections (r=0.300, p=0.003). Parity was positively associated with gestational age at delivery (r=0.515, p<0.001), but negatively correlated with intraoperative blood loss (r=-0.240, p=0.019) and maternal ICU stay (r=-0.245, p=0.017). Gestational age was inversely correlated with neonatal ICU stay (r=-0.381, p<0.001) and neonatal RDS (r=-0.405, p<0.001). Intraoperative blood loss showed strong positive correlations with erythrocyte transfusion (r=0.575, p<0.001) and maternal ICU stay (r=0.369, p<0.001). Erythrocyte transfusion was positively associated with maternal ICU stay (r=0.606, p<0.001) and hospital stay (r=0.481, p<0.001). In the uterus-preserving surgery group, maternal age was positively correlated with gravida (r=0.202, p=0.030) and parity (r=0.198, p=0.034). Gestational age showed negative correlations with neonatal ICU stay (r=-0.482, p<0.001) and neonatal RDS (r=-0.609, p<0.001). Intraoperative blood loss was positively associated with erythrocyte transfusion (r=0.730, p<0.001), maternal ICU stay (r=0.563, p<0.001), hospital stay (r=0.436, p<0.001), and neonatal ICU stay (r=0.299, p=0.001). Erythrocyte transfusion was positively correlated with maternal ICU stay (r=0.718, p<0.001) and hospital stay (r=0.557, p<0.001) (Table 7).

Table 8 presents the correlation analysis of maternal and neonatal outcomes between the anterior and posterior placenta groups. In the anterior placenta group, maternal age was positively correlated with gravida (r=0.227, p=0.002), parity (r=0.264, p<0.001), BMI (r=0.253, p<0.001), and the number of previous cesarean sections (r=0.210, p=0.004). The number of previous cesarean sections correlated positively with erythrocyte transfusion (r=0.172, p=0.018). Gestational age at delivery was negatively correlated with intraoperative blood loss (r=-0.239, p=0.001), NICU stay (r=-0.437, p<0.001), and neonatal RDS (r=-0.557, p<0.001). Intraoperative blood loss correlated positively with erythrocyte transfusion (r=0.717, p<0.001), maternal ICU stay (r=0.529, p<0.001), hospital stay (r=0.348, p<0.001), NICU stay (r=0.225, p=0.002), and neonatal RDS (r=0.261, p<0.001). Erythrocyte transfusion was significantly associated with maternal ICU stay (r=0.652, p<0.001) and hospital stay duration (r=0.483, p<0.001). In the posterior placenta group, gravida was strongly correlated with parity (r=0.884, p<0.001), BMI (r=0.490, p=0.021), and the number of previous cesarean sections (r=0.699, p<0.001). Parity was also associated with BMI (r=0.427, p=0.047) and the number of previous cesarean sections (r=0.781, p<0.001). BMI showed a significant positive correlation with the number of previous cesarean sections (r=0.512, p=0.015). Gestational age at delivery was negatively correlated with NICU stay (r=-0.568, p=0.006). Erythrocyte transfusion was positively correlated with maternal ICU stay duration (r=0.768, p<0.001) and hospital stay duration (r=0.670, p=0.001).

Discussion

In this retrospective analysis of 210 patients diagnosed with PAS, we investigated the impact of antenatal risk factors, clinical presentation, and management strategies on maternal and neonatal outcomes. Our findings demonstrate that planned surgical intervention was associated with reduced intraoperative blood loss, higher gestational age at delivery, and improved neonatal outcomes compared to emergency interventions. These results reinforce the critical role of antenatal diagnosis and timely delivery planning in optimizing outcomes for both the mother and the neonate.

The observed predominance of anterior placental location in our cohort (89.5%) aligns with prior studies reporting anterior implantation as a significant risk factor for severe placental invasion, particularly in patients with multiple prior cesarean sections[12]. Our data further indicate that anterior location was associated with higher rates of complete invasion and bladder involvement. These findings are consistent with earlier reports suggesting that anterior PAS may have a more aggressive clinical course and higher surgical complexity[13,14]. This underlines the importance of detailed prenatal imaging and multidisciplinary surgical preparation, especially in anteriorly located PAS cases.

Surgical management in our cohort favored hysterectomy in 58.6% of cases, with conservative uterus-preserving approaches used in 41.4% of cases, particularly in accreta and increta cases. This is comparable to previous large series, which reported hysterectomy rates ranging from 50% to 80% depending on disease severity and institutional protocols[15,16]. Moreover, accumulating evidence from recent high-quality studies strongly supports the clinical value of selective uterus-preserving surgical techniques in appropriately selected PAS patients[17-19]. These techniques, including localized resection of the invaded myometrium, partial myometrial excision with uterine reconstruction, stepwise devascularization, and the placenta left *in situ*

Table 7. Pearson correlation coefficients between clinical and neonatal variables in the hysterectomy and conservative surgery groups

			Gravida	Parity	BMI	Number of previous cesarean sections	Gestational age at delivery	Intraoperative blood loss	Erythrocyte transfusion	Maternal ICU stay duration	Hospital stay duration	Neonatal ICU stay duration	Neonatal respiratory distress syndrome
Hysterectomy	Age	Pearson correlation	0.285	0.232	0.300	0.205	0.057	-0.044	0.051	0.083	0.085	0.093	0.125
		p-value	**0.005**	**0.024**	**0.003**	**0.046**	0.586	0.669	0.622	0.425	0.411	0.368	0.228
	Gravida	Pearson correlation		0.864	0.269	0.332	0.167	-0.239	-0.255	-0.175	-0.103	0.237	0.131
		p-value		**<0.001**	**0.008**	**0.001**	0.106	**0.020**	**0.013**	0.091	0.321	**0.021**	0.206
	Parity	Pearson correlation			0.321	0.515	0.209	-0.240	-0.237	-0.245	-0.203	0.090	0.037
		p-value			**0.002**	**<0.001**	**0.042**	**0.019**	**0.021**	**0.017**	**0.048**	0.383	0.723
	BMI	Pearson correlation				0.188	0.169	-0.076	0.002	0.005	0.063	-0.079	0.061
		p-value				0.068	0.101	0.462	0.985	0.958	0.544	0.449	0.555
	Number of previous cesarean sections	Pearson correlation					0.060	-0.068	-0.009	-0.135	-0.227	-0.016	-0.094
		p-value					0.564	0.511	0.933	0.191	**0.027**	0.874	0.367
	Gestational age at delivery	Pearson correlation						-0.364	-0.065	-0.194	-0.113	-0.381	-0.405
		p-value						**<0.001**	0.533	0.060	0.274	**<0.001**	**<0.001**
	Intraoperative blood loss	Pearson correlation							0.575	0.369	0.199	0.142	0.236
		p-value							**<0.001**	**<0.001**	0.054	0.170	0.021
	Erythrocyte transfusion	Pearson correlation								0.606	0.481	-0.068	0.051
		p-value								**<0.001**	**<0.001**	0.512	0.624
	Maternal ICU stay duration	Pearson correlation									0.607	0.054	0.273
		p-value									**<0.001**	0.603	0.007
	Hospital stay duration	Pearson correlation										0.170	0.267
		p-value										**0.099**	**0.009**
	Neonatal ICU stay duration	Pearson correlation											0.710
		p-value											**<0.001**

Table 7. Continued

			Gravida	Parity	BMI	Number of previous cesarean sections	Gestational age at delivery	Intraoperative blood loss	Erythrocyte transfusion	Maternal ICU stay duration	Hospital stay duration	Neonatal ICU stay duration	Neonatal respiratory distress syndrome
Conservative Surgery	Age	Pearson correlation	0.121	0.202	0.198	0.177	0.042	0.023	0.055	0.097	0.042	-0.061	-0.090
		p-value	0.196	**0.030**	**0.034**	0.058	0.658	0.805	0.560	0.300	0.656	0.521	0.341
	Gravida	Pearson correlation		0.814	0.116	0.723	-0.179	0.049	0.033	-0.048	-0.052	0.011	0.117
		p-value		**<0.001**	0.217	**<0.001**	0.056	0.604	0.724	0.611	0.582	0.908	0.213
	Parity	Pearson correlation			0.158	0.825	-0.157	0.062	0.049	-0.021	-0.052	-0.013	0.050
		p-value			0.092	**<0.001**	0.093	0.507	0.600	0.826	0.584	0.886	0.596
	BMI	Pearson correlation				0.068	-0.096	-0.094	-0.085	-0.151	-0.131	-0.007	0.027
		p-value				0.473	0.308	0.315	0.369	0.106	0.161	0.941	0.772
	Number of previous cesarean sections	Pearson correlation					-0.143	0.149	0.210	0.163	0.164	0.079	0.178
		p-value					0.128	0.112	**0.025**	0.082	0.081	0.400	0.057
	Gestational age at delivery	Pearson correlation						-0.174	-0.072	-0.049	-0.035	-0.482	-0.609
		p-value						0.063	0.442	0.600	0.711	**<0.001**	**<0.001**
	Intraoperative blood loss	Pearson correlation							0.730	0.563	0.436	0.299	0.239
		p-value							**<0.001**	**<0.001**	**<0.001**	**0.001**	**0.010**
	Erythrocyte transfusion	Pearson correlation								0.718	0.557	0.196	0.269
		p-value								**<0.001**	**<0.001**	**0.036**	**0.004**
	Maternal ICU stay duration	Pearson correlation									0.652	0.190	0.274
		p-value									**<0.001**	**0.041**	**0.003**
	Hospital stay duration	Pearson correlation										0.210	0.316
		p-value										**0.024**	**0.001**
	Neonatal ICU stay duration	Pearson correlation											0.558
		p-value											**<0.001**

BMI: Body mass index, ICU: Intensive care unit. Statistically significant p values are indicated in bold

Table 8. Correlation analysis of maternal and neonatal outcomes in anterior and posterior placenta groups

			Gravida	Parity	BMI	Number of previous cesarean sections	Gestational age at delivery	Intraoperative blood loss	Erythrocyte transfusion	Maternal ICU stay duration	Hospital stay duration	Neonatal ICU stay duration	Neonatal respiratory distress syndrome
Anterior	Age	Pearson correlation	0.227	0.264	0.253	0.210	0.019	-0.003	0.060	0.092	0.049	0.008	-0.031
		p-value	**0.002**	**<0.001**	**<0.001**	**0.004**	0.794	0.965	0.415	0.208	0.506	0.918	0.672
	Gravida	Pearson correlation		0.841	0.162	0.521	-0.005	-0.108	-0.071	-0.088	-0.054	0.145	0.142
		p-value		**<0.001**	**0.026**	**<0.001**	0.941	0.139	0.333	0.230	0.462	**0.047**	0.052
	Parite	Pearson correlation			0.216	0.673	0.028	-0.098	-0.049	-0.103	-0.113	0.056	0.057
		p-value			**0.003**	**<0.001**	0.701	0.179	0.505	0.159	0.124	0.446	0.435
	BMI	Pearson correlation				0.086	0.031	-0.103	0.004	-0.045	0.029	-0.029	0.070
		p-value				0.243	0.675	0.158	0.956	0.541	0.689	0.695	0.341
	Number of previous cesarean sections	Pearson correlation					-0.061	0.059	0.172	0.055	-0.019	0.046	0.052
		p-value					0.408	0.424	**0.018**	0.456	0.797	0.533	0.479
	Gestational age at delivery	Pearson correlation						-0.239	-0.097	-0.133	-0.087	-0.437	-0.557
		p-value						**0.001**	0.183	0.070	0.234	**<0.001**	**<0.001**
	Intraoperative blood loss	Pearson correlation							0.717	0.529	0.348	0.225	0.261
		p-value							**<0.001**	**<0.001**	**<0.001**	**0.002**	**<0.001**
	Erythrocyte transfusion	Pearson correlation								0.652	0.483	0.090	0.178
		p-value								**<0.001**	**<0.001**	0.219	**0.015**
	Maternal ICU stay duration	Pearson correlation									0.623	0.141	0.292
		p-value									**<0.001**	0.054	**<0.001**
	Hospital stay duration	Pearson correlation										0.191	0.287
		p-value										**0.009**	**<0.001**
	Neonatal ICU stay duration	Pearson correlation											0.629
		p-value											**<0.001**

Table 8. Continued

			Gravida	Parity	BMI	Number of previous cesarean sections	Gestational age at delivery	Intraoperative blood loss	Erythrocyte transfusion	Maternal ICU stay duration	Hospital stay duration	Neonatal ICU stay duration	Neonatal respiratory distress syndrome
Posterior	Age	Pearson correlation	0.298	0.206	0.321	0.344	0.383	-0.294	-0.009	-0.106	0.184	0.089	0.222
		p-value	0.178	0.358	0.146	0.117	0.078	0.184	0.968	0.637	0.412	0.694	0.320
	Gravida	Pearson correlation		0.884	0.490	0.699	-0.170	-0.075	-0.261	-0.335	-0.099	0.074	-0.013
		p-value		**<0.001**	**0.021**	**<0.001**	0.448	0.741	0.240	0.127	0.662	0.745	0.953
	Parite	Pearson correlation			0.427	0.781	-0.277	-0.088	-0.248	-0.373	-0.096	-0.019	-0.040
		p-value			**0.047**	**<0.001**	0.213	0.697	0.266	0.087	0.671	0.935	0.859
	BMI	Pearson correlation				0.512	-0.024	-0.061	-0.404	-0.327	-0.334	-0.143	-0.157
		p-value				**0.015**	0.915	0.787	0.062	0.138	0.128	0.526	0.485
	Number of previous cesarean sections	Pearson correlation					-0.096	-0.196	-0.225	-0.196	0.033	0.007	0.140
		p-value					0.670	0.382	0.314	0.382	0.884	0.977	0.535
	Gestational age at delivery	Pearson correlation						-0.067	0.264	0.175	-0.046	-0.568	-0.268
		p-value						0.765	0.235	0.436	0.840	**0.006**	0.228
	Intraoperative blood loss	Pearson correlation							0.285	0.179	0.021	0.179	-0.069
		p-value							0.198	0.426	0.928	0.425	0.759
	Erythrocyte transfusion	Pearson correlation								0.768	0.670	0.004	0.178
		p-value								**<0.001**	**0.001**	0.986	0.429
	Maternal ICU stay duration	Pearson correlation									0.564	-0.030	0.130
		p-value									**0.006**	0.893	0.564
	Hospital stay duration	Pearson correlation										0.202	0.302
		p-value										0.368	0.172
	Neonatal ICU stay duration	Pearson correlation											0.654
		p-value											**0.001**

BMI: Body mass index, ICU: Intensive care unit. Statistically significant p values are indicated in bold

approach, have emerged as rational alternatives to routine peripartum hysterectomy, particularly in cases of focal or limited invasion and hemodynamic stability. Multiple observational series and meta-analyses have demonstrated that such uterus-preserving interventions are associated with significantly reduced operative time, lower intraoperative blood loss, and decreased transfusion requirements compared to hysterectomy, without compromising maternal survival[20]. In addition, uterus-preserving surgery confers important long-term advantages, including preservation of menstrual function and the potential for future pregnancy. From a healthcare systems perspective, these strategies have also been linked to reduced resource utilization—notably shorter ICU stays, fewer secondary surgical procedures, and lower overall hospital costs—when performed in tertiary referral centers with multidisciplinary PAS teams and standardized management protocols. Our present findings align closely with this growing body of evidence, reaffirming that the selective use of uterus-preserving techniques in appropriately selected patients, tailored to the extent of placental invasion, placental location, and maternal clinical condition, is pivotal for optimizing outcomes. Integrating precise antenatal imaging with multidisciplinary intraoperative coordination allows for balancing maternal safety with fertility preservation, thereby reflecting the contemporary paradigm shift from radical to selective management in PAS care.

A key statistical finding of our study was the strong and consistent negative correlation between intraoperative blood loss and postoperative hemoglobin/hematocrit levels across all subgroups, including anterior vs. posterior location, hysterectomy vs. uterus-preserving surgery, and emergency vs. planned deliveries. The magnitude of these correlations (Spearman r ranging from -0.45 to -0.68, all $p<0.001$) confirms the predictable hematologic impact of blood loss in PAS surgery. Moreover, multivariate logistic regression identified lower preoperative hematocrit as an independent predictor of emergency delivery (OR: 1.092; 95% CI: 1.007-1.185; $p=0.034$), suggesting that antenatal hematologic optimization may reduce the likelihood of urgent intervention. These findings are in agreement with previous reports that emphasize the importance of preoperative hemoglobin status in reducing intraoperative transfusion needs and improving hemodynamic stability[21,22]. These results also highlight the importance of meticulous surgical planning, early vascular control, and the availability of massive transfusion protocols. Emergency delivery was required in one-third of patients, most commonly due to PAS-related hemorrhage. Current guidelines emphasize rapid intervention in cases with impending or active hemorrhage, which aligns with our findings, as emergency deliveries were associated with markedly higher intraoperative blood loss, lower neonatal birth weight, and increased NICU admissions compared with planned procedures[23]. These results support previous studies reporting that unplanned surgery compromises maternal hemodynamic stability and worsens perinatal outcomes[24-26]. Moreover, the strong association between reduced preoperative hematocrit and the need for emergency delivery observed in our multivariate analysis suggests that antenatal optimization of maternal hematologic status may represent a modifiable risk factor for reducing the likelihood of unplanned intervention.

Neonatal outcomes in our cohort reflected the gestational age at delivery, with lower Apgar scores and higher respiratory distress rates in the emergency delivery group. This underscores the dual benefit of planned intervention: not only is maternal morbidity reduced, but neonatal maturity and stability at birth are improved. Our findings are in line with international guidelines recommending delivery at a gestational age balancing fetal maturity and maternal safety, often between 34 and 36 weeks in PAS cases[27-29].

Regarding long-term outcomes, several recent investigations have shown that uterus-preserving management may enable successful subsequent pregnancies in carefully selected patients, provided that rigorous follow-up and structured surveillance protocols are implemented[30]. However, subsequent pregnancies carry a measurable risk of recurrent abnormal placentation—most commonly placenta previa or recurrent PAS—highlighting the need for preconception counseling and delivery planning in tertiary centers with PAS expertise[31]. From a maternal health perspective, conservative strategies have been associated not only with preservation of reproductive potential but also with improved psychological, and quality-of-life outcomes, particularly among women desiring future fertility[32]. Long-term gynecologic sequelae, such as intrauterine adhesions or secondary infertility, appear uncommon when uterine repair is meticulous and postoperative infections are prevented through careful perioperative management. Moreover, structured and multidisciplinary care pathways that emphasize antenatal diagnosis, planned delivery, and optimized surgical coordination are consistently linked to lower blood transfusion requirements, shorter ICU stays, and reduced overall hospitalization time, translating into measurable cost savings for health systems. Economic analyses from recent multicenter studies indicate that planned conservative management, when applied in appropriate cases, can reduce total healthcare expenditure by up to 25-30% compared with emergency hysterectomy performed without prior antenatal diagnosis[33].

Study Limitations

A major strength of our study is the relatively large sample size of patients with histopathologically confirmed PAS, allowing for meaningful subgroup analyses by placental location, surgical approach, and timing of delivery. The inclusion of detailed maternal, surgical, and neonatal outcomes,

combined with correlation and regression analyses, provides a comprehensive assessment of the clinical course of PAS in a real-world tertiary care setting. Additionally, our focus on the predictive value of preoperative hematocrit for emergency delivery offers a potentially actionable clinical parameter for antenatal risk stratification.

However, several limitations should be acknowledged. The retrospective design inherently carries the risk of selection and information bias, particularly in the completeness of medical records. The study was conducted in a single tertiary referral center, which may limit the generalizability of the results to lower-resource or non-specialized settings. Furthermore, although surgical decision-making was standardized to an extent, variations in surgeon experience and intraoperative judgment could have influenced outcomes. In our center, although all procedures were performed by obstetric surgeons with expertise in high-risk obstetrics and PAS management, subtle differences in surgical judgment—such as the decision to proceed with uterus-preserving management versus radical management, the threshold for hysterectomy, or the intraoperative use of hemostatic and reconstructive techniques—may have impacted both maternal and neonatal outcomes. This inherent heterogeneity in operator experience is a well-recognized limitation in PAS research and contributes to interstudy variability reported in the literature. Differences in team composition, intraoperative resource availability, and surgeon familiarity with advanced uterus-preserving procedures may also act as confounding factors, particularly in retrospective analyses where allocation to a specific surgical approach cannot be fully randomized or blinded. Furthermore, emergent situations often necessitate rapid decision-making under suboptimal conditions, amplifying the effect of individual expertise on surgical outcomes. Although the use of institutional management protocols and multidisciplinary coordination minimizes this variability to some extent, the absence of a fully standardized decision-making algorithm across all surgeons remains an important source of potential bias. Finally, neonatal outcomes were influenced by multiple factors beyond the scope of PAS, including comorbidities and antenatal events, which could not be fully controlled in the analysis.

Conclusion

This study demonstrates that early diagnosis and planned delivery in cases of PAS are critical for optimizing both maternal and neonatal outcomes. Emergency deliveries were associated with lower gestational age at birth, increased intraoperative blood loss, and higher rates of adverse neonatal outcomes, including low birth weight, reduced Apgar scores, prolonged NICU stay, and increased risk of RDS and other serious complications. Surgical management strategies varied according to the type and extent of placental invasion, with uterus-preserving approaches more frequently adopted in focal PAS and hysterectomy preferred in complete invasion or percreta cases. The choice of uterine incision was also influenced by placental location and invasion type, underscoring the importance of individualized surgical planning.

These findings highlight the necessity of multidisciplinary collaboration and careful preoperative planning to reduce maternal morbidity and improve neonatal prognosis. Incorporating detailed antenatal imaging, risk stratification, and timely delivery planning into routine care pathways can significantly mitigate the risks associated with PAS. Future prospective, multicenter studies are warranted to validate these findings and refine management guidelines.

Ethics

Ethics Committee Approval: This retrospective cohort study was conducted at the Department of Obstetrics and Gynecology, İnönü University Faculty of Medicine, after obtaining approval from the Institutional Non-Interventional Clinical Research Ethics Committee (approval date: 02.04.2024; approval number: 2024/5875).

Informed Consent: Retrospective study.

Footnotes

Authorship Contributions

Concept: L.O., R.M., Design: L.O., R.M., E.Y., Data Collection or Processing: L.O., R.M., H.Ö., Analysis or Interpretation: Ş.Y., Literature Search: R.M., Writing: R.M., E.Y., H.Ö., Ş.Y.

Conflict of Interest: Ercan Yılmaz MD is editor-in-chief in Turkish Journal of Obstetrics and Gynecology. He had no involvement in the peer-review of this article and had no access to information regarding its peer-review.

Financial Disclosure: The authors declared that this study received no financial support.

References

1. Jauniaux E, Jurkovic D, Hussein AM, Burton GJ. New insights into the etiopathology of placenta accreta spectrum. Am J Obstet Gynecol. 2022;227:384-91.
2. Escobar MF, Gallego JC, Nasner D, Gunawardana K. Management of abnormal invasive placenta in a low- and medium-resource setting. Best Pract Res Clin Obstet Gynaecol. 2021;72:117-28.
3. Nieto-Calvache AJ, Palacios-Jaraquemada JM, Hussein AM, Jauniaux E, Milani Coutinho C, Rijken M. Management of placenta accreta spectrum in low- and middle-income countries. Best Pract Res Clin Obstet Gynaecol. 2024;94:102475.
4. Rauf M, Ebru C, Sevil E, Selim B. Conservative management of post-partum hemorrhage secondary to placenta previa-accreta with hypogastric artery ligation and endo-uterine hemostatic suture. J Obstet Gynaecol Res. 2017;43:265-71.
5. Waller J, Shamshirsaz A, Abuhamad A. Advances in imaging for placenta accreta spectrum disorder. Obstet Gynecol. 2025;145:621-7.
6. Patel-Lippmann KK, Planz VB, Phillips CH, Ohlendorf JM, Zuckerwise LC, Moshiri M. Placenta accreta spectrum disorders: update and pictorial review of the SAR-ESUR joint consensus statement for MRI. Radiographics. 2023;43:e220090.

7. Waller J, Abuhamad A. Imaging modalities for the diagnosis of placenta accreta spectrum. Clin Obstet Gynecol. 2025;68:242-50.
8. Collins SL, Alemdar B, van Beekhuizen HJ, Bertholdt C, Braun T, Calda P, et al.; International Society for Abnormally Invasive Placenta (IS-AIP). Evidence-based guidelines for the management of abnormally invasive placenta: recommendations from the International Society for Abnormally Invasive Placenta. Am J Obstet Gynecol. 2019;220:511-26.
9. Rosenthal EA, White A, Lafferty AK, Pruszynski JE, Spong CY, Herrera CL. Delivery timing of placenta accreta spectrum: later is feasible. Am J Obstet Gynecol. 2025:S0002-9378(25)00108-5.
10. Matsuzaki S, Einerson BD, Sentilhes L, Sibai BM, Saade GR, Saad AF, et al. Local resection after cesarean delivery for placenta accreta spectrum disorder: a systematic review and meta-analysis. Obstet Gynecol. 2025;145:639-53.
11. Shazly SA, Hortu I, Shih JC, Melekoglu R, Fan S, Ahmed FUA, et al.; and Middle East Obstetrics and Gynecology Graduate Education (MOGGE) foundation – Artificial intelligence (AI) unit. Prediction of clinical outcomes in women with placenta accreta spectrum using machine learning models: an international multicenter study. J Matern Fetal Neonatal Med. 2022;356644-53.
12. Jauniaux E, Ayres-de-Campos D, Langhoff-Roos J, Fox KA, Collins S; FIGO Placenta Accreta Diagnosis and Management Expert Consensus Panel. FIGO classification for the clinical diagnosis of placenta accreta spectrum disorders. Int J Gynaecol Obstet. 2019;146:20-4.
13. Liu H, Zhang B, Wang W, Li H, Huang X, Wang J, et al. Effect of placenta location detected by ultrasound on the severity of placenta accreta spectrum in patients with placenta previa and placenta accreta spectrum. BMC Pregnancy Childbirth. 2023;23:406.
14. White A, Malik M, Pruszynski JE, Do QN, Spong CY, Herrera CL. Contemporary placenta accreta spectrum disorder incidence and risk factors. Obstet Gynecol. 2025;145:665-73.
15. Pan S, Han M, Zhai T, Han Y, Lu Y, Huang S, et al. Maternal outcomes of conservative management and cesarean hysterectomy for placenta accreta spectrum disorders: a systematic review and meta-analysis. BMC Pregnancy Childbirth. 2024;24:463.
16. Sentilhes L, Seco A, Azria E, Beucher G, Bonnet MP, Branger B, et al.; PACCRETA Study Group. Conservative management or cesarean hysterectomy for placenta accreta spectrum: the PACCRETA prospective study. Am J Obstet Gynecol. 2022;226:839.e1-839.e24.
17. Pinto PV, Freitas G, Vieira RJ, Aryananda RA, Nieto-Calvache AJ, Palacios-Jaraquemada JM. Placenta accreta spectrum disorder: a systematic review and meta-analysis on conservative surgery. Int J Gynaecol Obstet. 2025 Jun 24.
18. Barinov SV, Di Renzo GC. A new technique to preserve the uterus in patients with placenta accreta spectrum disorders. Am J Obstet Gynecol. 2024;230:S1107-15.
19. Paping A, Bluth A, Al Naimi A, Mhallem M, Kolak M, Jaworowski A, et al.; IS-PAS. Opportunities for, and barriers to, uterus-preserving surgical techniques for placenta accreta spectrum. Acta Obstet Gynecol Scand. 2025;104(Suppl 1):8-19.
20. Hessami K, Kamepalli S, Lombaard HA, Shamshirsaz AA, Belfort MA, Munoz JL. Conservative management of placenta accreta spectrum is associated with improved surgical outcomes compared to cesarean hysterectomy: a systematic review and meta-analysis. Am J Obstet Gynecol. 2025;232:432-452.e3.
21. Kloka JA, Friedrichson B, Jasny T, Blum LV, Choorapoikayil S, Old O, et al. Anaemia and red blood cell transfusion in women with placenta accreta spectrum: an analysis of 38,060 cases. Sci Rep. 2024;14:4999.
22. Zhang B, Liu H, Li H, Wang J, Zhu H, Yu P, et al. Obstetric blood transfusion in placenta previa patients with prenatal anemia: a retrospective study. BMC Pregnancy Childbirth. 2024;24:92.
23. Bonanni G, Lopez-Giron MC, Allen L, Fox K, Silver RM, Hobson SR, et al. Guidelines on placenta accreta spectrum disorders: a systematic review. JAMA Netw Open. 2025;8:e2521909.
24. Zhan Y, Lu E, Xu T, Huang G, Deng C, Chen T, et al. Cesarean hysterectomy in pregnancies complicated with placenta previa accreta: a retrospective hospital-based study. BMC Pregnancy Childbirth. 2024;24:634.
25. Silver RM, Fox KA, Barton JR, Abuhamad AZ, Simhan H, Huls CK, et al. Center of excellence for placenta accreta. Am J Obstet Gynecol. 2015;212:561-8.
26. Morlando M, Schwickert A, Stefanovic V, Gziri MM, Pateisky P, Chalubinski KM, et al.; International Society for Placenta Accreta Spectrum (IS-PAS). Maternal and neonatal outcomes in planned versus emergency cesarean delivery for placenta accreta spectrum: a multinational database study. Acta Obstet Gynecol Scand. 2021;100(Suppl 1):41-9.
27. Allen L, Jauniaux E, Hobson S, Papillon-Smith J, Belfort MA; FIGO Placenta Accreta Diagnosis and Management Expert Consensus Panel. FIGO consensus guidelines on placenta accreta spectrum disorders: nonconservative surgical management. Int J Gynaecol Obstet. 2018;140:281-90.
28. Society of Gynecologic Oncology; American College of Obstetricians and Gynecologists and the Society for Maternal–Fetal Medicine; Cahill AG, Beigi R, Heine RP, Silver RM, Wax JR. Placenta accreta spectrum. Am J Obstet Gynecol. 2018;219:B2-16.
29. Jauniaux E, Alfirevic Z, Bhide AG, Belfort MA, Burton GJ, Collins SL, et al.; Royal College of Obstetricians and Gynaecologists. Placenta praevia and placenta accreta: diagnosis and management: green-top guideline no. 27a. BJOG. 2019;126:e1-e48.
30. Ohayon A, Castel E, Friedrich L, Mor N, Levin G, Meyer R, et al. Pregnancy outcomes after uterine preservation surgery for placenta accreta spectrum: a retrospective cohort study. Am J Perinatol. 2025;42:68-74.
31. Baldwin HJ, Nippita TA, Torvaldsen S, Ibiebele I, Ford JB, Patterson JA. Outcomes of subsequent births after placenta accreta spectrum. Obstet Gynecol. 2020;136:745-55.
32. Kuppermann M, Learman LA, Schembri M, Gregorich SE, Jackson RA, Jacoby A, et al. Contributions of hysterectomy and uterus-preserving surgery to health-related quality of life. Obstet Gynecol. 2013;122:15-25.
33. Morgan JC, Hripko EN, Einerson BD, Premkumar A. Intended conservative management versus caesarean hysterectomy for known or suspected placenta accreta spectrum: a cost-effectiveness analysis. BJOG. 2025;132:1096-103.

Clinical Investigation / Araştırma

DOI: 10.4274/tjod.galenos.2025.93384

Turk J Obstet Gynecol 2026;23(1):34-39

Preinvasive lesion creation prevalence of other HPV types other than HPV type 16-18

HPV tip 16-18 dışındaki diğer HPV tiplerinin preinvaziv lezyon oluşturma prevalansı

Tuğçe Baykara[1], İbrahim Serdar Serin[2], Mehmet Dolanbay[1], Bülent Özçelik[1], Enes Karaman[3]

[1]*Acıbadem Kayseri Hospital, Clinic of Obsterics and Gynecology, Kayseri, Türkiye*

[2]*Memorial Kayseri Hospital, Clinic of Obsterics and Gynecology, Kayseri, Türkiye*

[3]*Niğde Ömer Halisdemir University Faculty of Medicine, Department of Obstetrics and Gynecology, Niğde, Türkiye*

Abstract

Objective: This study aims to investigate the prevalence of preinvasive lesions in cytology cases of high-risk human papillomavirus (HR-HPV) types other than types 16-18.

Materials and Methods: A retrospective file scan of 342 patients with normal cytology was performed between January 2016 and April 2019 in our hospital's obstetrics and gynecology outpatient clinic. In the first group, with the exception of HR-HPV type positivity, normal cytology and preinvasive lesions were present as a result of biopsy. In the second group, women were HPV type 16-18 positive, had normal cervical cytology, and were found to have preinvasive lesions as a result of biopsy. At the end of the study, we calculated the percentages of HPV types seen in preinvasive lesions.

Results: Three hundred and forty-two patients with normal cytology were included in our study. The average age of women was 41.09±10.61. In 58 (16.9%) patients with 342 HR-HPV type positivity, preinvasive lesions were detected as a result of biopsy. High-grade squamous intraepithelial lesion-low-grade squamous intraepithelial lesion was reported in 54 (15.7%) cases, squamous cell carcinoma in 3 (0.92%) cases, and mixed surface epithelial carcinoma (endometrioid adenocarcinoma 95%, clear cell carcinoma 5%) in 1 (0.3%) case. The age variable was not significant in biopsy subgroups ($p>0.05$).

Conclusion: Among the biopsy results with preinvasive lesions, approximately half were positive for HPV type 16 or 18, and these cases were identified accordingly. Colposcopy and biopsy should be recommended in suspicious lesions, even if cytology is normal, since other HR-HPV types may also have certain rates of preinvasive and invasive lesions.

Keywords: Cervical cancer, human papilloma virus, colposcopy

Öz

Amaç: Bu çalışmanın amacı, 16-18 tipleri dışındaki diğer yüksek riskli insan papilloma virüsü (HR-HPV) tiplerinin pozitif olduğu sitoloji olgularında preinvaziv lezyonların prevalansını araştırmaktır.

Gereç ve Yöntemler: Ocak 2016-Nisan 2019 tarihleri arasında hastanemiz kadın hastalıkları ve doğum polikliniğinde normal sitolojiye sahip 342 hastanın dosyaları geriye dönük olarak incelendi. Birinci grupta; 16-18 dışındaki HR-HPV tipleri pozitif, sitolojisi normal, biyopsi sonucu preinvaziv lezyon saptanan hastalar yer aldı. İkinci grupta ise; HPV tip 16-18 pozitif, servikal sitolojisi normal, biyopsi sonucu preinvaziv lezyon saptanan hastalar yer aldı. Çalışma sonunda preinvaziv lezyonlarda görülen HPV tiplerinin yüzdeleri hesaplandı.

Bulgular: Normal sitolojiye sahip 342 hasta çalışmaya dahil edildi. Kadınların ortalama yaşı 41,09±10,61 idi. HR-HPV pozitifliği olan 342 hastadan 58'inde (%16,9) biyopsi sonucunda preinvaziv lezyon saptandı. Olguların 54'ünde (%15,7) yüksek dereceli skuamöz intraepitelyal lezyon-düşük

PRECIS: This study highlights that high-risk HPV types other than 16 and 18 may also play a significant role in the development of preinvasive cervical lesions, emphasizing that focusing solely on these two types may be insufficient for early detection.

Corresponding Author/Sorumlu Yazar: Asst. Prof. Enes Karaman,
Niğde Ömer Halisdemir University Faculty of Medicine, Department of Obstetrics and Gynecology, Niğde, Türkiye
E-mail: dr.eneskaraman@gmail.com **ORCID ID:** orcid.org/0000-0003-1459-0606

Received/Geliş Tarihi: 04.10.2025 **Accepted/Kabul Tarihi:** 01.11.2025 **Epub:** 22.01.2026 **Publication Date/Yayınlanma Tarihi:** 05.03.2026

Cite this article as: Baykara T, Serin İS, Dolanbay M, Özçelik B, Karaman E. Preinvasive lesion creation prevalence of other HPV types other than HPV type 16-18. Turk J Obstet Gynecol. 2026;23(1):34-39

dereceli skuamöz intraepitelyal lezyon, 3'ünde (%0,92) skuamöz hücreli karsinom, 1'inde (%0,3) ise miks yüzey epitelial karsinom (endometrioid adenokarsinom %95, berrak hücreli karsinom %5) rapor edildi. Yaş değişkeni biyopsi alt grupları arasında anlamlı bulunmadı (p>0,05).

Sonuç: Biyopsi sonucunda preinvaziv lezyon saptanan olguların oranı HPV tip 16-18 pozitif olanlarda daha yüksek bulunmuş olup, preinvaziv lezyon saptananların yaklaşık yarısında bu tipler belirlenmiştir. Sitoloji normal olsa bile, diğer HR-HPV tiplerinin de belirli oranlarda preinvaziv ve invaziv lezyonlara yol açabildiği göz önüne alınarak, şüpheli olgularda kolposkopi ve biyopsi önerilmelidir.

Anahtar Kelimeler: servikal kanser, insan papilloma virüsü, kolposkopi

Introduction

Zur Hausen, who found a 99.9% relationship between human papillomavirus (HPV) and cervical cancer, received the 2008 Nobel Prize in Physiology or Medicine. HPV can cause genital and laryngeal warts as well as preinvasive and invasive lesions[1]. In the 2014 guideline by the American Society for Colposcopy and Cervical Pathology, if the smear is normal and women test positive for HPV type 16 and/or 18, they undergo colposcopy. If the smear is normal and women aged 30 years or older, are positive for other HPV types, different follow-up is recommended. Cotest (smear + HPV) is recommended after 1 year. Today, as a result of research, HPV types that are defined as high-risk (HR)-HPV have been identified due to their association with cancer. HPV types with high oncogenic risk; 16, 18, 31, 33, 35, 39, 45, 51, 52, 56, 58, 59, 68, 73 and 82. The HPV types most frequently detected in invasive cervical carcinoma in Türkiye are 16, 18, 45, 31, and 33.
In this study, we evaluated biopsies with preinvasive lesions and HPV types 16 and 18 positivity in the follow-up of patients who were found to be positive for HR-HPV types other than types 16 and 18 at the Gynecology and Obstetrics outpatient clinic of Kayseri Erciyes University Faculty of Medicine between 2016 and 2019. By comparing it, we aimed to discuss the necessity of colposcopy and biopsy.

Materials and Methods

Our study was planned as a retrospective cohort study in the Gynecology and Obstetrics Clinic of Erciyes University Hospital. After obtaining ethical approval from the Clinical Research Ethics Committee of Erciyes University Hospital (approval number: 2019/430; date: 12.06.2019), 342 patients who applied to the gynecology outpatient clinic between January 2016 and April 2019 were examined. Cervical cytology was reported as normal in all of these patients. The common feature of these 342 patients was positivity for HR-HPV types other than HPV types 16 and 18. The control group consisted of patients with normal cervical cytology and positive results for HPV types 16-18 who were included in the study. All patients with normal cytology who tested positive for high-risk HPV types other than 16-18 between January 2016 and April 2019 at the Erciyes University Gynecology and Obstetrics Clinic were included. Patients who had abnormal cervical cytology, were positive for HPV types 6 or 11, or were under follow-up for premalignant or malignant cervical diseases were excluded from the study.

Statistical Analysis

Patient data, pathological diagnoses, ages, and HPV types were recorded in a computer database and analyzed using the IBM Statistical Package for the Social Sciences, version 20 (SPSS Inc., Chicago, IL, USA). Mean ± standard deviation values were reported for continuous variables and frequency (n) and percentage (%) for categorical variables. The normality of data distribution was assessed using histograms, Q-Q plots, and the Shapiro-Wilk test. Variance homogeneity was evaluated with Levene's test. For comparisons between groups, the independent samples t-test was applied to quantitative variables, and one-way analysis of variance was used for comparisons among more than two groups. The Pearson χ^2 test was used for the comparison of categorical data. A p-value of <0.05 was considered statistically significant. The results of precancerous lesions were compared by calculating frequencies and percentages (n, %).

Results

An abnormal cervical pathology was detected by biopsy in 58 (16.9%) of 342 patients who were HR-HPV-positive and had normal cytology. The ages of the patients included in the study ranged from 18 to 67 years, with a mean of 41.09±10.61 years. Among these 342 HR-HPV-positive patients, 54 (15.7%) had preinvasive lesions [high-grade squamous intraepithelial lesion (HGSIL) or low-grade squamous intraepithelial lesion (LGSIL)] according to biopsy results, 3 (0.92%) had squamous cell carcinoma (SCC), and 1 (0.3%) had mixed

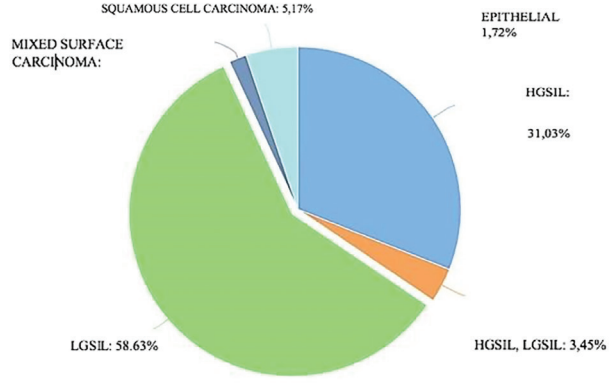

Figure 1. Distribution of abnormal bioscopy results in HR-HPV type positivities

HR-HPV: High-risk human papillomavirus, LGSIL: Low-grade squamous intraepithelial lesion, HGSIL: High-grade squamous intraepithelial lesion

surface epithelial carcinoma (endometrioid adenocarcinoma 95%, clear cell carcinoma 5%) (Figure 1).

The mean age of patients with HGSIL as a result of biopsy was 40.9±6.9, the mean age of patients with LGSIL was 34±1.4, the mean age of patients with mixed surface epithelial carcinoma was 63±2.3, and the mean age of patients with SCC was 52.6±5.7 (Figure 2).

The most common HPV type in patients with HGSIL was type 31 (27.7%) (Figure 3). The rates of other types were as follows: HPV 39 (11.1%); HPV 45, 51, 52, 56, 58, 59, and 66 (5.5%). Multiple HPV infections were detected as HPV 31+39 (5.5%), HPV 35+66 (5.5%), HPV 39+51 (5.5%), and HPV 51+58 (5.5%). In patients with LGSIL, the most common HPV types were HPV 58 (14.7%) and HPV 68 (14.7%), followed by HPV 31, 51, and 52 (8.8%), HPV 33, 45, 56, and 59 (5.8%), and HPV 35, 39, and 66 (2.9%). Among patients with SCC, HPV 31 (33.3% each), HPV 56 (33.3% each), and HPV 45 or 49 (33.3% each) were identified. In two cases positive for both HGSIL and LGSIL, HPV 31 (50%) and HPV 35 (50%) were detected. When all biopsy results were evaluated according to HPV type distribution, the most common types were HPV 31 (18%), HPV 58 (11%), HPV 68 (5.9%), HPV 51, 52, and 56 (4.7%), HPV 39, 45, and 59 (3.5%), HPV 33 and 66 (2.4%), HPV 35 (1.2%), and positivity for multiple other HPV types (9.16%).

HPV types 31 (17%), 56 (17%), 58 (17%), and 59 (17%) were the most common in the 18-30 age group. In the 30-45 age group, the most frequent types were HPV 31 (21%), HPV 68 (12%), HPV 45, 51, 52, and 58 (9%), HPV 39 and 56 (6%), and HPV 33, 35, 59, and 66 (3%). Among patients older than 45 years, HPV 31 (17%) and HPV 58 (11%) were the most common, followed by HPV 33, 35, 39, 51, 52, 56, 59, 66, and 68 (6%). Multiple HPV type infections were observed in 33% of patients aged 18-30, 9% of those aged 30-45, and 22% of those over 45 years (Figure 4).

The average age of patients with HPV type 16-18 positivity was found to be 41.49±9.26. The average age of HR-HPV type positivity was 41.09±10.61 (Table 1). The age variable was not statistically significant in HPV subgroups (p>0.05). HPV type is 16-18 positive, the average age of patients with HGSIL after biopsy is 42±7.85, the average age of patients with LGSIL is 41.53±8.9, the average age of patients with SCC is 46.12±7.12, the age of patients with adenocarcinoma the mean was found to be 46±12.04 (Table 2). Age variable was not significant in biopsy subgroups (p>0.05).

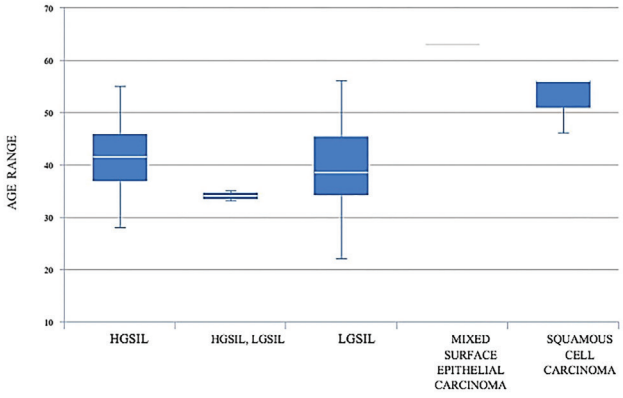

Figure 2. Numerical distribution of HR-HPV type positions abnormal biopsy results according to age range

HR-HPV: High-risk human papillomavirus, LGSIL: Low-grade squamous intraepithelial lesion, HGSIL: High-grade squamous intraepithelial lesion

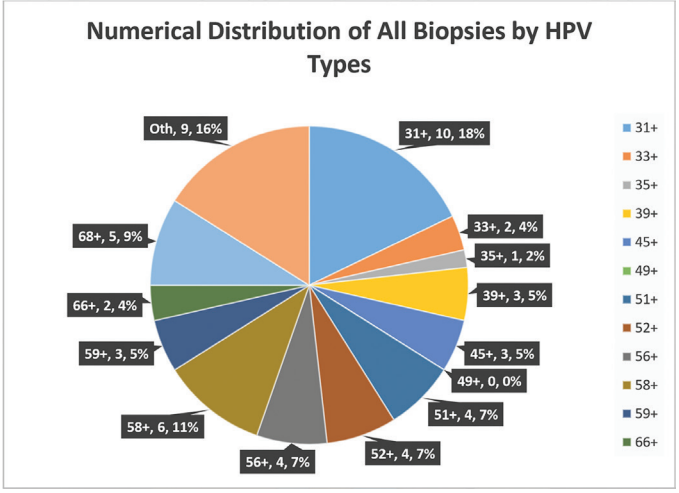

Figure 3. The ratio of all other high risk human papillomavirus types in preinvasive lesions

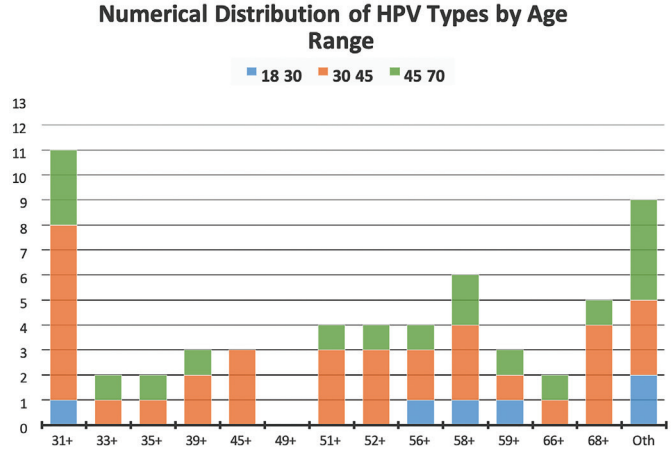

Figure 4. Numerical distribution of other high risk human papillomavirus types by age range

Table 1. Average age of HPV type 16-18 and HR-HPV types

HPV type	n	Mean
HPV type 16-18	209	41.49±9.26
Other HPV types	342	41.09±10.61

Data are expressed as ± standard deviation. P-value was calculated using two independent-samples t-test, HPV: Human papillomavirus

When the biopsies of 209 patients who were HPV type 16-18 positive were examined, 4 cases (1.91%) were diagnosed with adenocarcinoma, 40 cases (19.14%) with HGSIL, 30 cases (9.57%) with LGSIL, and 5 cases (2.39%) with SCC (Table 3).

A statistically significant difference was found between the HPV type variable and the biopsy variable (p>0.05). It was observed that the numbers of adenocarcinoma, HGSIL, and SCC were higher in the HPV type 16-18 group than in other HPV types. It was observed that the number of LGSIL in the HPV type 16/18 group was lower than the other HPV types.

Discussion

Screening programs for cervical cancer are becoming increasingly common, as the slow natural progression of the disease allows for early recognition of dysplastic lesions and prevention of their progression to invasive cancer[2]. Cervical cancer typically begins with mild dysplasia and progresses toward invasive carcinoma. Cervical dysplasia generally occurs in women in their 20s, carcinoma *in situ* in their 30s, and invasive disease after the age of 40[3]. With the introduction of liquid-based cytology, the accuracy of screening tests has improved, leading to better detection and treatment outcomes. However, despite the increased sensitivity and specificity of these tests, no single screening method has yet proven to be completely reliable. In one study, the sensitivity of the Pap test alone for detecting CIN 2-3 or cancer was reported to be between 33% and 94%, with a specificity of 87-98%. When HPV DNA testing was added, sensitivity increased to 87-100%, while specificity ranged from 69% to 95%[4]. In a meta-analysis published by Arbyn et al.[5], it was demonstrated that adding cytology to HPV DNA testing provides no additional diagnostic benefit. Accordingly, cytological examination does not hold significant value when colposcopy is performed in all HR patients identified by HPV genotyping. However, this approach leads to an increased number of colposcopies, biopsies, and pathological evaluations, which in turn raises the cost per patient for cervical cancer screening.

Table 2. Age average of patients according to HPV type 16-18 positive, smear negative preinvasive lesion types

Biopsy (n)	HGSIL 60	LGSIL 54	SCC 8	Adenocarcinoma 5
Age	42±7.85	41.53±8.9	46.12±7.12	46±12.04

Data are expressed as ± standard deviation. P-value was calculated using one-way analysis of variance, HPV: Human papillomavirus, LGSIL: Low-grade squamous intraepithelial lesion, HGSIL: High-grade squamous intraepithelial lesion, SCC: Squamous cell carcinoma

Table 3. Distribution of preinvasive lesions in HPV type 16-18 types

Preinvasive lesion	Number	Percentage
Adenocarcinoma	4	%1.914
HGSIL	40	%19.14
LGSIL	20	%9.569
SCC	5	%2.392

Data are expressed as% n.Pearson χ^2 analysis was used for HPV and biopsy variable, HPV: Human papillomavirus, LGSIL: Low-grade squamous intraepithelial lesion, HGSIL: High-grade squamous intraepithelial lesion

According to the ATHENA study conducted by Wright et al.[6], which included 42,209 participants over a three-year period in the United States, HPV DNA testing showed higher sensitivity than cytology or hybrid screening strategies for detecting CIN3+ lesions, particularly in women aged 25 years or older (28.3%) compared to those aged 30 years or older (24.3%). Studies have also shown that the risk of invasive cancer among HR-HPV carriers is significantly higher than in non-carriers. Similar results were observed in long-term follow-up studies of women enrolled in Kaiser Permanente cohorts in Portland, Oregon, and Northern California[7,8]. After five years of surveillance, the cumulative probability of CIN3 positivity was 0.17% [95% confidence interval (CI): 0.11-0.28] in HPV-negative women and 0.16% (95% CI: 0.06-0.39) in those negative for both cytology and HPV. Based on these findings and cost-effectiveness modeling analyses, both Australia and the Netherlands have adopted HPV testing as the primary screening method in their national cervical cancer prevention programs[9,10].

In the POBASCAM study conducted by Rijkaart et al.[11] in the Netherlands between January 1999 and September 2002, 22,420 women underwent cervical cancer screening. Among 19,999 women screened within the study group, 724 were classified as cytology-negative but HPV DNA-positive. Among these women, 31 (4.28%) had CIN2 and 29 (4.0%) had CIN3 lesions. In our study, colposcopic evaluation and biopsy of 342 patients with normal cytology revealed preinvasive lesions (HGSIL or LGSIL) in 54 (16.6%) cases, SCC in 3 (0.92%) cases, and mixed surface epithelial carcinoma (endometrioid adenocarcinoma 95%, clear cell carcinoma 5%) in 1 (0.3%) case. The rates of LSIL and HSIL in our study were higher than those reported in the POBASCAM trial.

In a study of 7,747 patients with cervical intraepithelial neoplasia in China, Wenbo Long et al.[12], reported that HPV type 16 was the most common carcinogenic subtype, followed by HPV 58 (15.2%) and HPV 33 (5.09%). In our study, HPV 58 was observed in 11% and HPV 33 in 4% of preinvasive lesions. Similarly, in a study by Chiang et al.[13] conducted in Taiwan involving 1,086 patients positive for HPV genotypes, HPV types 16 and 18 were detected in 21.3% of CIN2-3 cases among women over 50 years of age, while HPV 52, 58, and 33 were positive in 55.5% of cases.

In another study by Boumba et al.[14], HPV 16 (47.1%), HPV 33 (22.6%), HPV 18 (15%), HPV 31 (11.3%), and HPV 69 (3.7%) were the most common types detected. In invasive cervical cancer, HPV 33 (28.8%), HPV 18 (11.8%), HPV 31

(5%), and HPV 35 (1.7%) were reported. Overall, HPV 33 and HPV 31 were found to be the most common types in HGSIL and invasive cervical cancer, excluding HPV 16 and 18.

A 13-year study conducted by Andrea Piana et al.[15] in Italy reported HPV 16 (49%) as the most common type in patients diagnosed with invasive neoplasia, followed by HPV 51 (19.4%) and other HR types (excluding HPV 16 and 18) collectively with rates exceeding 20%. Matsumoto et al.[16] demonstrated that progression from LSIL to HSIL in women infected with HPV types 16, 18, 31, 33, 35, 52, and 58 occurred 3.5 times faster than in those with other HR types.

When considered in this context, cytological examination alone does not provide additional benefit if colposcopy is performed in all HR patients identified by HPV genotyping. However, this approach increases the number of colposcopies, biopsies, and histopathological examinations, consequently raising screening costs. To prevent missed preinvasive lesions and achieve early diagnosis, patient compliance with screening, diagnosis, and treatment should be improved. Therefore, colposcopy should be recommended for all patients positive for HR-HPV, despite the increased cost. Detection of low- and high-oncogenic-risk HPV DNA in cervical biopsy specimens is crucial for screening, early diagnosis, treatment planning, and follow-up in cervical cancer prevention. Based on the results of this study conducted at the Department of Obstetrics and Gynecology, Erciyes University Hospital, between January 2016 and April 2019, we believe that colposcopic biopsy in patients with HR-HPV positivity can significantly reduce the frequency of missed cervical lesions.

Despite ongoing research aimed at identifying the optimal global screening method, existing evidence indicates that HPV DNA testing is more effective than Pap smears, and the likelihood of missing preinvasive lesions decreases when a combined testing strategy is used. This study analyzed biopsy outcomes of patients with HR-HPV types excluding HPV 16 and 18, who were treated at the Obstetrics and Gynecology Outpatient Clinic of Kayseri Erciyes University Faculty of Medicine Hospital between January 2016 and April 2019. Similarly, Güzin et al.[17] reported that routine colposcopy in women with HR-HPV types other than 16 and 18 significantly increased the detection rates of CIN2+ lesions, even among those with normal cytology, emphasizing the importance of colposcopic evaluation in such cases.

Conclusion

Our objective was to demonstrate that various HR-HPV types may also necessitate colposcopic biopsy for the early detection of cervical cancer. Consequently, our research has shown that colposcopic evaluation and biopsy may be essential in cases where other HR-HPV types yield positive results despite normal cytology findings. It should be considered that in situations where other HR-HPV types are positive and cytology is normal but colposcopy is not performed according to established guidelines, cervical preinvasive lesions or even neoplasms may still be present.

Ethics

Ethics Committee Approval: Obtained ethical approval from the Clinical Research Ethics Committee of Erciyes University Hospital (approval number: 2019/430; date: 12.06.2019).

Informed Consent: Retrospective study.

Acknowledgment: This study is part of the MD thesis of Tugce Baykara.

Footnotes

Authorship Contributions

Surgical and Medical Practices: T.B., M.D., B.Ö., E.K., Concept: T.B., İ.S.S., B.Ö., E.K., Design: T.B., İ.S.S., B.Ö., E.K., Data Collection or Processing: T.B., M.D., B.Ö., E.K., Analysis or Interpretation: T.B., M.D., E.K., Literature Search: T.B., M.D., E.K., Writing: T.B., İ.S.S., E.K.

Conflict of Interest: No conflict of interest was declared by the authors.

Financial Disclosure: The authors declared that this study received no financial support.

References

1. Türkiye Klinikleri. HPV virolojisi, epidemiyolojisi ve genital kanser ilişkisi. Türkiye Klinikleri J Gynecol Obst. 2009;2:1-8.
2. Usubütün A, Alemany L, Küçükali T, Ayhan A, Yüce K, de Sanjosé S, et al. Human papillomavirus types in invasive cervical cancer specimens from Turkey. Int J Gynecol Pathol. 2009;28:541-8.
3. Hatch KD. Handbook of colposcopy: diagnosis and treatment of lower genital tract neoplasia and HPV infections. Boston: Little, Brown Medical Division; 1989.
4. Wright TC Jr, Schiffman M, Solomon D, Cox JT, Garcia F, Goldie S, et al. Interim guidance for the use of human papillomavirus DNA testing as an adjunct to cervical cytology for screening. Obstet Gynecol. 2004;103:304-9.
5. Arbyn M, Bergeron C, Klinkhamer P, Martin-Hirsch P, Siebers AG, Bulten J. Liquid compared with conventional cervical cytology: a systematic review and meta-analysis. Obstet Gynecol. 2008;111:167-77.
6. Wright TC, Stoler MH, Behrens CM, Sharma A, Zhang G, Wright TL. Primary cervical cancer screening with human papillomavirus: end-of-study results from the ATHENA study using HPV as the first-line screening test. Gynecol Oncol. 2015;136:189-97.
7. Schiffman M, Glass AG, Wentzensen N, Rush BB, Castle PE, Scott DR, et al. A long-term prospective study of type-specific human papillomavirus infection and risk of cervical neoplasia among 20,000 women in the Portland Kaiser Cohort Study. Cancer Epidemiol Biomarkers Prev. 2011;20:1398-409.
8. Katki HA, Kinney WK, Fetterman B, Lorey T, Poitras NE, Cheung L, et al. Cervical cancer risk for women undergoing concurrent testing for human papillomavirus and cervical cytology: a population-based study in routine clinical practice. Lancet Oncol. 2011;12:663-72.

9. National Cervical Screening Program. Renewal of the National Cervical Screening Program. Aust Fam Physician. 2014;43:293-6.
10. Cervical cancer screening in the Netherlands [Internet]. 2014 [cited 2014 Oct 14]. Available from: https://www.rivm.nl/en
11. Rijkaart DC, Berkhof J, Rozendaal L, van Kemenade FJ, Bulkmans NW, Heideman DA, et al. Human papillomavirus testing for the detection of high-grade cervical intraepithelial neoplasia and cancer: final results of the POBASCAM randomised controlled trial. Lancet Oncol. 2012;13:78-88.
12. Long W, Yang Z, Li X, Chen M, Liu J, Zhang Y, et al. HPV-16, HPV-58, and HPV-33 are the most carcinogenic HPV genotypes in Southwestern China and their viral loads are associated with severity of premalignant lesions in the cervix. Virol J. 2018;15:94.
13. Chiang YC, Cheng WF, Chen YL, Chang MC, Hsieh CY, Lin MC, et al. High-risk human papillomavirus, other than type 16/18, in predominantly older Taiwanese women with high-grade cervical preinvasive lesions. Taiwan J Obstet Gynecol. 2013;52:222-6.
14. Boumba LM, Hilali L, Mouallif M, Moukassa D, Ennaji MM. Specific genotypes of human papillomavirus in 125 high-grade squamous lesions and invasive cervical cancer cases from Congolese women. BMC Public Health. 2014;14:1320.
15. Piana A, Sotgiu G, Cocuzza C, Musumeci R, Marras V, Pischedda S, et al. High HPV-51 prevalence in invasive cervical cancers: results of a pre-immunization survey in North Sardinia, Italy. PLoS One. 2013;8:e63395.
16. Matsumoto K, Oki A, Furuta R, Maeda H, Yasugi T, Takatsuka N, et al.; Japan HPV and Cervical Cancer Study Group. Predicting the progression of cervical precursor lesions by human papillomavirus genotyping: a prospective cohort study. Int J Cancer. 2011;128:2898-910.
17. Güzin K, Duru N, Özyürek S, Aksoy H, Aksoy Ü, Yüce K. Colposcopy to all: does this approach increase detection rate of preneoplastic cervical lesions in cases with high-risk HPV. J Gynecol Reprod Health. 2024;2:1-4.

Clinical Investigation / Araştırma

DOI: 10.4274/tjod.galenos.2026.32784

Turk J Obstet Gynecol 2026;23(1):40-46

Role of postoperative renal ultrasound in identifying ureteral injury despite normal intraoperative jet flow

Normal intraoperatif jet akımına rağmen üreter yaralanmasının saptanmasında postoperatif renal ultrasonun rolü

Sercan Kantarcı[1], Alaattin Karabulut[1], Uğurcan Dağlı[1], Pınar Tuğçe Özer[2], Fatih Yıldırım[1], Alper İleri[1], Adnan Budak[1], Abdurrahman Hamdi İnan[1]

[1]University of Health Sciences Türkiye, İzmir Tepecik Education and Research Hospital, Department of Obstetrics and Gynaecology, İzmir, Türkiye
[2]İzmir University of Economics, Department of Obstetrics and Gynecology, İzmir, Türkiye

Abstract

Objective: This study evaluated the diagnostic utility of early postoperative renal ultrasound in detecting ureteral injury in patients who had undergone total laparoscopic hysterectomy (TLH) for benign indications, despite documented normal intraoperative ureteral jet flow on cystoscopy.

Materials and Methods: In this retrospective cohort study at a high-volume tertiary center, data from 3,170 patients who underwent TLH between January 2022 and October 2025 were analyzed. Inclusion required normal bilateral ureteral jet flow on routine intraoperative cystoscopy, a renal ultrasound within the first 24 postoperative hours, and at least 30 days of clinical follow-up. The primary outcome was the diagnostic yield of postoperative ultrasound for identifying ureteral injuries not apparent during surgery. Injuries were confirmed by advanced imaging or surgical exploration.

Results: The overall ureteral injury rate was 0.79% (n=25). Of these injuries, eight were diagnosed intraoperatively, while seventeen occurred despite documented normal bilateral ureteral jet flow during the procedure. Among the latter group, renal ultrasonography performed on postoperative day 1 detected 14 injuries, representing 56% of all injuries. Three injuries (12%) presented later, around postoperative day 10, and were not identified on initial imaging. Early postoperative ultrasonography demonstrated good sensitivity and a high negative predictive value as a screening tool. Comparison with preoperative baseline imaging enhanced diagnostic performance in identifying new-onset obstruction, particularly newly developed pelviectasis.

Conclusion: Normal intraoperative ureteral jet flow does not preclude ureteral injury, particularly those with delayed presentation, such as thermal damage. Early postoperative renal ultrasonography is a valuable non-invasive screening tool that identifies a significant proportion of injuries missed by cystoscopy alone. Comparative evaluation of routine postoperative ultrasonography with preoperative imaging may provide a meaningful contribution to the early diagnosis of ureteral injury following TLH.

Keywords: Ureteral injury, renal ultrasound, laparoscopic hysterectomy

Öz

Amaç: Bu çalışma, benign endikasyonlarla total laparoskopik histerektomi (TLH) uygulanan ve intraoperatif sistoskopide normal üreteral jet akımı izlenen hastalarda, erken postoperatif dönemde yapılan renal ultrasonografinin üreter yaralanmasını saptamadaki tanısal değerini değerlendirmeyi amaçlamıştır.

Gereç ve Yöntemler: Yüksek hacimli üçüncü basamak bir merkezde yürütülen bu retrospektif kohort çalışmasında, Ocak 2022-Ekim 2025 tarihleri arasında TLH uygulanan 3.170 hastanın verileri incelendi. Çalışmaya dahil edilme kriterleri; intraoperatif sistoskopide bilateral normal üreteral

PRECIS: In patients with normal intraoperative ureteral jet flow after total laparoscopic hysterectomy, early postoperative renal ultrasonography may contribute to the detection of some ureteral injuries and can be considered an adjunctive screening tool.

Corresponding Author/Sorumlu Yazar: Sercan Kantarcı MD,
University of Health Sciences Türkiye, İzmir Tepecik Education and Research Hospital, Department of Obstetrics and Gynaecology, İzmir, Türkiye
E-mail: sercan.kntrc@gmail.com **ORCID ID:** orcid.org/0000-0001-5608-060X

Received/Geliş Tarihi: 05.12.2025 **Accepted/Kabul Tarihi:** 05.02.2026 **Epub:** 17.02.2026 **Publication Date/Yayınlanma Tarihi:** 05.03.2026

Cite this article as: Kantarcı S, Karabulut A, Dağlı U, Özer PT, Yıldırım F, İleri A, et al. Role of postoperative renal ultrasound in identifying ureteral injury despite normal intraoperative jet flow. Turk J Obstet Gynecol. 2026;23(1):40-46

jet akımının doğrulanması, ilk 24 saat içinde renal ultrasonografi yapılması ve en az 30 günlük klinik takip bulunmasıydı. Birincil sonuç ölçütü, intraoperatif dönemde fark edilmeyen üreter yaralanmalarının postoperatif ultrason ile tanımlanma oranıydı. Yaralanmalar ileri görüntüleme yöntemleri veya cerrahi eksplorasyon ile doğrulandı.

Bulgular: Genel üreter yaralanması insidansı %0,79 (n=25) olup tüm yaralanmalar normal intraoperatif jet akımına rağmen meydana geldi. Postoperatif 1. gün renal ultrasonografi, yaralanmaların %56'sını (n=14) saptadı. Üç yaralanma (%12) postoperatif 10. gün civarında semptomatik hale geldi ve ilk görüntülemede görülmedi. Ultrason performans analizi, erken tarama için yüksek duyarlılık ve negatif prediktif değer gösterdi. Tanısal doğruluk, ultrason bulgularının preoperatif görüntüleme ile karşılaştırılarak yeni başlangıçlı obstrüktif hidronefroz şeklinde yorumlandığı durumlarda en yüksek seviyeye ulaştı; bu yaklaşım mükemmel özgüllük ve pozitif prediktif değer sağladı.

Sonuç: Normal intraoperatif üreteral jet akımı, özellikle gecikmiş termal hasar gibi durumlarda üreter yaralanmasını dışlamamaktadır. Erken postoperatif renal ultrasonografi, sistoskopinin saptayamadığı yaralanmaların önemli bir bölümünü ortaya koyan değerli ve non-invaziv bir tarama aracıdır. Rutin postoperatif ultrasonografinin, preoperatif görüntüleme ile karşılaştırmalı olarak değerlendirilmesi, TLH sonrası üreter hasarının erken tanısına anlamlı katkı sağlayabilir.

Anahtar Kelimeler: Üreter yaralanması, renal ultrason, laparoskopik histerektomi

Introduction

Ureteral injury remains one of the most significant yet relatively uncommon complications of gynecologic surgery. Despite advances in minimally invasive techniques, large contemporary studies report postoperative ureteral injury rates of approximately 0.4-0.8% for benign hysterectomy[1]. The anatomical complexity of the pelvic course of the ureter, the distortion of pelvic structures due to conditions like endometriosis or benign pelvic pathologies, and the widespread use of energy-based surgical instruments are the main factors that increase the risk of ureteral injury during hysterectomy[2]. Iatrogenic ureteral injury can occur in many different settings. Colorectal and abdominal vascular surgeries are known to place the ureters at risk of injury. Most iatrogenic ureteral injuries (52-82%) occur during gynecological procedures[3]. These observations emphasise the need for reliable strategies for early detection in routine surgical practice.

Multiple mechanisms contribute to ureteral injury during laparoscopic hysterectomy. In addition to direct trauma such as suturing, clamping, or devascularization, delayed thermal injury caused by lateral heat spread from energy devices poses a substantial risk. The extent of thermal spread varies with device type, energy settings, applied tissue tension, and duration of activation, and may lead to delayed obstruction, ischemia, or fistula formation, even when intraoperative findings appear normal[4,5]. Because thermal injuries may be clinically silent at the time of surgery, intraoperative detection remains challenging.

Intraoperative cystoscopy has been widely advocated as a means to identify occult injuries by assessing bilateral ureteral jet flow. While the visualization of normal jet flow is reassuring, evidence shows that it does not completely exclude the possibility of ureteral injury, particularly those caused by delayed thermal or ischemic mechanisms[6]. Although proponents of universal cystoscopy highlight its low risk, low cost, and increased detection rates, others favor selective use based on the low overall prevalence of injury and additional operative time required, leaving the debate unresolved[7].

Furthermore, meticulous evaluation of preoperative findings, such as renal pelvic ectasia, minimal hydronephrosis, or borderline pelvicalyceal dilation, is crucial. Accurate documentation of these baseline conditions allows clinicians to differentiate preexisting abnormalities from newly developed postoperative changes. This distinction prevents misinterpretation of mild preoperative dilation as postoperative ureteral injury, improves diagnostic accuracy, and provides medicolegal protection by demonstrating thorough perioperative assessment.

This study aims to evaluate the effectiveness of early postoperative renal ultrasonography in identifying ureteral injuries that occur despite normal intraoperative ureteral jet flow, and to determine whether routine early ultrasonographic screening can enhance early detection and improve clinical outcomes in this setting.

Materials and Methods

This retrospective cohort study, conducted at a high-volume tertiary referral center, evaluated data from 3,170 patients who underwent total laparoscopic hysterectomy (TLH) for benign gynecologic indications between January 2022 and October 2025. Institutional review board approval was obtained prior to study initiation (University of Health Sciences Türkiye, İzmir Tepecik Education and Research Hospital Non-Interventional Ethics Committee, decision no: 2025/10-13, date: 03.11.2025).

The primary analytic cohort was constructed by excluding the eight patients in whom ureteral injury was diagnosed intraoperatively from 25 patients with identified ureteral injuries, and by including only those in whom intraoperative cystoscopy demonstrated normal bilateral ureteral jet flow. Eligibility criteria required postoperative renal ultrasonography to be performed within the first 24 hours and at least 30 days of postoperative clinical follow-up. Preoperative urinary symptoms or ultrasonographic

abnormalities were not considered exclusion criteria, in order to better reflect real-world surgical practice.

All procedures were performed by an experienced minimally invasive gynecologic surgery team using a standardized TLH technique. Routine intraoperative cystoscopy was performed at the end of each operation, and bilateral ureteral jet flow was visually assessed and documented. Recognizing that normal jet flow does not exclude ureteral injury—particularly injuries related to thermal or ischemic mechanisms—all patients underwent postoperative gynecologic ultrasonographic evaluation, during which the renal pelvis and calyces were routinely examined; however, no separate or standardized renal ultrasonography protocol was applied. This targeted ultrasonographic assessment was used as an early screening tool to detect renal pelvic dilatation, new-onset pelvicalyceal enlargement (pelviectasis), or perirenal fluid collections. Patients with suspicious findings were referred for a urology consultation and further imaging, including contrast-enhanced computed tomography urography or retrograde pyelography. Ureteral injury was confirmed based on radiologic findings or direct intraoperative visualization.

Demographic characteristics (body mass index, parity, comorbidities) and perioperative variables (surgical indication, operative time, estimated blood loss, surgeon experience, and length of hospital stay) were recorded. Intraoperative cystoscopic observations, jet symmetry, and any deviations or complications were documented. Postoperative ultrasonographic assessments included hydronephrosis grade, pelvicalyceal system dilation, loss of jet flow, and perirenal fluid collections. For patients in whom ureteral injury was confirmed, the type of injury (suture or clip entrapment, kinking, laceration, thermal/ischemic damage) and the management approach [Double-J (DJ) stenting, ureterolysis, ureteroneocystostomy (UNC), reoperation, percutaneous nephrostomy, or conservative follow-up] were systematically recorded. A predefined subgroup analysis was performed in patients with normal bilateral intraoperative jet flow who were diagnosed with ureteral injury within 30 days postoperatively. Confirmation of injury required evidence of obstruction or contrast extravasation on computed tomography urography or retrograde pyelography; direct visualization of thermal or mechanical trauma during reoperation; or the need for therapeutic interventions such as DJ stenting or reconstructive ureteral surgery. Exclusion criteria included gynecologic malignancy; prior major urologic surgery (such as UNC, nephrectomy, renal transplantation, or extensive pelvic ureteral reconstruction); chronic kidney disease stage ≥3; concurrent intraoperative urologic or colorectal procedures; or incomplete cystoscopy, postoperative imaging, or follow-up records.

The primary outcome of the study was the diagnostic rate of postoperative renal ultrasonography in identifying ureteral injuries among patients with normal intraoperative jet flow. Secondary outcomes included the overall incidence of ureteral injury, timing of diagnosis, proportion of asymptomatic cases, frequency of delayed injury despite preserved jet flow, management strategies, early postoperative complications, and length of hospital stay.

Statistical Analysis

Statistical analyses were performed using IBM SPSS Statistics version 26 (IBM Corp., Armonk, NY, USA). Normally distributed continuous variables were expressed as mean ± standard deviation, while non-normally distributed variables were reported as median (minimum-maximum). Categorical variables were presented as numbers and percentages. Group comparisons were performed using the Student's t-test or the Mann-Whitney U test, as appropriate. For comparisons involving more than two groups, one-way ANOVA or Kruskal-Wallis tests were applied, followed by post-hoc procedures when significant differences were observed. Categorical variables were analyzed using the chi-square test or Fisher's exact test when indicated. A two-sided p-value of <0.05 was considered statistically significant.

Results

Among the 3,170 adult patients evaluated, approximately 5% (n=158) had incidental ultrasonographic findings documented on preoperative imaging that were unrelated to ureteral trauma and did not cause obstruction. On postoperative ultrasonographic assessments, these findings were interpreted not as newly developed pathology but as consistent with preoperative baseline imaging. The most common incidental findings included simple cortical renal cysts, mild non-obstructive pelviectasis, small asymptomatic renal calculi, and subtle increases in renal parenchymal echogenicity.

During the study period, a total of 3,170 TLH were performed, and 25 ureteral injuries were identified, corresponding to an overall incidence of 0.79%. Among these injuries, 8 were diagnosed intraoperatively, whereas the remaining 17 were identified postoperatively despite documented normal bilateral intraoperative ureteral jet flow. Of these injuries, 14 cases (56%) were diagnosed on postoperative day 1, 8 cases (32%) were detected intraoperatively, and 3 cases (12%) represented delayed presentations. Early postoperative ureteroscopy revealed suture-related obstruction, stricture, or kinking in 8 patients, all were successfully treated with DJ stenting followed by elective removal at 3 months; in 3 patients, complete ureteral defects requiring early UNC were observed; and in 3 patients, severe edema or complex injury was initially managed with percutaneous nephrostomy and subsequently treated with delayed UNC at 3 months. Intraoperative injuries included five primary ureteral repairs with DJ stenting, one UNC, and two cases with undocumented repair details. Three late-presenting injuries occurred despite

normal day 1 ultrasonography and manifested around postoperative day 10 with fever, flank pain, or vaginal urinary leakage. Imaging demonstrated subcapsular urine collections, and all injuries were ultimately attributed to thermal injury with delayed tissue necrosis. Treatment information for these delayed cases was not fully documented. Notably, postoperative day 1 renal ultrasonography enabled detection of 14 injuries that occurred despite preserved intraoperative jet flow, highlighting its value as a complementary early screening tool (Figure 1).

Postoperative day 1 renal ultrasonography demonstrated a high negative predictive value (NPV) for ruling out ureteral injury in patients with normal intraoperative ureteral jet flow. Among the 3,162 patients evaluated (after excluding 8 cases diagnosed intraoperatively), hydronephrosis detected on day-1 ultrasound correctly identified 14 ureteral injuries. In 158 cases, ultrasonographic findings represented incidental, non-obstructive findings unrelated to ureteral trauma, while 2,987 patients without hydronephrosis showed no evidence of injury during the follow-up period. Three injuries were not detected on day 1 imaging and subsequently presented as delayed thermal injuries approximately postoperative day 10. Based on these findings, day-1 renal ultrasound yielded a sensitivity of 82.4%, a specificity of 95.0%, a positive predictive value (PPV) of 8.1%, and a NPV of 99.9%, confirming its value as an early screening tool despite preserved intraoperative jet flow (Table 1).

When all hydronephrosis findings were considered (Scenario A), diagnostic performance mirrored these results; however, restricting the analysis to new-onset obstructive hydronephrosis confirmed by comparison with preoperative ultrasonography (Scenario B) markedly improved accuracy. All 14 ureteral injuries exhibited new-onset obstruction with no false-positive cases, resulting in 100% specificity and 100% PPV, while the NPV remained high at 99.9%. Collectively, these findings indicate that although any hydronephrosis on day 1 ultrasound provides excellent sensitivity and NPV, new-onset obstructive hydronephrosis offers the highest diagnostic accuracy and clearly distinguishes true ureteral injuries from incidental or preexisting renal findings (Table 2).

Discussion

Although rare, ureteral injuries remain a clinically significant concern following benign gynecologic hysterectomy because diagnostic delays can lead to serious complications such as

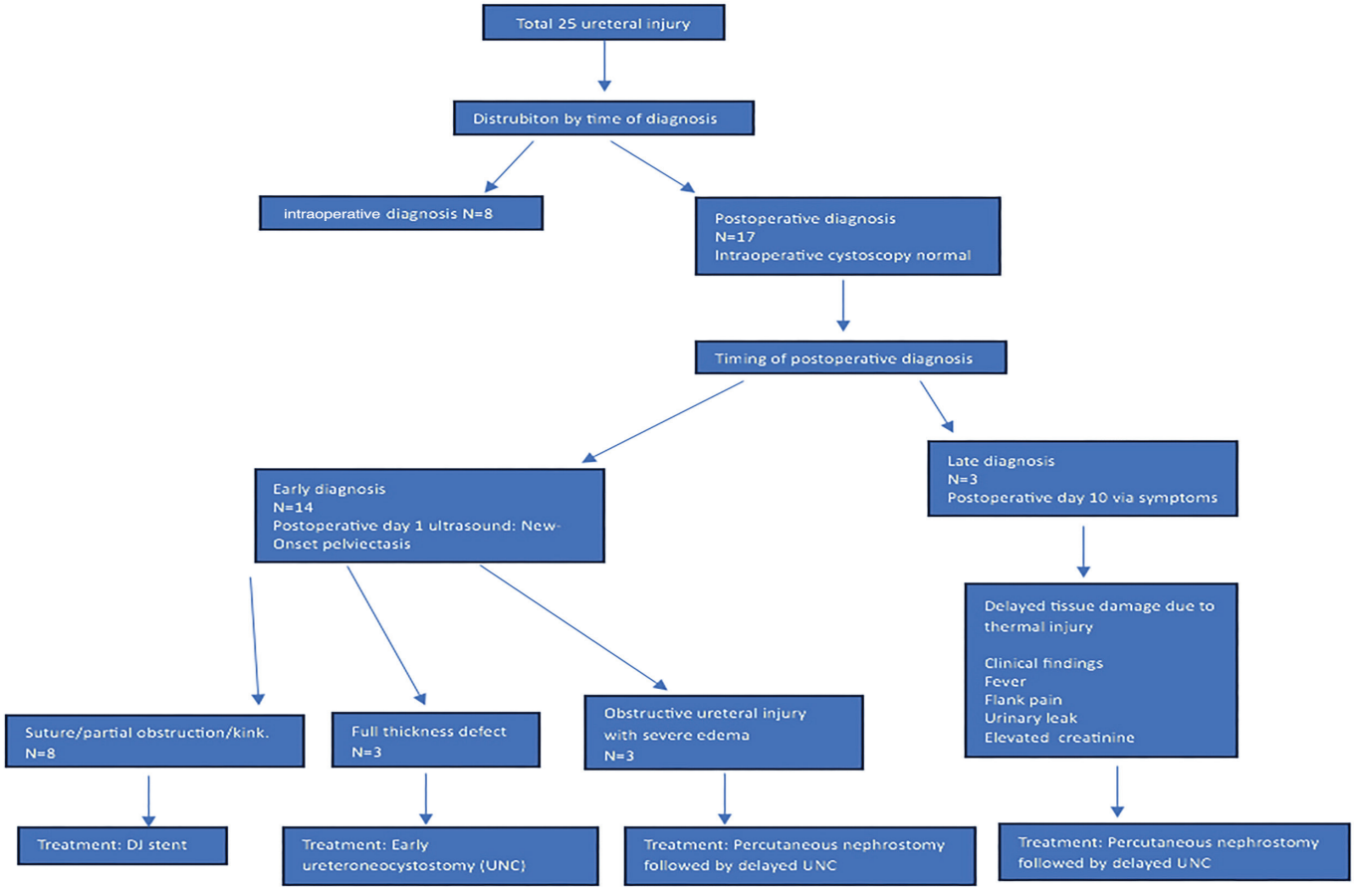

Figure 1. Management algorithm for iatrogenic ureteral injuries

Table 1. Day-1 renal ultrasound for early detection of ureteral injury

Day-1 renal ultrasound	Ureteral injury (+)	Ureteral injury (–)
Hydronephrosis (+)	14 (true positives)	158 (incidental findings)
Hydronephrosis (–)	3 (missed delayed thermal injuries)	2987 (true negatives)

Note: Eight patients diagnosed intraoperatively were excluded from the total cohort (n=3,170), as they did not require further postoperative screening for injury detection

Table 2. Renal ultrasound performance metrics in early ureteral injury detection

Day-1 renal ultrasound	Ureteral injury (+)	Ureteral injury (–)	Sensitivity	Specificity	PPV	NPV
A. All hydronephrosis findings (reflecting common clinical practice)	14	158	82.4%	95.0%	8.1%	99.9%
B. Only new-onset obstructive hydronephrosis (compared with preoperative USG)	14	0	82.4%	100%	100%	99.9%

PPV: Positive predictive value, NPV: Negative predictive value, USG: Ultrasonography

obstructive nephropathy, urinoma, infection, sepsis, and permanent loss of renal function[8,9]. Although intraoperative cystoscopy and jet flow evaluation are useful for detecting mechanical injuries, studies have shown that normal jet flow can be preserved in a significant proportion of delayed thermal or ischemic injuries, particularly those associated with energy devices[10]. Therefore, intraoperative evaluation alone cannot completely rule out an injury, and additional imaging strategies in the early postoperative period may provide diagnostic value. Our study aims to demonstrate the contribution of renal ultrasonography, performed within the first 24 hours postoperatively, to the early diagnosis of ureteral injuries in patients with normal intraoperative jet flow and to evaluate the impact of early screening on clinical outcomes. The non-invasive, widely accessible, and low-cost nature of ultrasonography renders its feasibility as a systematic screening tool in the early period clinically important. Early postoperative ultrasonographic evaluation enhances patient safety following benign total TLH, even when intraoperative jet-flow findings are within normal limits. Accordingly, it is hypothesized that early ultrasonography offers significant diagnostic value in detecting postoperative complications, thereby justifying its routine use regardless of intraoperative assessments.

Intraoperative cystoscopy with ureteral jet evaluation remains a valuable tool for identifying mechanical ureteral injuries; however, its limitations become apparent in the context of energy device-related thermal damage, where preserved ureteral perfusion can yield normal jet flow despite underlying injury[11]. Our findings confirm that normal ureteral jet flow during cystoscopy does not definitively exclude ureteral compromise. While complete transections are often recognized intraoperatively, partial injuries such as thermal damage, kinking, or ischemic lesions may not disrupt jet flow because of partial lumen patency, thereby delaying diagnosis[12]. The absence of jet flow is a significant indicator of injury; however, its presence does not entirely exclude injury[13]. The pathophysiology of energy-induced thermal injury involves progressive tissue necrosis, often with preservation of initial mucosal integrity and ureteral perfusion. This preservation explains why jet flow may appear normal initially, with clinical manifestations emerging 7-14 days postoperatively as necrosis develops[14]. The three delayed-presentation cases in our cohort, which became symptomatic around postoperative days 7-10, are consistent with this mechanism. This finding is consistent with the literature documenting postoperative ureteral injuries despite normal intraoperative cystoscopy, highlighting the limitation of relying solely on intraoperative cystoscopy to detect such injuries[15]. We recommend supplementing postoperative day 1 renal ultrasonography with a repeat study at the first follow-up visit, around postoperative day 10. This two-step imaging approach is critical for detecting late-presenting thermal and ischemic ureteral lesions.

During benign gynecologic surgery, unilateral ureteral injuries often do not cause a significant elevation in serum creatinine because renal functional reserve and contralateral compensatory hyperfiltration produce a biochemical masking effect[16]. In our series, most radiologically confirmed cases of ureteral obstruction did not show a meaningful rise in serum creatinine, which likely reflects rapid contralateral renal compensation; therefore, a normal creatinine level does not exclude ureteral injury. Research demonstrates that while the affected kidney's glomerular filtration rate (GFR) decreases

rapidly, the contralateral kidney increases its GFR by 25-35%, maintaining overall renal function within normal limits[17]. This compensatory mechanism can preserve normal serum creatinine levels even in complete unilateral obstruction, particularly in patients with normal baseline renal function. Given the low diagnostic sensitivity of serum creatinine for detecting unilateral ureteral injury, reliance on biochemical parameters alone is insufficient[18]. Consequently, renal ultrasonography emerges as an essential diagnostic tool that reliably detects obstructive changes and prevents diagnostic delays. The timing of ureteral injury management is one of the most critical determinants of postoperative outcomes, as early recognition significantly reduces the risk of obstructive nephropathy, urinoma, infection, sepsis, and permanent loss of renal function[19]. When identified early, injuries can often be successfully managed with minimally invasive interventions such as endoscopic stenting, primary repair, or early UNC, whereas delayed diagnosis markedly decreases the likelihood of successful treatment. Contemporary guidelines from the American Urological Association and the European Association of Urology emphasize that injuries recognized intraoperatively or within the first 24-72 hours should undergo prompt intervention, as this approach yields substantially better outcomes compared with delayed repair[20]. In this context, early postoperative imaging, integrated into routine evaluation, facilitates timely diagnosis, particularly of injuries that may not be apparent intraoperatively. Therefore, in high-risk procedures such as laparoscopic hysterectomy, early identification of ureteral injury remains essential for preserving renal function and preventing long-term morbidity.

Early ureteral repair consistently demonstrates higher success rates and lower complication rates compared with delayed intervention; historical reconstructive urology series have reported success rates of 89-95% when repair is performed within the first 72 hours[21]. In contrast, injuries diagnosed more than seven days postoperatively are associated with reduced success rates (50-65%) due to inflammation, fibrosis, urinoma formation, and tissue necrosis, all of which complicate reconstruction[21]. More recent studies highlight that energy-related thermal injuries, common in minimally invasive gynecologic surgery, may remain clinically silent in the early postoperative period, and that delayed diagnosis increases the technical complexity and morbidity of surgical repair[22]. Consequently, the literature consistently supports early imaging-based detection and timely repair as the strongest predictors of renal functional preservation, lower reoperation rates, and improved patient outcomes.

The key strengths of this study include the use of data derived from a high-volume, minimally invasive gynecologic surgery center, enhancing the representativeness of the study population. The large case volume supports the robustness of the observed clinical patterns and improves the generalizability of the findings. In addition, the integrated use of preoperative ultrasonography, routine intraoperative cystoscopy, and postoperative renal ultrasonography within the same clinical setting facilitates early recognition and timely management of ureteral injuries.

Study Limitations

Despite the clinical relevance and methodological strengths of the present study, several important limitations should be carefully considered when interpreting the findings. The retrospective study design is inherently associated with risks of selection bias and incomplete or inconsistent clinical documentation. In addition, a formal cost-effectiveness analysis of the proposed diagnostic strategy was not conducted, limiting the ability to draw definitive conclusions about its economic impact. Furthermore, although the overall study cohort was relatively large, the limited number of ureteral injury cases necessitates cautious interpretation of diagnostic performance metrics, particularly PPV and NPVs. Importantly, the PPV observed in this study should not be regarded as a definitive diagnostic outcome, but rather as a hypothesis-generating observation that provides clinically meaningful insight and informs future research directions. Accordingly, the present findings warrant validation in larger, prospective, and well-controlled studies.

Conclusion

The findings of this study indicate that the presence of normal intraoperative ureteral jet flow does not reliably exclude ureteral injury. Renal ultrasonography, when integrated into the routine postoperative clinical assessment performed at our center, allows identification of newly developed pelviectasis and thereby facilitates early recognition of ureteral obstruction. When considered not as an additional screening test but as a natural extension of the standard postoperative evaluation, this approach may reduce morbidity associated with delayed diagnosis. Accordingly, postoperative renal ultrasonography, particularly when interpreted relative to preoperative baseline imaging, appears to be a practical adjunct for the early detection of ureteral injury.

Ethics

Ethics Committee Approval: Institutional review board approval was obtained prior to study initiation (University of Health Sciences Türkiye, İzmir Tepecik Education and Research Hospital Non-Interventional Ethics Committee, decision no: 2025/10-13, date: 03.11.2025).

Informed Consent: Retrospective cohort study.

Footnotes

Authorship Contributions

Surgical and Medical Practices: S.K., Concept: S.K., A.K., A.B., Design: S.K., A.K., U.D., A.H.İ., Data Collection or Processing: U.D., P.T.Ö., F.Y., Analysis or Interpretation: S.K.,

F.Y., Literature Search: S.K., A.İ., A.B., A.H.İ., Writing: S.K., A.İ., A.H.İ.

Conflict of Interest: No conflict of interest was declared by the authors.

Financial Disclosure: The authors declared that this study received no financial support.

References

1. Dickson B, Tessier KM, Green IC, et al. Urinary tract injury during benign hysterectomy for endometriosis: an NSQIP study. J Minim Invasive Gynecol. 2025;32:898-905.e1.
2. Adelman MR, Bardsley TR, Sharp HT. Urinary tract injuries in laparoscopic hysterectomy: a systematic review. J Minim Invasive Gynecol. 2014;21:558-66.
3. Smith AP, Bazinet A, Liberman D. Iatrogenic ureteral injury after gynecological surgery. Can Urol Assoc. 2019;13(6 Suppl4):S51-5.
4. Sutton PA, Awad S, Perkins AC, Lobo DN. Comparison of lateral thermal spread using monopolar and bipolar diathermy, the harmonic Scalpel and the Ligasure. Br J Surg. 2010;97:428-33.
5. Capozzi VA, Monfardini L, Scarpelli E, Barresi G, Rotondella I, De Finis A, et al. Urologic complication after laparoscopic hysterectomy in gynecology oncology: a single-center analysis and narrative review of the literature. Medicina (Kaunas). 2022;58:1869.
6. Galhotra S, Zeng K, Hu C, Norton T, Mahnert N, Smith R, et al. The effect of patient positioning on ureteral efflux during intraoperative cystoscopy: a randomized controlled trial. J Minim Invasive Gynecol. 2023;30:13-8.
7. Polan RM, Barber EL. Association between cystoscopy at the time of hysterectomy performed by a gynecologic oncologist and delayed urinary tract injury. Int Gynecol Cancer. 2022;32:62-8.
8. Chan JK, Morrow J, Manetta A. Prevention of ureteral injuries in gynecologic surgery. Am J Obstet Gynecol. 2003;188:1273-7.
9. Blackwell RH, Kirshenbaum EJ, Shah AS, Kuo PC, Gupta GN, Turk TMT. Complications of recognized and unrecognized ıatrogenic ureteral injury at time of hysterectomy: a population based analysis. J Urol. 2018;199:1540-5.
10. Teeluckdharry B, Gilmour D, Flowerdew G. Urinary tract injury at benign gynecologic surgery and the role of cystoscopy. Obstet Gynecol. 2015;126:1161-9.
11. Wu HH, Yang PY, Yeh GP, Chou PH, Hsu JC, Lin KC. The detection of ureteral injuries after hysterectomy. J Minim Invasive Gynecol. 2006;13:403-8.
12. Oh BR, Kwon DD, Park KS, Ryu SB, Park YI, Presti JCJ. Late presentation of ureteral injury after laparoscopic surgery. Obstet Gynecol. 2000;95:337-9.
13. Anand M, Casiano ER, Heisler CA, Weaver AL, Borah BJ, Wagie AE, et al. Utility of intraoperative cystoscopy in detecting ureteral injury during vaginal hysterectomy. Female Pelvic Med Reconstr Surg. 2015;21:70-6.
14. Maheswaran R, Beisland C, Bergesen AK, Almås B. A delayed diagnosis of iatrogenic ureteral injury results in increased morbidity. Sci Rep. 2024;14:13771.
15. Dandolu V, Mathai E, Chatwani A, Harmanli O, Pontari M, Hernandez E. Accuracy of cystoscopy in the diagnosis of ureteral injury in benign gynecologic surgery. Int Urogynecol J Pelvic Floor Dysfunct. 2003;14:427-31.
16. Walter AJ, Magtibay PM, Morse AN, Hammer RA, Hentz JG, Magrina JF. Perioperative changes in serum creatinine after gynecologic surgery. Am J Obstet Gynecol. 2002;186:1315-9.
17. Ito K, Chen J, El Chaar M, Stern JM, Seshan SV, Khodadadian JJ, et al. Renal damage progresses despite improvement of renal function after relief of unilateral ureteral obstruction in adult rats. Am J Physiol Renal Physiol. 2004;287:F1283-93.
18. Gosmanova EO, Baumgarten DA, O'Neill WC. Acute kidney injury in a patient with unilateral ureteral obstruction. Am J Kidney Dis. 2009;54:775-9.
19. Burks FN, Santucci RA. Management of iatrogenic ureteral injury. Ther Adv Urol. 2014;6:115-24.
20. Kitrey ND, Campos-Juanatey F, Hallscheidt P, Mayer E, Serafetinidis E, Waterloos M, et al. EAU Guidelines on Urological Trauma. Arnhem (Netherlands): European Association of Urology (EAU); 2025. Available from: https://d56bochluxqnz.cloudfront.net/documents/full-guideline/EAU-Guidelines-on-Urological-Trauma-2025.pdf
21. Brandes S, Coburn M, Armenakas N, McAninch J. Diagnosis and management of ureteric injury: an evidence-based analysis. BJU Int. 2004;94:277-89.
22. Taqi KM, Nassr MM, Al Jufaili JS, Abu-Qasida AI, Mathew J, Al-Qadhi H. Delayed diagnosis of ureteral injury following penetrating abdominal trauma: a case report and review of the literature. Am J Case Rep. 2017;18:1377-81.

Clinical Investigation / Araştırma

DOI: 10.4274/tjod.galenos.2026.37165

Turk J Obstet Gynecol 2026;23(1):47-55

Inflammatory indices, machine learning and artificial intelligence in tubal ectopic pregnancy management

Tubal ektopik gebelik yönetiminde enflamatuvar indeksler, makine öğrenmesi ve yapay zeka

Uğurcan Zorlu[1], Senem Arda Düz[2], Gül Kurtaran[3], Mohammad İbrahim Halilzade[3], Burak Elmas[4]

[1]*Ankara Bilkent City Hospital, Clinic of Perinatology, Ankara, Türkiye*

[2]*İnönü University Faculty of Medicine, Department of Obstetrics and Gynecology, Malatya, Türkiye*

[3]*Ankara Bilkent City Hospital, Clinic of Obstetrics and Gynecology, Ankara, Türkiye*

[4]*Acıbadem Maslak Hospital, Clinic of Obstetrics and Gynecology, İstanbul, Türkiye*

Abstract

Objective: To assess the predictive value of hematologic and biochemical inflammatory indices for methotrexate (MTX) treatment outcomes in tubal ectopic pregnancy (TEP) and to develop machine learning (ML) models for individualized risk stratification.

Materials and Methods: This retrospective cohort included 293 hemodynamically stable TEP patients who were treated with a single dose of MTX between January 2019 and December 2023. Demographic, clinical, ultrasonographic, and laboratory data were analyzed. Inflammatory indices—including neutrophil-to-lymphocyte ratio (NLR), platelet-to-lymphocyte ratio, systemic immune-inflammation index, systemic inflammation response index (SIRI), aggregate index of systemic inflammation (AISI), and fibrinogen-to-albumin ratio (FAR)—were calculated. Outcomes were categorized as single-dose MTX success, requirement for additional MTX, or surgery. Predictive accuracy of five supervised ML algorithms was evaluated using receiver operating characteristic analysis.

Results: Single-dose MTX was successful in 65.5% of patients; 18.4% required an additional dose, and 16.0% underwent surgery. AISI had the highest predictive accuracy for surgery [area under the curve (AUC)=0.929], followed by SIRI (AUC=0.899) and FAR (AUC=0.847). NLR best predicted the need for additional MTX (AUC=0.675). Na¨ve Bayes achieved the highest performance for surgical prediction (accuracy=98.3%, AUC=0.998), while random forest and gradient boosting were most effective in predicting the need for additional MTX (accuracy=83.1%, AUC=0.884-0.896). Feature importance analyses consistently ranked AISI, SIRI, and FAR as top predictors.

Conclusion: AISI, SIRI, and FAR are strong predictors of MTX failure and surgical intervention in TEP. Combining these biomarkers with ML models markedly improves predictive performance and supports a personalized approach to TEP management. Multicenter prospective validation is needed before clinical application.

Keywords: Ectopic pregnancy, inflammation, inflammatory markers, machine learning, methotrexate

Öz

Amaç: Tubal ektopik gebelikte (TEG) metotreksat (MTX) tedavi sonuçlarını öngörmede hematolojik ve biyokimyasal enflamatuvar indekslerin tahmin gücünü değerlendirmek ve bireyselleştirilmiş risk sınıflaması için makine öğrenmesi (MÖ) modelleri geliştirmektir.

Gereç ve Yöntemler: Bu retrospektif kohort çalışmaya Ocak 2019-Aralık 2023 tarihleri arasında tek doz MTX ile tedavi edilen 293 hemodinamik olarak stabil TEG hastası dahil edildi. Demografik, klinik, ultrasonografik ve laboratuvar verileri analiz edildi. Nötrofil-lenfosit oranı (NLR), trombosit-lenfosit oranı, sistemik immün-enflamasyon indeksi, sistemik enflamasyon yanıt indeksi (SIRI), toplu sistemik enflamasyon indeksi (AISI)

PRECIS: Using inflammatory indices and machine learning models, we evaluated predictors of methotrexate failure and surgical intervention in patients with tubal ectopic pregnancy.

Corresponding Author/Sorumlu Yazar: Uğurcan Zorlu MD,
Ankara Bilkent City Hospital, Clinic of Perinatology, Ankara, Türkiye
E-mail: ugurcanzorlu@gmail.com **ORCID ID:** orcid.org/0000-0002-8912-0812

Received/Geliş Tarihi: 11.01.2026 **Accepted/Kabul Tarihi:** 18.02.2026 **Epub:** 20.02.2026 **Publication Date/Yayınlanma Tarihi:** 05.03.2026

Cite this article as: Zorlu U, Arda Düz S, Kurtaran G, Halilzade Mİ, Elmas B. Inflammatory indices, machine learning and artificial intelligence in tubal ectopic pregnancy management. Turk J Obstet Gynecol. 2026;23(1):47-55

ve fibrinojen/albümin oranı (FAR) gibi enflamatuvar indeksler hesaplandı. Tedavi sonuçları; tek doz MTX başarısı, ek doz MTX gereksinimi ve cerrahi müdahale olarak sınıflandırıldı. Tahmin doğruluğu, ROC analizi ve beş farklı denetimli MÖ algoritması ile değerlendirildi.

Bulgular: Tek doz MTX tedavisi %65,5 oranında başarılı olurken; %18,4 hastada ek doz MTX gereksinimi oluştu, %16,0 hastaya ise cerrahi müdahale uygulandı. Cerrahi tahmininde en yüksek doğruluk AISI'ye ait olup eğrinin altındaki alan (AUC) değeri 0,929 olarak bulundu; bunu SIRI (AUC=0,899) ve FAR (AUC=0,847) izledi. Ek MTX ihtiyacını en iyi öngören indeks NLR oldu (AUC=0,675). Na¨ve Bayes algoritması, cerrahi öngörüsünde en yüksek başarıyı sağladı (doğruluk=%98,3; AUC=0,998); rastgele orman (random forest) ve gradyan artırma (gradient boosting) algoritmaları ise ek MTX ihtiyacını öngörmede en etkili modellerdi (doğruluk=%83,1; AUC=0,884-0,896). Özellik önem analizleri, AISI, SIRI ve FAR indekslerini tutarlı şekilde en güçlü öngörücüler olarak belirledi.

Sonuç: AISI, SIRI ve FAR, TEG'de MTX tedavi başarısızlığını ve cerrahi müdahale gereksinimini öngörmede güçlü biyobelirteçlerdir. Bu biyobelirteçlerin MÖ modelleriyle entegrasyonu, tahmin performansını önemli ölçüde artırarak TEG yönetiminde kişiselleştirilmiş bir yaklaşımı destekler. Klinik uygulamaya geçmeden önce çok merkezli prospektif çalışmalarla doğrulama gereklidir.

Anahtar Kelimeler: Ektopik gebelik, enflamasyon, enflamatuvar belirteçler, makine öğrenmesi, metotreksat

Introduction

Tubal ectopic pregnancy (TEP) remains a significant contributor to maternal morbidity and mortality during the first trimester and constitutes more than 90% of all ectopic pregnancies[1]. The use of systemic methotrexate (MTX) has substantially changed the management of hemodynamically stable patients, as single-dose regimens provide a less invasive alternative to surgical intervention[2]. However, the clinical response to MTX is heterogeneous, and a subset of patients experiences treatment failure, necessitating additional MTX administration or surgical management[3,4]. For this reason, the early identification of patients at increased risk for unsuccessful medical treatment is essential to enable individualized therapeutic strategies and improve overall prognosis. In recent years, hematologic and biochemical inflammatory indices obtained from routine laboratory testing, such as the systemic immune-inflammation index (SII), platelet-to-lymphocyte ratio (PLR), neutrophil-to-lymphocyte ratio (NLR), and fibrinogen-to-albumin ratio (FAR), have been increasingly investigated as potential predictors of disease course and treatment response in obstetric and gynecologic disorders[4,5].These markers reflect systemic immune activation, coagulation status, and metabolic changes, all of which may influence MTX efficacy in TEP[6,7]. Although several studies have explored their predictive role, findings remain inconsistent, particularly regarding their ability to forecast the need for surgical intervention versus additional MTX administration[8,9].

Alongside biomarker research, advances in artificial intelligence and machine learning (ML) offer novel opportunities to improve clinical decision-making in TEP. ML algorithms can process complex, multidimensional datasets to identify nonlinear relationships between clinical, ultrasonographic, and laboratory variables, potentially outperforming traditional statistical approaches[10,11]. However, integration of ML-based prediction models into routine ectopic pregnancy management remains limited, with few studies systematically comparing their performance against established clinical predictors.

Given these gaps, the present retrospective cohort study aimed to evaluate the predictive accuracy of inflammatory indices for treatment success, the requirement for additional MTX, and surgical intervention in TEP patients, and to develop and validate ML-based prediction models for individualized risk stratification. By combining traditional statistical methods with advanced computational modeling, this study seeks to establish a more precise, data-driven framework for optimizing TEP management.

Materials and Methods

This retrospective cohort study was conducted in the Department of Obstetrics and Gynecology of a tertiary referral hospital between January 2019 and December 2023. All clinical, laboratory, and imaging data were retrieved from the institutional electronic medical record system and radiology archives. The study protocol was reviewed and approved by the Ankara Bilkent City Hospital Institutional Ethics Committee (approval no: TABED 2-25-1311, date: 11.06.2025), and all procedures were conducted in accordance with the Declaration of Helsinki.

All women diagnosed with TEP during the study period were evaluated for eligibility. A definitive diagnosis was established based on transvaginal ultrasonography findings and/or serial serum beta human chorionic gonadotropin (β-hCG) measurements. Only hemodynamically stable patients who were initially managed with a single-dose intramuscular MTX regimen and had complete clinical, laboratory, and imaging records were included. Patients presenting with hemodynamic instability, suspected or confirmed tubal rupture, immediate indications for surgical intervention, contraindications to MTX therapy (e.g., hepatic, renal, or hematologic disorders), non-tubal ectopic pregnancies (including cervical, interstitial, or ovarian locations), or those treated primarily with multi-dose MTX protocols were excluded from the analysis.

All eligible patients received a single intramuscular dose of MTX at 50 mg/m² on day 0. Serum β-hCG levels were measured on days 0, 4, and 7 following treatment. A decline of at least 15% in β-hCG levels between day 4 and day 7 was considered indicative of an adequate therapeutic response. Patients who failed to achieve this decline received an additional dose of MTX and were classified as requiring further medical treatment. Those who developed worsening clinical

symptoms such as increasing abdominal pain, hemodynamic deterioration, signs of tubal rupture, or persistent elevation of β-hCG levels despite medical therapy were referred for surgical management.

Demographic characteristics including age, gravidity, and parity, as well as clinical features such as abdominal pain and vaginal bleeding at presentation, were recorded for each patient. Laboratory parameters included serum β-hCG levels at baseline, day 4, and day 7; complete blood count values; and concentrations of C-reactive protein, fibrinogen, and albumin. Ultrasonographic evaluation provided data on adnexal mass size and Doppler-derived ipsilateral ovarian artery systolic/diastolic ratio and pulsatility index. Based on complete blood count parameters, several hematologic and inflammatory indices were calculated, including NLR, monocyte-to-lymphocyte ratio (MLR), PLR, eosinophil-to-lymphocyte ratio (ELR), white blood cell-to-neutrophil ratio, SII, systemic inflammation response index (SIRI), aggregate index of systemic inflammation (AISI), and FAR.

The primary outcomes of the study were defined as the successful resolution of ectopic pregnancy with a single dose of methotrexate, the requirement for an additional MTX dose, and the need for surgical intervention following medical treatment. Secondary outcomes included the identification of clinical and laboratory predictors associated with treatment failure, the assessment of the diagnostic performance of inflammatory indices in predicting treatment outcomes, and the evaluation of ML models for predicting surgical intervention or the need for an additional dose of methotrexate.

Statistical Analysis

All analyses were conducted using IBM SPSS Statistics version 25.0 (IBM Corp., Armonk, NY, USA) and Python 3.10 with standard scientific libraries. Data distribution was assessed with the Shapiro-Wilk test. Parametric data were reported as mean ± standard deviation and compared using the Student's t-test or one-way ANOVA, whereas nonparametric variables were expressed as median (interquartile range) and analyzed with the Mann-Whitney U or Kruskal-Wallis tests. Categorical variables were compared using the chi-square test or Fisher's exact test, as appropriate. A two-sided p-value <0.05 was considered statistically significant.

Receiver operating characteristic (ROC) analyses were performed to assess the ability of inflammatory indices to predict surgical intervention and the requirement for an additional dose of methotrexate. Area under the curve (AUC) values and 95% confidence intervals (CIs) were calculated using the DeLong method. Optimal cut-off points were identified with the Youden Index, and sensitivity, specificity, positive predictive value, and negative predictive value were subsequently derived.

Machine Learning Analysis

A supervised ML framework was applied to construct predictive models addressing two binary classification objectives: identifying patients requiring surgical intervention and predicting the need for an additional dose of methotrexate. These models were designed to support individualized risk stratification in the management of tubal ectopic pregnancy. A supervised ML framework was applied using standardized variables, an 80:20 stratified train–test split, and five-fold cross-validation, with performance evaluated using accuracy, AUC, and F1 score.

Prior to model training, comprehensive data preprocessing was undertaken. All continuous clinical, hematologic, and inflammatory variables were standardized using Z-score transformation to eliminate scale-related bias and ensure equal contribution of features during model learning. The proportion of missing data was low, accounting for less than two percent of all entries, and was addressed through mean imputation for continuous variables and mode imputation for categorical variables. The class distribution was examined for imbalance; because surgical intervention outcomes demonstrated moderate skewness, class-weighting strategies were incorporated into algorithms sensitive to class imbalance, such as logistic regression and support vector machines, to enhance model stability and predictive accuracy. For feature selection, all available hematologic and inflammatory indices were initially included as candidate predictors. The relative importance of each variable was subsequently evaluated using two complementary approaches. First, the mean decrease in impurity derived from random forest models was calculated to assess each feature's contribution to reducing classification error. Second, permutation-based importance analysis was performed to quantify the change in model performance following random shuffling of individual features, thereby directly measuring their impact on predictive accuracy. The results of these analyses are presented in Figures 1 and 2.

For predictive modeling, commonly used supervised classification algorithms were applied: logistic regression with L2 regularization, random forest, Gaussian naïve Bayes, support vector machine with a radial basis function kernel, and gradient boosting. Model hyperparameters were optimized using grid search strategies, with the number of trees in the random forest set to 500 and the optimal tree depth determined algorithmically. For the support vector machine model, the penalty parameter was tuned to achieve optimal classification performance, while gradient boosting models were trained using a learning rate of 0.1, with depth parameters refined through cross-validation.

To ensure robust evaluation, the dataset was randomly divided into training and testing subsets at an 80:20 ratio, stratified according to outcome categories, and a fixed random seed was applied to guarantee reproducibility. Hyperparameter tuning was conducted using five-fold cross-validation within

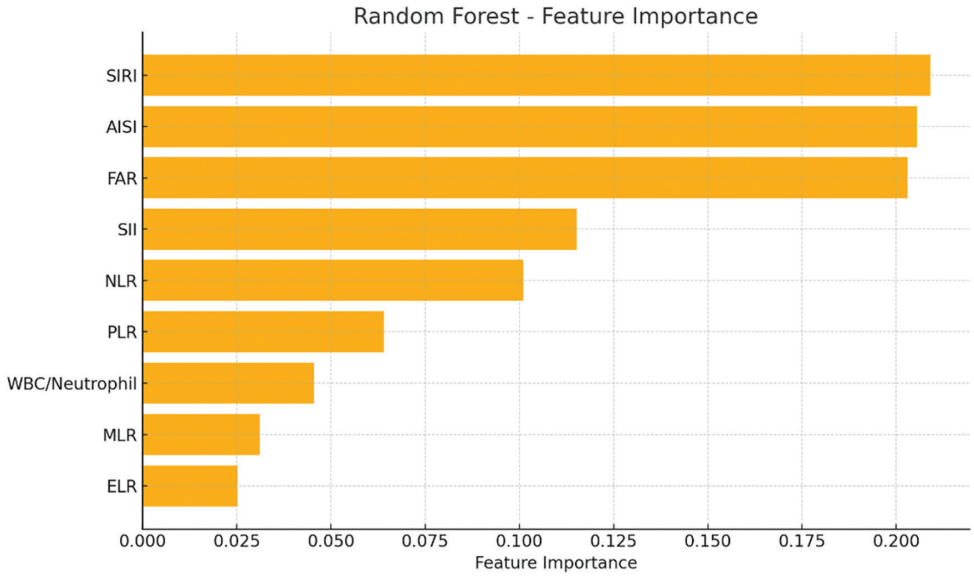

Figure 1. Top predictors of surgical requirement (random forest feature importance)

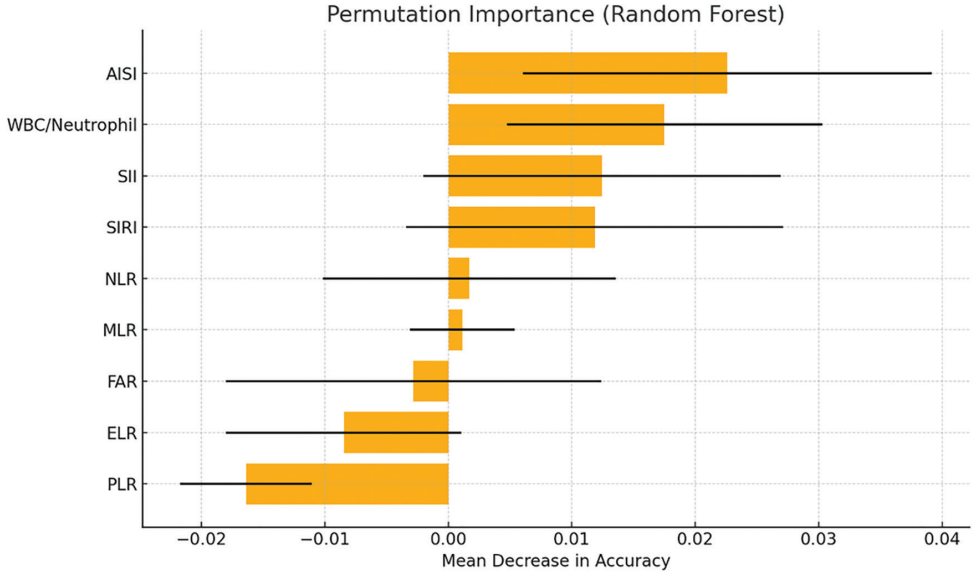

Figure 2. Permutation-based feature importance for predicting surgical intervention in ectopic pregnancy using random forest classifier

the training dataset. Final model performance was assessed on the independent test dataset. For feature-importance analyses and graphical representations, models were subsequently retrained on the entire dataset to maximize statistical power and enhance generalizability.

Model performance was quantified using multiple complementary metrics. Overall classification accuracy was calculated to determine the proportion of correctly classified cases. Discriminative capacity, independent of decision thresholds, was assessed using the area under the ROC curve. The F1 score was employed to capture the balance between precision and recall, and confusion matrices were generated to examine the distribution of false-positive and false-negative predictions.

To identify the most influential variables associated with surgical intervention, feature importance analyses were performed using the final random forest model trained on the complete dataset. Variable contributions were first assessed using mean decrease in impurity, which reflects the relative importance of each feature in reducing classification error across decision trees. In addition, permutation-based importance analysis was conducted by randomly shuffling individual features and quantifying the resulting decline in model accuracy, thereby directly measuring the dependence

of predictive performance on each variable. Both methods were applied to ensure consistency and robustness of feature ranking. Across both approaches, aggregate index of systemic inflammation, systemic inflammation response index, and FAR consistently emerged as the most influential predictors, followed by neutrophil-to-lymphocyte and PLR ratios. All machine-learning analyses and visualizations were performed using the scikit-learn library and Matplotlib.

Results

A total of 293 women diagnosed with TEP between January 2019 and December 2023 were included in this retrospective study. Among these patients, 192 (65.5%) achieved complete resolution with a single intramuscular dose of methotrexate, 54 (18.4%) required an additional dose of medical therapy, and 47 (16.0%) ultimately underwent surgical management.

Clinical Characteristics

A comparative analysis of clinical features by treatment outcome is presented in Table 1. The mean age did not differ significantly among the single-dose MTX group, the additional-dose group, and the surgical intervention group (p=0.195). Baseline serum β-hCG concentrations, adnexal mass dimensions, and gestational age at diagnosis were also comparable across the three groups, with no statistically significant differences observed (p=0.552, p=0.376, and p=0.203, respectively).

Vaginal bleeding at presentation was observed more frequently in patients who required an additional dose of MTX than in those who responded to a single dose or who proceeded to surgery; this difference was statistically significant (p=0.038). In contrast, the occurrence of abdominal pain was similar across all groups and was not significantly associated with treatment outcome (p=0.616).

Doppler ultrasonographic findings revealed marked differences between groups. The ipsilateral ovarian artery systolic/diastolic ratio was significantly higher in patients who underwent surgery than in those who were successfully treated with a single dose of MTX or who required an additional dose of MTX (p<0.001). Likewise, the pulsatility index was substantially elevated in the surgical group compared with both medical treatment groups, indicating increased vascular resistance in patients progressing to surgical management (p<0.001).

Hematologic and Inflammatory Parameters

Detailed comparisons of hematologic and inflammatory indices are provided in Table 2. The NLR demonstrated a stepwise increase across outcome groups, being lowest in patients successfully treated with a single dose of methotrexate, higher in those requiring an additional dose, and highest among patients undergoing surgical intervention (p<0.001).

A similar pattern was observed for the MLR, PLR, and eosinophil-to-lymphocyte ratio, all of which were significantly elevated in patients who required further medical treatment or surgery, compared with those who responded to initial therapy (p<0.01 for MLR and PLR; p=0.048 for ELR). Systemic inflammatory markers, including the systemic immune-inflammation index, systemic inflammation response index, aggregate index of systemic inflammation, and fibrinogen-to-albumin ratio, were also significantly higher in the additional-dose and surgical groups than in the single-dose group (all p<0.05). Consistent with these findings, C-reactive protein levels increased progressively across groups, with the highest values observed in patients who underwent surgery (p=0.002). In contrast, the white blood cell-to-neutrophil ratio was significantly lower in the surgical intervention group than in patients successfully treated with a single dose of methotrexate, suggesting a shift toward neutrophil predominance in more severe disease (p=0.032).

ROC Analysis for Predicting Surgical Intervention

The ROC analysis results for inflammatory markers predicting surgical intervention are presented in Table 3. The AISI demonstrated the highest discriminatory ability, with an AUC of 0.929 (95% CI: 0.892–0.963) at a cut-off value of

Table 1. Clinical parameters by treatment outcome in patients with ectopic pregnancy (mean ± SD or %)

Parameter	Single-dose MTX	Additional-dose MTX	Surgical intervention	p-value
Age (years)	28.00±6.02	27.83±5.46	26.27±6.03	0.195
Serum β-hCG (beta-human chorionic gonadotropin, IU/L)	3263.72±1210.15	3418.07±1163.36	3433.58±1237.33	0.552
Adnexal mass size (cm)	2.79±0.70	2.93±0.61	2.87±0.63	0.376
Gestational age (weeks)	5.60±0.31	5.55±0.20	5.65±0.28	0.203
Vaginal bleeding (presence, %)	56.8%	75.9%	59.6%	0.038
Abdominal pain (presence, %)	68.8%	74.1%	74.5%	0.616
Ipsilateral ovarian artery S/D	3.14±0.52	3.53±0.39	4.03±0.53	<0.001
Ipsilateral ovarian artery PI	1.11±0.20	1.32±0.20	1.61±0.24	<0.001

MTX: Methotrexate, β-hCG: Beta-human chorionic gonadotropin, SD: Standard deviation, S/D: Systolic/diastolic ratio, PI: Pulsatility index

221.678, yielding a sensitivity of 95.7% and a specificity of 77.2%. This was followed by the systemic inflammation response index (SIRI) (AUC=0.899, 95% CI: 0.846-0.944; cut-off 738.615; sensitivity 72.3%; specificity 95.5%) and the fibrinogen-to-albumin ratio (FAR) (AUC=0.847, 95% CI: 0.761-0.920; cut-off 0.129; sensitivity 76.6%; specificity 80.5%).

Other markers such as NLR, MLR, PLR, and SII also demonstrated good discriminatory performance (AUC range: 0.793–0.835), whereas the white blood cell to neutrophil ratio showed poor predictive value(AUC=0.241).

Model Performance for Surgical Intervention

The performances of ML models using inflammatory markers as predictors are summarized in Table 4. The Naive Bayes (NB) model achieved the highest overall performance, with an accuracy of 98.3%, an ROC AUC of 0.998, and an F1 score of 0.982.

Logistic Regression (accuracy 96.6%, ROC AUC 0.996, F1=0.964) and Support Vector Machine (accuracy 94.9%, ROC AUC 0.996, F1=0.948) also demonstrated excellent predictive performance. Random Forest and Gradient Boosting yielded slightly lower accuracies (93.2% each) but maintained high ROC AUC values (0.991 and 0.989, respectively).

Feature importance rankings from the Random Forest analysis are illustrated in Figure 1, highlighting AISI, SIRI, and FAR as the most influential predictors of surgical requirement. Figure 2 depicts permutation-based feature importance, confirming the predominance of these indices.

ROC Analysis for Predicting Additional-dose MTX Requirement

The ROC analysis for predicting additional-dose MTX is shown in Table 5.

Table 2. Comparison of hematologic indices by treatment outcome in patients with tubal ectopic pregnancy (mean ± SD)

Parameter	Single-dose MTX	Additional-dose MTX	Surgical intervention	p-value
NLR	2.91±1.00	4.33±1.19	4.98±1.87	<0.001
MLR	0.26±0.08	0.32±0.09	0.38±0.09	<0.01
PLR	115.55±28.22	139.51±32.60	162.10±41.02	<0.01
ELR	0.042±0.020	0.063±0.030	0.067±0.026	0.048
WBC/neutrophil ratio	1.60±0.31	1.50±0.28	1.33±0.19	0.032
SII ($\times 10^9$/L)	0.83±0.32	1.05±0.41	1.34±0.50	<0.001
SIRI	526.33±108.91	661.72±133.04	789.45±146.37	<0.001
AISI	152.80±49.90	212.75±64.35	279.93±73.12	<0.001
FAR	0.10±0.02	0.12±0.02	0.14±0.03	0.017
CRP (mg/L)	4.2±1.1	6.5±1.3	9.8±2.1	0.002

MTX: Methotrexate, NLR: Neutrophil-to-lymphocyte ratio, MLR: Monocyte-to-lymphocyte ratio, PLR: Platelet-to-lymphocyte ratio, ELR: Eosinophil-to-lymphocyte ratio, WBC: White blood cell, SII: Systemic immune-inflammation index, SIRI: Systemic inflammation response index, AISI: Aggregate index of systemic inflammation, FAR: Fibrinogen-to-albumin ratio, CRP: C-reactive protein, SD: Standard deviation

Table 3. ROC analysis of inflammatory markers for predicting surgical intervention in patients with tubal ectopic pregnancy using the Youden Index method

Parameter	AUC	95% CI	Cut-off (Youden)	Sensitivity	Specificity
NLR	0.800	0.725-0.877	4.360	0.638	0.841
MLR	0.764	0.699-0.830	0.338	0.787	0.659
PLR	0.793	0.705-0.869	145.869	0.681	0.797
ELR	0.700	0.618-0.774	0.0646	0.532	0.785
WBC/neutrophil ratio	0.241	0.186-0.295	1.191	0.979	0.057
SII	0.835	0.759-0.900	1.14	0.830	0.728
SIRI	0.899	0.846-0.944	738.615	0.723	0.955
AISI	0.929	0.892-0.963	221.678	0.957	0.772
FAR	0.847	0.761-0.920	0.129	0.766	0.805

NLR: Neutrophil-to-lymphocyte ratio, MLR: Monocyte-to-lymphocyte ratio, PLR: Platelet-to-lymphocyte ratio, ELR: Eosinophil-to-lymphocyte ratio, WBC: White blood cell, SII: Systemic immune-inflammation index, SIRI: Systemic inflammation response index, AISI: Aggregate index of systemic inflammation, FAR: Fibrinogen-to-albumin ratio, AUC: Area under the curve, CI: Confidence interval, ROC: Receiver operating characteristic

Among the evaluated markers, NLR exhibited the highest predictive capacity (AUC=0.675, 95% CI: 0.603-0.747) with an optimal cut-off value of 3.842 (sensitivity 90.7%, specificity 43.5%). PLR (AUC=0.642) and ELR (AUC=0.626) provided moderate discrimination, whereas WBC/Neutrophil ratio (AUC=0.435) demonstrated poor predictive value.

Machine Learning Model Performance for Additional-dose MTX Prediction

As presented in Table 6, the best-performing models for predicting additional-dose MTX requirement were random forest and gradient boosting. Both models achieved an accuracy of 83.1%; their ROC AUC values were 0.884 and 0.896 for random forest and gradient boosting, respectively. A Support Vector Machine achieved an accuracy of 81.4% with an ROC AUC of 0.809. In contrast, Logistic Regression and Naive Bayes models achieved moderate accuracy (72.9%) and similar ROC AUC values (0.805 and 0.807, respectively).

Table 4. Machine learning model performance for predicting surgical intervention in patients with tubal ectopic pregnancy using NLR, MLR, PLR, ELR, WBC/Neutrophil ratio, SII, SIRI, AISI, and FAR

Model	Accuracy	ROC-AUC	F1 score
Logistic regression	0.966	0.996	0.964
Random forest	0.932	0.991	0.931
Naive bayes	0.983	0.998	0.982
Support vector machine	0.949	0.996	0.948
Gradient boosting	0.932	0.989	0.930

NLR: Neutrophil-to-lymphocyte ratio, MLR: Monocyte-to-lymphocyte ratio, PLR: Platelet-to-lymphocyte ratio, ELR: Eosinophil-to-lymphocyte ratio, WBC: White blood cell, SII: Systemic immune-inflammation index, SIRI: Systemic inflammation response index, AISI: Aggregate index of systemic inflammation, FAR: Fibrinogen-to-albumin ratio, ROC-AUC: Receiver operating characteristic-area under the curve, F1 Score: Harmonic mean of precision and recall

Table 5. ROC analysis of hematologic and inflammatory markers for predicting additional-dose MTX requirement in patients with tubal ectopic pregnancy using the Youden Index method

Parameter	AUC	95% CI	Cut-off (Youden)	Sensitivity	Specificity
NLR	0.675	0.603-0.747	3.842	0.907	0.435
MLR	0.557	0.477-0.630	0.296	0.722	0.427
PLR	0.642	0.563-0.717	129.492	0.815	0.448
ELR	0.626	0.530-0.719	0.058	0.611	0.686
WBC/neutrophil ratio	0.435	0.360-0.515	1.219	0.019	0.996
SII	0.590	0.505-0.671	0.994	0.574	0.624
SIRI	0.611	0.523-0.692	621.223	0.667	0.573
AISI	0.602	0.520-0.682	190.456	0.630	0.585
FAR	0.578	0.494-0.658	0.112	0.537	0.616

MTX: Methotrexate, NLR: Neutrophil-to-lymphocyte ratio, MLR: Monocyte-to-lymphocyte ratio, PLR: Platelet-to-lymphocyte ratio, ELR: Eosinophil-to-lymphocyte ratio, WBC: White blood cell, SII: Systemic immune-inflammation index, SIRI: Systemic inflammation response index, AISI: Aggregate index of systemic inflammation, FAR: Fibrinogen-to-albumin ratio, AUC: Area under the curve, CI: Confidence interval

Table 6. Performance metrics of machine learning models for predicting the need for additional-dose methotrexate (MTX) in patients with tubal ectopic pregnancy

Model	Accuracy	ROC-AUC	F1 score
Logistic regression	0.729	0.805	0.511
Random forest	0.831	0.884	0.545
Naive bayes	0.729	0.807	0.513
Support vector machine	0.814	0.809	0.521
Gradient boosting	0.831	0.896	0.543

MTX: Methotrexate, ROC-AUC: Receiver operating characteristic-area under the curve, F1 Score: Harmonic mean of precision and recall

Discussion

This study provides robust evidence that specific inflammatory indices, particularly AISI, SIRI, and FAR, strongly predict MTX treatment failure and the need for surgical intervention in TEP. Furthermore, our results demonstrate that ML algorithms, especially Naïve Bayes and logistic regression, can achieve excellent predictive accuracy, outperforming traditional cut-off-based approaches.

Our findings are in line with recent studies investigating the prognostic utility of hematologic markers in ectopic pregnancy. Bilir et al.[8] reported that hemogram-based indices such as NLR, PLR, and SII were significantly higher in patients requiring surgical management after MTX therapy, with AISI emerging as the most discriminatory parameter. Dinc and Issın[5] showed that elevated SII values at presentation correlated strongly with the risk of tubal rupture, underscoring the role of systemic inflammation in the progression of ectopic pregnancy. Seyfettinoglu and Adiguzel[9] further highlighted that combining multiple indices improved predictive performance compared to single parameters.

The application of ML in ectopic pregnancy prognosis remains nascent but shows promise. Chen et al.[11] used gradient boosting and random forest models to predict MTX success in ectopic pregnancy and found ROC-AUC values up to 0.94-comparable to the performance observed in our Na¨ve Bayes model (AUC=0.998). Our inclusion of Doppler ultrasonography parameters alongside inflammatory indices may partly explain the superior performance, as ultrasonographic vascular indices reflect tubal perfusion and inflammatory status. ROC-derived cut-off values should be interpreted as supportive risk indicators rather than absolute clinical thresholds and must be integrated with clinical assessment and β-hCG dynamics.

Clinically, integrating these biomarkers with ML-based prediction tools could facilitate personalized management strategies. High-risk patients identified at diagnosis could receive closer monitoring, earlier consideration for surgery, and tailored counseling, potentially reducing the incidence of rupture and associated morbidity.

Strengths of this study include its relatively large sample size for a single tertiary center, simultaneous evaluation of multiple inflammatory indices, and the methodological rigor in comparing classical statistical methods with diverse ML algorithms. The use of two independent feature importance approaches (mean decrease in impurity and permutation) strengthens the validity of our predictive variable ranking.

Study Limitations

However, several limitations should be noted. The retrospective design carries an inherent risk of selection bias. All data were derived from a single center, which may limit generalizability. Potential confounders, such as subclinical infections or inflammatory comorbidities, could influence hematologic indices but were not systematically excluded. Although model performance was high, external validation in multicenter prospective cohorts is necessary before clinical adoption.

Future research should focus on validating these findings in larger and more diverse populations, integrating additional biomarkers (e.g., cytokines, cell-free DNA), and developing real-time decision support tools within electronic medical record systems. Randomized controlled trials assessing whether ML-guided treatment decisions improve clinical outcomes compared to current practice would be of particular value. Additional limitations include the single-center design, the potential residual confounding affecting inflammatory markers, and the lack of external validation. Therefore, prospective multicenter studies are required before routine clinical implementation.

Conclusion

This study indicates that AISI, SIRI, and FAR are strong predictors of MTX outcomes in tubal ectopic pregnancy. Integrating these biomarkers into machine-learning models, particularly Na¨ve Bayes and logistic regression, significantly enhances predictive accuracy and supports individualized risk stratification. The routine use of these indices in clinical practice may facilitate earlier decision-making, optimize treatment selection, and reduce complication rates. However, multicenter prospective studies are required to validate these findings and to explore the added value of advanced imaging and novel molecular biomarkers.

Ethics

Ethics Committee Approval: The study protocol was reviewed and approved by the Ankara Bilkent City Hospital Institutional Ethics Committee (approval no: TABED 2-25-1311, date: 11.06.2025), and all procedures were conducted in accordance with the Declaration of Helsinki.

Informed Consent: Retrospective study.

Footnotes

Authorship Contributions

Surgical and Medical Practices: U.Z., G.K., M.İ.H., B.E., Concept: U.Z., Design: U.Z., Data Collection or Processing: G.K., M.İ.H., Analysis or Interpretation: U.Z., B.E., Literature Search: U.Z., S.A.D., G.K., M.İ.H., B.E., Writing: U.Z., S.A.D., G.K., M.İ.H., B.E.

Conflict of Interest: No conflict of interest was declared by the authors.

Financial Disclosure: The authors declared that this study received no financial support.

References

1. Varma R, Gupta J. Tubal ectopic pregnancy. BMJ Clin Evid. 2012;2012:1406.
2. Gervaise A, Capella-Allouc S, Audibert F, Rongières-Bertrand C, Vincent Y, Fernandez H. Methotrexate for the treatment of unruptured tubal pregnancy: a prospective nonrandomized study. JSLS. 2003;7:233-8.
3. Baskiran Y, Uçkan K, Karacor T, Çeleğen I, Acar Z. The impact of maternal electrolyte and albumin levels on the efficacy of single-dose methotrexate treatment for ectopic pregnancies. Turk J Obstet Gynecol. 2023;20:214-8.
4. Tong S, Skubisz MM, Horne AW. Molecular diagnostics and therapeutics for ectopic pregnancy. Mol Hum Reprod. 2015;21:126-35.
5. Dinc K, Issın G. Novel marker to predict rupture risk in tubal ectopic pregnancies: the systemic immune-inflammation index. Ginekol Pol. 2023;94:320-5.
6. Akkaya H, Uysal G. Can hematologic parameters predict treatment of ectopic pregnancy? Pak J Med Sci. 2017;33:937-42.
7. Baskiran Y, Uçkan K, Çeleğen I. Can failure be predicted in methotrexate treatment with the modified parameter? Arch Gynecol Obstet. 2024;310:477-83.
8. Bilir C, Soysal C, Biyik I, Ulas O, Erbakirci NM, Sari H, et al. The relationship between hemogram-based inflammatory indices and prognosis in ectopic pregnancy cases treated with methotrexate. Sci Rep. 2025;15:23114.
9. Seyfettinoglu S, Adiguzel FI. Prediction of tubal rupture in ectopic pregnancy using methotrexate treatment protocols and hematological markers. J Clin Med. 2023;12:6459.
10. Dereli ML, Savran Üçok B, Ozkan S, Sucu S, Topkara S, Firatligil FB, et al. The importance of blood-count-derived inflammatory markers in predicting methotrexate success in patients with tubal ectopic pregnancy. Int J Gynaecol Obstet. 2024;167:789-96.
11. Chen S, Chen XF, Qiu P, Huang YX, Deng GP, Gao J. Association between white blood cells at baseline and treatment failure of methotrexate for ectopic pregnancy. Front Med (Lausanne). 2021;8:722963.

Clinical Investigation / Araştırma

DOI: 10.4274/tjod.galenos.2025.93630

Turk J Obstet Gynecol 2026;23(1):56-63

The effect of tinzaparin sodium and leuprolide acetate in an experimental mouse model of endometriosis: The rol of the WNT/beta-catenin pathway

Endometriyozis deneysel fare modelinde tinzaparin sodyum ve löprolid asetatın etkisi: WNT/beta-katenin yolaklarının rolü

Yasemin Albak[1], Gamze Sönmez Ünal[2], Çağlar Yıldız[3], Meral Çetin[4], Sevgi Durna Daştan[5], Erkan Gümüş[6], Ahmet Şevki Taşkıran[7], Ali Çetin[8]

[1]*Defa Life Hospital, Clinic of Obstetrics and Gynecology, Gaziantep, Türkiye*
[2]*Numune Hospital, Clinic of Obstetrics and Gynecology, Sivas, Türkiye*
[3]*Cumhuriyet University Faculty of Medicine, Department of Obstetrics and Gynecology, Sivas, Türkiye*
[4]*Cumhuriyet University Faculty of Medicine, Department of Obstetrics and Gynecology, Retired, Sivas, Türkiye*
[5]*Cumhuriyet University Faculty of Science, Deparment of Biology, Division of Molecular Biology, Sivas, Türkiye*
[6]*Adnan Menderes University Faculty of Medicine, Department of Histology and Embryology, Aydın, Türkiye*
[7]*Cumhuriyet University Faculty of Medicine, Department of Physiology, Sivas, Türkiye*
[8]*University of Health Sciences Türkiye, İstanbul Haseki Training and Research Hospital, Department of Obstetrics and Gynecology, İstanbul, Türkiye*

Abstract

Objective: Endometriosis is a benign condition driven by estrogen and inflammation in which endometrial-like tissue develops in ectopic locations. We aimed to determine whether non-steroidal agents acting on the WNT/beta-catenin signaling axis could provide therapeutic benefit in this disease.

Materials and Methods: Forty adult female mice underwent surgical creation of endometriotic implants and were then distributed into five experimental arms: untreated controls, early leuprolide (leup1d), early tinzaparin (tnz1d), delayed leuprolide (leup7d), and delayed tinzaparin (tnz7d). Early treatment groups received drug treatment beginning at postoperative hour 24, whereas delayed groups began treatment on postoperative day 8. At two weeks post-surgery, lesions were harvested for RNA extraction and transcript profiling. Tissues were also processed for hematoxylin-eosin staining with semi-quantitative grading. Immunostaining was performed using antibodies against HIF1a and WNT2.

Results: The tnz7d group exhibited decreased inflammatory markers, while the leup7d group displayed reduced epithelial content; both changes resulted in lower disease severity scores. WNT2 and HIF1a immunostaining revealed greater reductions in score in the tnz7d group compared with controls and other treatment arms, but these differences were not statistically significant.

Conclusion: Further investigation is warranted to determine how tinzaparin sodium and leuprolide acetate modulate the WNT/β-catenin axis for the management of endometriosis.

Keywords: Endometriosis, tinzaparin sodium, leuprolide acetate, WNT/beta-catenin pathway, immunohistochemistry

PRECIS: This study investigates effects of tinzaparin sodium and leuprolide acetate on surgically induced endometriosis in mice, focusing on their impact on the WNT/beta-catenin pathway through gene expression, histopathological, immunohistochemical analyses.

Corresponding Author/Sorumlu Yazar: Gamze Sönmez Ünal, MD,
Numune Hospital, Clinic of Obstetrics and Gynecology, Sivas, Türkiye
E-mail: gmzsnmz@hotmail.com **ORCID ID:** orcid.org/0000-0002-3818-5552

Received/Geliş Tarihi: 26.09.2025 **Accepted/Kabul Tarihi:** 17.12.2025 **Epub:** 29.01.2026 **Publication Date/Yayınlanma Tarihi:** 05.03.2026

Cite this article as: Albak Y, Sönmez Ünal G, Yıldız Ç, Çetin M, Durna Daştan S, Gümüş E, et al. The effect of tinzaparin sodium and leuprolide acetate in an experimental mouse model of endometriosis: the rol of the WNT/beta-catenin pathway. Turk J Obstet Gynecol. 2026;23(1):56-63

Öz

Amaç: Endometriozis, iyi huylu, östrojen bağımlı bir enflamatuvar hastalık olup, ektopik endometriyal implantlarla karakterizedir. Bu çalışma, insanlarda endometriozis tedavisi için WNT/beta-katenin yoluna odaklanan yeni non-steroid ilaçların potansiyelini araştırmayı amaçlamıştır.

Gereç ve Yöntemler: Çalışmaya 40 yetişkin dişi fare dahil edilmiştir. Farelerde cerrahi olarak endometriotik odaklar oluşturulduktan sonra, fareler rastgele beş gruba ayrıldı: 1- Kontrol, 2- Profilaktik leuprolid asetat grubu (leup1d), 3- Profilaktik tinzaparin sodyum grubu (tnz1d), 4- Terapötik leuprolid asetat grubu (leup7d), 5- Terapötik tinzaparin sodyum grubu (tnz7d). Leup1d ve tnz1d gruplarına ameliyat sonrası 24. saatten itibaren profilaktik dozlarda ilaçlar verildi. Leup7d ve tnz7d gruplarına ise ameliyat sonrası 8. günden itibaren terapötik dozlarda ilaçlar verildi. Ameliyat sonrası 14. günde, çıkarılan endometriotik odaklar üzerinde toplam RNA izolasyonu ve gen ekspresyonu analizleri yapıldı. Ek olarak, odaklar hematoksilen ve eozin ile boyandı ve endometriozis için yarı kantitatif olarak puanlandı. HIF1a ve WNT2 için birincil antikorlar kullanılarak immünohistokimyasal analiz yapıldı.

Bulgular: Tinzaparin 7 günlük grupta enflamasyonda azalma görülürken, leuprolid 7 günlük grupta epitel dokusunda azalma görülmüş ve bu da endometriozis skorunda düşüşe yol açmıştır. WNT2 ve HIF1a ile yapılan immünohistokimyasal boyama, kontrol grubu ve diğer gruplara kıyasla tinzaparin 7 günlük grupta endometriozis skorunda daha belirgin bir azalma olduğunu göstermiştir, ancak bu istatistiksel olarak anlamlı değildir.

Sonuç: Endometriozis tedavisinde tinzaparin sodyum ve leuprolid asetatın WNT/beta-katenin yolakları üzerindeki etkilerini doğrulamak için daha fazla çalışma yapılması gerekmektedir.

Anahtar Kelimeler: Enometriyozis, tinzaparin sodyum, löprolid asetat, WNT/beta-katenin, immünhistokimya

Introduction

Endometriosis stands as one of the leading benign gynecological disorders, presenting as a persistent, hormone-dependent inflammatory state that leads to extrauterine deposition of glandular and stromal components[1]. Affected individuals commonly report cyclic pelvic discomfort, menstrual irregularities, difficulty conceiving, pain during intercourse, urinary symptoms, and bowel complaints. Although the condition is widespread, definitive diagnosis typically lags 7-10 years behind symptom onset due to heterogeneous clinical presentations, complex underlying mechanisms, and insufficient rapid diagnostic options[2,3].

The precise origins of this condition remain incompletely understood, with evidence pointing to multiple interacting factors. Scientific work has implicated dysregulated WNT/beta-catenin signaling as a contributor to disease pathobiology[4,5]. Although exact pathogenic sequences remain debated, retrograde menstruation followed by peritoneal implantation represents the prevailing explanatory model. Central to this framework are cellular migration and tissue invasion, which are prerequisites for lesion formation[1-6]. Multiple WNT-responsive genes govern cell growth, directional movement, and matrix penetration[7,8]. Current findings indicate that aberrant pathway activation may enhance the migratory and invasive capacity of shed endometrial cells in patients with this condition[9].

Although classified as non-malignant based on histological criteria, endometriosis exhibits certain biological behaviors resembling cancer. Analogous to neoplastic processes, these lesions demonstrate a capacity for both local extension and distant dissemination[10]. Tinzaparin, a low-molecular-weight heparin, has exhibited cytostatic properties by interfering with the WNT/beta-catenin pathway in cellular studies[11]. Beyond anticoagulation, tinzaparin has shown diverse antitumor activities in preclinical investigations[12].

Estrogen stands as the sole definitively established factor promoting disease development[13]. Therapeutic objectives center on alleviating symptoms, arresting progression, and preserving reproductive capacity. Gonadotropin-releasing hormone (GnRH) agonists are first-line pharmacological options that achieve efficacy by inducing a low-estrogen environment. Leuprolide, acting as a GnRH-receptor agonist, suppresses gonadotropin secretion during sustained administration, inducing a reversible ovarian quiescence that mimics menopause[14].

This investigation systematically evaluated the preventive and therapeutic applications of tinzaparin sodium and leuprolide acetate in a surgically induced mouse model of endometriosis, with emphasis on the involvement of WNT/beta-catenin signaling.

Materials and Methods

All procedures received institutional ethical endorsement from Sivas Cumhuriyet University (approval number: 307; date: 03.09.2019) and adhered to established animal welfare principles. Funding was provided by the university's Scientific Research Unit (grant: T879). The study population consisted of 40 sexually mature female mice (body weight 20-25 g) obtained from the institutional animal facility at Sivas Cumhuriyet University. Housing conditions included an ambient temperature of 21±2 °C, relative humidity of 60±5%, and a standard 12-hour photoperiod. Animals had unrestricted access to standard chow and water. Daily environmental monitoring, weekly body weight assessments, and general health evaluations were conducted throughout the study period.

Induction of Endometriosis

The Vernon-Wilson technique was employed, representing the most widely validated approach for establishing peritoneal endometriosis via autologous uterine tissue grafting[15]. Anesthesia was induced by intramuscular injection of ketamine (50 mg/mL, Ketalar; Eczacibasi Warner-Lambert, İstanbul, Türkiye) combined with xylazine (20 mg/mL,

Rompun; Bayer, İstanbul, Türkiye), each administered in a volume of 1 mL. Following anesthetic stabilization, the right uterine segment was ligated and surgically removed. A 15 mm tissue specimen was obtained using microsurgical instruments and temporarily stored in isotonic saline. The harvested segment was incised longitudinally and fixed to the peritoneal surface adjacent to the mesenteric vasculature, preserving myometrial architecture. The procedure was completed by abdominal closure.

Following surgery, animals were randomized into five experimental cohorts (n=8 each): (1) Untreated controls; (2) Early leuprolide group (100 µg/day, subcutaneously); (3) Early tinzaparin group (10 mg/kg, subcutaneously), with treatment initiated at 24 hours post-surgery for 14 days; (4) Delayed leuprolide group (100 µg/day, subcutaneously); and (5) Delayed tinzaparin group (10 mg/kg, subcutaneously), with treatment initiated on day 7 post-surgery for 14 days.

Tissue Collection

RNA Isolation and Gene Expression Analysis

Terminal procedures were performed on postoperative day 14 by exsanguination. Repeat laparotomy permitted the identification and careful harvesting of established implants. Specimens were transferred to sterile 1.5 mL tubes containing 1 mL of RNA-preservation solution (Ribo Saver, Gene All, Seoul, Korea) and stored at -80 °C until processing.

Total RNA Isolation and cDNA Collection

Total RNA was extracted using the GeneAll® Hybrid-RTM kit according to the manufacturer's specifications (Cat. no.: 305-101; Lot: 30519L09056; Seoul, Korea). Tissue disruption was performed using magnetic bead homogenization. Purified RNA was reconstituted in 100 µL of nuclease-free water, and the concentration was assessed by spectrophotometry (Denovix DS nanodrop). Specimens yielded 20-40 ng of RNA. Reverse transcription was performed using WizScript™ cDNA Synthesis reagents (South Korea), following the recommended thermal parameters.

Gene Expression Analyses

Transcript quantification was performed using SYBR-based detection chemistry (GeneAll Real Amp TM SYBR master mix, Seoul, Korea) on an Applied Biosystems StepOnePlus platform (USA). SYBR Green served as the reporter dye, with ROX as the passive reference dye. Amplification reactions (10 µL total) contained 2X master mix, 50X ROX, gene-specific primers (10 pmol each), nuclease-free water, and template cDNA. Thermal cycling included initial denaturation (95 °C, 10 min) followed by 40 cycles of denaturation (95 °C, 15 sec) and annealing/extension (60 °C, 60 sec). ACTB served as an endogenous control. Relative quantification was performed using the comparative Ct approach (2^-ΔΔCt) to calculate fold-change values.

Histopathological Evaluation

Harvested implants were fixed in 10% phosphate-buffered formalin for 30-36 hours. After standard paraffin processing, 5 µm sections were prepared and subjected to hematoxylin-eosin staining for morphological assessment. Quantitative grading followed established protocols[16]. Stromal tissue proportion was determined by averaging coverage across 10 randomly selected high-magnification fields, while glandular density reflected mean gland counts within these fields. Composite scoring employed was as follows: Grade 0: absent stromal or glandular elements; Grade 1: <25% stromal coverage with a single gland; Grade 2: 25-50% stromal coverage with 2-3 glands; Grade 3: >50% stromal coverage with ≥4 glands.

Immunohistochemical Evaluation

Protein expression of WNT2 and HIF1a was assessed immunohistochemically. Deparaffinized sections underwent antigen retrieval via thermal treatment in citrate buffer (0.01 M, pH 6.0) for 10 minutes. Endogenous peroxidase was quenched using 3% hydrogen peroxide. Non-specific binding was blocked with Ultra V reagent (Thermo Fisher Scientific). Primary antibody incubation (WNT2, 1:100, BT-LAB/BT-AS00007; HIF1α, 1:100, BT-LAB/BT-AP00156) was performed overnight at 4 °C. Sequential application of Primary Antibody Enhancer (TL-015-PB; Thermo Fisher Scientific, USA; 20 min) followed by HRP-conjugated polymer (TL-015-PH; Thermo Fisher Scientific, USA; 30 min at room temperature) preceded chromogenic development with DAB substrate. Harris hematoxylin counterstaining facilitated nuclear visualization under bright-field microscopy (Olympus BX50). Immunoreactivity scoring incorporated staining intensity (0=absent, 1=faint, 2=moderate, 3=intense) and percentage of positive cells (0=none, 1=1-10%, 2=11-50%, 3=>50%)[17]. Final scores (range 0-9) were derived by multiplying these parameters.

Statistical Analysis

Normality of the data distribution was verified prior to analysis. Statistical analyses were performed using GraphPad Prism 5, and outcomes are reported as mean ± standard error of the mean. Intergroup comparisons for transcript data were performed using one-way ANOVA with Tukey's post-hoc correction. Statistical significance was set at $p<0.05$.

Results

Drug treatment effects on messenger RNA levels for 12 target genes in control and experimental groups bearing surgical implants are shown in Figure 1.

Histological and Immunohistochemical Staining of Endometriotic Foci

No observable adverse reactions occurred during the experimental period, with body weights remaining

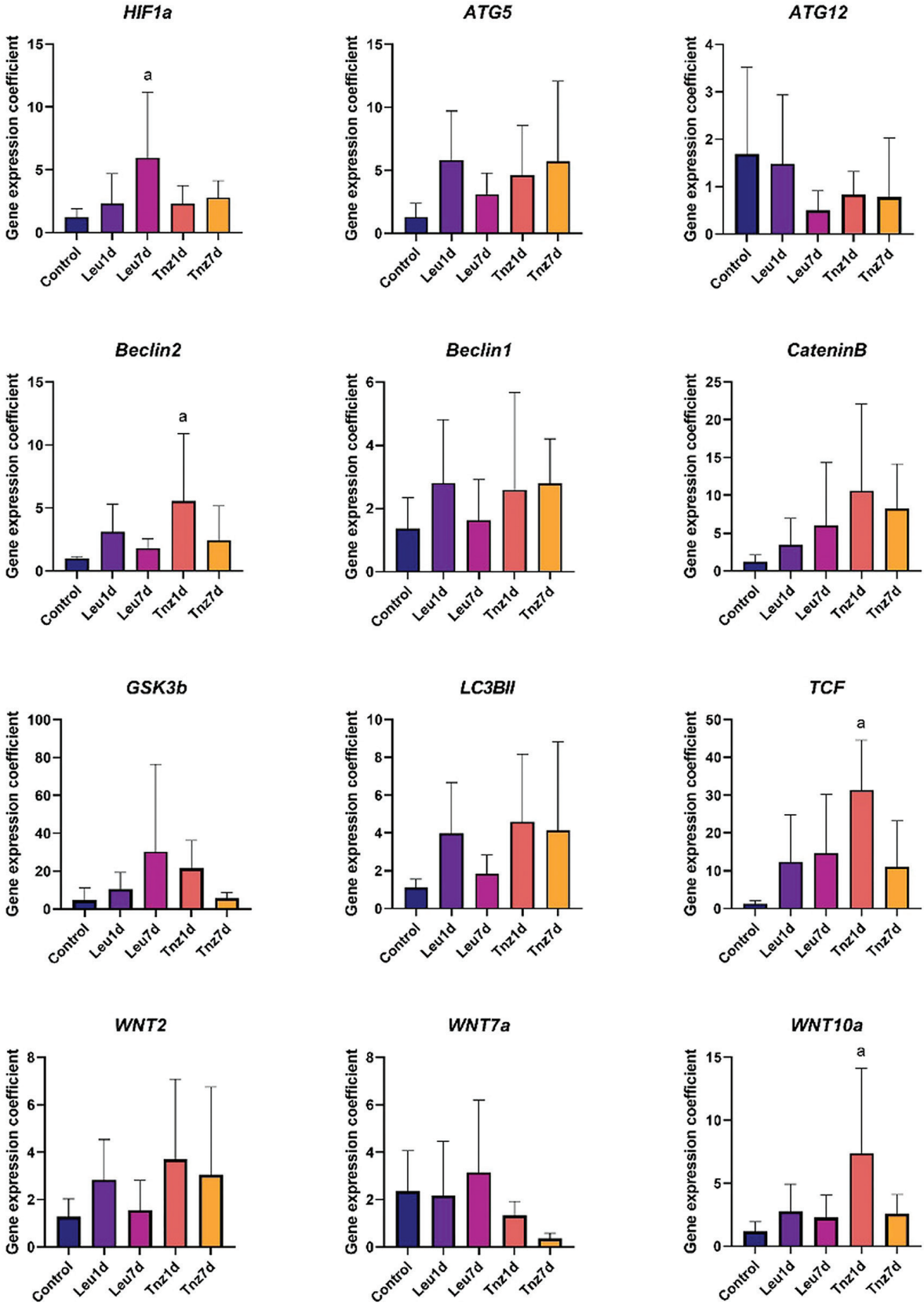

Figure 1. Transcript abundance profiles for control, leu1d, leu7d, tnz1d, and tnz7d groups encompassing WNT2, HIF1a, and related pathway components. Values represent the median and interquartile range

comparable between baseline and endpoint measurements. Representative histological and immunohistochemical preparations showing the expression patterns of WNT2 and HIF1a after treatment with tinzaparin sodium and leuprolide acetate are shown in Figure 2.

Endometriosis Score and Immunohistochemical Staining Score

Comparative analysis revealed that the tnz7d group achieved a statistically significant reduction in disease score, primarily due to decreased inflammatory indices, compared with untreated controls ($p<0.05$; Figure 3). The leup7d group also demonstrated a significant attenuation of epithelial components compared with controls ($p<0.05$; Figure 3). Immunostaining scores for WNT2 and HIF1a did not differ significantly between either treatment group and the controls ($p>0.05$; Figure 3). Furthermore, no significant inter-drug differences emerged ($p>0.05$, Figure 3).

Discussion

This study systematically evaluated the effects of tinzaparin and leuprolide on surgically-induced murine endometriotic implants by integrated immunohistochemical profiling of WNT2 and HIF1a. Both pharmacological agents demonstrated the capacity to attenuate disease severity scores. Although

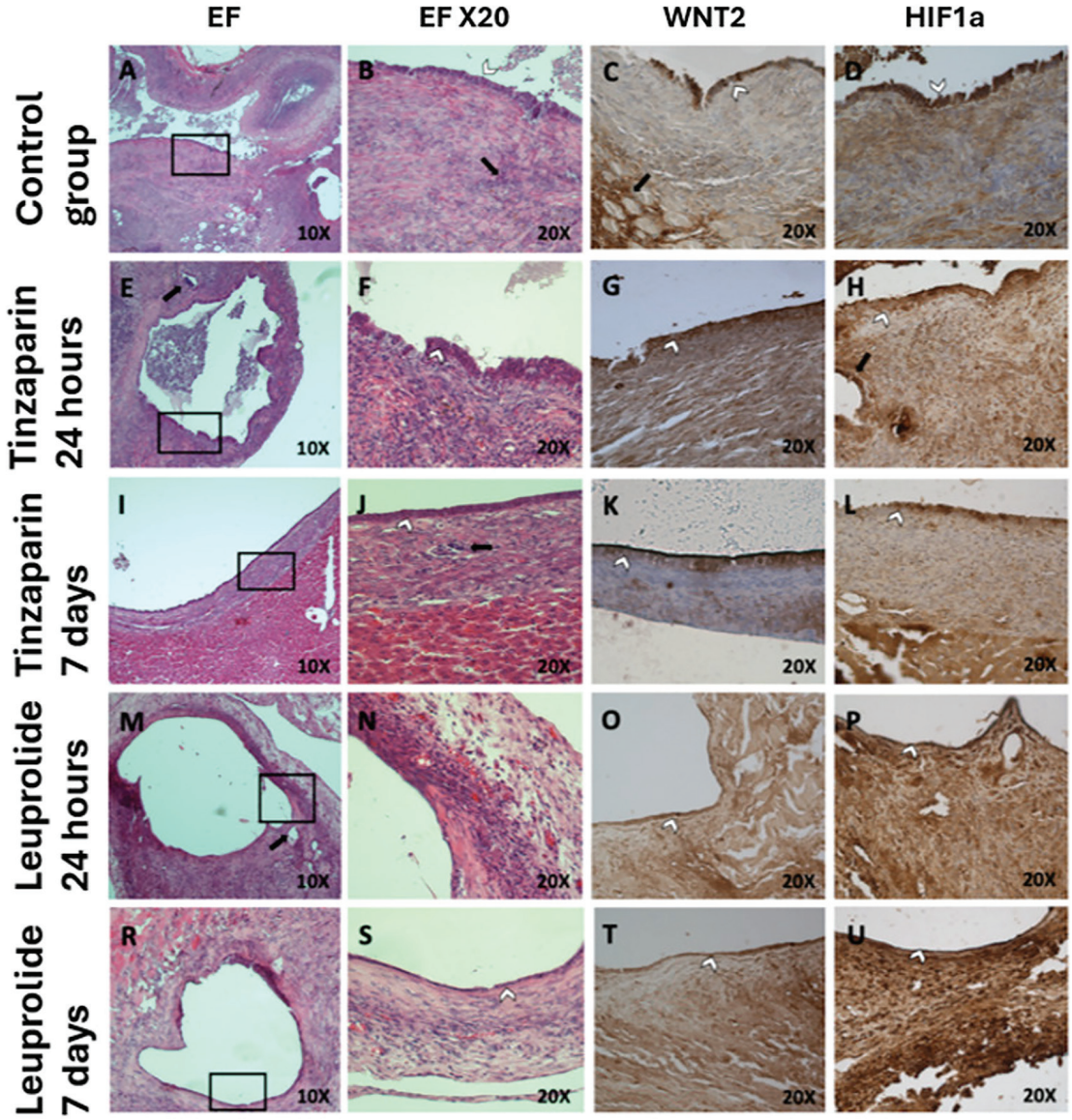

Figure 2. Histological and immunohistochemical findings in endometriotic foci following tinzaparin sodium and leuprolide acetate administration

EF: Endometriotic foci, X20: 20-fold optical magnification

early-treatment groups (initiated on day 1) exhibited numerical reductions in scores relative to untreated controls, these differences were not statistically significant. Notably, the delayed tinzaparin group (tnz7d) produced marked suppression of inflammation, whereas the corresponding leuprolide group (leup7d) significantly reduced epithelial tissue content, and collectively reduced disease burden. Immunostaining analysis revealed that day-7 tinzaparin produced numerically greater score reductions than controls and other treatment arms, although these differences did not reach statistical significance. Leuprolide treatment produced no discernible alteration in immunohistochemical markers relative to controls. The leup7d group exhibited significantly elevated HIF1a transcript levels compared with untreated controls, whereas the tnz1d group showed significant upregulation of BECLIN2/TCF and WNT10a mRNA levels.

The etiopathogenesis of endometriosis and optimal therapeutic approaches have generated sustained scientific discourse. Currently available interventions cannot prevent disease onset. Epidemiological data indicate an approximately 6-7-fold increase in disease frequency among first-degree biological relatives of affected individuals compared with background population rates[18]. Concordance studies in monozygotic twins reveal heritability estimates approaching 75%[19], substantiating genetic predisposition as a significant determinant of susceptibility.

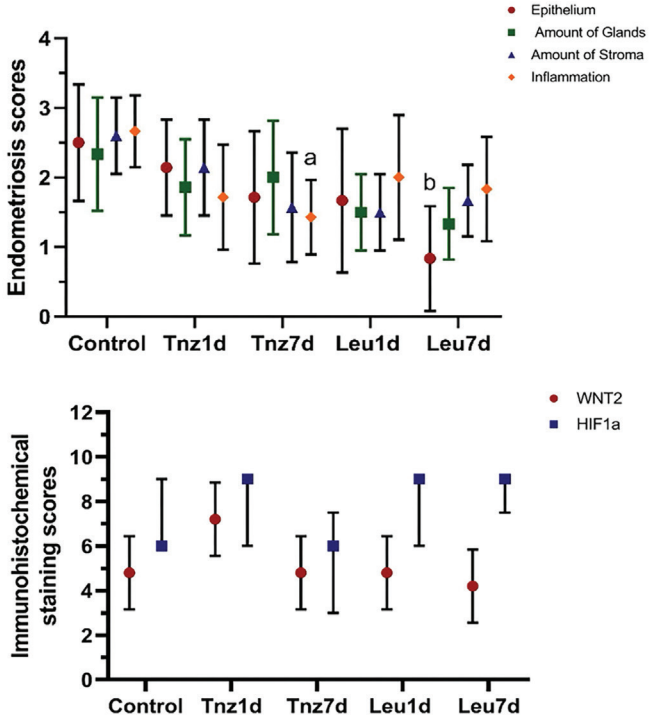

Figure 3. Disease severity scores and immunostaining indices across all experimental groups (control, tnz1d, tnz7d, leup1d, leup7d). Data are shown as median (interquartile range). Inflammatory scores in tnz7d were significantly reduced compared with controls (designated 'a'; $p<0.05$), and epithelial scores in leup7d were significantly decreased compared with the control and tnz1d groups (designated 'b'; $p<0.05$)

Despite an unremarkable cellular architecture, endometriotic lesions exhibit several pathobiological features characteristic of malignancy. Paralleling neoplastic behavior, these implants demonstrate a propensity for regional tissue invasion and dissemination to anatomically remote sites. Such lesions exhibit adhesive properties, enabling attachment to and penetration of adjacent structures. Nevertheless, distinguishing features include the absence of a sustained proliferative drive and of cachexia-inducing metabolic perturbations; fatal outcomes are exceptional[20]. Importantly, endometriosis constitutes an inflammatory condition, and chronic inflammatory states have established associations with elevated malignancy risk.

Selection of tinzaparin derived from encouraging cellular assay data demonstrating cytotoxic efficacy against transformed cells through WNT/beta-catenin pathway interference, supplemented by established clinical safety for thromboembolic prophylaxis across diverse patient populations including pregnant women[11]. These attributes positioned tinzaparin as a rational candidate for evaluating the involvement of pathways in the pathogenesis of endometriosis. Published literature documents tinzaparin's antimetastatic and antiangiogenic activities and its modulation of the WNT pathway; however, systematic investigation in endometriosis, which shares metastatic and angiogenic phenotypes, has remained unexplored.

Over the past five years, investigations have substantiated the functional significance of WNT/β-catenin signaling in governing cellular proliferation, migration, and epithelial–mesenchymal phenotypic transitions in endometriotic cell populations[21,22]. Consequently, pathway-targeting has garnered attention as a promising intervention strategy. Given that the transcriptomic panel examined in our design encompasses WNT-associated elements, our observations demonstrate concordance with prevailing scientific understanding. Nonetheless, given the intricate nature of WNT signaling and its extensive crosstalk with parallel regulatory networks, comprehensive pathway characterization remains necessary to elucidate mechanisms.

Previous reports have documented that heparin-class compounds and structural derivatives possess the capacity to suppress neoplastic cell proliferation, directional migration, and invasive behavior, and potentially enhance chemotherapeutic responsiveness[23]. The pronounced attenuation of inflammation observed in the tnz7d group provides supportive evidence of previously characterized antiangiogenic and anti-inflammatory biological properties. However, definitive determination of whether tinzaparin exerts direct modulatory effects on WNT/β-catenin signaling awaits additional mechanistic investigations.

Our experimental approach examined the relationships of leuprolide and tinzaparin with WNT/beta-catenin pathway activity, which is hypothesized to participate in the establishment of endometriosis. The results demonstrated that both pharmacological interventions modified the transcript abundance of pathway-associated genetic elements. Furthermore, findings indicated that both prophylactic and therapeutic dosing schedules produced detectable alterations in gene expression profiles. Nevertheless, subsequent investigations are necessary to ascertain whether either agent can induce lesion regression or achieve complete resolution, and to delineate optimal therapeutic dosing parameters. This work provides a preliminary characterization of prophylactic versus therapeutic applications of leuprolide and tinzaparin in a murine endometriosis paradigm, emphasizing WNT/beta-catenin pathway contributions to treatment response. Establishing molecular-level cellular effects will require expanded mechanistic studies.

In the current investigation, the effects of tinzaparin and leuprolide on experimentally induced ectopic implants were systematically evaluated in a murine model. Both compounds reduced disease severity metrics, with the delayed-tinzaparin group exhibiting significant inflammatory suppression and the corresponding leuprolide group demonstrating a notable reduction in epithelial tissue. These observations align with accumulating evidence supporting the critical involvement of WNT/β-catenin signaling and HIF1α-driven hypoxia/angiogenesis pathways in disease pathophysiology.

Methodological strengths of this investigation include: (1) parallel assessment of preventive and therapeutic treatment paradigms; and (2) integrated use of histopathological, immunohistochemical, and transcriptomic analyses.

Study Limitations

Recognized study limitations include: (1) Modest experimental group sizes, potentially constraining statistical power; (2) Restricted pathway coverage, with analysis limited to selected target transcripts; (3) Absence of functional cellular assays corroborating molecular observations; (4) Lack of assessment of extended treatment duration; (5) Inherent constraints on translational applicability from murine models to human disease. This work explored alternative pharmacological approaches to the management of endometriosis, investigated disease-prevention potential, and characterized molecular pathways that contribute to lesion development. Our findings are significant for advancing the development of novel therapeutics and expanding clinical drug indications for human patients.

Conclusion

In summary, this investigation provides preliminary evidence suggesting that tinzaparin and leuprolide exert measurable effects on endometriotic tissue. Nonetheless, comprehensive characterization of the involvement of the WNT/β-catenin and HIF1α pathways, coupled with validation studies in human tissue specimens and extended molecular profiling, remains essential for establishing therapeutic potential and clinical translatability.

The authors express appreciation to all contributing investigators whose efforts enabled the completion of this experimental study.

Ethics

Ethics Committee Approval: All procedures received institutional ethical endorsement from Sivas Cumhuriyet University (approval number: 307; date: 03.09.2019).
Informed Consent: Not necessary.

Footnotes

Authorship Contributions

Surgical and Medical Practices: G.S.Ü., Y.A., Ç.Y., Concept: G.S.Ü., Y.A., Ç.Y., M.Ç., A.Ç., A.Ş.T., Design: G.S.Ü., Y.A., M.Ç., S.D.D., E.G., A.Ç., Data Collection or Processing: G.S.Ü., Y.A., S.D.D., E.G., Analysis or Interpretation: G.S.Ü., S.D.D., E.G., A.Ç., Literature Search: G.S.Ü., A.Ç., Writing: G.S.Ü., A.Ç.
Conflict of Interest: No conflict of interest was declared by the authors.
Financial Disclosure: Funding was provided by the university's Scientific Research Unit (grant: T879).

References

1. Giudice LC. Clinical practice. Endometriosis. N Engl J Med. 2010;362:2389-98.
2. Eisenberg VH, Weil C, Chodick G, Shalev V. Epidemiology of endometriosis: a large population-based database study from a healthcare provider with 2 million members. BJOG. 2018;125:55-62.
3. Tomassetti C, D'Hooghe T. Endometriosis and infertility: insights into the causal link and management strategies. Best Pract Res Clin Obstet Gynaecol. 2018;51:25-33.
4. Matsuzaki S, Darcha C, Maleysson E, Canis M, Mage G. Impaired down-regulation of E-cadherin and beta-catenin protein expression in endometrial epithelial cells in the mid-secretory endometrium of infertile patients with endometriosis. J Clin Endocrinol Metab. 2010;95:3437-45.
5. Wu Y, Kajdacsy-Balla A, Strawn E, Basir Z, Halverson G, Jailwala P, et al. Transcriptional characterizations of differences between eutopic and ectopic endometrium. Endocrinology. 2006;147:232-46.
6. Hull ML, Escareno CR, Godsland JM, Doig JR, Johnson CM, Phillips SC, et al. Endometrial-peritoneal interactions during endometriotic lesion establishment. Am J Pathol. 2008;173:700-15.
7. Klaus A, Birchmeier W. WNT signalling and its impact on development and cancer. Nat Rev Cancer. 2008;8:387-98.
8. Wend P, Holland JD, Ziebold U, Birchmeier W. WNT signaling in stem and cancer stem cells. Semin Cell Dev Biol. 2010;21:855-63.
9. Dufour A, Zucker S, Sampson NS, Kuscu C, Cao J. Role of matrix metalloproteinase-9 dimers in cell migration: design of inhibitory peptides. J Biol Chem. 2010;285:35944-56.

10. Wilbur M, Shih I-M, Segars J, Fader A. Cancer implications for patients with endometriosis. Semin Reprod Med. 2017;35:110-6.
11. Pfankuchen DB, Baltes F, Batool T, Li JP, Schlesinger M, Bendas G. Heparin antagonizes cisplatin resistance of A2780 ovarian cancer cells by affecting the Wnt signaling pathway. Oncotarget. 2017;8:67553-66.
12. Pfankuchen DB, Stölting DP, Schlesinger M, Royer HD, Bendas G. Low molecular weight heparin tinzaparin antagonizes cisplatin resistance of ovarian cancer cells. Biochem Pharmacol. 2015;97:147-57.
13. Gurates B, Bulun SE. Endometriosis: the ultimate hormonal disease. Semin Reprod Med. 2003;21:125-34.
14. Anglin HP, Foster WG, Agarwal SK. GnRH agonists and antagonists in endometriosis and adenomyosis therapy. In: Endometriosis and Adenomyosis: Global Perspectives Across the Lifespan. Cham: Springer International Publishing; 2022. p. 577-91.
15. Vernon MW, Wilson EA. Studies on the surgical induction of endometriosis in the rat. Fertil Steril. 1985;44:684-94.
16. Kilico I, Kokcu A, Kefeli M, Kandemir B. Regression of experimentally induced endometriosis with a new selective cyclooxygenase-2 enzyme inhibitor. Gynecol Obstet Invest. 2014;77:35-9.
17. Ragnum HB, Røe K, Holm R, Vlatkovic L, Nesland JM, Aarnes EK, et al. Hypoxia-independent downregulation of hypoxia-inducible factor 1 targets by androgen deprivation therapy in prostate cancer. Int J Radiat Oncol Biol Phys. 2013;87:753-60.
18. Kennedy S, Hadfield R, Westbrook C, Weeks DE, Barlow D, Golding S. Magnetic resonance imaging to assess familial risk in relatives of women with endometriosis. Lancet. 1998;352:1440-1.
19. Foti PV, Farina R, Palmucci S, Vizzini IAA, Libertini N, Coronella M, et al. Endometriosis: clinical features, MR imaging findings and pathologic correlation. Insights Imaging. 2018;9:149-72.
20. Greene AD, Lang SA, Kendziorski JA, Sroga-Rios JM, Herzog TJ, Burns KA. Endometriosis: where are we and where are we going? Reproduction. 2016;152:R63-78.
21. Zhang M, Xu T, Tong D, Li S, Yu X, Liu B, et al. Research advances in endometriosis-related signaling pathways: a review. Biomed Pharmacother. 2023;164:114909.
22. Zhang Y, Sun X, Li Z, Han X, Wang W, Xu P, et al. Interactions between miRNAs and the Wnt/β-catenin signaling pathway in endometriosis. Biomed Pharmacother. 2024;171:116182.
23. Ma SN, Mao ZX, Wu Y, Liang MX, Wang DD, Chen X, et al. The anti-cancer properties of heparin and its derivatives: a review and prospect. Cell Adh Migr. 2020;14:118-28.

Clinical Investigation / Araştırma

DOI: 10.4274/tjod.galenos.2026.05763

Turk J Obstet Gynecol 2026;23(1):64-70

The relationship between oocyte maturation and follicle size: A comparative analysis of 2D and 3D ultrasound

Oosit olgunlaşması ve folikül boyutu arasındaki ilişki: 2D ve 3D ultrasonun karşılaştırmalı analizi

Özge Karaosmanoğlu, Ayşen Yücetürk, Nuri Peker, Ömür Albayrak, Burak Elmas, İlke Özer Aslan, Bülent Tıraş

Acıbadem Maslak Hospital, In Vitro Fertilization Center, İstanbul, Türkiye

Abstract

Objective: To compare the ability of three-dimensional (3D) and conventional two-dimensional (2D) ultrasound to predict oocyte maturity during in vitro fertilization cycles, and to evaluate their contribution to trigger timing and to the determination of optimal cut-off values for maximizing metaphase II (MII) oocyte yield using automated volume-calculation software.

Materials and Methods: Forty-three infertile women who had ≤5 follicles, were younger than 40 years, had a body mass index <30, and had no previous oocyte maturation problems were included in this retrospective study. Follicle diameter was measured using 2D ultrasound, while follicle volume was measured using 3D ultrasound with SonoAVC software. The obtained values were compared with those from MII oocytes, and receiver operating characteristic (ROC) analysis and logistic regression were performed.

Results: A total of 203 oocytes were analyzed; 70% of them were in the MII stage. In the ROC analysis, the optimal cut-off for 2D measurement was determined to be 17.05 mm [area under curve (AUC)=0.737], and for 3D measurement, it was 1.83 cm³ (AUC=0.709). 2D measurements showed specificity, while 3D measurements showed sensitivity. In logistic regression analysis, both 2D diameter and 3D volume were found to be independent predictors of MII oocyte development.

Conclusion: Our findings suggest that 3D ultrasound measurements may provide greater sensitivity for predicting oocyte maturity. However, false-positive results may occur in the presence of multiple or nested follicles, and observer dependence cannot be completely eliminated. Therefore, optimization and large-scale validation studies are needed to improve the accuracy of the method.

Keywords: Oocyte maturation, in vitro fertilization, ultrasonography, imaging, three-dimensional

Öz

Amaç: Bu çalışmada, in vitro fertilizasyon sikluslarında oosit olgunluğunu öngörmede üç boyutlu (3D) ultrason ile ölçülen folikül hacmi ile geleneksel iki boyutlu (2D) ultrason ölçümlerinin karşılaştırılması ve triger zamanlamasında klinik katkılarının araştırılması amaçlanmıştır. Ayrıca, yapay zeka tabanlı otomatik hacim hesaplama yazılım desteğiyle ovaryen hiperstimülasyon döngülerinde maksimum metafaz II (MII) oosit elde edilebilmesi için en uygun cut-off değerinin belirlenmesi hedeflenmiştir.

Gereç ve Yöntemler: Retrospektif olarak planlanan çalışmaya, ≤5 folikülü bulunan, 40 yaş altı, vücut kitle indeksi <30 olan ve daha önce oosit maturasyon problemi bulunmayan 43 infertil kadın dahil edilmiştir. Folikül çapı 2D ultrason ile, folikül hacmi ise SonoAVC yazılımı kullanılarak 3D

PRECIS: Two-dimensional (2D) follicle diameter and three-dimensional follicular volume provide complementary clinical information for predicting oocyte maturity and guiding trigger timing in IVF cycles.

Corresponding Author/Sorumlu Yazar: Özge Karaosmanoğlu MD,
Acıbadem Maslak Hospital, In Vitro Fertilization Center, İstanbul, Türkiye
E-mail: ozge61@gmail.com **ORCID ID:** orcid.org/0000-0001-8184-4747

Received/Geliş Tarihi: 23.12.2025 **Accepted/Kabul Tarihi:** 19.01.2026 **Epub:** 29.01.2026 **Publication Date/Yayınlanma Tarihi:** 05.03.2026

Cite this article as: Karaosmanoğlu Ö, Yücetürk A, Peker N, Albayrak Ö, Elmas B, Özer Aslan İ, et al. The relationship between oocyte maturation and follicle size: a comparative analysis of 2D and 3D ultrasound. Turk J Obstet Gynecol. 2026;23(1):64-70

ultrason ile ölçülmüştür. Elde edilen değerler MII oositler ile karşılaştırılmış, alıcı işletim karakteristiği (ROC) analizi ve lojistik regresyon testleri uygulanmıştır.

Bulgular: Toplam 203 oosit analiz edilmiştir; bunların %70'i MII evresinde bulunmuştur. ROC analizinde 2D ölçüm için en uygun cut-off 17,05 mm [eğrinin altındaki alan (AUC)=0,737], 3D ölçüm için ise 1,83 cm³ (AUC=0,709) olarak belirlenmiştir. 2D ölçümler özgüllük açısından, 3D ölçümler ise duyarlılık açısından daha yüksek performans göstermiştir. Lojistik regresyon analizinde hem 2D çap hem de 3D hacim MII oosit gelişimi için bağımsız prediktör bulunmuştur.

Sonuç: Bulgularımız, literatür ile uyumlu olarak 3D ultrason ölçümlerinin oosit olgunluğunu öngörmede duyarlılık avantajı sağlayabileceğini göstermektedir. Ancak çok sayıda veya iç içe folikül varlığında yanlış pozitif sonuçlar oluşabilmekte, ayrıca gözlemci bağımlılığı tamamen ortadan kalkmamaktadır. Bu nedenle yöntemin doğruluğunun artırılmasına yönelik optimizasyon ve geniş ölçekli doğrulama çalışmalarına ihtiyaç vardır.

Anahtar Kelimeler: Oosit maturasyonu, in vitro fertilizasyon, ultrasonografi, görüntüleme, üç boyutlu

Introduction

Infertility is a significant health issue affecting millions of individuals worldwide. In vitro fertilization (IVF) procedures, which are part of assisted reproductive technologies, are among the most commonly used and promising treatment methods for infertile couples. IVF success has many components; however, oocyte maturity, particularly the number of metaphase II (MII) oocytes, is a critical factor directly affecting embryo quality, implantation rates, and live birth rates[1-3].

Three-dimensional ultrasound (3D-US), a significant milestone in gynecological and obstetric diagnostic imaging, has been increasingly adopted clinical practice in recent years. In obstetrics, it is widely used to examine fetal malformations and to perform facial assessments[4,5]. In gynecology, its primary applications include the evaluation of uterine anomalies using sonohysterography and the detection of intracavitary pathologies. However, antral follicle counting and follicle monitoring are still routinely performed using two-dimensional ultrasound (2D-US)[5,6]. This raises the question of whether 3D ultrasound can replace 2D ultrasound for assessing oocyte maturity via follicular volume measurements and for determining trigger timing.

Transvaginal 2D ultrasound has been widely used in recent years for the evaluation, treatment planning, and follow-up of infertile women. This method has become the preferred approach for determining the number, size, and volume of follicles in real time. However, follicle monitoring with 2D-US has limitations such as manual measurements, interobserver variability, increased time requirements, and errors related to follicle shape[7,8]. In contrast, 3D-US allows imaging of the entire ovarian tissue in a single sonographic section. Follicle count, diameter, and volume measurements are performed using automated volume calculation software. This software automatically identifies fluid-filled structures in the area of interest and reports the size and volume information for each follicle. Although 3D-US has been shown to provide reliable estimates of follicle size, it is still used to a limited extent to monitor ovarian response to stimulation[9-11]. Thus, current studies indicate that the contribution of 3D-US to predicting oocyte maturity and trigger timing remains incompletely clarified in clinical terms[12,13].

This study aimed to compare follicle volume measured by 3D-US with 2D diameter measurements in predicting oocyte maturity during IVF cycles and to investigate their contributions to more accurate trigger timing. Additionally, the study aimed to determine the optimal cut-off value to achieve the maximum number of MII oocytes during ovarian hyperstimulation cycles using artificial intelligence-based software.

Materials and Methods

Study Design and Participants

This retrospective study included 43 infertile women who presented to the IVF center at Acıbadem Hospital and underwent IVF with controlled ovarian stimulation.

Inclusion criteria were defined as patients who started stimulation for IVF with an antagonist protocol, were under 40 years of age, and had ≤5 follicles in both ovaries. Patients with a history of oocyte maturation problems, endometrioma, or smoking, or who had a body mass index (BMI) ≥30, were excluded from the study.

The study was approved by the Acıbadem Medical Research Ethics Committee (Acıbadem) under decision number 2025-08/61, dated: 22.05.2025. Informed consent was obtained from all participants.

Ovarian Stimulation Protocol

During controlled ovarian hyperstimulation, the gonadotropin-releasing hormone antagonist (Cetrorelix, Merck Serono, Darmstadt, Germany) was initiated at 250 µg/day when the leading follicle diameter reached ≥14 mm and was continued until the trigger day.

The trigger was administered when at least half of the follicles were ≥17 mm in diameter as determined by ultrasound. For this purpose, recombinant human chorionic gonadotropin (1000-2000 IU, Ovitrelle, Merck, Lyon, France) and triptorelin acetate, 0.1 mg/mL (two doses; Gonapeptyl, Ferring Pharmaceuticals) were used. Oocyte retrieval (OPU) was performed under sedation 36 hours after the trigger.

Ultrasound Evaluations

Patients' ultrasonographic examinations were performed by a single specialist with at least 10 years of experience in IVF. All

evaluations were performed using a Voluson S8 (GE Medical Systems, Zipf, Austria) equipped with a 5-9 MHz transvaginal volume probe.

First, follicles were measured using 2D ultrasound, and their number and size in both ovaries were recorded. Then the ovary's maximum diameter was measured, and the image was fixed for 3D volume scanning. Follicle volumes were calculated semi-automatically using SonoAVC software.

In cases where the software mistakenly evaluated vascular cross-sections or free fluid areas as follicles, the cross-sections were reacquired and volume measurements were repeated (Figure 1).

Since the primary goal was to track each oocyte individually and match it to the MII stage, cases with a large number (>20) of follicles were excluded because reliable follicle-oocyte matching could not be performed (Figure 2).

Oocyte Retrieval and Evaluation

Follicles marked on ultrasound were aspirated individually during OPU. Oocytes were evaluated by embryologists after denudation, and their maturity status was recorded.

Statistical Analysis

Descriptive statistics were calculated for all variables. Continuous variables [2D follicle measurements (mm) and 3D follicle volumes (cm^3)] were summarized as mean ± standard deviation when normally distributed and as median (minimum-maximum) when not normally distributed. Normality was assessed using the Shapiro-Wilk test. Categorical variables were presented as counts and percentages. Receiver operating characteristic (ROC) curve analyses were performed separately for 2D and 3D measurements to evaluate the discriminatory power of follicle size to predict MII oocytes. The area under the curve (AUC) and 95% confidence intervals (CIs) were reported. The optimal cut-off points were determined using the Youden index, and diagnostic performance was summarized by sensitivity, specificity, positive predictive value (PPV), and negative predictive value (NPV). Additionally, logistic regression analyses were performed to predict MII outcome from follicle size. Logistic regression analyses were performed using univariate models. In model 1, 3D follicular volume was used as a continuous variable; in model 2, volume was categorized according to a cut-off value of 1.83 cm^3 (<1.83 vs. ≥1.83 cm^3). The same analyses were performed in parallel for 2D measurements. All analyses were performed using R software (version 4.4.2). P<0.05 was considered statistically significant.

Results

Among the analyzed oocytes, the mean 2D follicle measurement was 16.54±3.66 mm (range: 6.4-24.0 mm), and the mean 3D follicle volume was 2.37±1.26 cm^3 (range: 0.20-5.41 cm^3). Of the 203 oocytes evaluated, 142 (70.0%) were in the MII stage, 14 (6.9%) were in the metaphase I (MI) stage, and 15 (7.4%) were in the germinal vesicle stage. Additionally, 13 (6.0%) of the 202 oocytes examined were at the MA stage (Table 1).

ROC analysis of 2D follicular measurements determined an optimal cut-off value of 17.05 mm (sensitivity=0.67, specificity=0.79, PPV=0.88, NPV=0.51). Below this threshold, the MII rate was 49.5% (47/95), while above the threshold, this rate increased to 88.0% (95/108). This finding indicates that larger 2D follicular diameters are significantly associated with the likelihood of reaching MII (Figure 3; Table 2).

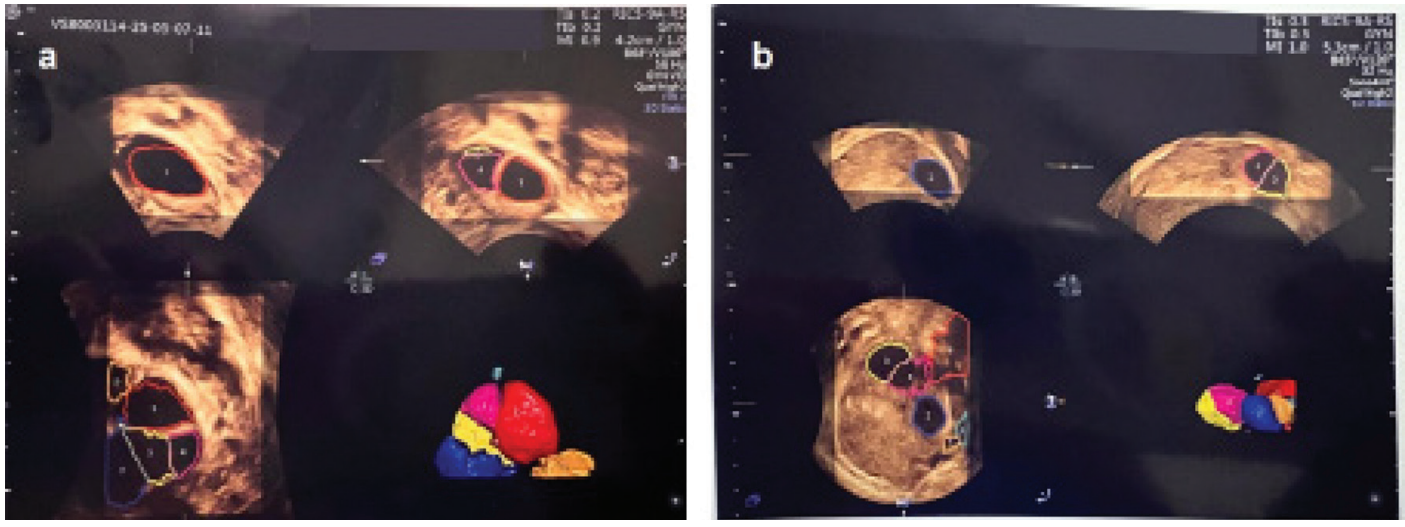

Figure 1. Examples of semi-automatic measurement of follicle volumes using three-dimensional ultrasound and SonoAVC software. Each follicle is marked with a different color and numbered. (a) Number "2" was incorrectly identified as a follicle by the software and required manual correction as it was a blood vessel section. (b) Number "1" is an example of free fluid around the ovary being detected as a follicle by the software

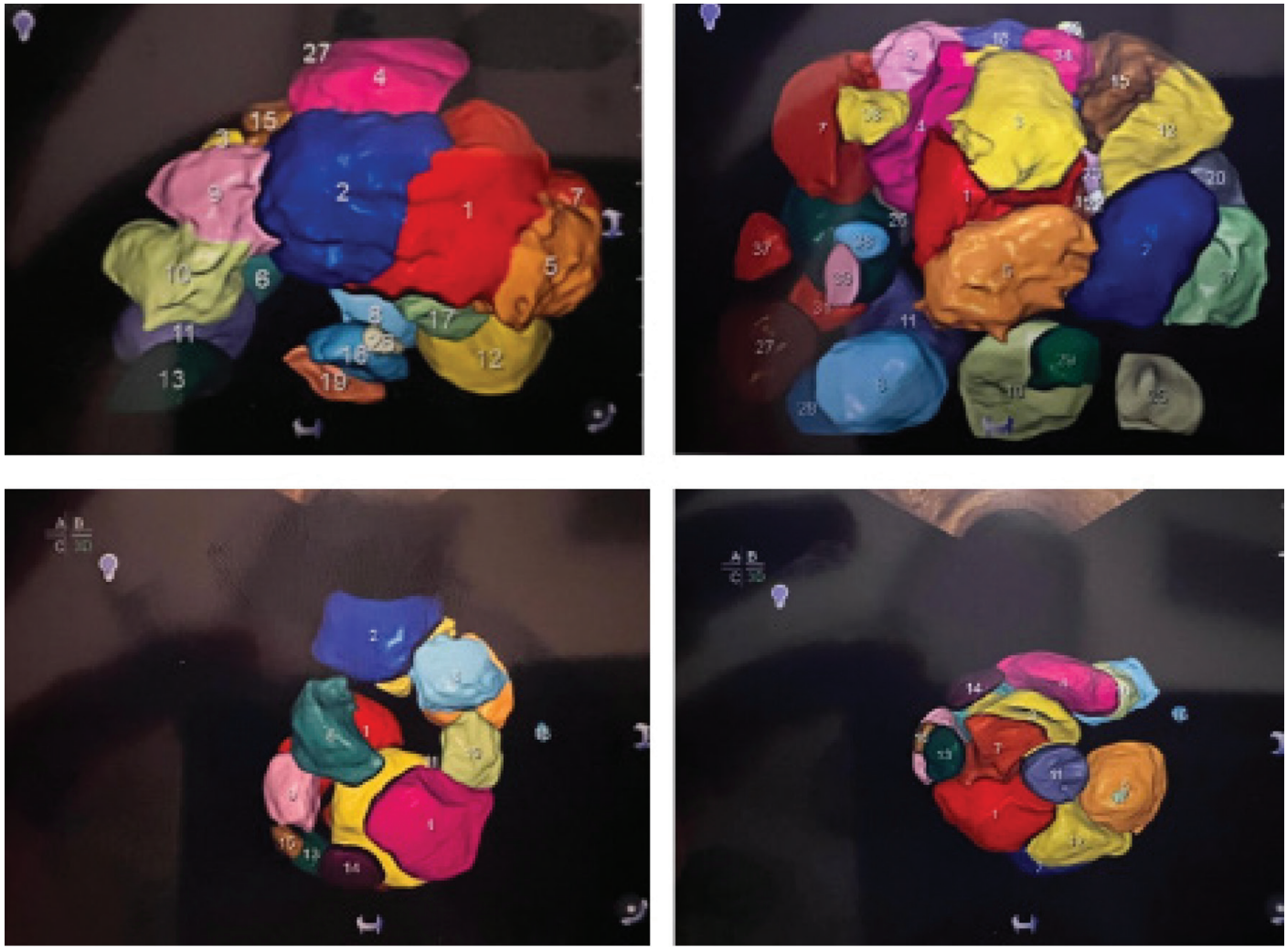

Figure 2. Examples of volume reconstruction using three-dimensional ultrasound and SonoAVC software in different cases with multiple follicles. Each follicle is marked with a different color and numbered. Since follicle-oocyte matching cannot be reliably performed in such cases, they were not included in the study to maintain methodological consistency

Table 1. Distribution of oocytes according to 2D follicle measurements, 3D follicle volumes, and maturation stages

Variable	Mean	SD	Min	Max
2D measurement	16.54	3.66	6.4	24.00
3D volume	2.37	1.26	0.2	5.41
	N	Count (1)	Count (0)	% (1)
MII	203	142	61	70
MI	203	14	189	6.9
GV	203	15	188	7.4
MA	202	13	189	6.0

SD: Standard deviation, MII: Metaphase II, MI: Metaphase I, GV: Germinal vesicle, MA: Metaphase arrest, Min: Minimum, Max: Maximum, 3D: Three-dimensional, 2D: Two-dimensional

The cut-off value of 17.05 mm, determined for 2D measurement, provided a meaningful distinction for predicting MII oocytes. The MII rate in follicles below this threshold value was approximately half that in follicles above the threshold, where a significantly higher rate of 88.0% was observed. This finding supports the utility of 2D measurements in clinical decision-making.

ROC analysis revealed an AUC of 0.709 for 3D follicular volume. This value indicates that 3D volume measurement has moderate discriminatory power for distinguishing oocytes that reach the MII stage. In the literature, AUC values between 0.70 and 0.80 are considered acceptable, between 0.80 and 0.90 are considered good, and values >0.90 are considered to indicate excellent discriminatory power. The ROC curve lying above the diagonal reference line indicates that the model performed better than random guessing. Furthermore,

the curve approaching the upper left corner indicates that certain cutoff points (e.g., 1.83 cm³) provide an appropriate balance between sensitivity and specificity. Clinically, follicles with larger 3D volumes were more likely to reach the MII stage (Figure 4).

Table 2. MII rates according to 2D follicle diameter cut-off values

2D cut-off group	Follicle count	MII number	Ratio (%)
<17.05 mm	95	47	49.5%
≥17.05 mm	108	95	88.0%

MII: Metaphase, 2D: Two-dimensional

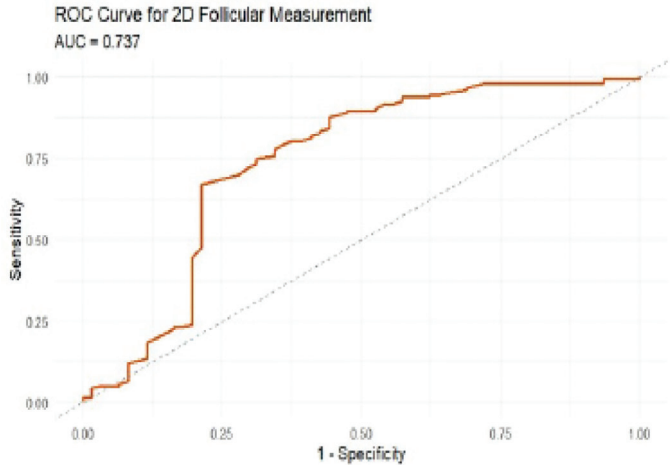

Figure 3. ROC curve for 2D follicle measurement. The analysis determined a cutoff value of 17.05 mm as the optimal threshold (AUC=0.737). This value has moderate discriminatory power in predicting oocytes that reach the metaphase II stage. The curve indicates an appropriate balance between sensitivity and specificity

ROC: Receiver operating characteristic, AUC: Area under the curve, 2D: Two-dimensional

Table 3. MII rates according to the 3D follicular volume cut-off value

3D cut-off group	Follicle count	MII number	Ratio (%)
<1.83 cm³	74	34	45.9%
≥1.83 cm³	129	108	83.7%

3D: Three-dimensional, MII: Metaphase

This analysis contributes to the objective selection of a specific cut-off value and to the decision-making process in clinical practice (Table 3).

ROC analysis for 3D follicular volume determined an optimal cut-off value of 1.83 cm³. Below this threshold, the MII rate was 45.9% (34/74), while above the threshold, this rate increased to 83.7% (108/129). At this cut-off value, sensitivity was 0.76, specificity was 0.66, PPV was 0.84, and NPV was 0.54. These findings indicate that 3D follicular volume has significant discriminatory ability to predict the likelihood of reaching MII.

Logistic regression analysis showed that both 2D follicular diameter and 3D follicular volume are meaningful predictors of MII oocyte development. Larger follicle size was associated with a significantly increased probability of reaching MII, both when analyzed as a continuous variable and when categorized using cutoff values from ROC analysis (Table 4). Both 2D follicle diameter and 3D follicle volume were found to be significant predictors of reaching the MII stage. For continuous variables, each one-unit increase significantly increased the likelihood of achieving MII. When ROC-derived cut-off values were applied, larger follicle sizes also were associated with a marked increase in the likelihood of achieving MII.

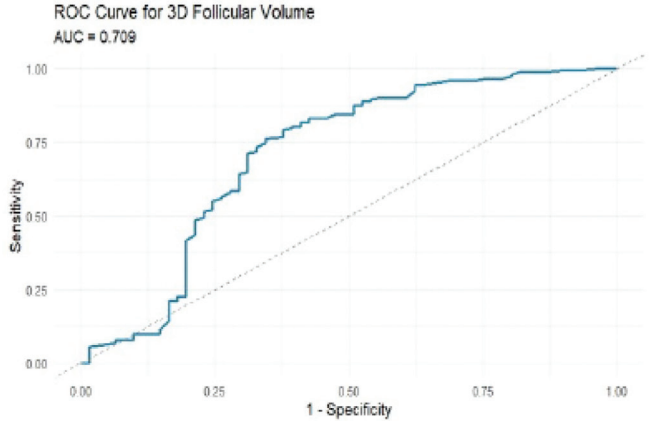

Figure 4. ROC curve for 3D follicular volume. The curve indicates that the model has moderate discriminatory power in predicting oocytes that reach the metaphase II stage (AUC=0.709)

ROC: Receiver operating characteristic, AUC: Area under the curve, 3D: Three-dimensional

Table 4. Logistic regression analysis showing the relationship between follicle size and the probability of obtaining MII oocytes

Variable	OR	95% CI	p-value
3D volume (continuous)	1.85	(1.42; 2.47)	0.0000126000
3D volume (≥1.83 vs. <1.83 cm³)	6.05	(3.18; 11.82)	0.0000000681
2D diameter (continuous)	1.30	(1.19; 1.44)	0.0000000521
2D diameter (≥17.05 vs. <17.05 mm)	7.46	(3.78; 15.62)	0.0000000235

OR: Odds ratio, CI: Confidence interval, MII: Metaphase

3D volume (continuous): For each 1 cm³ increase, the odds of achieving MII increased 1.85-fold [odds ratio (OR) = 1.85, 95% CI: 1.42-2.47].
For 3D volume (cut-off ≥1.83 cm³), follicles above this threshold showed a sixfold higher probability of obtaining MII compared to those with smaller volumes (OR=6.05, 95% CI: 3.18-11.82).
2D diameter (continuous): Each 1-mm increase was associated with a 1.30-fold higher likelihood of achieving MII (OR=1.30, 95% CI: 1.19-1.44).
2D diameter (cut-off ≥17.05 mm): Larger follicles had approximately 7.5-fold higher odds of MII than smaller ones (OR=7.46, 95% CI: 3.78-15.62).

Discussion

Many researchers have recently questioned the accuracy of the aforementioned 2D measurement approach, particularly during controlled ovarian hyperstimulation cycles, due to the irregular shape of follicles.[5,6] Measuring follicle size often yields inaccurate results because follicles, which are actually 3D structures, are assessed as 2D structures, even in ovaries containing few or small follicles. Current literature on the accuracy of 3D and 2D ultrasound in IVF follicular assessment shows that 3D ultrasound is more accurate than real-time 2D ultrasound in measuring follicular size and volume[14,15]. However, software errors and technical limitations have been observed in 3D ultrasound measurements, and the accuracy and clinical utility of the method require further optimization. In this study, both 2D-US and 3D-US measurements were found to be valuable in predicting oocyte maturity. Analyses revealed that 2D measurements reduced false positives, whereas 3D measurements were more sensitive in detecting mature oocytes. These findings indicate that both methods contribute to determining trigger timing from different perspectives and may be complementary. 3D-US provides practical benefits in assessing maturity, especially in patients with few follicles, but 2D examinations remain important in the clinical process to validate the measurements. Additionally, these results suggest that 3D-US may offer a significant advantage in clinical practice, particularly in patients with a low follicle count and a BMI <30.
Our findings are consistent with the existing literature. For instance, Shmorgun et al.[15] reported that 3D volume measurements showed a higher, though limited, correlation with oocyte maturation than did 2D diameter measurements. Hernández et al.[16] demonstrated a significant relationship between follicle volume classes and the number of mature oocytes based on automatic volume measurements performed with SonoAVC software. In a more recent study, Rodr´guez-Fuentes et al.[2] showed that a follicular volume >0.56 cm³ on the trigger day could predict the retrieval of mature oocytes, but sensitivity and specificity were moderate. Similarly, in our study, 3D volume measurements showed moderate discriminatory power, and our analyses determined the most appropriate cut-off value to be 1.83 cm³. This finding indicates that threshold values may vary across populations, but 3D-US generally offers greater sensitivity. In addition, a newly published study by Yang et al.[14] reported that follicular sphericity was predictive only in patients with normal ovarian reserve, had limited discriminatory power for MII oocytes, and showed no correlation with clinical outcomes in the low-reserve group. These findings indicate that the clinical use of volume- and shape-based 3D parameters still requires optimization and larger, multicenter validation studies.
These studies commonly conclude that the conventional approach based on follicle diameter has limitations and that volume-based assessment has the potential to guide clinical decisions more accurately. Our study supports these findings, particularly among a homogeneously selected group of patients with few follicles.
Automated 3D ultrasound software, such as SonoAVC, saves clinicians time by enabling rapid evaluation of follicles in the correct sections and significantly reduces observer dependence often seen in manual 2D measurements. However, in this study evaluation was difficult in patients with a large number of follicles, because closely adjacent or intertwined follicles were sometimes perceived as a single follicle. This situation necessitated that the physician performing the ultrasound also conduct a 2D examination to verify the measurements. Furthermore, vascular structures in the ovarian section or surrounding fluids can also be interpreted as follicles by the software, potentially leading to misleading results in volume measurements. Indeed, these limitations reported in early studies such as Coelho Neto et al.[7] and Vandekerckhove et al.[17], these limitations, which have been reported in early studies, are still valid in some other recent studies [Rodr´guez-Fuentes et al.[2]], highlighting the need for optimization and validation in the clinical use of the method.
Our findings indicate that 2D-US follicle diameter remains reliable for routine trigger decisions, whereas 3D follicle volume measurement may provide additional value in specific clinical scenarios, particularly for patients with low follicle counts or borderline follicle growth. The higher sensitivity of 3D-US may help clinicians avoid premature triggering in such cases. However, due to software limitations and the risk of false-positive measurements caused by overlapping follicles, the routine use of 3D ultrasonography should be reserved for complex or uncertain cases, rather than replacing traditional 2D assessment.

Study Limitations

The main limitations of this study include its retrospective nature and its relatively small, homogeneous study population. These conditions may also limit the generalizability of the findings. The exclusion of patients with a high number of follicles raises questions regarding the applicability. Furthermore, when interpreting the results, the technical

limitations of automated 3D volume measurements and the absence of clinical outcomes beyond oocyte maturity should be considered.

Conclusion

Our study demonstrates that follicular volume measurements obtained by 3D ultrasound may be clinically valuable for predicting oocyte maturity and determining trigger timing. However, significant limitations of the method include the possibility of measurement errors, particularly in patients with multiple or overlapping follicles, and the potential for misidentification of blood vessels or areas of free fluid as follicles by the software. Therefore, while 3D measurements offer clinical benefits, further optimization studies are needed for the method's clinical application.

Ethics

Ethics Committee Approval: The study was approved by the Acıbadem Medical Research Ethics Committee (Acıbadem) under decision number 2025-08/61, dated: 22.05.2025.
Informed Consent: Informed consent was obtained from all participants.

Footnotes

Authorship Contributions

Surgical and Medical Practices: Ö.K., A.Y., N.P., Ö.A., B.E., İ.Ö.A., B.T., Concept: Ö.K., A.Y., N.P., Ö.A., B.E., İ.Ö.A., B.T., Design: Ö.K., A.Y., N.P., Ö.A., B.E., İ.Ö.A., B.T., Data Collection or Processing: Ö.K., A.Y., N.P., Ö.A., B.E., İ.Ö.A., B.T., Analysis or Interpretation: Ö.K., A.Y., N.P., Ö.A., B.E., İ.Ö.A., B.T., Literature Search: Ö.K., A.Y., N.P., Ö.A., B.E., İ.Ö.A., B.T., Writing: Ö.K., A.Y., N.P., Ö.A., B.E., İ.Ö.A., B.T.
Conflict of Interest: No conflict of interest was declared by the authors.
Financial Disclosure: The authors declared that this study received no financial support.

References

1. Practice Committee of the American Society for Reproductive Medicine. Electronic address: asrm@asrm.org; Practice Committee of the American Society for Reproductive Medicine. Testing and interpreting measures of ovarian reserve: a committee opinion. Fertil Steril. 2020;114:1151-7.
2. Rodr´guez-Fuentes A, Hernández J, Rouleau JP, Mart´n-Vasallo P, Palumbo A. A follicular volume of >0.56 cm3 at trigger is the cutoff to predict oocyte maturity: a starting point for novel volume-based triggering criteria. Fertil Steril. 2024;121:991-9.
3. Sunkara SK. Number of oocytes and IVF outcomes: real-world evidence. Best Pract Res Clin Obstet Gynaecol. 2023;89:102341.
4. Coticchio G, Dal Canto M, Mignini Renzini M, Guglielmo MC, Brambillasca F, Turchi D, et al. Oocyte maturation: gamete–somatic cell interactions, meiotic resumption, cytoskeletal dynamics and cytoplasmic reorganization. Hum Reprod Update. 2015;21:427-54.
5. Salim R, Woelfer B, Backos M, Regan L, Jurkovic D. Reproducibility of three-dimensional ultrasound diagnosis of congenital uterine anomalies. Ultrasound Obstet Gynecol. 2003;21:578-82.
6. Hirshfeld-Cytron J. Three-dimensional follicle measurements: coming soon to a clinic near you? Fertil Steril. 2024;121:964-5.
7. Coelho Neto MA, Ludwin A, Borrell A, Benacerraf B, Dewailly D, da Silva Costa F, et al. Counting ovarian antral follicles by ultrasound: a practical guide. Ultrasound Obstet Gynecol. 2018;51:10-20.
8. Rodrigues ARDO, de Sá RA, Velarde GC, Valle MP, Nóbrega BN, Roque M, et al. Comparing two- and three-dimensional antral follicle count in patients with endometriosis. J Med Ultrasound. 2022;30:282-6.
9. Kyprianou MA, Dakou K, Lainas GT, Xenariou M, Makris A, Lainas TG. Two-dimensional ultrasound results in underestimation of the ovarian follicle size compared to automated three-dimensional imaging in women undergoing IVF. J Ultrasound. 2025;28:27-33.
10. Singh N, Usha BR, Malik N, Malhotra N, Pant S, Vanamail P. Three-dimensional sonography-based automated volume calculation (SonoAVC) versus two-dimensional manual follicular tracking in in vitro fertilization. Int J Gynaecol Obstet. 2015;131:166-9.
11. Peres Fagundes PA, Chapon R, Olsen PR, Schuster AK, Mattia MMC, Cunha-Filho JS. Evaluation of three-dimensional SonoAVC ultrasound for antral follicle count in infertile women: its agreement with conventional two-dimensional ultrasound and serum levels of anti-Müllerian hormone. Reprod Biol Endocrinol. 2017;15:96.
12. Abdallah A, Shawki H, Abdel-Rasheed M, Salem S, Hosni M. Role of 3-D transvaginal ultrasonography in women undergoing in vitro fertilization/intra-cytoplasmic sperm injection. Ultrasound Med Biol. 2020;46:1424-7.
13. Revelli A, Martiny G, Delle Piane L, Benedetto C, Rinaudo P, Tur-Kaspa I. A critical review of bi-dimensional and three-dimensional ultrasound techniques to monitor follicle growth: do they help improving IVF outcome? Reprod Biol Endocrinol. 2014;12:107.
14. Yang J, Wang M, Zhou D, Ye H, Huang G, Lian X, et al. Follicular sphericity based on three-dimensional transvaginal ultrasound algorithms predicts ovarian responsiveness to in vitro fertilization. J Ovarian Res. 2025;18:197.
15. Shmorgun D, Hughes E, Mohide P, Roberts R. Three-dimensional follicular volume measurements have a stronger correlation with the number of mature oocytes retrieved than 2-D measurements. Fertil Steril. 2010;93:606-10.
16. Hernández J, Rodr´guez-Fuentes A, Puopolo M, Palumbo A. Follicular volume predicts oocyte maturity: a prospective cohort study using three-dimensional ultrasound and SonoAVC. Reprod Sci. 2016;23:1442-8.
17. Vandekerckhove F, Bracke V, De Sutter P. The value of automated follicle volume measurements in IVF/ICSI. Front Surg. 2014;1:18.

Clinical Investigation / Araştırma

DOI: 10.4274/tjod.galenos.2026.94515

Turk J Obstet Gynecol 2026;23(1):71-80

A preliminary investigation of gene expression and levels of FSH, IL-10, and TNF-α and histological staining in natural aging mice

Doğal yaşlanan farelerde gen ifadesi ve FSH, IL-10 ve TNF-α düzeyleri ile histolojik boyama üzerine bir ön araştırma

Yulice Soraya Nur Intan[1,2], Soetrisno Soetrisno[2,3], Abdurahman Laqif[3], Dono Indarto[4,5]

[1]*Universitas Islam Sultan Agung Faculty of Medicine, Department of Obstetrics and Gynecology, Semarang, Indonesia*

[2]*Universitas Sebelas Maret Faculty of Medicine, Doctoral Program of Medical Sciences, Surakarta, Indonesia*

[3]*Universitas Sebelas Maret Faculty of Medicine, Dr. Moewardi General Hospital, Department of Obstetrics and Gynecology, Surakarta, Indonesia*

[4]*Universitas Sebelas Maret Faculty of Medicine, Department of Physiology, Surakarta, Indonesia*

[5]*Universitas Sebelas Maret Faculty of Medicine, Biomedical Laboratory, Surakarta, Indonesia*

Abstract

Objective: This study aimed to compare estrous cycle patterns, serum hormone and cytokine levels, gene expression, and ovarian morphology between healthy and aging mice, to evaluate their potential as models of reproductive aging.

Materials and Methods: Female BALB/c mice older than 9 months were used as the aged group and were compared with healthy controls (6-8 weeks old). Estrous phases were monitored for six days using vaginal cytology. Ovarian morphology was analyzed using hematoxylin and eosin staining and immunohistochemistry. Serum levels of follicle-stimulating hormone (FSH), interleukin (IL)-10, and tumor necrosis factor-alpha (TNF-α) were measured by enzyme-linked immunosorbent assay. Gene expression of IL-10 and TNF-α was assessed by reverse transcription polymerase chain reaction.

Results: Healthy mice cycled through all estrous phases, whereas aging mice were predominantly arrested in diestrus and exhibited increased immune-cell infiltration and inflammatory changes. Ovarian histology showed enlargement, fibrosis, and the presence of non-functional structures. Follicle counts were reduced in aging mice, though the reduction was not statistically significant. Serum FSH (1.37±0.20 vs. 1.10±0.03 pg/mL) and TNF-α (37.05±17.31 vs. 21.57±4.62 pg/mL) were significantly elevated, whereas IL-10 was significantly decreased (4.53±0.32 vs. 6.23±0.99 pg/mL) ($p<0.05$). TNF-α mRNA levels increased and IL-10 mRNA levels decreased; however, these changes were not statistically significant.

Conclusion: Aging BALB/c mice exhibit disrupted estrous cycles, ovarian fibrosis, increased FSH and TNF-α, and reduced IL-10, changes that resemble those associated with menopause. These findings support the use of aging BALB/c mice as a model for reproductive aging and therapeutic studies.

Keywords: Aging, estrous cycle, FSH, IL-10, TNF-α

Öz

Amaç: Bu çalışma, reprodüktif yaşlanma modelleri olarak potansiyellerini değerlendirmek amacıyla, sağlıklı ve yaşlanan fareler arasında östrus döngüsü paternlerini, serum hormon ve sitokin düzeylerini, gen ifadesini ve yumurtalık morfolojisini karşılaştırmayı amaçlamıştır.

Gereç ve Yöntemler: Dokuz aydan büyük dişi BALB/c fareler yaşlı grup olarak kullanıldı ve sağlıklı kontrollerle (6-8 haftalık) karşılaştırıldı. Östrus fazları altı gün boyunca vajinal sitoloji kullanılarak izlendi. Yumurtalık morfolojisi hematoksilen ve eozin boyama ve immünohistokimya kullanılarak

PRECIS: This study demonstrates that aging BALB/c mice exhibit disrupted estrous cycles, ovarian fibrosis, altered cytokine expression, and hormonal changes, supporting their use as a model for reproductive aging.

Corresponding Author/Sorumlu Yazar: Dono Indarto, MD, PhD,
Universitas Sebelas Maret Faculty of Medicine, Department of Physiology; Universitas Sebelas Maret Faculty of Medicine, Biomedical Laboratory, Surakarta, Indonesia
E-mail: dono@staff.uns.ac.id **ORCID ID:** orcid.org/0000-0001-7420-5816

Received/Geliş Tarihi: 17.10.2025 **Accepted/Kabul Tarihi:** 28.01.2026 **Epub:** 17.02.2026 **Publication Date/Yayınlanma Tarihi:** 05.03.2026

Cite this article as: Intan YSN, Soetrisno S, Laqif A, Indarto D. A preliminary investigation of gene expression and levels of FSH, IL-10, and TNF-α and histological staining in natural aging mice. Turk J Obstet Gynecol. 2026;23(1):71-80

analiz edildi. Folikül uyarıcı hormon (FSH), interlökin (IL)-10 ve tümör nekroz faktörü-alfa (TNF-α) serum düzeyleri enzim bağlantılı immünosorbent testi ile ölçüldü. IL-10 ve TNF-α gen ifadesi ters transkripsiyon polimeraz zincir reaksiyonu ile değerlendirildi.

Bulgular: Sağlıklı fareler tüm östrus evrelerinden geçerken, yaşlanan fareler ağırlıklı olarak diöstrus evresinde kaldı ve artmış immün hücre infiltrasyonu ve enflamatuvar değişiklikler sergiledi. Yumurtalık histolojisi, büyüme, fibrozis ve işlevsiz yapıların varlığını gösterdi. Folikül sayısı yaşlanan farelerde azalmış olsa da, bu azalma istatistiksel olarak anlamlı değildi. Serum FSH (1,37±0,20'ye karşı 1,10±0,03 pg/mL) ve TNF-α (37,05±17,31'e karşı 21,57±4,62 pg/mL) anlamlı derecede yükselirken, IL-10 anlamlı derecede azaldı (4,53±0,32'ye karşı 6,23±0,99 pg/mL) (p<0,05). TNF-α mRNA seviyeleri arttı ve IL-10 mRNA seviyeleri azaldı, ancak bu değişiklikler istatistiksel olarak anlamlı değildi.

Sonuç: Yaşlanan BALB/c farelerinde bozulmuş östrus döngüleri, yumurtalık fibrozisi, artmış FSH ve TNF-α ve azalmış IL-10 görülmektedir; bu değişiklikler menopozla ilişkili olanlara benzemektedir. Bu bulgular, yaşlanan BALB/c farelerinin reprodüktif yaşlanma ve terapötik çalışmalar için bir model olarak kullanılmasını desteklemektedir.

Anahtar Kelimeler: Yaşlanma, östrus döngüsü, FSH, IL-10, TNF-α

Introduction

Menopause is a physiological phase that occurs naturally in women with advancing age and is characterized by the permanent cessation of ovarian function and the absence of menstrual cycles for at least 12 consecutive months[1]. Reduced production and circulating levels of estrogen and progesterone lead to metabolic disorders, decreased bone density, and an increased risk of cardiovascular and inflammatory diseases[1,2]. Significant changes occurring during menopause include an increase in systemic inflammation, which contributes to accelerated tissue aging in the ovary[3].

The primary challenge in menopause studies is the complexity of biological changes and the difficulty of studying this process directly in humans, given individual variability and ethical constraints[4]. To advance our understanding of menopause, it is essential to utilize animal models that accurately reflect the biological and molecular changes characteristic of this condition. Rodent models, particularly mice, are widely employed for this purpose due to their physiologically comparable reproductive cycles and the ease with which they can be manipulated and analyzed at the histological and molecular levels[5].

Some animal models of menopause have been developed, but the most commonly used is ovariectomy, in which the ovaries are removed to create an estrogen-deficient condition[6,7]. However, this model neither reflects the ovaries' natural aging process nor demonstrates the gradual changes in the estrous cycle[8]. The ovariectomy model also fails to replicate the chronic inflammation observed during menopause[7,9]. Therefore, naturally aged mice may serve as an alternative model that matches physiological conditions, such as molecular and degenerative changes in the ovaries.

In this study, we used female BALB/c mice aged over nine months as a model of natural aging and compared them with healthy young adult female mice. We evaluated estrous cycle dynamics, levels of follicle-stimulating hormone (FSH) and pro- and anti-inflammatory cytokines [tumor necrosis factor-alpha (TNF-α) and interleukin (IL)-10], expression of inflammation-related mRNAs, and ovarian morphology, assessed by histological and immunohistochemical analyses. This study not only offers an alternative approach to understanding natural reproductive aging but also creates opportunities to develop anti-inflammatory therapeutic interventions targeting menopausal conditions.

Materials and Methods

Research Design

The model employed in this study consisted of female BALB/c mice divided into two groups: Naturally aged mice older than 9 months and healthy young adult females (6-8 weeks old), with five mice per group. All animals were housed in standard laboratory cages and provided ad libitum access to standard feed and drinking water. Environmental conditions were carefully maintained at 26 °C, 50-60% relative humidity, and a 12-hour light/dark cycle to ensure experimental consistency. Healthy young adult mice (6-8 weeks old) underwent a one-week acclimatization period prior to experimental procedures to minimize stress and allow adaptation to the laboratory environment. In contrast, the naturally aging mice older than 9 months had been maintained under laboratory conditions prior to study initiation, and a defined acclimatization or incubation period had not been applied to this group. The study was conducted in accordance with ethical principles for animal research. The protocol was reviewed and approved by the Institutional Review Board/Animal Ethics Committee of Universitas Islam Sultan Agung, Semarang, Indonesia (approval no: 561/XII/2024/Komisi Bioetik, date: 30.12.2024).

Evaluation of Estrous Cycle

The estrous cycle was monitored through vaginal smear cytology for six consecutive days. The smears were collected each morning at the same time to avoid daily hormonal variation. Briefly, a drop of sterile 0.9% NaCl solution was gently instilled into the mouse's vagina to a depth of approximately 0.5-1 cm without causing tissue injury. The fluid was then aspirated, applied to a glass slide[10], air-dried, and subsequently stained with Giemsa (Sigma-Aldrich, USA) according to the manufacturer's protocol[11]. After staining and drying, the slides were examined using a light microscope (Zeiss, Germany) at 100× and 400× magnifications. The estrous cycle phase was determined by observing the dominant cell types (nucleated epithelial cells, cornified epithelial cells, and leukocytes).

Measurements of FSH, IL-10, and TNF-α Levels

According to the kit protocol, IL-10, FSH, and TNF-α levels in mouse serum were measured using the enzyme-linked immunosorbent assay (Elabscience Biotechnology Inc., USA). Blood was collected from mice following cervical dislocation, and serum was separated by centrifugation at 3,000 rpm for 15 minutes. The resulting serum was stored at -80 °C until analysis.

The assay was performed separately for each cytokine and hormone using microtiter plates pre-coated with specific antibodies against IL-10, FSH, and TNF-α (Elabscience, USA). 100 µL of serum or standard solution was added to each well, and the wells were incubated at 37 °C for 90 minutes. After washing, the biotinylated detection antibody solution was added, followed by incubation at 37 °C for 1 hour. After further washing, the horseradish peroxidase-conjugate solution was added and incubated for 30 minutes. 3,3',5,5'-tetramethylbenzidine substrate was then added and incubated until color development occurred, after which the reaction was stopped by adding the stop solution. Absorbance was measured at 450 nm using a microplate reader. Concentrations of IL-10, FSH, and TNF-α were calculated from the standard curve and expressed in pg/mL.

Gene Expression of IL-10 and TNF-α

NA was extracted from ovarian tissues using TRIzol reagent (Invitrogen, Massachusetts, USA) according to the manufacturer's instructions. Approximately 50 mg of tissue was placed into 1 mL of TRIzol, incubated, and then 200 µL of chloroform was added, followed by vigorous shaking for 15 seconds. The mixture was centrifuged at 20,000 × g for 15 minutes at 4 °C, and the upper aqueous phase containing RNA was transferred to a new tube. Isopropanol (0.5 mL per 1 mL of TRIzol) was added, gently mixed, and incubated at room temperature for 10 minutes. After centrifugation at 20,000 × g for 15 minutes, the supernatant was discarded, and the RNA pellet was washed with 75% ethanol and centrifuged at 15,000 × g for 5 minutes. The RNA pellet was dissolved in 100 µL nuclease-free water. RNA concentration and purity were measured on a NanoDrop spectrophotometer (Thermo Fisher Scientific, USA) using absorbance ratios at 260/280 nm and 260/230 nm.

cDNA synthesis was performed using one µg of total RNA with SuperScript II reverse transcriptase (Invitrogen, USA) and oligo(dT) primers, with an initial incubation at 70 °C for 10 minutes, followed by synthesis at 45 °C for 30 minutes. Quantitative reverse transcription polymerase chain reaction (qRT-PCR) was conducted using a PCRmax Eco 48 system (Illumina, USA) with a reaction volume of 20 µL, comprising 10 µL of SYBR Green Master Mix (KAPA Biosystems, Sigma-Aldrich, USA), 1 µL of forward primer, 1 µL of reverse primer, 2 µL of cDNA, and 6 µL of nuclease-free water. Specific primers targeted the IL-10 and TNF-α genes, with glyceraldehyde-3-phosphate dehydrogenase (GAPDH) as the reference gene. The thermal cycling protocol included an initial denaturation at 95 °C for 3 minutes, followed by 40 cycles of denaturation at 95 °C for 15 seconds and annealing/extension at 60 °C for 1 minute. Gene expression levels were determined based on cycle threshold values and analyzed using Eco v5.0 software (Illumina, USA). Relative expression was calculated using the 2^−ΔΔCt (Livak) method, normalized to GAPDH, and results were presented as fold changes relative to the healthy group.

Ovary Histology

Ovarian tissues were collected and carefully examined for macroscopic features. Each ovary was photographed to document gross morphology prior to histological processing. For microscopic examination, 3-4 µm-thick ovarian tissue sections were cut from paraffin blocks, dried at 37 °C, and heated on a slide warmer at 60 °C. Deparaffinization was performed by sequentially immersing the tissue sections in three xylene solutions (Xylol I, II, and III) (Sigma-Aldrich, St. Louis, Missouri, USA), followed by rehydration through a graded series of alcohol solutions (absolute, 96%, and 80%). The slides were then rinsed with running water.

Tissue staining was conducted using hematoxylin and eosin (H&E). The slides were first immersed in hematoxylin solution (Sigma-Aldrich, St. Louis, Missouri, USA) to stain the cell nuclei and were then rinsed with running water. Next, eosin (Sigma-Aldrich, St. Louis, Missouri, USA) was applied to stain the cytoplasm and other tissue structures, and the slides were rinsed again. The bluing process was performed using Tacha Bluing solution (Biocare Medical, California, USA), followed by a final rinse with water.

The slides then underwent gradual dehydration in graded alcohols (80% and 96%) and were cleared using xylene (Xylol I, II, and III). The mounting process was performed using Ecomount (Biocare Medical, California, USA) and was covered with a coverslip. The stained ovarian tissue preparations were observed under a light microscope (Olympus, Germany) at 100× magnification in five fields of view.

Statistical Analysis

Data were analyzed using SPSS software. One-way analysis of variance was performed, followed by a post hoc least significant difference test. Results were presented as mean ± standard deviation, with the significance level at $p<0.05$.

Results

Mice Vaginal Cytology

Vaginal smear cytology illustrates the cellular composition of the vaginal epithelium across the four phases of the estrous cycle, highlighting the morphological changes that reflect hormonal fluctuations and tissue activity in each phase. Figure 1A shows the proestrus phase, characterized by a predominance of nucleated epithelial cells with some cornified cells, indicating

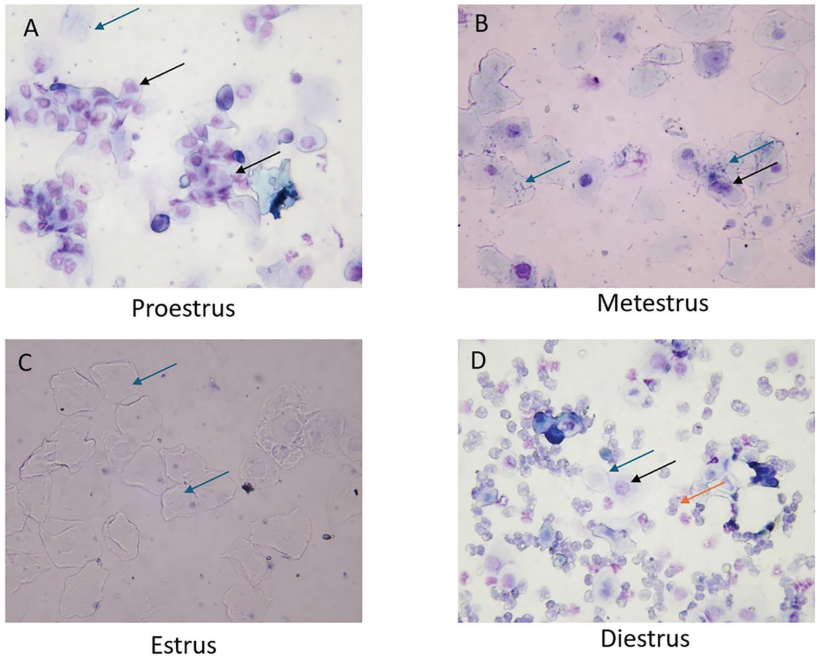

Figure 1. Vaginal smear cytology in different estrous cycle phases in mice. Black arrows indicate nucleated epithelial cells, blue arrows indicate cornified epithelial cells, and orange arrows indicate immune cells. (A) In the proestrus phase, nucleated epithelial cells (black arrows) and cornified epithelial cells (blue arrows) are observed, with nucleated cells being dominant. (B) Only cornified epithelial cells (blue arrows) are present during the estrus phase. (C) In the metestrus phase, cornified epithelial cells (blue arrows) are still visible, but nucleated epithelial cells (black arrows) begin to reappear. (D) In the diestrus phase, a mixture of nucleated epithelial cells (black arrows), cornified epithelial cells (blue arrows), and immune cells (orange arrows) is observed

epithelial proliferation in response to estrogen stimulation, without complete keratinization. Figure 1B depicts the estrus phase, marked by fully cornified epithelial cells, reflecting complete keratinization under maximal estrogen influence, coinciding with the peak of sexual receptivity. Figure 1C shows the metestrus phase, characterized by dominance of cornified cells and the reappearance of nucleated epithelial cells. This pattern indicates a decline in estrogen levels, an increase in progesterone levels, and the initiation of epithelial regeneration. Figure 1D displays the diestrus phase, in which nucleated epithelial cells, cornified epithelial cells, and immune cells are observed. This reflects progesterone dominance, immune-mediated tissue remodeling, and the resting phase before the cycle begins anew.

Estrous Cycle in Mice

The estrous cycle graph comparing healthy and aging mice shows differences in hormonal patterns over a 6-day observation period, as illustrated in Figure 2A. In healthy mice (represented by circle symbols), the estrous cycle shows a regular phase transition from day to day. The dynamic changes from proestrus to estrus, metestrus, and diestrus reflect a normal, cyclical reproductive pattern influenced by regular fluctuations in estrogen and progesterone. In contrast, aged mice (represented by square symbols) spent most of the observation period in the diestrus phase. Diestrus is generally the resting phase in the estrous cycle, characterized by low estrogen levels and the absence of ovulation. The prolonged diestrus phase in aging mice indicates that ovarian follicles no longer develop and ovulation does not occur. This is a hallmark of reproductive aging, characterized by the decline or cessation of ovarian function, which resembles the physiological condition of menopause in humans.

The doughnut diagram in Figure 2B visually emphasizes this difference. In healthy mice, the distribution of time spent in each of the four estrous phases, proestrus, estrus, metestrus, and diestrus, appears relatively balanced. This balanced phase distribution reflects a regular estrous cycle and active endocrine signaling. However, in aging mice, the diagram is dominated by the light gray color representing the diestrus phase, indicating that most of the time is spent in this non-reproductive phase. This change reflects a significant decline in ovarian activity due to disrupted or weakened hormonal signaling, particularly in estrogen production.

Histological analysis of vaginal smears further supports these findings. In healthy mice during the estrus phase, as shown in Figure 2C, the epithelial layer is dominated by cornified epithelial cells (blue arrows), which are flattened, anucleate cells resulting from complete keratinization of the epithelium. This cellular profile is characteristic of the estrous phase, when estrogen levels peak, stimulating epithelial maturation and preparing the reproductive tract for potential

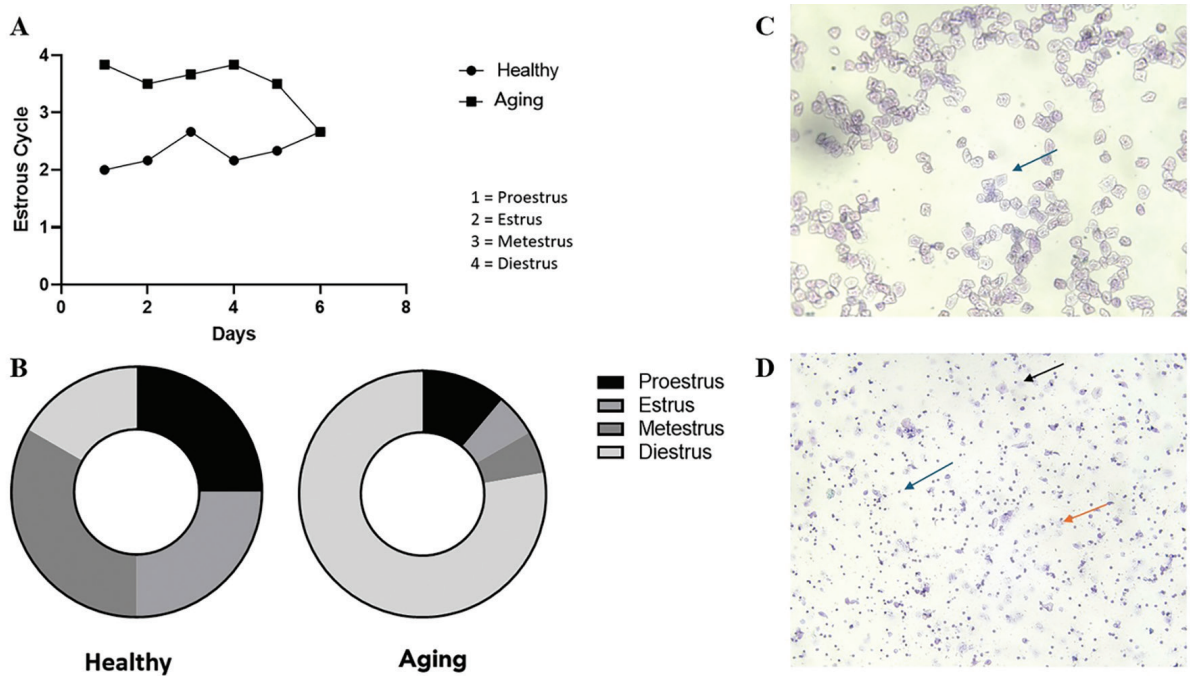

Figure 2. Observation of estrous cycle in healthy and aging mice. (A) The estrous cycle graph of healthy and aging mice shows that during the 6-day observation period, healthy mice undergo regular estrous phase transitions. (B) Donut diagram of estrous phase distribution in healthy and aging mice. (C) In healthy mice during the estrus phase, numerous cornified epithelial cells are observed (indicated by blue arrows). (D) Aging mice show fewer cornified epithelial cells, more nucleated epithelial cells (black arrows), and immune cells (orange arrows)

fertilization. The absence of immune cells during this phase indicates the lack of inflammation, consistent with an optimal physiological reproductive state. However, in aging mice, the cellular composition appears markedly different. Figure 2D shows fewer cornified epithelial cells, whereas nucleated epithelial cells (black arrows) and immune cells (orange arrows) are more numerous. Nucleated cells indicate incomplete keratinization, a sign of insufficient estrogen stimulation. Meanwhile, the increased number of immune cells reflects tissue remodeling or mild inflammation, possibly in response to epithelial regression in the reproductive tract resulting from decreased ovarian hormone production. These cytological findings align with the hormonal and behavioral signs of menopause in rodents and serve as reliable indicators for assessing reproductive aging[6].

Cellular and Tissue Morphology of Mice Ovary

During the aging transition, significant changes occur in ovarian morphology due to altered hormonal regulation and tissue remodeling processes[1]. In aging mice, the ovaries appear larger than those of healthy mice. As shown in Figure 3, this enlargement may be caused by the accumulation of non-functional structures such as fibrotic tissue, cysts, residual follicles, and stromal tissue. These structural abnormalities are most likely the result of hormonal imbalances and degenerative processes associated with aging.

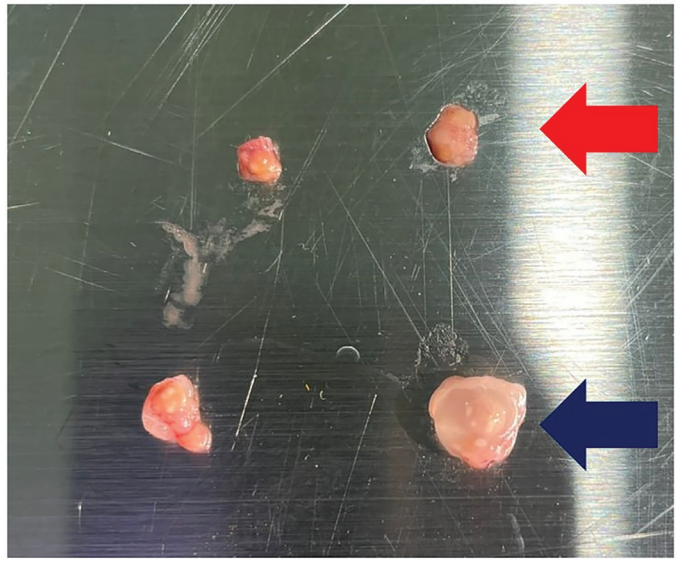

Figure 3. The macroscopic appearance of ovaries in healthy mice (red arrow) and aging mice (blue arrow) shows differences in organ size

Histological analysis of ovarian tissue from aging mice revealed differences in follicle number and types compared with the healthy group. The healthy group exhibited a greater number of follicles at various developmental stages, particularly primary, secondary, and antral follicles (Figure 4B).

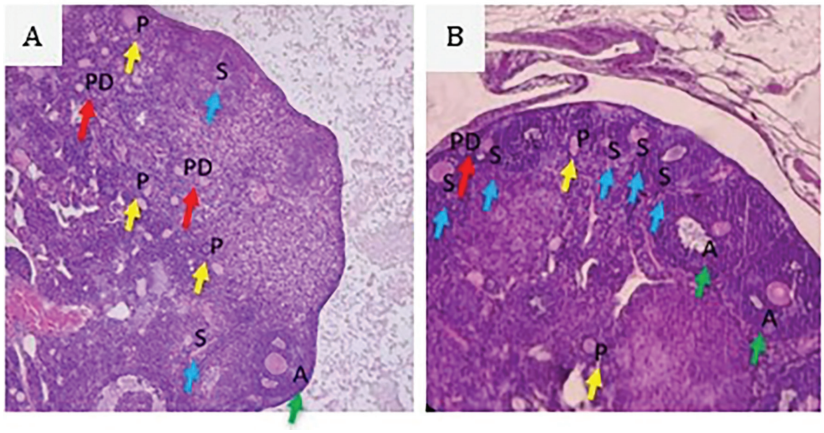

Figure 4. Results of hematoxylin and eosin staining assay show various stages of ovarian follicle development in mice, namely primordial follicles (yellow arrows), primary follicles (red arrows), secondary follicles (blue arrows), and antral follicles (green arrows). (A) Aging mice show fewer secondary and antral follicles compared to healthy mice. (B) Healthy mice show a higher number of secondary and antral follicles compared to aging mice

By contrast, in the aging group the total number of follicles decreased, with a predominance of early-stage follicles (primordial and primary), whereas secondary and antral follicles were rare or undetectable (Figure 4A).

The number of each follicle type was lower in the aging group than in the healthy group, although the differences were not statistically significant (Figure 5). This downward trend remains consistent with the histological appearance of aging ovaries (Figure 4), in which the process of follicular atresia progresses more rapidly than follicular recruitment and maturation proceed. This condition leads to menopausal ovaries that are dominated by primordial and primary follicles that fail to develop into the secondary and antral stages[12].

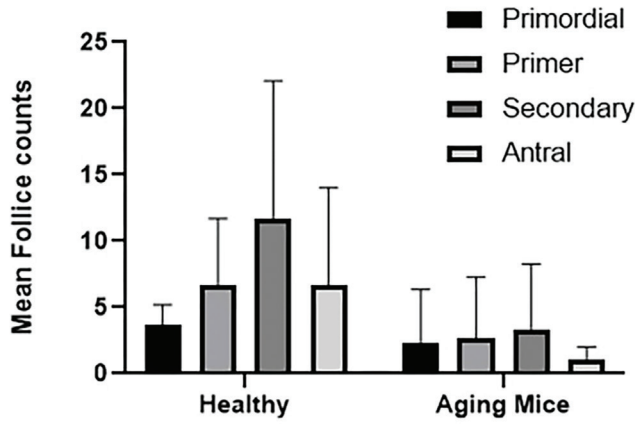

Figure 5. The total number of follicles in healthy and aging mice. The number of follicles decreased in aging mice due to the degeneration of ovarian function. Data are presented as mean ± standard deviation

FSH, TNF-α, and IL-10 Level in Mice Serum

To investigate differences in hormonal imbalances and systemic inflammation between healthy and aging mice, we measured serum levels of FSH, IL-10, and TNF-α. As shown in Figure 6A, serum FSH levels were significantly higher in aged mice (1.37±0.20 pg/mL) than in healthy controls (1.10±0.03 pg/mL) ($p<0.05$). This elevation in FSH is a well-established hallmark of menopause, reflecting the diminished negative feedback from ovarian hormones such as estrogen, which typically decline with ovarian aging. Additionally, Figure 6B illustrates that serum TNF-α, a pro-inflammatory cytokine, was significantly increased in aging mice (37.05±17.31 pg/mL) compared with healthy mice (21.57±4.62 pg/mL) ($p<0.05$). This finding indicates heightened systemic inflammation in aging mice, consistent with the low-grade chronic inflammatory state often associated with reproductive aging. In contrast, as shown in Figure 6C, serum IL-10 levels, an anti-inflammatory cytokine, were significantly reduced in aging mice (4.53±0.32 pg/mL) compared to healthy controls (6.23±0.99 pg/mL) ($p<0.05$). The decrease in IL-10 may contribute to the imbalance between pro- and anti-inflammatory signaling, further supporting the presence of an inflammatory state during menopause.

Expression of TNF-α and IL-10 in Mice Ovary

qRT-PCR analysis assessed the differences in mRNA expression levels of TNF-α and IL-10 between healthy and aging mice. As shown in Figure 7A, TNF-α mRNA expression was significantly increased in aged mice (4.75±2.21) compared with healthy mice (1.06±0.53; $p<0.05$), indicating an upregulation of pro-inflammatory gene expression associated with aging. Conversely, Figure 7B shows that IL-10 mRNA expression was lower in aged mice (0.45±0.22) than in healthy mice (1.02±0.69); however, this difference was not statistically significant. This trend suggests a possible decline in anti-inflammatory signaling in aging mice, consistent

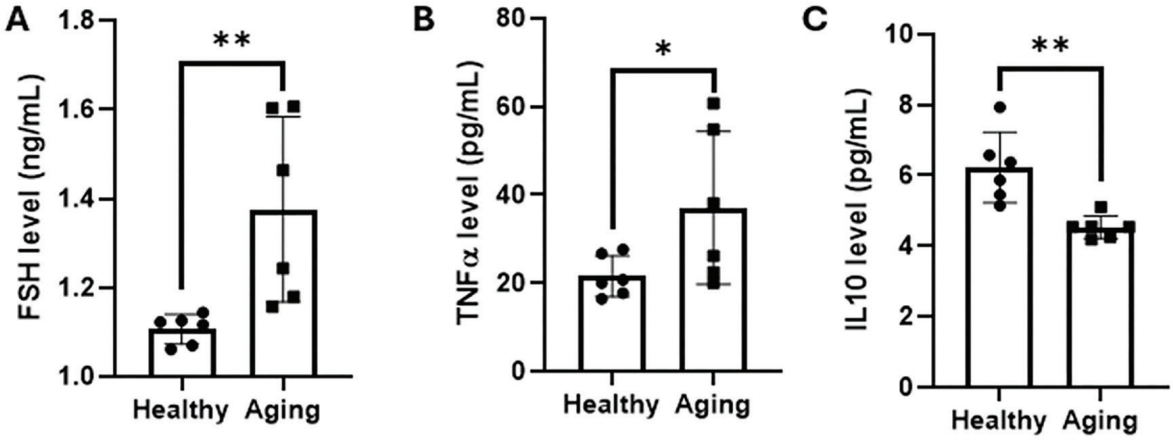

Figure 6. Differences in serum levels of FSH, TNF-α, and IL-10 between healthy and aging mice. (A) There was a significant difference between the healthy and aging mouse groups ($p<0.05$), with serum FSH levels markedly higher in aging mice than in healthy mice. (B) There was a significant difference between the healthy and aging mouse groups ($p<0.05$), with a significant increase in serum TNF-α levels in aging mice compared to healthy mice. (C) There was a significant difference between the healthy and aging mouse groups ($p<0.05$), with a clear reduction in serum IL-10 levels in aging mice compared to healthy mice. Significance indicators: *: $p<0.05$; **: $p<0.01$

FSH: Follicle-stimulating hormone, IL-10: Interleukin-10, TNF-α: Tumor necrosis factor-alpha

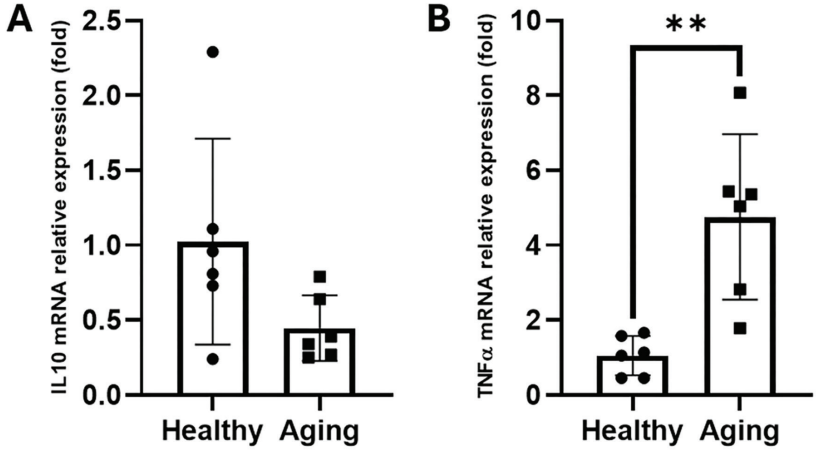

Figure 7. Differences in TNF-α and IL-10 mRNA expression between healthy and aging mice. (A) There was a significant difference between the healthy and aging mice groups ($p<0.05$), with a significant increase in TNF-α mRNA expression in aging mice compared to healthy mice. (B) There was no significant difference between the healthy and aging mouse groups ($p>0.05$). However, IL-10 mRNA expression decreased in aging mice compared to healthy mice, although this difference was not statistically significant Significance indicators: **: p<0.0

IL-10: Interleukin-10, TNF-α: Tumor necrosis factor-alpha 1

with a shift towards a more pro-inflammatory environment, despite the absence of a statistically significant difference. These findings support the serum cytokine level results and further strengthen the hypothesis that menopause may lead to transcriptional changes that contribute to systemic inflammation.

Discussion

This study demonstrates that aged female BALB/c mice (>9 months of age) exhibit physiological and molecular changes resembling human menopause. The key findings indicate that the diestrus phase predominates in the estrous cycle and is characterized by increased levels of FSH and TNF-α, decreased levels of IL-10, and structural changes in the ovaries. These results confirm that this model effectively represents menopause. Estrous cycle analysis revealed that aging mice primarily remained in the diestrus phase and exhibited immune cells and nucleated epithelial cells. In contrast, healthy mice displayed dynamic transitions between estrous phases. These observations are consistent with previous

studies reporting that aged mice experience disrupted estrous cycles and tend to remain in diestrus due to declining ovarian activity[13,14]. However, estrous cycle monitoring was limited to six consecutive days, which is shorter than the 14-20 days commonly recommended to define persistent diestrus[15]. Therefore, the conclusion regarding estrous cycle disruption should be interpreted with caution, and longer monitoring is needed in future studies.

The significant increase in FSH levels observed in aging mice in this study reflects the disruption of ovarian hormonal feedback, particularly the decline in estrogen with age[16]. Previous studies have reported that mice with aging ovaries exhibit surges in FSH, which serve as key indicators of endocrine dysfunction associated with menopause[17]. Concurrently, increased TNF-α and decreased IL-10 levels observed in aging mice in this study indicate an immune imbalance leading to a systemic pro-inflammatory state. These findings are consistent with earlier studies showing that aging rats exhibit elevated expression of pro-inflammatory cytokines (such as TNF-α and IL-6) and reduced expression of anti-inflammatory cytokines (such as IL-10), reflecting the low-grade chronic inflammation characteristic of menopause[18-20].

Furthermore, the increased TNF-α mRNA expression and decreased IL-10 mRNA expression in aging mice in this study suggest transcriptional regulatory changes in immune-related genes. Although the decrease in IL-10 expression was not statistically significant, the observed direction of change aligns with a shift toward a systemic pro-inflammatory state. However, given the limited estrous monitoring duration and small sample size, these molecular changes should be regarded as indicative rather than definitive. Previous studies have found that the ovaries of aging rats exhibit increased expression of pro-inflammatory genes and decreased anti-inflammatory regulators, contributing to tissue damage and oxidative stress[18,21,22].

The natural aging model used in this study offers advantages over the ovariectomized (OVX) model for evaluating anti-inflammatory therapeutic strategies. In contrast to OVX, which induces an abrupt and artificial loss of ovarian hormones, natural aging is characterized by a gradual decline in ovarian function, accompanied by progressive endocrine and immune alterations[23]. The concurrent increase in TNF-α and decrease in IL-10 observed in aging mice reflect a chronic, low-grade inflammatory state rather than an acute inflammatory response arising from natural aging processes, whereas OVX-induced low-grade inflammation occurs through immune cell-driven mechanisms that are distinct from the age-associated inflammatory pathways[23,24]. Ovary-intact aging models preserve residual ovarian tissue and ongoing immune-endocrine interactions, which more accurately reflect the physiological and molecular features of human menopause, including anestrus and reduced gonadal steroid levels[25].

Morphological observations revealed changes in the ovaries of mice. Aged mice exhibited enlarged ovaries containing non-functional lesions, including fibrotic tissue and cysts, indicating tissue degeneration due to chronic hormonal imbalance. Previous studies have shown that the ovaries of aged mice exhibit increased fibrosis, decreased numbers of mature follicles, and stromal accumulation due to reduced estrogenic activity and increased oxidative stress[26-28]. Additionally, H&E analysis showed a reduction in the number of follicles in aging mice compared with healthy mice. These findings are consistent with previous research demonstrating an age-related decline in ovarian follicle numbers in Egyptian spiny mice[29]. With advancing age, the number of ovarian follicles in women decreases due to follicular atresia and ovulation[29]. This reduction is accompanied by a decline in the number of ovarian granulosa cells, which are the leading producers of estradiol and inhibin B. Levels of anti-Müllerian hormone (AMH), also produced by granulosa cells, similarly decrease. The diminished production of estrogen and inhibins A and B leads to the loss of inhibition of gonadotropin secretion, resulting in increased FSH and luteinizing hormone levels[30]. This reduction in estrogen levels also disrupts the balance of the hypothalamic-pituitary-ovarian axis[31]. As a result, endometrial development fails, leading to irregular menstrual cycles and, eventually, complete cessation of menstruation (menopause)[1,32].

Study Limitations

The molecular scope of this study was limited to IL-10 and TNF-α and did not include other important inflammatory and hormonal markers, such as IL-6, estradiol, and AMH, which could provide a more comprehensive understanding of reproductive aging. Although the histological analyses successfully revealed ovarian changes, more detailed molecular and ultrastructural assessments would strengthen the interpretation of tissue degeneration. The small sample size (n=5 per group) represents a major limitation; the findings should be interpreted with caution. Moreover, estrous cycle monitoring was limited to six days, which is insufficient to definitively establish persistent cycle arrest. Finally, caution is needed when extrapolating these findings to humans, as physiological differences between the estrous cycle in mice and the menstrual cycle in women may limit direct comparability.

Conclusion

Our findings indicate that aged female mice exhibit physiological and molecular signs of menopause, making them suitable models for experimental studies of reproductive aging and for the development of therapeutic interventions targeting inflammation and ovarian dysfunction associated with menopause.

Ethics

Ethics Committee Approval: The protocol was reviewed and approved by the Institutional Review Board/Animal Ethics Committee of Universitas Islam Sultan Agung, Semarang, Indonesia (approval no: 561/XII/2024/Komisi Bioetik, date: 30.12.2024).
Informed Consent: Not necessary.

Footnotes

Authorship Contributions

Surgical and Medical Practices: S.S., Concept: Y.S.N.I., D.I., Design: Y.S.N.I., S.S., Data Collection or Processing: Y.S.N.I., A.L., Analysis or Interpretation: Y.S.N.I., A.L., D.I., Literature Search: S.S., Writing: Y.S.N.I., A.L., D.I.
Conflict of Interest: No conflict of interest was declared by the authors.
Financial Disclosure: The authors declared that this study received no financial support.

References

1. Peacock K, Carlson K, Ketvertis KM. Menopause [Internet]. In: StatPearls. Treasure Island (FL): StatPearls Publishing; 2025 [cited 2025 June 12]. Available from: http://www.ncbi.nlm.nih.gov/books/NBK507826/
2. Santoro N, Roeca C, Peters BA, Neal-Perry G. The menopause transition: signs, symptoms, and management options. J Clin Endocrinol Metab. 2021;106:1-15.
3. McCarthy M, Raval AP. The peri-menopause in a woman's life: a systemic inflammatory phase that enables later neurodegenerative disease. J Neuroinflammation. 2020;17:317.
4. Barber K, Charles A. Barriers to accessing effective treatment and support for menopausal symptoms: a qualitative study capturing the behaviours, beliefs and experiences of key stakeholders. Patient Prefer Adherence. 2023;17:2971-80.
5. Koebele SV, Bimonte-Nelson HA. Modeling menopause: the utility of rodents in translational behavioral endocrinology research. Maturitas. 2016;87:5-17.
6. Diaz Brinton R. Minireview: translational animal models of human menopause: challenges and emerging opportunities. Endocrinology. 2012;153:3571-8.
7. Oishi Y, Manabe I. Macrophages in age-related chronic inflammatory diseases. Npj Aging Mech Dis. 2016;2:16018.
8. Brinton RD. Investigative models for determining hormone therapy-induced outcomes in brain: evidence in support of a healthy cell bias of estrogen action. Ann N Y Acad Sci. 2005;1052:57-74.
9. Gilmer G, Bean AC, Iijima H, Jackson N, Thurston RC, Ambrosio F. Uncovering the "riddle of femininity" in osteoarthritis: a systematic review and meta-analysis of menopausal animal models and mathematical modeling of estrogen treatment. Osteoarthritis Cartilage. 2023;31:447-57.
10. Quignon C. Collection and analysis of vaginal smears to assess reproductive stage in mice. Curr Protoc 2023;3:e887.
11. Musyayyadah H, Wulandari F, Nangimi AF, Anggraeni AD, Ikawati M, Meiyanto E. The growth suppression activity of diosmin and PGV-1 co-treatment on 4T1 breast cancer targets mitotic regulatory proteins. Asian Pac J Cancer Prev APJCP. 2021;22:2929-38.
12. Park SU, Walsh L, Berkowitz KM. Mechanisms of ovarian aging. Reprod Camb Engl. 2021;162:R19-33.
13. Umehara T, Winstanley YE, Andreas E, Morimoto A, Williams EJ, Smith KM, et al. Female reproductive life span is extended by targeted removal of fibrotic collagen from the mouse ovary. Sci Adv. 2022;8:eabn4564.
14. Herrera-Pérez JJ, Hernández-Hernández OT, Flores-Ramos M, Cueto-Escobedo J, Rodr´guez-Landa JF, Mart´nez-Mota L. The intersection between menopause and depression: overview of research using animal models. Front Psychiatry [Internet] 2024 [cited 2025 June 25];15. Available from: https://www.frontiersin.org/journals/psychiatry/articles/10.3389/fpsyt.2024.1408878/full
15. Quignon C. Collection and analysis of vaginal smears to assess reproductive stage in mice. Curr Protoc. 2023;3:e887.
16. Spicer J, Malaspina D, Blank SV, Goosens KA. Follicle-stimulating hormone: more than a marker for menopause: FSH as a frontier for women's mental health. Psychiatry Res. 2025;345:116239.
17. Xiong J, Kang SS, Wang M, Wang Z, Xia Y, Liao J, et al. FSH and ApoE4 contribute to Alzheimer's disease-like pathogenesis via C/EBPβ/δ-secretase in female mice. Nat Commun. 2023;14:6577.
18. Lliberos C, Liew SH, Zareie P, La Gruta NL, Mansell A, Hutt K. Evaluation of inflammation and follicle depletion during ovarian ageing in mice. Sci Rep. 2021;11:278.
19. Zhu Z, Xu W, Liu L. Ovarian aging: mechanisms and intervention strategies. Med Rev (2021). 2022;2:590-610.
20. Ameho S, Klutstein M. The effect of chronic inflammation on female fertility. Reprod Camb Engl. 2025;169:e240197.
21. Wu Y, Li M, Zhang J, Wang S. Unveiling uterine aging: much more to learn. Ageing Res Rev. 2023;86:101879.
22. Isola JVV, Hense JD, Osório CAP, Biswas S, Alberola-Ila J, Ocañas SR, et al. Reproductive ageing: Inflammation, immune cells, and cellular senescence in the aging ovary. 2024 [cited 2025 June 25]; Available from: https://rep.bioscientifica.com/view/journals/rep/168/2/REP-23-0499.xml
23. Zakaria R, Said RM, Othman Z, Azman KF, Aziz CBA. Menopause rodent models: suitability for cognitive aging research. Int Med J. 2019;26:450-2.
24. Benedusi V, Martini E, Kallikourdis M, Villa A, Meda C, Maggi A. Ovariectomy shortens the life span of female mice. Oncotarget. 2015;6:10801-11.
25. McCarthy M, Raval AP. The peri-menopause in a woman's life: a systemic inflammatory phase that enables later neurodegenerative disease. J Neuroinflammation. 2020;17:317.
26. Briley SM, Jasti S, McCracken JM, Hornick JE, Fegley B, Pritchard MT, et al. Reproductive age-associated fibrosis in the stroma of the mammalian ovary. Reprod Camb Engl. 2016;152:245-60.
27. Zhang Z, Schlamp F, Huang L, Clark H, Brayboy L. Inflammaging is associated with shifted macrophage ontogeny and polarization in the aging mouse ovary. 2020 [cited 2025 June 25]; Available from: https://rep.bioscientifica.com/view/journals/rep/159/3/REP-19-0330.xml
28. Guo Y, Xue L, Tang W, Xiong J, Chen D, Dai Y, et al. Ovarian microenvironment: challenges and opportunities in protecting against chemotherapy-associated ovarian damage. Hum Reprod Update. 2024;30:614-47.

29. Bellofiore N, George E, Vollenhoven B, Temple-Smith P. Reproductive aging and menopause-like transition in the menstruating spiny mouse (Acomys cahirinus). Hum Reprod Oxf Engl. 2021;36:3083-94.
30. Hall JE. Endocrinology of the menopause. Endocrinol Metab Clin North Am. 2015;44:485-96.
31. Tanbo TG, Fedorcsak PZ. Can time to menopause be predicted? Acta Obstet Gynecol Scand. 2021;100:1961-8.
32. McNeil MA, Merriam SB. Menopause. Ann Intern Med. 2021;174:ITC97-112.

Clinical Investigation / Araştırma

DOI: 10.4274/tjod.galenos.2026.98440

Turk J Obstet Gynecol 2026;23(1):81-87

Inverted microscopy as a high performance tool for pre denudation evaluation of oocyte nuclear maturity

Denüdasyon öncesi oosit nükleer matürasyonunun değerlendirilmesinde yüksek performanslı bir araç olarak invert mikroskopi

Nuri Peker[1], Ayşen Yücetürk[1], Özge Karaosmanoğlu[1], Esra Tığlı[2], Burak Elmas[1], İlke Özer Aslan[1], Sadık Doğan[1], Bülent Tıraş[3]

[1]*Acıbadem Maslak Hospital, In Vitro Fertilization Center, İstanbul, Türkiye*

[2]*Kütahya University Faculty of Medicine, Kütahya, Türkiye*

[3]*Acıbadem Mehmet Ali Aydınlar University School of Medicine, Department of Obstetrics & Gynecology and Reproductive Endocrinology, İstanbul, Türkiye*

Abstract

Objective: We aimed to show that inverted microscope is a reliable and highly accurate method for evaluating oocyte nuclear maturation before cumulus-oocyte complex (COC) denudation.

Materials and Methods: This single-center prospective observational study was conducted between 15 October and 15 November 2025. Non-dominant follicles with a diameter <10 mm were retrieved and evaluated under an inverted microscope to predict oocyte nuclear maturation prior to COC denudation. A total of 974 oocytes were retrieved from 59 patients; 250 COCs obtained from follicles <10 mm were analyzed. COCs were divided into three groups: (i) COCs with germinal vesicle (GV) oocytes, (ii) COCs with non-GV oocytes, and (iii) unclassified COCs. Two hours later, COCs were denuded, and the diagnostic accuracy of the inverted microscope was assessed.

Results: Ninety-seven COCs were classified as GV, 127 as non-GV, and 26 as unidentified. After denudation, 94 of 97 COCs were confirmed as GV oocytes, and 124 of 127 COCs were confirmed as non-GV oocytes. The accuracy of the inverted microscope in identifying nuclear maturation for GV and non-GV oocytes was 96.91% and 97.64%, respectively. No statistically significant difference in diagnostic accuracy was observed between embryologists.

Conclusion: Currently, no method can definitively determine oocyte nuclear maturation before COC denudation. This method allows the prediction of oocyte nuclear maturation before denudation with high accuracy, potentially improving in vitro maturation outcomes by preserving cumulus-oocyte communication.

Keywords: Nuclear maturation, inverted microscope, in vitro maturation, germinal vesicle, polar body

Öz

Amaç: Bu çalışmada, invert mikroskobun, kümülüs-oosit kompleksi (KOK) denüdasyonundan önce oosit nükleer matürasyonunu değerlendirmek için güvenilir bir yöntem olduğunu göstermeyi amaçladık.

Gereç ve Yöntemler: Bu tek merkezli prospektif gözlemsel çalışma,15 Ekim-15 Kasım 2025 tarihleri arasında gerçekleştirilmiştir. Çapı <10 mm olan foliküllerden elde edilen KOK'lar denüdasyondan önce oosit nükleer maturasyonunu tahmin etmek amacıyla invert mikroskop altında değerlendirilmiştir. Toplam 59 hastadan 974 oosit toplanmış, ve <10 mm foliküllerden elde edilen 250 KOK analiz edilmiştir. KOK'lar üç gruba ayrılmıştır: (i) germinal vezikül (GV) oosit içeren KOK'lar, (ii) GV olmayan oosit içeren KOK'lar ve (iii) sınıflandırılamayan KOK'lar. İki saat sonra, KOK'lar denüdasyona tabi tutulmuş ve invert mikroskobun tanısal doğruluğu değerlendirilmiştir.

PRECIS: Inverted microscope allows the prediction of oocyte nuclear maturation before denudation with high accuracy, potentially improving in vitro maturation outcomes by preserving cumulus-oocyte communication.

Corresponding Author/Sorumlu Yazar: Nuri Peker MD,
Acıbadem Maslak Hospital, In Vitro Fertilization Center, İstanbul, Türkiye
E-mail: dr.nuripeker@gmail.com **ORCID ID:** orcid.org/0000-0002-4854-3851

Received/Geliş Tarihi: 02.02.2026 **Accepted/Kabul Tarihi:** 02.03.2026 **Publication Date/Yayınlanma Tarihi:** 05.03.2026

Cite this article as: Peker N, Yücetürk A, Karaosmanoğlu Ö, Tığlı E, Elmas B, Özer Aslan İ, et al. Inverted microscopy as a high performance tool for pre denudation evaluation of oocyte nuclear maturity. Turk J Obstet Gynecol. 2026;23(1):81-87

Bulgular: İnvert mikroskop ile değerlendirme sonrası 97 KOK GV oosit içeriyor, 127 KOK GV olmayan oosit içeriyor ve 26 KOK ise tanımlanamayan olarak sınıflandırıldı. Denüdasyondan sonra, 97 KOK'un 94'ü GV oosit, 127 KOK'un 124'ü ise GV olmayan oosit olarak doğrulandı. İnvert mikroskobun GV ve GV olmayan oositler için nükleer olgunlaşmayı belirlemedeki doğruluğu sırasıyla %96,91 ve %97,64 idi. Embriyologlar arasında tanı doğruluğunda istatistiksel olarak anlamlı bir fark gözlenmedi.

Sonuç: Günümüzde, KOK içindeki oositin nükleer matürasyonunu, KOK'u denüde etmeden önce belirleyebilecek bir yöntem bulunmamaktadır. Tanımladığımız bu yöntem ile denüdasyon öncesi oosit nükleer maturasyonu yüksek doğrulukla tahmin edilebilmektedir. Böylelikle KOK denüde edilmeden oosit nükleer matürasyonu belirlenebilecek ve in vitro olgunlaştırma sonuçları potansiyel olarak iyileştirilebilecektir.

Anahtar Kelimeler: Nükleer matürasyon, invert mikroskop, in vitro olgunlaştırma, germinal vezikül, polar body

Introduction

In vitro maturation (IVM) is a treatment modality nearly as old as in vitro fertilization (IVF) itself, first described by Pincus and Enzmann in 1935 and later defined by Edwards in 1962[1]. Classically, immature oocytes are collected and matured outside the body under laboratory conditions. Four main IVM protocols are described: (i) standard IVM, (ii) biphasic IVM, (iii) human chorionic gonadotropin (hCG)-primed IVM, and (iv) rescue IVM. In standard IVM, oocytes are retrieved after a short (2-3-day) stimulation period without an hCG trigger, and maturation is completed *in vitro* in one step[1]. In biphasic IVM, a pre-culture phase temporarily prevents meiosis to allow cytoplasmic maturation. In rescue IVM, germinal vesicle (GV) oocytes obtained after denudation in a conventional IVF cycle are matured *in vitro*. Rescue IVM is performed to obtain a higher number of metaphase-II oocytes, 2-pronuclear (2PN) zygotes and blastocysts, particularly in patients with diminished ovarian reserve (DOR), poor ovarian response (POR), or premature ovarian failure[2-4]. However, the success rate of rescue IVM has been reported as low because denudation disrupts the bidirectional interaction between oocytes and cumulus cells[3,4].

Currently, there is no definitive method for detecting oocyte nuclear maturation before denudation. Although several studies have attempted to estimate oocyte maturity by assessing cumulus-oocyte complex (COC) morphology under a microscope, these approaches have proven unreliable. Recently, Peker et al.[5] investigated the relationship between COC morphology and oocyte nuclear maturation and concluded that morphology alone is an unreliable indicator.

The objective of this study was to present a new method that enables the highly accurate prediction of oocyte nuclear maturation prior to denudation.

Materials and Methods

We conducted a single-center prospective observational study between July 1 and September 1, 2025. The study was reviewed and approved by the Acıbadem University Ethics Committee and was performed in accordance with the principles of the 1975 Declaration of Helsinki, as revised in 2000 (approval no: 2025-14/541, date: 18.09.2025). Informed consent was obtained from all participants prior to inclusion.

On day 2 or 3 of the menstrual cycle, antral follicles were counted by transvaginal sonography. All patients received an antagonist protocol, and follicles were triggered using hCG, gonadotropin-releasing hormone agonist, or a combination of both. Oocyte retrieval was performed 36 hours after triggering, under sedation, using a 17-G needle.

Three embryologists participated in the study. Two embryologists, blinded to each other's evaluations, assessed oocytes using an inverted microscope, while a third embryologist, also blinded, performed denudation. During oocyte retrieval, dominant follicles and those larger than 10 mm were first aspirated and placed in a four-well dish. The remaining non-dominant follicles (<10 mm) were collected separately and examined under an inverted microscope by one of the two embryologists. First, follicular fluid was examined under a stereomicroscope to determine the presence of COCs. When COCs were detected, they were evaluated in a Petri dish using an inverted microscope. After assessment, the embryologists classified each COC into three groups: (i) COCs containing GV oocytes, (ii) COCs containing non-GV oocytes (including metaphase-I and metaphase-II oocytes), and (iii) COCs that could not be clearly identified as GV or non-GV. Two hours later, denudation was performed by the third embryologist and the accuracy of the inverted microscope evaluation was determined.

Evaluation of COCs Under Inverted Microscope

Follicular fluid was poured into a 90-mm Petri dish, which was then tilted at a 30-45 °C angle to spread and visualize the COCs. COCs were subsequently examined using the same dish under an inverted microscope to determine nuclear maturation. Immediately before observation, the cumulus was gently spread laterally with a pipette to improve visualization of the oocyte.

Under the inverted microscope, oocytes displaying a GV were recorded as GV oocytes, while those with a visible polar body were categorized as non-GV oocytes. Oocytes lacking both a GV and a polar body were designated as having undefined nuclear maturity. Figure 1 illustrates images of a GV (GV oocyte) and a polar body [metaphase II (MII) oocyte].

Statistical Analyses

All data obtained in the study were analyzed using SPSS (IBM SPSS Statistics version 2.5, Chicago, IL, USA). Data distributions are presented as medians and percentages. Normality was assessed using Kolmogorov-Smirnov tests (n>30). The chi-square test was applied to categorical

variables, and the Mann-Whitney U test was applied to continuous variables. A 95% confidence level was adopted for all analyses.

Results

A total of 100 patients were initially enrolled in the study. In 41 patients, no COCs could be retrieved from follicles <10 mm; therefore, these patients were excluded. A total of 974 oocytes obtained from 59 patients were analyzed. Of these, 724 oocytes originated from follicles ≥10 mm, and 250 from follicles <10 mm were included as the study group.

Table 1 summarizes the success rate in identifying mature and immature oocytes using the inverted microscope. Among the 250 COCs evaluated, 97 were classified as GV oocytes. After denudation, 94 oocytes were confirmed as GV, 2 as MII, and 1 as metaphase I (MI). Of the 127 COCs classified as non-GV, 124 were confirmed as non-GV and three were GV after denudation (108 MII, 16 MI). Twenty-six COCs could not be classified and were designated as unidentified. The overall accuracy of the inverted microscope in detecting oocyte nuclear maturation was 96.91% for GV oocytes and 97.64% for non-GV oocytes.

Table 2 presents the performance of embryologist 1 in predicting oocyte nuclear maturation using the inverted microscope. A total of 120 COCs were assessed; 38 were classified as GV, 69 as non-GV, and 13 as unidentified (group 3). The success rate for detecting oocyte nuclear maturation was 97.10% for GV oocytes and 97.37% for non-GV oocytes.

Table 3 presents the performance of embryologist 2. A total of 130 COCs were evaluated; 59 were classified as GV, 58 as non-GV, and 13 as unidentified (group 3). The accuracy rates were 98.28% for GV and 96.91% for non-GV oocytes. No statistically significant difference was found between the two embryologists in diagnostic accuracy for GV versus non-GV classification.

The diagnostic performance of the imaging method was further compared using area under the curve (AUC) values. Figure 2 shows the receiver operating characteristic (ROC) curve for the inverted microscope. The ROC AUC was 0.99, indicating excellent predictive accuracy for oocyte nuclear maturation (R^2=0.989, mean absolute error=0.127, root mean square error=0.252).

Figure 3 shows the regression analysis results for the inverted microscope. The regression line corresponded closely with denudation scores, showing minimal deviations and a balanced distribution. These results demonstrate that measurements obtained with the inverted microscope show a strong linear correlation with oocyte nuclear maturation outcomes.

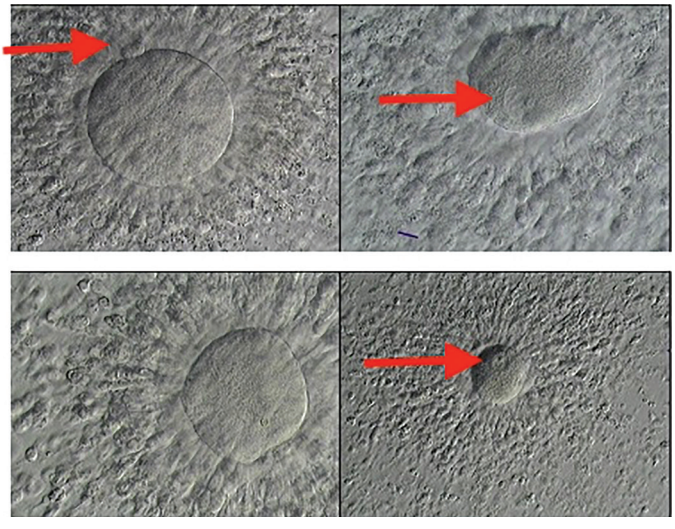

Figure 1. The upper-left image represents an oocyte (in metaphase 2) and was taken using an inverted microscope. Red arrow indicates a polar body (i.e., at 12 o'clock). The upper-right and the bottom-right photos show a GV as observed under an inverted microscope (red arrow). The bottom-left image depicts neither GV nor the polar body. Therefore, whether this image is a GV or MII oocyte remains uncertain

GV: Germinal vesicle, MII: Metaphase II

Table 1. Diagnostic accuracy of inverted microscopy in identifying GV and non-GV oocytes prior to denudation

	Mature (%)	Immature (%)	p-value
Embryologist 1	97.37	97.10	>0.05
Embryologist 2	96.61	98.28	>0.05
Total	96.91	97.64	

GV: Germinal vesicle

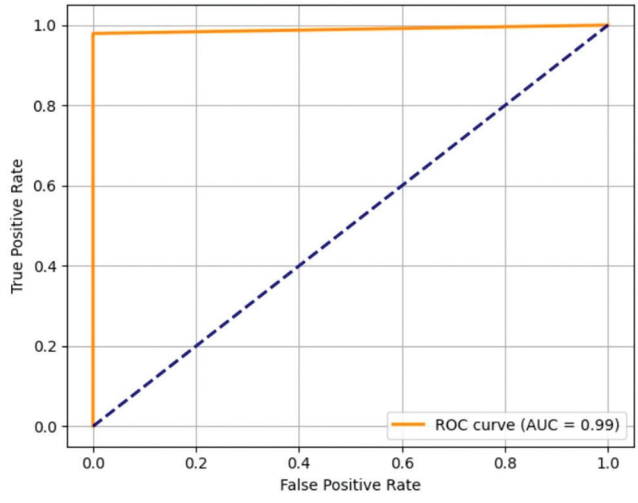

Figure 2. ROC curve, the new "inverted microscope" method has a very high success rate in predicting oocyte nuclear maturation before denudation. R^2=0.989, MAE=0.127, RMSE=0.252, ROC AUC=0.99

ROC: Receiver operating characteristic, RMSE: Root mean square error, AUC: Area under the curve, MAE: Mean absolute error

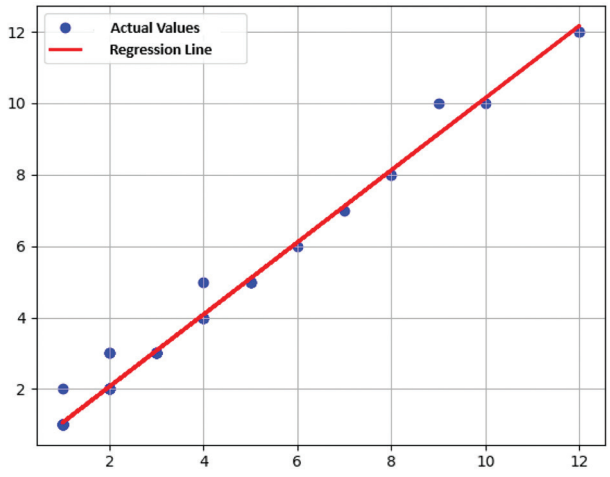

Figure 3. Regression analysis. The regression line matches the denudation score trend well. Deviation from a linear relationship is minimal and the distribution is balanced. Taken together, these data demonstrate that the inverted microscope is capable of reliably predicting oocyte nuclear maturation

Discussion

Rescue in vitro maturation (r-IVM) refers to the IVM of denuded, immature oocytes after triggering with hCG and/or a GnRH agonist during a conventional IVF cycle[6]. This approach can increase the number of mature oocytes obtained in a single cycle, particularly in patients with DOR, POR, or primary ovarian insufficiency. However, its effectiveness is limited because denudation disrupts the bidirectional communication between cumulus cells and the oocyte[6,7].

In a study by Qin et al.[4], the reproductive outcomes of rescue IVM were evaluated by comparing two groups: (i) 2112 women who underwent intracytoplasmic sperm injection (ICSI) and (ii) 490 women who underwent ICSI followed by rescue IVM. In the ICSI + r-IVM group, the number of MII oocytes, 2-pronuclear (2PN) embryos and day-3 embryos was higher than in the ICSI-only group. Similarly, Shani et al.[8] conducted a retrospective cohort study to assess the maturation potential of immature oocytes undergoing IVM, and reported that the fertilization rates of MI-rescue IVM and GV-rescue IVM oocytes were comparable to those of sibling MII oocytes. However,

Table 2. Diagnostic performance of embryologist 1 in predicting oocyte nuclear maturation under-inverted microscope

ID	COCs obtained from follicles <10 mm (n)	GV under inverted microscope (n)	GV after denudation (n)	Non-GV under inverted microscope (n)	Non-GV after denudation (n)	Unidentified cases under inverted microscope (n)	MII after denudation (n)	MI after denudation (n)	GV after denudation (n)
1	4	4	4	0	0	0	0	0	0
2	1	1	1	0	0	0	0	0	0
3	7	7	7	0	0	0	0	0	0
4	3	3	2	0	0	0	0	0	0
5	1	1	1	0	0	0	0	0	0
6	2	2	2	0	0	0	0	0	0
7	3	1	1	1	1	1	1	0	0
8	7	1	1	0	0	6	6	0	0
9	5	1	1	2	2	2	2	0	0
10	3	1	1	1	1	1	0	0	1
11	9	1	1	8	8	0	0	0	0
12	3	0	0	3	3	0	0	0	0
13	3	0	0	3	3	0	0	0	0
14	2	1	1	1	1	0	0	0	0
15	2	0	0	1	1	1	1	0	0
16	2	1	1	1	1	0	0	0	0
17	6	1	1	5	5	0	0	0	0
18	1	0	0	1	1	0	0	0	0
19	6	0	0	6	6	0	0	0	0
20	4	4	4	0	0	0	0	0	0

Table 2. Continued

ID	COCs obtained from follicles <10 mm (n)	GV under inverted microscope (n)	GV after denudation (n)	Non-GV under inverted microscope (n)	Non-GV after denudation (n)	Unidentified cases under inverted microscope (n)	MII after denudation (n)	MI after denudation (n)	GV after denudation (n)
21	2	2	2	0	0	0	0	0	0
22	1	1	1	0	0	0	0	0	0
23	2	0	0	2	2	0	0	0	0
24	1	0	0	1	1	0	0	0	0
25	3	2	2	1	1	0	0	0	0
26	1	0	0	1	1	0	0	0	0
27	4	0	0	2	2	2	0	1	1
28	1	0	0	1	1	0	0	0	0
29	12	0	0	12	12	0	0	0	0
30	6	1	1	5	4	0	0	0	0
31	12	2	2	10	9	0	0	0	0
32	1	0	0	1	1	0	0	0	0
Total	120	38	37	69	67	13	10	1	2

GV: Germinal vesicle, MII: Metaphase II, MI: Metaphase I, COC: Cumulus-oocyte complex

Table 3. Diagnostic performance of embryologist 2 in predicting GV and non-GV oocytes under inverted microscope

ID	COCs obtained from follicles <10 mm	GV under inverted microscope	GV after denudation	Non-GV under inverted microscope	Non-GV after denudation	Unidentified cases under inverted microscope	MII after denudation	MI after denudation	GV after denudation
1	2	1	1	1	1	0	0	0	0
2	5	4	4	1	1	0	0	0	0
3	3	1	1	2	2	0	0	0	0
4	5	3	3	2	2	0	0	0	0
5	1	1	1	0	0	0	0	0	0
6	15	12	12	3	3	0	0	0	0
7	5	4	4	1	1	0	0	0	0
8	2	1	1	1	1	0	0	0	0
9	7	5	5	2	2	0	0	0	0
10	2	0	0	2	2	0	0	0	0
11	3	3	2	0	0	0	0	0	0
12	9	1	1	8	8	0	0	0	0
13	9	2	1	4	4	3	0	2	1
14	1	1	1	0	0	0	0	0	0
15	5	2	2	3	3	0	0	0	0
16	1	1	1	0	0	0	0	0	0
17	4	0	0	2	2	2	1	0	1
18	3	0	0	3	3	0	0	0	0

Table 3. Continued

ID	COCs obtained from follicles <10 mm	GV under inverted microscope	GV after denudation	Non-GV under inverted microscope	Non-GV after denudation	Unidentified cases under inverted microscope	MII after denudation	MI after denudation	GV after denudation
19	12	2	2	10	10	0	0	0	0
20	12	5	5	2	2	5	4	0	1
21	2	1	1	1	1	0	0	0	0
22	3	0	0	1	1	2	0	1	1
23	1	1	1	0	0	0	0	0	0
24	3	1	1	2	2	0	0	0	0
25	5	2	2	2	2	1	1	0	0
26	6	3	3	3	2	0	0	0	0
27	4	2	2	2	2	0	0	0	0
Total	130	59	57	58	57	13	6	3	4

GV: Germinal vesicle, MII: Metaphase II, MI: Metaphase I, COC: Cumulus-oocyte complex

early cleavage and blastulation rates were significantly lower in r-IVM group. Despite this, the euploid blastocyst and good-quality blastocyst rates were comparable with MII siblings, suggesting that r-IVM may enhance transferable blastocyst yield and overall IVF success[8]. Conversely, Bartolacci et al.[9] published a meta-analysis demonstrating that fertilization, cleavage, blastulation, and clinical pregnancy rates were significantly lower for r-IVM oocytes than for sibling MII oocytes. Several studies have attributed these poorer outcomes to the loss of COC. Cumulus cells play a critical role in supporting oocyte growth, development, and maturation by secreting regulatory molecules such as cAMP and cGMP. They also produce metabolic energy and facilitate nutrient transport to the oocyte[10-12]. Preserving this communication is, therefore, essential. Accurate identification of GV oocytes before denudation allows IVM to proceed without disrupting these interactions, potentially improving maturation and fertilization rates.

Only a limited number of studies have investigated the identification of mature and immature oocytes before denudation. Batsry et al.[13] reported that experienced embryologists could identify 90% of mature and 72.7% of immature oocytes before denudation. Similarly, Peker et al.[5] found that embryologists correctly identified 69% of immature and 80% of mature oocytes based on COC morphology. Hammitt et al.[14] further assessed embryologists' ability to predict nuclear maturation and reported correct prediction rates of 74%, 64%, and 47% for three observers. Across these studies, the predictive accuracy for nuclear maturation did not exceed 90%, suggesting that COC morphology alone is insufficient for reliable classification.

In our study, we developed and validated a new method, using inverted microscopy, to assess oocyte nuclear maturation before denudation. After evaluation, 96.91% of immature oocytes and 97.64% of non-GV oocytes were correctly identified. We believe that determining oocyte nuclear maturation before COC denudation represents a potentially transformative step in IVF practice. GV oocytes detected under an inverted microscope can be left to mature *in vitro* with their cumulus cells intact, thereby maintaining bidirectional communication and improving maturation rates.

Conclusion

Inverted microscopy provides a highly accurate, non-invasive method for assessing oocyte nuclear maturation prior to COC denudation. This technique may improve IVM outcomes, particularly in patients with limited oocyte yield. Its integration into standard IVF workflows could preserve cumulus-oocyte interactions, thereby enhancing oocyte maturation, fertilization, embryo development, and pregnancy rates. Moreover, in classical and biphasic IVM protocols, COCs can be evaluated using inverted microscopy before denudation, allowing an extended IVM period for immature oocytes to achieve the MII stage. Future studies should be multicenter, prospective, and incorporate molecular markers of oocyte maturation.

Ethics

Ethics Committee Approval: The study was reviewed and approved by the Acıbadem University Ethics Committee and was performed in accordance with the principles of the 1975 Declaration of Helsinki, as revised in 2000 (approval no: 2025-14/541, date: 18.09.2025).

Informed Consent: Informed consent was obtained from all participants prior to inclusion.

Footnotes

Authorship Contributions

Surgical and Medical Practices: N.P., A.Y., Ö.K., E.T., Concept: N.P., B.T., Design: N.P., E.T., B.T., Data Collection or Processing: N.P., A.Y., Ö.K., E.T., B.E., İ.Ö.A., S.D., Analysis or Interpretation: N.P., A.Y., S.D., B.T., Literature Search: N.P., Writing: N.P., E.T., B.T.

Conflict of Interest: No conflict of interest was declared by the authors.

Financial Disclosure: The authors declared that this study received no financial support.

References

1. Racca A, Rodriguez I, Garcia S, Arroyo G, Polyzos NP. Double versus single stimulation in young low prognosis patients followed by a fresh embryo transfer: a randomized controlled trial (DUOSTIM-fresh). Hum Reprod. 2024:deae104. Erratum in: Hum Reprod. 2025;40:397.
2. Esbert M, Garc´a C, Cutts G, Lara-Molina E, Garrido N, Ballestros A, et al. Oocyte rescue in-vitro maturation does not adversely affect chromosome segregation during the first meiotic division. Reprod Biomed Online. 2024;48:103379.
3. Sankari S, Elanchezhian M, Selvamani D, Nagarajan M, Gopikrishnan D. Live Birth after rescue *in vitro* maturation-intracytoplasmic sperm injection in type 1 diabetes, polycystic ovary syndrome patient using clomiphene-antagonist protocol. J Hum Reprod Sci. 2018;11:75-8.
4. Qin DY, Jiang HH, Yao QY, Yao W, Yuan XQ, Wang Y, et al. Rescue *in vitro* maturation may increase the pregnancy outcomes among women undergoing intracytoplasmic sperm injection. Front Endocrinol (Lausanne). 2022;13:1047571.
5. Peker N, Karaosmanoğlu Ö, Albayrak Ö, Elmas B, Aslan İÖ, Yücetürk A. Prediction of oocyte maturity before denudation: is the assessment of COC morphology a reliable option?. Turk J Obstet Gynecol. 2025;22:194-8.
6. Coticchio G, Cimadomo D, De Vos M, Ebner T, Esbert M, Escribá MJ, et al. To rescue or not to rescue immature oocytes: prospects and challenges. Fertil Steril. 2025;123:749-58.
7. Jie H, Zhao M, Alqawasmeh OAM, Chan CPS, Lee TL, Li T, et al. *In vitro* rescue immature oocytes - a literature review. Hum Fertil (Camb). 2022;25:640-50.
8. Shani AK, Haham LM, Balakier H, Kuznyetsova I, Bashar S, Day EN, et al. The developmental potential of mature oocytes derived from rescue in vitro maturation. Fertil Steril. 2023;120:860-9.
9. Bartolacci A, Busnelli A, Pagliardini L, de Girolamo S, De Santis L, Esposito S, et al. Assessing the developmental competence of oocytes matured following rescue in vitro maturation: a systematic review and meta-analysis. J Assist Reprod Genet. 2024;41:1939-50.
10. Gilchrist RB, Smitz J. Oocyte in vitro maturation: physiological basis and application to clinical practice. Fertil Steril. 2023;119:524-39.
11. Chen YR, Yin WW, Jin YR, Lv PP, Jin M, Feng C. Current status and hotspots of in vitro oocyte maturation: a bibliometric study of the past two decades. J Assist Reprod Genet. 2025;42:459-72.
12. Fakhar-I-Adil M, Angel-Velez D, Araftpoor E, Amin QA, Hedia M, Bühler M, et al. Biphasic CAPA-IVM improves equine oocyte quality and subsequent embryo development without inducing genetic aberrations. Int J Mol Sci. 2025;26:5495.
13. Batsry L, Orvieto R, Mor-Hadar D, Yung Y, Gitman H, Shimon C, et al. Can we predict oocyte maturation prior to denudation for intracytoplasmic sperm injection? Gynecol Endocrinol. 2020;36:265-7.
14. Hammitt DG, Syrop CH, Van Voorhis BJ, Walker DL, Miller TM, Barud KM, et al. Prediction of nuclear maturity from cumulus-coronal morphology: influence of embryologist experience. J Assist Reprod Genet. 1992;9:439-46.

Clinical Investigation / Araştırma

DOI: 10.4274/tjod.galenos.2026.53358

Turk J Obstet Gynecol 2026;23(1):88-94

Differential expression of c-kit, E-cadherin, and beta-catenin in endometriosis and normal endometrial tissue

Endometriozis ve normal endometriyal dokuda c-kit, E-kadherin ve beta-kateninin farklı ekspresyonları

Esra Ayhan Atasayar[1], Fatih Şendağ[2], Gürdeniz Serin[3], Ali Akdemir[2]

[1]*University of Health Sciences Türkiye, İzmir Tepecik Training and Research Hospital, Department of Obstetrics and Gynaecology, İzmir, Türkiye*
[2]*Ege University Faculty of Medicine Hospital, Department of Obstetrics and Gynaecology, İzmir, Türkiye*
[3]*Ege University Faculty of Medicine Hospital, Department of Pathology, İzmir, Türkiye*

Abstract

Objective: C-kit, E-cadherin and beta-catenin adhesion molecules and proto-oncogenes are thought to be associated with molecular mechanisms related to the invasion, implantation and persistence of ectopic endometrial cells. Comparing the expression levels of these molecules in endometriomas, other types of endometriosis, and normal endometrial tissue may provide further insight into the mechanisms driving endometriosis development. The present study sought to examine the molecular pathophysiological roles of these molecules by determining their expression profiles in different types of endometriosis and in the healthy endometrium.

Materials and Methods: Retrospective data from 180 cases were analyzed, comprising 60 endometriomas, 60 cases of other types of endometriosis (superficial and deep), and 60 normal proliferative endometrial tissue samples. Immunohistochemical staining for c-kit, E-cadherin, and beta-catenin was performed. The expression levels of E-cadherin and beta-catenin were quantified using the H-score method.

Results: C-kit positivity was found in 9% of endometriomas and 10% of other endometriosis tissues, but was absent in normal endometrium. Beta-catenin H-scores were significantly lower in endometriosis tissues compared with normal endometrial tissues ($p<0.001$). E-cadherin levels showed no significant difference between the groups. A post-hoc power analysis confirmed that the study was adequately powered to detect group differences in E-cadherin, indicating that the non-significant finding likely reflects a true absence of a difference.

Conclusion: Increased c-kit expression, along with reduced beta-catenin expression in endometriosis samples, suggests that these molecules contribute to endometriosis pathogenesis. However, because no significant difference was found in E-cadherin expression, a definitive conclusion cannot be made regarding the involvement of E-cadherin in endometriosis development.

Keywords: Endometriosis, endometrioma, c-kit, E-cadherin, beta-catenin

Öz

Amaç: C-kit, E-kaderin ve beta-katenin gibi adezyon molekülleri ve proto-onkogenlerin, ektopik endometriyal hücrelerin invazyonu, implantasyonu ve persistansı ile ilişkili moleküler mekanizmalarla bağlantılı olduğu düşünülmektedir. Bu çalışma, farklı endometriozis tiplerinde ve sağlıklı endometriyumda bu moleküllerin ekspresyon profillerini belirleyerek moleküler patofizyolojik rollerini incelemeyi amaçlamıştır.

Gereç ve Yöntemler: Yüz seksen olgunun retrospektif verileri analiz edildi; bunlar arasında 60 endometrioma, 60 diğer endometriozis türü (yüzeyel ve derin) ve 60 normal proliferatif endometriyal doku örneği bulunmaktaydı. C-kit, E-kadherin ve beta-katenin için immünohistokimyasal boyama yapıldı. E-kadherin ve beta-katenin ekspresyon düzeyleri H-skor yöntemi kullanılarak ölçüldü.

PRECIS: This retrospective case-control study evaluates immunohistochemical expression of c-kit, E-cadherin, and beta-catenin in endometriotic and normal endometrial tissues, revealing molecular differences linked to endometriosis pathogenesis.

Corresponding Author/Sorumlu Yazar: Esra Ayhan Atasayar MD,
University of Health Sciences Türkiye, İzmir Tepecik Training and Research Hospital, Department of Obstetrics and Gynaecology, İzmir, Türkiye
E-mail: esraayhanatasayar@gmail.com **ORCID ID:** orcid.org/0000-0002-1178-2525

Received/Geliş Tarihi: 26.09.2025 **Accepted/Kabul Tarihi:** 25.02.2026 **Epub:** 02.03.2026 **Publication Date/Yayınlanma Tarihi:** 05.03.2026

Cite this article as: Ayhan Atasayar E, Şendağ F, Serin G, Akdemir A. Differential expression of c-kit, E-cadherin, and beta-catenin in endometriosis and normal endometrial tissue. Turk J Obstet Gynecol. 2026;23(1):88-94

Bulgular: C-kit pozitifliği endometriomaların %9'unda ve diğer endometriozis dokularının %10'unda saptandı, ancak normal endometriyumda gözlenmedi. Beta-katenin H-skorları, normal endometrial dokulara kıyasla endometriozis dokularında anlamlı olarak daha düşüktü (p<0,001). E-kaderin düzeyleri gruplar arasında anlamlı farklılık göstermedi. Post-hoc güç analizi, çalışmanın E-kadherin'deki grup farklılıklarını tespit etmek için yeterli güce sahip olduğunu doğruladı ve bu da anlamlı olmayan bulgunun muhtemelen gerçek bir farkın olmadığını yansıttığını gösterdi.

Sonuç: Endometriozis dokularında artmış c-kit ekspresyonu ile azalmış beta-katenin ekspresyonu, bu moleküllerin endometriozis patogenezine katkıda bulunabileceğini düşündürmektedir. Ancak, E-kaderin ekspresyonunda önemli bir fark bulunmadığından, endometriozis gelişiminde E-kaderinin rolünü kesin olarak belirlemek mümkün değildir.

Anahtar Kelimeler: Endometriozis, endometriyoma, c-kit, E-kadherin, beta-katenin

Introduction

Endometriosis is a chronic inflammatory disease that affects 5-10% of women during their reproductive years, characterized by endometrial glands and stroma located outside the uterine cavity[1]. Although asymptomatic cases are observed, common symptoms of endometriosis include pelvic pain and infertility. Endometriosis has negative effects on patients' daily activities, overall well-being, and sexual function. It is often associated with fatigue and depression, resulting in work loss and a significant economic burden[2]. There are three phenotypes of endometriosis: Superficial endometriosis, ovarian endometrioma and deep infiltrating endometriosis[3]. Understanding the pathogenesis of endometriosis is crucial for achieving effective treatment. Although the disease is common and reduces patients' overall well-being, the underlying molecular and cellular processes remain incompletely elucidated. Key questions, such as the origins of different types of endometriosis and why deep infiltrating endometriosis exhibits cancer-like behavior, remain unanswered. Even though endometriosis is a non-malignant condition, it mimics tumor cells through its formation of new blood vessels, tissue infiltration, and ectopic implantation into distant organs[4,5]. Studies have shown that adhesion molecules and proto-oncogenes involved in tumor pathogenesis may also play a role in the development of endometriosis. In this study, we analyzed the roles of stem cells and adhesion molecules, such as c-kit, E-cadherin, and beta-catenin, potentially involved in endometriosis pathogenesis.

The c-kit receptor (CD117), the gene product of c-kit, constitutes a transmembrane glycoprotein. Several studies provide evidence that the stem cell factor/c-kit signaling axis is involved in the molecular mechanisms driving endometriosis. The E-cadherin/beta-catenin complex is involved in epithelial cell-cell adhesion. Disruption of this integrity and the reduction or absence of adhesion molecules has been associated with the proliferation, migration, and invasion of tumor cells. Endometrial cells located outside the uterus in patients with endometriosis invade other tissues and organs in a manner resembling tumor cells. Various studies have been conducted based on the hypothesis that stem cell expression increases and adhesion molecule levels decrease to enable endometrial cells to migrate and invade other areas during the development of endometriosis, similar to tumor progression. While some studies report increased c-kit proto-oncogene expression and decreased E-cadherin and beta-catenin levels in endometriosis, findings remain inconsistent[6-8]. In order to better understand the mechanisms underlying endometriosis, we analyzed pathological preparations from 180 cases, focusing on the proto-oncogene c-kit and the cell-cell adhesion molecules E-cadherin and beta-catenin.

Materials and Methods

Patient and Tissue Sample Selection

This retrospective case-control study was approved by the Ege University Research Ethics Committee, İzmir, Türkiye (decision number: 21-7T/50, dated 08.07.2021), and was designed following the approval. Between 2015 and 2021, patients aged 18-55 years who underwent surgery for endometriosis or other benign conditions and had pathological examinations were retrospectively selected from the archives of the Department of Obstetrics and Gynecology, Ege University Faculty of Medicine. Pathology slides from the selected cases were retrieved from the medical pathology archive. The slides were examined under a microscope in the presence of a pathologist, and samples containing an adequate number of assessable epithelial and stromal cells were selected for analysis. Based on the review of surgical notes and definitive pathology reports, patients were divided into three groups: those with ovarian endometriotic cysts were assigned to the endometrioma group; those with endometriosis foci in tissues other than the ovary were assigned to the endometriosis group; and those with proliferative endometrium obtained for benign reasons were assigned to the control group. Sixty patients were selected from each group. Patients with genital system malignancies and those with insufficient endometriosis tissue in paraffin blocks were excluded from the study.

Immunohistochemical Examination

Histological evaluation was performed on 3-5 μm-thick sections obtained from formalin-fixed paraffin blocks using immunohistochemical staining for E-cadherin (monoclonal, clone 36, JO1182, Ventana, ready to use), beta-catenin (monoclonal, clone 14, V0003124, Cellmarque, ready-to-use),

and c-kit (CD117, monoclonal, clone YR145, Cellmarque, concentrate; 1:100). Paraffin sections were deparaffinized in xylene and rehydrated sequentially with graded alcohol using a fully automated immunohistochemical staining device (Benchmark XT; Ventana Medical Systems), following the manufacturers' instructions.

Focal limited staining was observed in endometriosis foci with the c-kit antibody and was considered positive. Samples showing no staining were considered negative. Evaluation of E-cadherin and beta-catenin expression was performed separately based on the percentage of stained cells and staining intensity. The percentage of staining was determined as the ratio of stained cells to the total number of cells (0-100%). Staining intensity was classified into four groups: 0=no staining, 1=weak, 2=moderate, and 3=strong staining intensity. The histochemical scoring method (H-score), obtained by multiplying the percentage of cells at each staining intensity by the corresponding intensity score, was used to evaluate staining extent and intensity together, as previously described by McCarty et al.[9].

Since E-cadherin staining was observed only in epithelial cells, it was evaluated exclusively in these cells. However, because beta-catenin staining was observed in both epithelial and stromal cells, these two components were evaluated separately. Representative images of c-kit, E-cadherin, and beta-catenin staining are shown in Figure 1.

Statistical Data Analysis Methods

IBM SPSS Statistics 25.0 (IBM Corp., Released 2017. IBM SPSS Statistics for Windows, Version 25.0. Armonk, NY: IBM Corp.) was used for statistical analyses.

The normality of numerical variables was assessed using the Kolmogorov-Smirnov test within subgroups. Numerical variables were compared among the three groups using the Kruskal-Wallis test, and Dunn's test with Bonferroni correction was applied for post-hoc pairwise comparisons when significant differences were detected. Ordinal variables were analyzed using the chi-square test (with exact probabilities calculated), and cells contributing to significant differences were identified by adjusted residual Z-scores ($z>1.96$ or $z<-1.96$). A p-value <0.05 was considered statistically significant.

Results

Although no significant difference was found between the endometrioma and endometriosis groups in terms of c-kit positivity rates, both groups exhibited a marked elevation relative to the control group (p=0.005). C-kit positivity rates for each group are presented in Table 1.

No notable difference was detected among the groups in terms of E-cadherin H-scores. The E-cadherin H-scores across the groups are shown in Table 1. E-cadherin staining intensities were also similar among the groups, as shown in Table 2 (p=0.14).

When beta-catenin H-scores were evaluated, a significant difference was observed among the groups (p<0.001). Comparisons between individual groups showed no significant difference between the endometrioma and endometriosis groups (p=0.53), whereas both groups had significantly lower beta-catenin H-scores than the control group (p<0.001). Beta-catenin H-scores for each group are detailed in Tables 1, 3, and 4.

Beta-catenin epithelial and stromal staining intensities were evaluated separately, and a significant difference was found among the groups (p<0.001). Beta-catenin epithelial and stromal staining intensities are summarized in Table 5. Tables 1 and 4 show significant differences in age distribution among the three groups (p<0.001). The mean age in both study groups was lower than that of the control group (p<0.001). The correlation between age and immunohistochemical variables was then analyzed. Table 3 shows a statistically significant but weak positive correlation between beta-catenin H-scores (epithelial and stromal intensity) and age across all cases. Because no significant differences in age distribution were observed among the endometriosis, endometrioma, and control groups with respect to beta-catenin expression, this weak positive correlation was considered not to be clinically meaningful, and no additional statistical analyses were performed.

Discussion

In this study, we evaluated the expression of c-kit, E-cadherin, and beta-catenin—molecules recognized for their role in stem cell signaling and cell-cell adhesion—in different types of endometriosis and compared them with normal proliferative endometrium. Our results demonstrated a significant increase in c-kit expression and a significant decrease in beta-catenin expression in endometriosis tissues. These findings contribute to the growing evidence that stem cell-related pathways and adhesion molecules could play a role in the molecular mechanisms underlying endometriosis, particularly in the initiation and persistence of ectopic lesions.

The significantly higher c-kit expression detected in endometriosis samples relative to normal endometrium supports the hypothesis that the stem cell factor (SCF)/c-kit axis could be involved in endometriosis development. Previous studies have demonstrated elevated SCF levels in the peritoneal fluid of women with endometriosis[10] and increased c-kit expression in ectopic endometrial tissue[10,11]. Our findings are consistent with these reports and suggest that c-kit may contribute to lesion formation and persistence. Although Osuga et al.[10] detected c-kit mRNA expression in both eutopic and ectopic endometrium, this finding may be attributed to the high sensitivity of everse transcription polymerase chain reaction, which allows detection of even very low levels of gene expression. In addition, although Pacchiarotti et al.[11] reported low-level c-kit expression

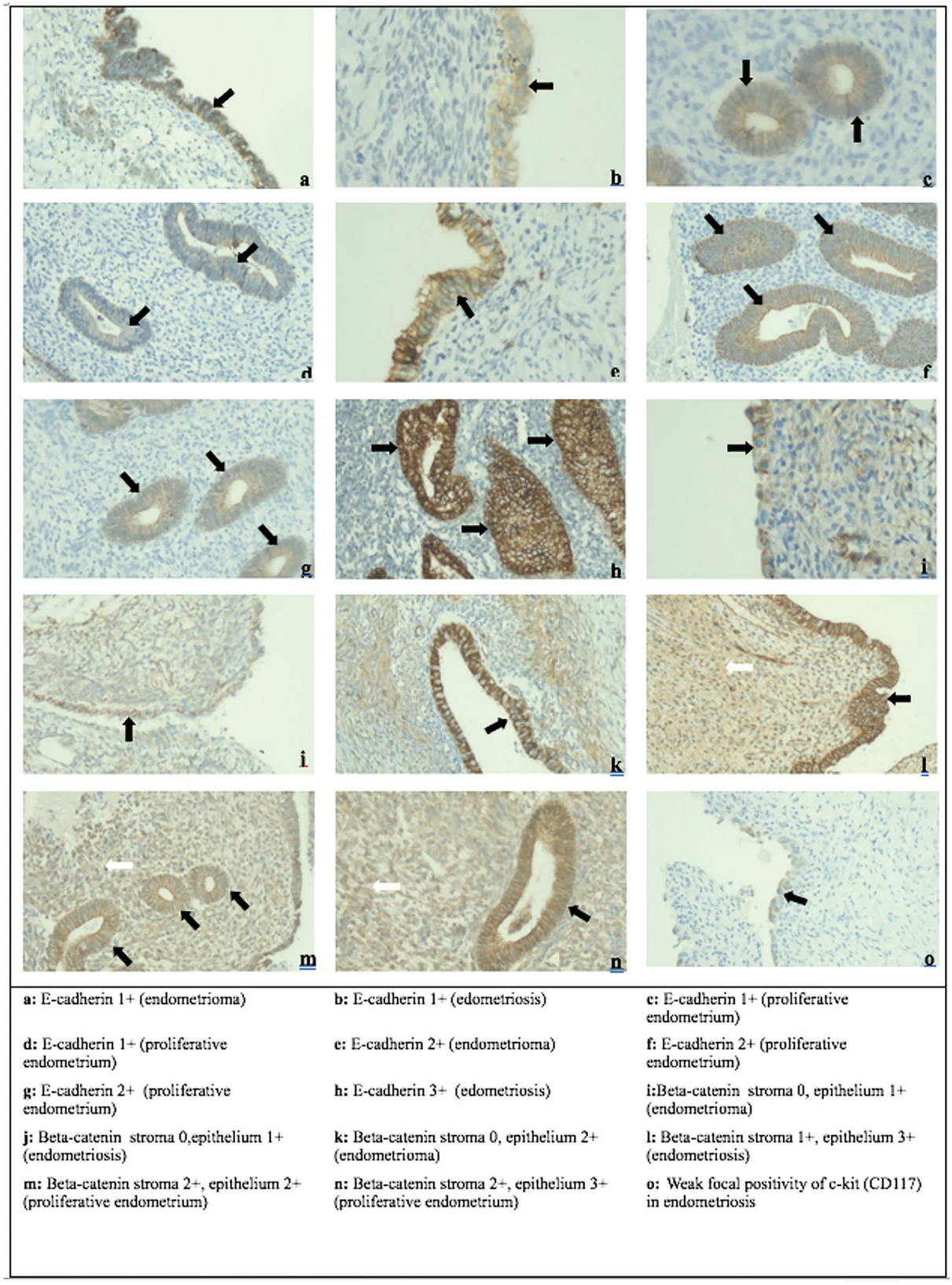

Figure 1. Immunohistochemical staining of c-kit, E-cadherin, and beta-catenin

**Immunopositive cells are indicated by arrows. Black arrows indicate epithelial positivity, and white arrows indicate stromal positivity. Staining intensity was graded as 0 (negative), 1+ (weak), 2+ (moderate), and 3+ (strong), and was semi-quantitatively scored separately in epithelial and stromal components, with higher scores indicating stronger immunoreactivity. For beta-catenin, both epithelial and stromal staining patterns are shown*

Table 1. Comparison of demographic and clinical characteristics among the endometriosis, endometrioma, and control groups

		Endometriosis	Endometrioma	Control group
E-cadherin H-score	Mean	241.33	236.67	251.83
	Std. deviation	34.369	39.172	31.000
	Median	250	240	255
	Minimum	150	150	160
	Maximum	290	300	300
	IQR	48	70	30
	p-value	0.12		
Beta-catenin H-score	Mean	237.83	225	259
	Std. deviation	30.426	42.486	24.886
	Median	240	240	260
	Minimum	160	80	180
	Maximum	300	290	300
	IQR	40	50	30
	p-value	<0.001		
Age	Mean	33.38	35.12	40.85
	Std. deviation	6.268	8.201	7.813
	Median	33	34	42.5
	Minimum	23	21	20
	Maximum	48	48	53
	IQR	10	16	8
	p-value	<0.001		
C-kit	C-kit (-) n (%)	50 (83.3)	51 (85.0)	60 (100.0)
	C-kit (+) n (%)	10 (16.7)	9 (15.0)	0 (0)
	p-value	0.005		

c-kit (+/-): Indicates the presence or absence of c-kit expression. Statistical analyses were performed using the Kruskal-Wallis test for continuous variables and Fisher's exact test for categorical variables. IQR: Interquartile range, Std.: Standard

in eutopic endometrium, no c-kit immunoreactivity was detected in eutopic endometrial samples in the present study. This discrepancy may be explained by the inherently minimal expression of c-kit in eutopic endometrium and by the possibility that immunohistochemistry may fall below the detection threshold, particularly in retrospective studies.

Similar to our study, Pacchiarotti et al.[11] and Osuga et al.[10] did not perform a separate analysis comparing deep and superficial endometriosis. Future studies could be designed to evaluate c-kit expression specifically in deep versus superficial lesions.

Table 2. Distribution of E-cadherin staining intensity among the endometriosis, endometrioma, and control groups

	E-cadherin staining intensity			
	1	2	3	p-value
	n (%)	n (%)	n (%)	
Endometriosis	2 (3.3)	17 (28.3)	41 (68.3)	0.14
Endometrioma	5 (8.3)	19 (31.7)	36 (60.0)	
Control group	1 (1.7)	11 (18.3)	48 (80.0)	

In contrast to c-kit, beta-catenin expression was significantly decreased in endometriosis tissues, particularly within the stromal compartment. Beta-catenin is a key component of the E-cadherin-mediated adhesion complex and plays an important role in maintaining epithelial integrity and cell-cell adhesion[7]. Reduced beta-catenin expression may weaken intercellular adhesion, thereby facilitating cellular detachment, migration, and implantation of endometrial cells at ectopic sites. This finding is consistent with previous studies reporting diminished beta-catenin levels in endometriotic lesions[7,12]. The similar reduction in beta-catenin observed in both endometrioma and other types of endometriosis suggests that impaired adhesion mechanisms may represent a shared molecular feature underlying different endometriosis phenotypes rather than being specific to invasiveness.

E-cadherin, another important adhesion molecule, did not show significant differences in expression levels among the groups in our study. This finding is consistent with several previous reports[7,12,13], although conflicting data exist in the literature. For example, Jedryka et al.[14] reported reduced E-cadherin levels in the serum or peritoneal fluid of patients with endometriosis, whereas other studies have linked decreased expression primarily to recurrent or deep infiltrative forms of the disease[15,16]. These discrepancies may be attributed to methodological heterogeneity, differences in sample type (circulating versus tissue-based measurements), and variability in disease stage or phenotype. Importantly, our findings suggest that alterations in E-cadherin expression may not represent a universal feature of endometriosis but may instead be restricted to specific clinical subtypes or more advanced disease, which could explain the inconsistent results across studies.

Study Limitations

This study presents certain limitations. Due to its retrospective nature, a potential for selection bias exists, which could restrict causal inferences. Although the sample size was adequate to detect significant differences in c-kit and beta-catenin expression, detailed subgroup analyses according to disease phenotype were not performed.

Table 3. Correlation between age and immunohistochemical variables

	Immunohistochemical variables			Endometriosis group			Endometrioma group			Control group		
	Coef	n	p-value	Coef	n	p-value	Coef	n	p-value	Coef	n	p-value
E-cadherin H-score	0.008	180	0.92	0.087	60	0.51	-0.123	60	0.35	-0.084	60	0.52
E-cadherin severity	-0.044	180	0.56	0.010	60	0.94	-0.128	60	0.33	-0.226	60	0.08
Beta-catenin H-score	0.215	180	0.004	0.114	60	0.39	0.288	60	0.03	-0.144	60	0.27
Beta-catenin severity	0.184	180	0.01	0.129	60	0.32	0.181	60	0.17	-0.129	60	0.33
Beta-catenin stromal severity	0.273	180	<0.001	0.250	60	0.05	-0.222	60	0.09	0.053	60	0.69

Coef: Correlation coefficient, n: Sample size

Table 4. Statistical comparison of beta-catenin H-scores and age among the endometrioma, endometriosis, and control groups

Groups	p-value for beta-catenin H-scores	p-value for age
Endometrioma-endometriosis	0.53	0.55
Endometrioma-control group	**<0.001**	**<0.001**
Endometriosis-control group	**<0.001**	**<0.001**

Table 5. Distribution of beta-catenin epithelial and stromal staining intensity among the endometriosis, endometrioma, and control groups

	Beta-catenin epithelial staining intensity				Beta-catenin stromal staining intensity				
	1	2	3	p-value	0	1	2	3	p-value
	n (%)	n (%)	n (%)		n (%)	n (%)	n (%)	n (%)	
Endometriosis	2 (3.3)	18 (30.0)	40 (66.7)	**p<0.001**	23 (38.3)	26 (43.3)	10 (16.7)	1 (1.7)	**p<0.001**
Z-score	-0.7	0.7	-0.3		**4.7**	**2.4**	**-2.4**	**-4.6**	
Endometrioma	6 (10.0)	24 (40.0)	30 (50.0)		11 (18.3)	26 (43.3)	16 (26.7)	7 (11.7)	
Z-score	**2.2**	**2.9**	**-3.7**		-0.1	**2.4**	-0.2	**-2.3**	
Control group	1 (1.7)	6 (10.0)	53 (88.3)		0 (0.0)	5 (8.3)	24 (40.0)	31 (51.7)	
Z-score	**-1.5**	**-3.6**	**4.1**		**-4.6**	**-4.8**	**2.6**	**6.9**	

Z-score: Adjusted residual z-score from chi-square analysis

Immunohistochemistry provided semi-quantitative protein expression data but did not allow functional or molecular-level evaluation. In addition, clinical variables such as prior treatment and disease duration could not be fully controlled.

Conclusion

This study demonstrates that altered expression of c-kit and beta-catenin is associated with the pathogenesis of endometriosis, highlighting their potential roles in lesion formation and maintenance. In contrast, E-cadherin expression did not show a consistent association. These findings provide insight into molecular mechanisms underlying endometriosis and may guide future diagnostic and therapeutic strategies.

Acknowledgement: We are grateful to Mr. Mehmet Atasayar, Mr. Hakan İnke for her help with text formatting, editing figures and tables.

Ethics

Ethics Committee Approval: This retrospective case-control study was approved by the Ege University Research Ethics Committee, İzmir, Türkiye (decision number: 21-7T/50, dated 08.07.2021), and was designed following the approval.
Informed Consent: Informed consent was obtained from all patients who participated in the study.

Footnotes

Authorship Contributions

Surgical and Medical Practices: E.A.A., F.Ş., A.A., G.S., Concept: E.A.A., F.Ş., G.S., Design: E.A.A., G.S. F.Ş., Data Collection or Processing: E.A.A., Analysis or Interpretation: E.A.A., G.S., Literature Search: E.A.A., Writing: E.A.A.
Conflict of Interest: No conflict of interest was declared by the authors.

Financial Disclosure: This study was supported by a grant from the Scientific Research Projects Coordination Unit (BAP) of Ege University.

References

1. Taylor HS, Kotlyar AM, Flores VA. Endometriosis is a chronic systemic disease: clinical challenges and novel innovations. Lancet. 2021;397:839-52.
2. Giudice LC, Kao LC. Endometriosis. Lancet. 2004;364:1789-99.
3. Chapron C, Marcellin L, Borghese B, Santulli P. Rethinking mechanisms, diagnosis and management of endometriosis. Nat Rev Endocrinol. 2019;15:666-82.
4. Sancakli Usta C, Turan G, Bulbul CB, Usta A, Adali E. Differential expression of Oct-4, CD44, and E-cadherin in eutopic and ectopic endometrium in ovarian endometriomas and their correlations with clinicopathological variables. Reprod Biol Endocrinol. 2020;18:116.
5. Siufi Neto J, Kho RM, Siufi DF, Baracat EC, Anderson KS, Abrão MS. Cellular, histologic, and molecular changes associated with endometriosis and ovarian cancer. J Minim Invasive Gynecol. 2014;21:55-63.
6. Uzan C, Cortez A, Dufournet C, Fauvet R, Siffroi JP, Dara¨ E. Endometrium from women with and without endometriosis, and peritoneal, ovarian and bowel endometriosis, show different c-kit protein expression. J Reprod Immunol. 2005;65:55-63.
7. Shaco-Levy R, Sharabi S, Benharroch D, Piura B, Sion-Vardy N. Matrix metalloproteinases 2 and 9, E-cadherin, and beta-catenin expression in endometriosis, low-grade endometrial carcinoma and non-neoplastic eutopic endometrium. Eur J Obstet Gynecol Reprod Biol. 2008;139:226-32.
8. Okamoto I, Kawano Y, Tsuiki H, Sasaki J, Nakao M, Matsumoto M, et al. CD44 cleavage induced by a membrane-associated metalloprotease plays a critical role in tumor cell migration. Oncogene. 1999;18:1435-46.
9. McCarty KS Jr, Miller LS, Cox EB, Konrath J, McCarty KS Sr. Estrogen receptor analyses: correlation of biochemical and immunohistochemical methods using monoclonal antireceptor antibodies. Arch Pathol Lab Med. 1985;109:716-21.
10. Osuga Y, Koga K, Tsutsumi O, Igarashi T, Okagaki, Takai Y, et al. Stem cell factor (SCF) concentrations in peritoneal fluid of women with or without endometriosis. Am J Reprod Immunol. 2000;44:231-5.
11. Pacchiarotti A, Caserta D, Sbracia M, Moscarini M. Expression of oct-4 and c-kit antigens in endometriosis. Fertil Steril. 2011;95:1171-3.
12. Matsuzaki S, Darcha C, Maleysson E, Canis M, Mage G. Impaired down-regulation of E-cadherin and beta-catenin protein expression in endometrial epithelial cells in the mid-secretory endometrium of infertile patients with endometriosis. J Clin Endocrinol Metab. 2010;95:3437-45.
13. Béliard A, Donnez J, Nisolle M, Foidart JM. Localization of laminin, fibronectin, E-cadherin, and integrins in endometrium and endometriosis. Fertil Steril. 1997;67:266-72.
14. Jedryka M, Goluda M, Kuliczkowski K, Sozański L. E-kadheryna w surowicy i płynie otrzewnowym kobiet z endometrioza [E-cadherin in the serum and the peritoneal fluid of women with endometriosis]. Ginekol Pol. 2001;72:418-21. Polish.
15. Donnez O, Orellana R, Van Kerk O, Dehoux JP, Donnez J, Dolmans MM. Invasion process of induced deep nodular endometriosis in an experimental baboon model: similarities with collective cell migration? Fertil Steril. 2015;104:491-7.e2.
16. Wu T, Zhang R, Jiang Q, Li Z, Wu R. Expression of cellular adherent and invasive molecules in recurrent ovarian endometriosis. J Int Med Res. 2020;48:300060520971993.

Clinical Investigation / Araştırma

DOI: 10.4274/tjod.galenos.2026.26098

Turk J Obstet Gynecol 2026;23(1):95-100

Inverted microscopy-based assessment reveals major maturation gap between denuded and non-denuded GV oocytes: A novel r-IVM approach

İnvert mikroskopi ile yapılan değerlendirme, denüdasyon uygulanan ve uygulanmayan GV oositler arasında belirgin bir maturasyon farkı ortaya koyuyor: Yenilikçi bir r-IVM yaklaşımı

Nuri Peker[1], Ayşen Yücetürk[1], Özge Karaosmanoğlu[1], Esra Tığlı[2], Burak Elmas[1], İlke Özer Aslan[1], Burcu Aksu Türan[1], Bülent Tıraş[3]

[1]*Acıbadem Maslak Hospital, In Vitro Fertilization Center, İstanbul, Türkiye*

[2]*Kütahya University Faculty of Medicine, Kütahya, Türkiye*

[3]*Acıbadem Mehmet Ali Aydınlar University School of Medicine, Department of Obstetrics & Gynecology and Reproductive Endocrinology, İstanbul, Türkiye*

Abstract

Objective: To compare the maturation rate and developmental potential of immature oocytes subjected to and spared from cumulus-oocyte complex (COC) denudation.

Materials and Methods: This single-center prospective observational study was conducted between 15 November-15-December 2025. Germinal vesicle (GV) oocytes were allocated to two groups: Group 1 included oocytesobtained from follicles >10 mm and identified as GV following denudation, whereas group 2 included immature oocytes retrieved from non-dominant follicles with diameter <10 mm, and assessed under an inverted microscope immediately after oocyte retrieval and placed into culture medium without being denuded. All immature oocytes were cultured separately in Continuous Single Culture-NX Complete medium, supplemented with gentamicin and human serum albumin, for 24 hours. COCs in group 2 were subsequently denuded and evaluated for nuclear maturation. Oocytes reaching metaphase II (MII) underwent intracytoplasmic sperm injection. The primary outcome was the MII maturation rate; secondary outcomes included 2PN formation rate and cleavage-stage embryo rate.

Results: A total of 885 oocytes were retrieved from 52 patients. Group 1 included 84 denuded GV oocytes, and group 2 comprised 141 non-denuded COCs. After 24 hours of culture, maturation rates in groups 1 and 2 were 3/84 (2.37%) and 52/141 (36.9%), respectively. In group 1, only one oocyte was fertilized, and the resulting embryo arrested on day 3. In group 2, the fertilization and day-3 embryo rates were 23/48 (47.9%) and 14/23 (73.4%), respectively.

Conclusion: Non-denuded immature oocytes demonstrated significantly higher maturation, fertilization, and embryo development rates compared with denuded oocytes.

Keywords: Inverted microscope, germinal vesicle, immature oocyte, in vitro maturation

Öz

Amaç: Kümülüs-oosit kompleksi (KOK) denüdasyonu uygulanan ve uygulanmayan immatür oositlerin 24 saatlik kültür sonrası maturasyon oranı ve embriyo gelişim potansiyelinin karşılaştırılması amaçlandı.

Gereç ve Yöntemler: Bu tek merkezli prospektif gözlemsel çalışma 15 Kasım-15 Aralık 2025 tarihleri arasında gerçekleştirildi. İşlem sırasında elde edilen germinal vezikül (GV) evresindeki oositler iki gruba ayrıldı. Grup 1, denüdasyon sonrası GV olarak tanımlanan ve 10 mm üzeri foliküllerden

PRECIS: The maturation rate of non-denuded immature oocytes was found to be significantly higher than that of denuded oocytes.

Corresponding Author/Sorumlu Yazar: Nuri Peker, MD,
Acıbadem Maslak Hospital, In Vitro Fertilization Center, İstanbul, Türkiye
E-mail: dr.nuripeker@gmail.com **ORCID ID:** orcid.org/0000-0002-4854-3851

Received/Geliş Tarihi: 02.02.2026 **Accepted/Kabul Tarihi:** 02.03.2026 **Publication Date/Yayınlanma Tarihi:** 05.03.2026

Cite this article as: Peker N, Yücetürk A, Karaosmanoğlu Ö, Tığlı E, Elmas B, Özer Aslan İ, et al. Inverted microscopy-based assessment reveals major maturation gap between denuded and non-denuded GV oocytes: a novel r-IVM approach. Turk J Obstet Gynecol.2026;23(1):95-100

elde edilen oositlerden; grup 2 ise KOK denüdasyonu yapılmaksızın inverted mikroskop altında değerlendirilen ve çapı 10 mm'nin altında olan foliküllerden elde edilen GV oositlerden oluştu. Tüm oositler, gentamisin ve insan serum albümini içeren Continuous Single Culture NX Complete ortamında 24 saat ayrı ayrı kültüre edildi. Grup 2'deki KOK'lar inkübasyon sonunda denude edilerek nükleer maturasyon açısından değerlendirildi. Metafaz II (MII) evresine ulaşan oositlere intrasitoplazmik sperm enjeksiyonu uygulandı. Birincil sonuç ölçütü MII'ye ulaşma oranı, ikincil sonuç ölçütleri ise 2PN oranı, klivaj evresi embriyo oranıydı.

Bulgular: Çalışmaya dahil edilen 52 hastadan toplam 885 oosit elde edildi. Grup 1'de 84 denüde edilmiş GV oositi, grup 2'de ise 141 denüde edilmemiş GV oositi değerlendirildi. Yirmi dört saatlik kültür sonrası MII oranları sırasıyla 3/84 (%2,37) ve 52/141 (%36,9) olarak bulundu. Grup 1'de yalnızca bir oosit fertilize oldu ve embriyo 3. günde gelişimini durdurdu. Grup 2'de fertilizasyon ve klivaj oranları sırasıyla 23/48 (%47,9) ve 14/23 (%73,4) olarak saptandı.

Sonuç: Denüde edilmemiş immatür oositlerde maturasyon, fertilizasyon ve embriyo gelişim oranları denüde edilmiş oositlere kıyasla istatistiksel olarak anlamlı derecede daha yüksekti.

Anahtar Kelimeler: İnvert mikroskop, germinal vezikül, immatür oosit, in vitro maturasyon

Introduction

In vitro maturation (IVM) is defined as the maturation of immature oocytes, either germinal vesicle (GV) or metaphase 1 (MI) stage oocytes in a laboratory culture system to obtain a metaphase 2 (MII) stage oocyte[1]. Several IVM types have been defined across various classification systems; the most commonly used are categorized into three main groups: classical IVM, biphasic IVM, and rescue IVM[1-3]. In classical and biphasic IVM, oocytes are matured *ex vivo* without prior denudation; however, in rescue-IVM (r-IVM), oocytes are collected following a conventional in vitro fertilization (IVF) cycle, denuded, and cultured in IVM medium[1-3]. r-IVM has been particularly used in patients with diminished ovarian reserve (DOR) and poor ovarian response, as well as in those yielding a limited number of mature oocytes, to increase the total number of MII oocytes available[1-3]. Although r-IVM allows the retrieval of additional MII oocytes, the procedure has several important limitations that hinder its widespread adoption. The most notable limitations include low maturation rates and significantly lower blastocyst formation rates compared with those observed in *in vivo*-matured oocytes[2].

In the literature, maturation and blastocyst development rates in IVM cycles vary considerably, with reported blastocyst formation rates falling below 20%[2,3]. It has been suggested that even when nuclear maturation occurs and an MII oocyte is formed, blastocyst development rates remain low owing to insufficient cytoplasmic maturation. Disruption of communication between the cumulus cells and the oocyte, following denudation, is considered one of the most important causes of deficient cytoplasmic maturation. In addition, aberrant mitochondrial distribution and reduced ATP generation may further compromise embryo competence[4,5].

Materials and Methods

We conducted a single-center, prospective, observational study from 15 November to 15 December 2025. The study was reviewed and approved by the Acıbadem University Ethics Committee and was performed in accordance with the principles of the 1975 Declaration of Helsinki as revised in 2000 (approval no: 2025-17/627, date: 30.10.2025). Informed consent was obtained from all participants before study enrollment.

Cumulus-oocyte complexes (COCs) obtained from follicles <10 mm in diameter were included into the study group (group 2). At oocyte retrieval, follicle diameters were measured by transvaginal ultrasonography; COCs from follicles <10 mm in diameter were allocated to a separate well of a 4-well dish. Immediately thereafter, the COCs were examined under an inverted microscope to assess oocyte nuclear maturation. Those identified as MII were isolated and, approximately 2-3 hours later, denuded and subjected to intracytoplasmic sperm injection (ICSI). COCs containing GV oocytes were separated and were not denuded; instead, they were transferred to the same culture medium as group 1 and incubated for 24 hours, after which they were denuded and assessed for nuclear maturation. The control group (Group 1) was composed of GV oocytes obtained from COCs collected from follicles with diameter larger than 10 mm during the OPU procedure. These denuded GV oocytes were then cultured in culture medium for 24 hours, after which their nuclear maturation status was re-evaluated. Subsequently, oocytes from both groups that had progressed to MII were evaluated and subjected to ICSI. In both groups, 2PN formation, cleavage-stage embryo development were monitored.

The primary outcome was the MII maturation rate. The secondary outcomes were the 2PN rate and the cleavage-stage embryo rate.

Ovarian Hyperstimulation Protocol

All patients received a GnRH antagonist protocol and final oocyte maturation was triggered using human chorionic gonadotropin, gonadotropin-releasing hormone agonist, or both. Oocyte retrieval was performed 36 hours after triggering, using a 17-G needle under sedation.

Evaluation of COCs Under Inverted Microscope

Follicular fluid was poured into a 90-mm Petri dish, which was then tilted at a 30-45 °C angle to spread the fluid and visualize the COCs. COCs were subsequently examined under an inverted microscope, using the same dish, to

assess nuclear maturation status. Just before observation, the cumulus was gently spread laterally with a pipette to improve visualization of the oocyte. Figure 1 illustrates a MII oocyte and a GV as viewed under an inverted microscope.

Immature Oocyte Maturation Culture

Immature oocytes in both groups were cultured separately in Continuous Single Culture-NX Complete medium supplemented with gentamicin and human serum albumin for 24 hours. Subsequently, COCs in Group 2 were denuded and assessed for nuclear maturation. Oocytes that had progressed to MII in both groups were subsequently subjected to ICSI.

Results

A total of 885 oocytes were retrieved from 52 patients. Group 1 included 84 denuded immature oocytes, whereas group 2 contained 141 nondenuded COCs. In both groups, the immature oocytes were incubated in culture medium for 24 hours and subsequently evaluated for nuclear maturation. Table 1 summarizes the numbers of MII oocytes, fertilization rates, day-3 embryo rates, for both groups. In group 1, only 3 of the 84 immature oocytes matured to the MII stage following denudation. Of these three MII oocytes, only one fertilized, forming a 2PN zygote; however, this embryo arrested at the cleavage stage. In group 2, 141 COCs were identified as containing immature oocytes. Following 24 hours of culture, COCs were denuded: 52 (36.9%) oocytes had progressed to MII, 27 (19.2%) had progressed to MI, and 62 (43.9%) remained immature. ICSI was not performed on the MI oocytes. Notably, in one patient with azoospermia, the limited number of available spermatozoa precluded ICSI on the MII oocytes (n=4) that matured from immature oocytes; therefore, the available sperm were reserved for ICSI on MII oocytes retrieved from dominant follicles. ICSI was performed on 48 of the 52 MII oocytes; 23 (47.9%) of these demonstrated 2PN formation. Of the 23 2PN zygotes, 14 developed into day-3 embryos.

Discussion

In the present study, nuclear maturation was assessed without COC denudation, using an inverted microscope, which enabled distinction between mature and immature oocytes. When COCs containing immature oocytes were maintained in culture medium for 24 hours without denudation, a 36.9%

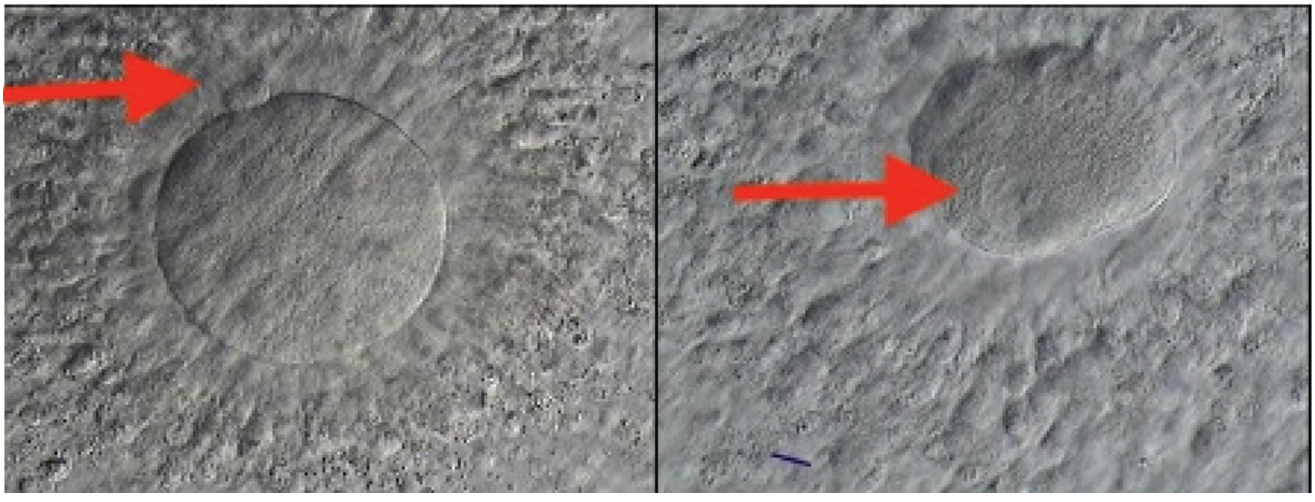

Figure 1. Visualization of the nuclear maturation of the oocytes under an inverted microscope. The red arrow in the left panel indicates a polar body, consistent with an metaphase II oocyte. The red arrow on the right panel indicates a germinal vesicle, consistent with an immature oocyte

Table 1. Comparison of group 1 and group 2 with respect to MII oocyte, 2PN, day-3 embryo, and blastocyst numbers and rates

Variable	Group 1 (denuded)	Group 2 (non-denuded)
Immature oocyte number	84	141
MII oocyte number (maturation rate)	3/84 (2.37%)	52/141 (36.9%)
2PN number/rate	1/3 (33.3%)	23/52 (47.9%)
Day-3 embryo number/rate	0	14/23 (73.4%)

MII: Metaphase II

maturation rate (GV to MII), a 47.9% fertilization rate, and a 73.4% day-3 embryo rate were observed. Although these rates are lower than those reported in the literature for r-IVM, no IVM-specific maturation medium was used in our protocol. To the best of our knowledge, this is the first study to assess oocyte nuclear maturation and to allow immature oocytes to undergo IVM without COC denudation.

The study conducted at our clinic was not designed to investigate the IVM of immature oocytes or to evaluate the outcomes of standard IVM protocols. Instead, our objective was to identify immature oocytes within COCs using an inverted microscope without denudation, to keep these COCs in culture for 24 hours, and to assess their maturation outcomes. Notably, IVM is not routinely performed at our center. Our routine protocol involves maintaining oocytes in culture medium for 2-3 hours following retrieval, after which they are denuded. ICSI is then performed on MII-stage oocytes, whereas immature oocytes undergo an additional 24-hour incubation, after which nuclear maturation is re-evaluated and ICSI is performed on those that have progressed to MII.

Tracing its historical development, rescue IVM entered clinical use in the late 1990s; however, it did not become a routine clinical practice, as adequate numbers of mature oocytes could not be consistently obtained and prolonged culture durations accelerated oocyte aging[6,7]. From the 2020s onward, rescue IVM continued to be employed in patients with DOR or in those yielding only a limited number of MII oocytes, with the aim of deriving mature oocytes from immature ones and thereby improving IVF outcomes[1,6,7]. Nevertheless, the lack of complete cytoplasmic maturation led to lower fertilization rates, reduced blastocyst formation, and lower euploidy rates[8]. Furthermore, the absence of standardized IVM culture media further contributed to these low success rates[9]. In a study conducted by Ahmad et al.[2], the effectiveness of r-IVM between women with DOR and those with normal ovarian response was compared, reporting higher rates of oocyte maturity, fertilization, and embryo quality in the DOR group. Although the study populations and comparators differ, these findings collectively underscore that r-IVM outcomes may be influenced by multiple factors beyond ovarian reserve, including oocyte handling prior to culture. Qin et al.[10] compared patients who underwent conventional IVF alone with those who additionally received r-IVM. The latter group demonstrated significantly improved IVF outcomes, including higher numbers of MII oocytes, 2PN rates, and day-3 embryo rates. In a systematic review and meta-analysis of 27 r-IVM trials, oocyte maturation rates were reported as 57% for MI-to-MII and 68% for GV-to-MII progression[11]. The blastulation rates were 16% for oocytes that matured from GV to MII. Additionally, that review demonstrated that clinical pregnancy and live birth rates were significantly higher in r-IVM cycles[11]. Similarly, Wei et al.[12] reported that r-IVM improved clinical pregnancy and live birth rates in patients with fewer than 9 MII oocytes. In a 2024 meta-analysis, 24 studies were evaluated, comprising a total of 74,136 oocytes. Among these oocytes, 59,144 were MII, 11,326 were MI, and 3,666 were GV oocytes. When maturation rates were assessed, 38.8% of MI oocytes and 58.2% of GV oocytes reached maturity[13]. In that meta-analysis, fertilization, cleavage, and blastocyst development rates, and consequently clinical pregnancy and live-birth rates, of GV-derived oocytes were significantly lower than those of *in vivo*-matured MII oocytes collected within the same cycle[13]. Although a direct comparison is limited by differences in culture conditions and by the absence of a dedicated IVM medium in our protocol, the maturation rates observed in the non-denuded group suggest that preservation of COC integrity may contribute to oocyte developmental competence during *in vitro* culture. A common feature of all these studies is that r-IVM was applied to immature oocytes following COC denudation. However, studies have demonstrated bidirectional communication between cumulus cells and the oocyte, in which cumulus cells transmit cytokines and growth factors to the oocyte through gap junctions. It has been shown that cAMP, cGMP, amino acids, pyruvate, ions, and various cytokines maintain the oocyte in meiotic arrest, prevent premature maturation, and provide the energy required for proper maturation. Following the early denudation of COCs, the bidirectional communication between cumulus cells and the oocyte is disrupted; as a result, while nuclear maturation occurs prematurely, cytoplasmic maturation is delayed, compromising the developmental potential of the oocyte[14,15].

In the present study, the maturation rate in group 1 was significantly lower than that in group 2. We attribute this outcome primarily to early cumulus cell removal and to the absence of a dedicated IVM medium. When discussing the effects of cumulus cells on oocyte maturation, it is important to emphasize that these cells possess significant antioxidant and cytoprotective functions[16]. Cumulus cells rapidly eliminate reactive oxygen species (ROS) present in the environment, thereby reducing or completely preventing the damaging effects that ROS may exert on the oocyte cytoplasm, meiotic spindle apparatus, mitochondrial DNA, and other cytoplasmic organelles[17]. In addition, cumulus cells help maintain stable glutathione (GSH) levels in the microenvironment, providing further antioxidant protection. Since the oocyte has a limited capacity to synthesize GSH, this support is crucial for achieving high-quality maturation[17,18]. Furthermore, bidirectional and dynamic communication exists between cumulus cells and the oocyte. Through gap-junctional signaling, this communication ensures that nuclear maturation and cytoplasmic maturation proceed in a coordinated and well-regulated manner[19,20]. When this communication

is disrupted, premature nuclear maturation occurs while cytoplasmic maturation remains insufficient, ultimately preventing the oocyte from reaching full developmental competence[19,20]. The markedly lower maturation rates observed in denuded oocytes are largely explained by the loss of this antioxidant protection and intercellular communication. We attribute the higher oocyte maturation rates in the non-denuded COC group to the antioxidant effects of the cumulus cells surrounding the oocyte and to the preservation of intact bidirectional communication that prevents premature nuclear maturation.

The absence of an appropriate IVM medium is one of the major contributing factors to the low maturation rates. IVM media are culture systems formulated to support maturation of immature oocytes under controlled laboratory conditions. They differ significantly from standard IVF media because immature oocytes have far more complex biological requirements, necessitating a microenvironment that mimics the natural follicular milieu by incorporating growth factors, hormones, and antioxidants[19]. Although patient characteristics, age, and related clinical variables can influence oocyte maturation rates, the use of sibling oocytes makes it unlikely that individual patient variables alone fully explain the magnitude of the observed difference between groups. Therefore, we consider the culture conditions and the degree of cumulus cell preservation to be the primary determinants of the observed discrepancy.

Study Limitations

The present study has several limitations. The first limitation is the relatively small sample size. The secondand most critical limitation is the absence of a dedicated IVM medium. Third, the study does not include pregnancy outcomes, which precludes a complete assessment of the clinical potential of non-denuded r-IVM. Nevertheless, our work represents a novel and potentially significant contribution to the field of r-IVM.

Conclusion

With the adoption of optimized and standardized IVM media, r-IVM protocols performed without prior COC denudation may yield higher maturation rates, improved blastocyst development rates, and ultimately increased live birth rates.

Ethics

Ethics Committee Approval: The study was reviewed and approved by the Acıbadem University Ethics Committee and was performed in accordance with the principles of the 1975 Declaration of Helsinki as revised in 2000 (approval no: 2025-17/627, date: 30.10.2025).

Informed Consent: Informed consent was obtained from all participants before study enrollment.

Footnotes

Authorship Contributions

Surgical and Medical Practices: N.P., A.Y., Concept: N.P., A.Y., E.T., B.T., Design: N.P., A.Y., Ö.K., E.T., B.T., Data Collection or Processing: N.P., A.Y., Ö.K., B.E., İ.Ö.A., B.A.T., Analysis or Interpretation: N.P., B.A.T., B.T., Literature Search: N.P., E.T., Writing: N.P., E.T., B.T.

Conflict of Interest: No conflict of interest was declared by the authors.

Financial Disclosure: The authors declared that this study received no financial support.

References

1. Gilchrist RB, Smitz J. Oocyte in vitro maturation: physiological basis and application to clinical practice. Fertil Steril. 2023;119:524-39.
2. Ahmad MF, Mohd Nor NY, Mohammad Ramadneh MM, Roseli NI, Elias MH, Mat Jin N, et al. Comparative analysis of rescue-in vitro-maturation (r-IVM) outcomes in women with diminished ovarian reserve (DOR) versus normal ovarian reserve (NOR). Biomedicines. 2025;13:1084.
3. Shani AK, Haham LM, Balakier H, Kuznyetsova I, Bashar S, Day EN, et al. The developmental potential of mature oocytes derived from rescue in vitro maturation. Fertil Steril. 2023;120:860-9.
4. Kirillova A, Smitz JEJ, Sukhikh GT, Mazunin I. The role of mitochondria in oocyte maturation. Cells. 2021;10:2484.
5. Buratini J, Soares ACS, Barros RG, Dellaqua TT, Lodde V, Franciosi F, et al. Physiological parameters related to oocyte nuclear differentiation for the improvement of IVM/IVF outcomes in women and cattle. Reprod Fertil Dev. 2021;34:27-35.
6. Jie H, Zhao M, Alqawasmeh OAM, Chan CPS, Lee TL, Li T, et al. *In vitro* rescue immature oocytes - a literature review. Hum Fertil (Camb). 2022;25:640-50.
7. De Vos M, Grynberg M, Ho TM, Yuan Y, Albertini DF, Gilchrist RB. Perspectives on the development and future of oocyte IVM in clinical practice. J Assist Reprod Genet. 2021;38:1265-80.
8. Yuan Y, Reed L, Swain JE, Schoolcraft WB, Katz-Jaffe MG. Rescue in vitro maturation and the transfer of a euploid blastocyst provided improved chances for patients with poor prognosis to conceive. Fertil Steril. 2024;121:121-2.
9. Soler N, Cimadomo D, Escrich L, Grau N, Galán A, Alamá P, et al. Rescue in vitro maturation of germinal vesicle oocytes after ovarian stimulation: the importance of the culture media. Hum Reprod. 2025;40:1504-15.
10. Qin DY, Jiang HH, Yao QY, Yao W, Yuan XQ, Wang Y, et al. Rescue *in vitro* maturation may increase the pregnancy outcomes among women undergoing intracytoplasmic sperm injection. Front Endocrinol (Lausanne). 2022;13:1047571.
11. Coffey H, Thomson A, Popa T, Morgan R, Iliev D, Taneja J, et al. O-183 evaluating the role of rescue IVM and rescue ICSI in ART: a systematic review and meta-analysis of outcomes in low/failed maturation and fertilisation cases. Hum Reprod. 2025;40(Suppl 1).
12. Wei J, Luo Z, Dong X, Jin H, Zhu L, Ai J. Cut-off point of mature oocyte for routine clinical application of rescue IVM: a retrospective cohort study. J Ovarian Res. 2023;16:226.
13. Bartolacci A, Busnelli A, Pagliardini L, de Girolamo S, De Santis L, Esposito S, et al. Assessing the developmental competence of oocytes

matured following rescue in vitro maturation: a systematic review and meta-analysis. J Assist Reprod Genet. 2024;41:1939-50.

14. Zhou CJ, Wu SN, Shen JP, Wang DH, Kong XW, Lu A, et al. The beneficial effects of cumulus cells and oocyte-cumulus cell gap junctions depends on oocyte maturation and fertilization methods in mice. PeerJ. 2016;4:e1761.
15. Xie J, Xu X, Liu S. Intercellular communication in the cumulus-oocyte complex during folliculogenesis: a review. Front Cell Dev Biol. 2023;11:1087612.
16. Hatırnaz Ş, Ata B, Hatırnaz ES, Dahan MH, Tannus S, Tan J, et al. Oocyte *in vitro* maturation: a systematic review. Turk J Obstet Gynecol. 2018;15:112-25.
17. Rohn MCH, Simeone JM, Doctorman S, Ge P, Hernandez A, Das S, et al. The functional role of cumulus cells and their influence on oocyte quality: a systematic review. Reprod Sci. 2025;32:2877-902.
18. Nikoloff N. The key role of cumulus cells in oocytes in vitro maturation protocols. Fertil Steril. 2021;116:1663.
19. Liu W, Chen C, Gao Y, Cui X, Zhang Y, Gu L, et al. Transcriptome dynamics and cell dialogs between oocytes and granulosa cells in mouse follicle development. Genomics Proteomics Bioinformatics. 2024;22:qzad001.
20. Martinez CA, Rizos D, Rodriguez-Martinez H, Funahashi H. Oocyte-cumulus cells crosstalk: new comparative insights. Theriogenology. 2023;205:87-93.

Review / Derleme

DOI: 10.4274/tjod.galenos.2026.02391

Turk J Obstet Gynecol 2026;23(1):101-114

The letrozole use in reproductive medicine: Beyond aromatase inhibition - a comprehensive review

Üreme tıbbında letrozol kullanımı: Aromataz inhibisyonunun ötesi - kapsamlı derleme

Gerçek Aydın[1,2], Şafak Hatırnaz[3], Ebru Saynur Hatırnaz[4], Mehmet Bilge Çetinkaya[5], Muhterem Akdeniz[5], Nur Dokuzeylül Güngör[6], Oğuz Güler[7], Merdan Ali Merdanoğlu[8], Asiye Uzun[9], Semra Eroğlu[10], Önder Tosun[11], Ali Bahadırlı[12], Engin Yurtçu[13], Betül Keyif[13], Huri Güvey[14], Naziye Gürkan[5], Pervin Karlı[15], Zehra Yılmaz[16], Giorgio Maria Baldini[17], Aziz İhsan Tavuz[18], Radmila Sparic[19,20], Nikoleta Tabakova[21], Andrea Tinelli[22], Mingju Cao[22], Seang Lin Tan[23], Oğuz Hatırnaz[24], Michael Dahan[25]

[1]*İstanbul Health and Technology University Faculty of Medicine, Department of Obstetrics and Gynecology, İstanbul, Türkiye*
[2]*Eurofertil IVF Center, Bursa, Türkiye*
[3]*Kent University School of Health Sciences, İstanbul, Türkiye*
[4]*Maltepe University Faculty of Medicine, Department of Histology and Embryology, İstanbul, Türkiye*
[5]*Medical Park Samsun Hospital, IVF Center, Samsun, Türkiye*
[6]*Bahçeşehir University Faculty of Medicine, Department of Obstetrics and Gynecology, İstanbul, Türkiye*
[7]*Private Gazi Hospital, Clinic of Obstetrics and Gynecology, İstanbul, Türkiye*
[8]*Yunus Emre State Hospital, IVF Center, Eskişehir, Türkiye*
[9]*Medipol University Faculty of Medicine, Department of Obstetrics and Gynecology, İstanbul, Türkiye*
[10]*Samsun University Faculty of Medicine, Department of Obstetrics and Gynecology, Samsun, Türkiye*
[11]*University of Health Sciences Türkiye, Zeynep Kamil Maternity and Children Training and Research Hospital, İstanbul, Türkiye*
[12]*Bursa City Hospital, Bursa, Türkiye*
[13]*Düzce University Faculty of Medicine, Department of Obstetrics and Gynecology, Düzce, Türkiye*
[14]*Kütahya Health Sciences University Faculty of Medicine, Department of Medical Education and Informatics, Kütahya, Türkiye*
[15]*Private Office, Samsun, Türkiye*
[16]*Private Clinic, Samsun, Türkiye*
[17]*MOMO' FertiLIFE, IVF Clinic, Bisceglie, Italy*
[18]*Momart IVF Center, İstanbul, Türkiye*
[19]*Faculty of Medicine, University of Belgrade, Belgrade, Serbia*
[20]*Clinic for Gynecology and Obstetrics, University Clinical Centre of Serbia, Belgrade, Serbia*
[21]*Medical University of Varna, Varna, Bulgaria*
[22]*Department of Obstetrics and Gynecology, "Veris delli Ponti" Hospital, CEntro di RIcerca Clinico SALentino (CERICSAL), "Veris delli Ponti" Hospital, Scorrano, Italy*
[23]*Originelle Women's Health and Fertility Center, Quebec, Canada*
[24]*Ondokuz Mayıs University Faculty of Medicine, Samsun, Türkiye*
[25]*Reproductive Medicine Center, McGill University Faculty of Medicine, Quebec, Canada*

Corresponding Author/Sorumlu Yazar: Asst. Prof. Gerçek Aydın,
İstanbul Health and Technology University Faculty of Medicine, Department of Obstetrics and Gynecology; Eurofertil IVF Center, İstanbul, Bursa, Türkiye
E-mail: gercekay@yahoo.com **ORCID ID:** orcid.org/0000-0002-5638-3675

Received/Geliş Tarihi: 10.12.2025 **Accepted/Kabul Tarihi:** 04.02.2026 **Epub:** 17.02.2026 **Publication Date/Yayınlanma Tarihi:** 05.03.2026

Cite this article as: Aydın G, Hatırnaz Ş, Saynur Hatırnaz E, Çetinkaya MB, Akdeniz M, Dokuzeylül Güngör N, et al. The letrozole use in reproductive medicine: beyond aromatase inhibition - a comprehensive review. Turk J Obstet Gynecol. 2026;23(1):101-114

Abstract

Letrozole and other aromatase inhibitors are increasingly recognized as first-line ovulation induction (OI) medications, offering an efficient and physiologic approach to ovarian stimulation that enhances outcomes in reproductive medicine. By selectively inhibiting aromatase and maintaining lower peripheral estrogen levels, letrozole supports mono- or bi-follicular development while reducing the risk of supraphysiologic estradiol exposure seen with traditional gonadotropin regimens. These pharmacological characteristics have contributed to its expanding use not only in OI but also in various assisted reproductive technologies. To evaluate the clinical benefits, effectiveness, and safety of using letrozole in in vitro fertilization (IVF), in vitro maturation (IVM), and OI, with particular attention to reproductive outcomes, ovarian response, endometrial effects, cycle characteristics, and treatment-related adverse events. A comprehensive systematic search covering the period from December 2000 to November 2025 was conducted across major electronic databases including PubMed, Embase, the Cochrane Library, and Google Scholar. The search strategy incorporated predefined keywords related to letrozole, aromatase inhibition, OI, IVF, and IVM. Studies involving randomized controlled trials, observational cohorts, and meta-analyses were included, while non-clinical and non-reproductive data were excluded. Relevant outcomes were extracted and synthesized qualitatively. Letrozole demonstrates broad clinical utility in reproductive medicine, spanning assisted reproductive techniques, ovarian stimulation strategies, and the management of ovarian hyperstimulation syndrome risk, ectopic pregnancy, and endometriosis-related infertility. Its targeted estrogen suppression, cost-effectiveness, and favorable safety profile make it a valuable component of individualized treatment protocols. Nonetheless, further high-quality research is required to refine optimal dosing strategies, identify ideal patient populations, and clarify long-term reproductive and obstetric safety.

Keywords: Letrozole, assisted reproductive medicine, infertility, in vitro fertilization, in vitro maturation

Öz

Letrozol ve diğer aromataz inhibitörleri, giderek artan biçimde birinci basamak ovülasyon indüksiyonu (Oİ) ajanları olarak kabul edilmekte olup, üreme tıbbında sonuçları iyileştiren etkili ve fizyolojik bir over stimülasyon yaklaşımı sunmaktadır. Aromatazı selektif olarak inhibe ederek periferal östrojen düzeylerini düşürmesi, geleneksel gonadotropin protokollerinde görülen suprafizyolojik östradiol maruziyetini azaltırken, mono- veya bifolliküler gelişimi desteklemektedir. Bu farmakolojik özellikler, letrozolün yalnızca Oİ'de değil, çeşitli yardımcı üreme tekniklerinde de kullanım alanının genişlemesine katkı sağlamıştır. Letrozolün in vitro fertilizasyon (IVF), in vitro maturasyon (IVM) ve Oİ'deki klinik faydalarını, etkinliğini ve güvenlilik profilini değerlendirmek; özellikle üreme sonuçları, over yanıtı, endometriyal etkiler, siklus karakteristikleri ve tedaviye bağlı advers olaylara odaklanmak. Aralık 2000 ile Kasım 2025 dönemini kapsayan kapsamlı bir sistematik tarama, PubMed, Embase, Cochrane Library ve Google Scholar gibi temel elektronik veri tabanlarında gerçekleştirilmiştir. Arama stratejisinde letrozol, aromataz inhibisyonu, Oİ, IVF ve IVM ile ilgili önceden belirlenmiş anahtar kelimeler kullanılmıştır. Randomize kontrollü çalışmalar, gözlemsel kohortlar ve meta-analizler dahil edilmiş; klinik dışı ve üreme tıbbıyla ilişkili olmayan veriler dışlanmıştır. İlgili sonuçlar çıkarılmış ve niteliksel olarak sentezlenmiştir. Letrozol, yardımcı üreme tedavileri, over stimülasyon stratejileri ve yumurtalık hiperstimülasyon sendromu risk yönetiminden ektopik gebelik ve endometriozis ilişkili infertiliteye kadar geniş bir klinik kullanım yelpazesi göstermektedir. Hedefe yönelik östrojen baskılanması, maliyet etkinliği ve olumlu güvenlilik profili ile bireyselleştirilmiş tedavi protokollerinin değerli bir bileşenidir. Bununla birlikte, optimal dozlama stratejilerinin netleştirilmesi, ideal hasta gruplarının belirlenmesi ve uzun dönem üreme ile obstetrik güvenliğin aydınlatılması için daha yüksek kaliteli çalışmalara ihtiyaç vardır.

Anahtar Kelimeler: Letrozol, yardımcı üreme tıbbı, infertilite, in vitro fertilizasyon, in vitro maturasyon

Introduction

Despite remarkable advancements in reproductive medicine, many conditions continue to limit treatment success and patients' quality of life. As the field increasingly moves toward individualized, physiology-based therapies, agents that modulate estrogen pathways while maintaining favorable safety profiles have gained renewed clinical relevance.

Targeted blockade of estrogen production is a cornerstone treatment strategy for estrogen-sensitive tumors; aromatase inhibitors have been used for this purpose[1]. It was then discovered, coincidentally, that a decrease in estrogen produces a feedback-driven increase in endogenous follicle-stimulating hormone (FSH) secretion, and that aromatase inhibitors were found to be strong ovulation inducers nearly two decades ago[2].

Letrozole, a non-steroidal oral third-generation aromatase inhibitor (AI), reversibly blocks the cytochrome P450 aromatase enzyme, a key enzyme in the biosynthesis of estrogens from androgens[1,3].

Legro et al.[2] published the first article on the use of letrozole as a sole ovulation-induction agent in 2004, and since then, letrozole has been used worldwide, even in the USA, where the Food and Drug Administration (FDA) disapproved the use of letrozole as an agent for infertility.

Although decades have passed since aromatase inhibitors were introduced in reproductive endocrinology, data remain fragmented across heterogeneous populations and diverse clinical scenarios. To accurately define the present role of letrozole and to anticipate its future place in reproductive practice, a comprehensive synthesis of current insights, clinical applications, and safety considerations is essential. In this review, we aimed to consolidate existing knowledge across all major domains of the use of letrozole, clarify areas of controversy, and provide clinicians with an updated, evidence-based framework for its responsible and informed application.

Methods

A comprehensive systematic search from 2000 to November 2025 was conducted in the databases PubMed, Embase, the Cochrane Library, and Google Scholar, using the following keywords: "in vitro fertilization" or "IVF", "in vitro maturation" or "IVM", "letrozole", "clomiphene citrate", "ovulation induction" or "OI", "ovarian hyperstimulation

syndrome" or "ovarian hyperstimulation syndrome (OHSS)", "ectopic pregnancy", "complications". The search strategy involved combining keywords using the Boolean operator 'AND'. After retrieving the related articles, the authors also evaluated the reference lists and citations for additional eligible data. All relevant articles were available in full text and English.

Inclusion Criteria

Regardless of study design, we included studies of letrozole for IVF, IVM, and OI. Articles comparing letrozole with clomiphene citrate, discussing letrozole-related complications, and addressing letrozole use for ectopic pregnancy were also retrieved.

Exclusion Criteria

Articles published before 2000 were excluded, except for selective references, to capture more recent data. Non-systematic reviews were excluded because of the risk of selection bias. Expert opinions and opinion-based papers were also excluded.

Data Collection and Analysis

Three review authors (MHD, AT and SH) independently checked for overlaps (duplications) among selected studies, assessed risk of bias, and extracted data.

Two Cell Two Gonadotropin Theory

Estrogen biosynthesis in the ovary is governed by the coordinated actions of theca and granulosa cells, as outlined in the "two-cell, two-gonadotropin theory." Ovarian steroidogenesis requires cooperative interactions between theca and granulosa cells, which are mainly controlled by luteinizing hormone (LH) and FSH. Falck first demonstrated the ovary as the site of estrogen production in rat microtransplantation studies[4]. Short[5] later proposed that theca cells convert progesterone to estrogens, further supporting this model.

According to this theory, LH stimulates theca cells to produce androgens, while FSH promotes aromatization of these androgens into estrogens within granulosa cells. Aromatase (CYP19), localized predominantly in granulosa cells, catalyzes this conversion, whereas 17α-hydroxylase (CYP17A1) is confined to the theca compartment, confirming functional specialization[6,7].

During follicular development, theca cells express LH receptors, P450scc (CYP11A1), and 3β-HSD, enabling cholesterol transport and conversion to pregnenolone. Androgen synthesis progresses via CYP17A1, and these androgens diffuse into granulosa cells, where FSH-dependent aromatase converts them into estrone and estradiol[7,8]. Rising estradiol exerts negative feedback on pituitary gonadotropin release.

FSH remains essential for early folliculogenesis, whereas LH supports terminal follicle maturation by increasing androgen substrate availability, enhancing dominant follicle selection, and promoting atresia of smaller follicles[9].

Aromatase Enzyme Activity; Both Sides of Reaction and Implications of Inhibition

Aromatase, an enzyme that catalyzes the demethylation of carbon-19 from androgens to produce phenolic 18-carbon estrogens, is a member of the cytochrome P450 superfamily. This superfamily includes more than 480 members and is the product of the *CYP19* gene. This reaction, catalyzed by aromatase, occurs mainly in the ovary[10]. Its expression in granulosa cells is regulated by cAMP and gonadotropins[11].

Letrozole competitively binds to aromatase due to structural similarity to androgen substrates, suppressing estrogen synthesis by up to 99%[12,13]. Reduced estradiol relieves negative feedback on gonadotropin-releasing hormone (GnRH), increasing FSH secretion and enhancing follicular recruitment[14].

Inhibition of aromatization increases intraovarian androgens, which support early follicular growth by stimulating granulosa-cell mitosis and FSH-receptor expression[15,16]. While moderate androgen exposure promotes folliculogenesis, excessive androgen levels in late follicular stages may induce atresia[17].

Aromatase is also expressed in extragonadal tissues, including adipose tissue, bone, brain, and vascular endothelium, contributing to systemic estrogen production[18]. Consequently, aromatase inhibition has therapeutic applications beyond reproductive medicine.

Third-generation aromatase inhibitors such as letrozole, anastrozole, and exemestane suppress systemic estrogen levels by over 95%[19,20].

Clinical Applications Beyond Infertility

Hormone-sensitive Breast Cancer

Aromatase inhibitors are cornerstone therapies for postmenopausal women with estrogen receptor (ER)-positive breast cancer. By depriving cancer cells of estrogen, AIs reduce tumor proliferation and recurrence, and thus offer superior outcomes compared with selective ER modulators like tamoxifen[21].

Endometriosis Management

Endometriosis, the expression and growth of endometrial tissue (both glands and stroma) outside the uterus, is associated with greatly increased aromatase activity compared with eutopic endometrium. Estrogen dependence in endometriotic lesions makes aromatase inhibition a promising approach. Studies have reported reduced lesion size and symptomatic relief in women treated with letrozole or other agents. This is particularly the case when combined with GnRH agonist suppression of ovarian estradiol production[22,23].

Bone Health: While the reduction in systemic estrogen levels seen with long-term AI use, commonly prescribed

for ER-positive cancers, poses a risk of loss of bone mineral density, concurrent use of bisphosphonates or selective ER modulators can mitigate this side effect[24].

Research into the combination of aromatase inhibitors with other therapeutic agents holds promise for enhancing efficacy and reducing resistance. For instance, combining AIs with selective ER degraders or targeted molecular therapies is under investigation for advanced breast cancer[25].

In reproductive medicine, tailoring AI protocols based on individual ovarian reserve markers and genetic predispositions could optimize outcomes and minimize adverse effects[26]. Large doses of letrozole, up to 20 mg daily, have been used to induce multifollicular development in women with decreased ovarian reserve undergoing IVF, resulting in significant cost savings compared with gonadotropins[27].

Although aromatase inhibitors are generally well-tolerated, clinicians must remain vigilant regarding potential adverse effects, including musculoskeletal pain, hot flashes, and lipid profile alterations[28]. Monitoring and individualized patient management are essential to balance therapeutic benefits against risks.

Aromatase Inhibitors and Their Clinical Use

The development of AIs began with first-generation agents such as aminoglutethimide, which inhibited not only aromatase but also enzymes involved in the synthesis of cortisol, aldosterone, and thyroid hormones[29]. Fadrazole, a more potent and selective inhibitor than aminoglutethimide, was approved in Japan for estrogen-dependent postmenopausal breast cancer, but was never marketed in the United States[30]. Formestane, a steroidal aromatase inhibitor, significantly reduces circulating estrogen levels and demonstrates antitumor activity in postmenopausal women with breast cancer. Its side-effect profile is more favorable than that of aminoglutethimide[31,32]. Currently, three third-generation oral aromatase inhibitors—anastrozole, letrozole, and exemestane—are FDA-approved for the treatment of hormone-receptor-positive breast cancer in postmenopausal women. Large clinical trials have shown that AIs are generally more effective and better tolerated than tamoxifen, with superior response rates and longer time to progression[33,34]. These third-generation agents exhibit high selectivity for aromatase with minimal cross-reactivity[35].

Exemestane, the only steroidal oral AI, is widely used, particularly in combination with everolimus, for human epidermal growth factor receptor 2-negative, hormone-receptor-positive advanced breast cancer[36]. Exemestane is an active, well-tolerated third-line hormonal therapy for postmenopausal patients with advanced breast cancer who do not respond to standard first- and second-line hormonal therapies[37]. Comparative studies among exemestane, anastrozole, and letrozole have shown comparable efficacy[38,39]. Notably, all three AIs demonstrated superior efficacy to the ER antagonist tamoxifen in large head-to-head clinical trials for the treatment of postmenopausal estrogen-dependent breast cancer[34]. Vorozole was evaluated in Europe and Canada, but never received FDA approval[39].

Letrozole, an oral non-steroidal aromatase inhibitor, lowers estrogen levels in postmenopausal women by inhibiting cytochrome P450 aromatase, the enzyme that converts testosterone to estrogen. It does not stop the production of estrogen in the ovaries. It decreases the growth of hormone-receptor-positive breast cancer cells by reducing the amount of estrogen[40,41].

Letrozole: Molecular Structure and Mechanism of Action

Letrozole (code name: CGS-20267), a non-steroidal type II AI with a triazole ring, enables high-affinity, reversible binding at the aromatase substrate site[42]. With each successive generation, AIs have become increasingly powerful and specialized. Letrozole has the chemical formula C17H11N5 (illustrated in Figure 1) and a molecular weight of 285.31 g/mol[43]. Due to its favorable pharmacokinetic profile, letrozole can inactivate more than 98% of peripheral aromatase even at low daily doses of 0.5-2.5 mg[44]. It is rapidly absorbed with nearly 100% bioavailability, is 60% protein-bound (primarily to albumin), has a 42-hour half-life, and is hepatically metabolized to an inactive carbinol derivative that is excreted renally.

Letrozole competitively inhibits the aromatization of androstenedione and testosterone into estrone and estradiol,

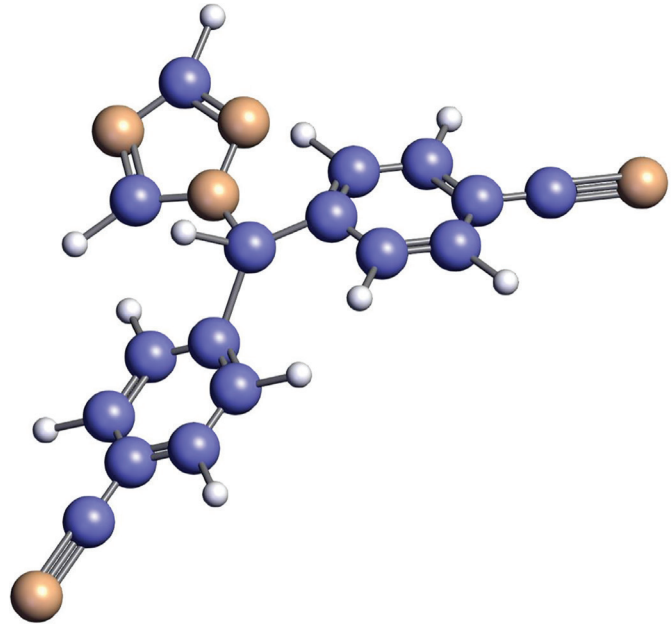

Figure 1. Chemical formula of letrozole (C17H11N5)

This figure illustrates the 3D ball-and-stick representation of letrozole, a non-steroidal aromatase inhibitor characterized by a triazole ring and substituted benzene moieties. The spatial configuration highlights key functional groups responsible for its high-affinity, reversible binding to the aromatase enzyme, underpinning its potent estrogen-suppressive activity

respectively. This inhibition creates a biochemical shift toward increased androgens and decreased estrogens. Its triazole structure coordinates to the heme iron of aromatase, effectively blocking hydroxylation reactions essential for aromatization and thereby achieving high potency and specificity[45].

Reduced estrogen levels remove negative feedback on the hypothalamic-pituitary axis, resulting in increased FSH secretion and stimulation of follicular development[46]. Increased intraovarian androgens further enhance follicular sensitivity to FSH and insulin-like growth factor-1 signaling. Because letrozole does not antagonize ERs in the brain, normal endocrine feedback resumes once the drug is cleared, promoting monofollicular development and reducing the risk of multifollicular development[47].

Decreased estrogen levels in the circulation and peripheral tissues, resulting from potent aromatase inhibition by letrozole, cause upregulation of ERs in the endometrium. Therefore, when estrogen secretion is restored, rapid endometrial growth is observed[48]. This is necessary for healthy implantation.

Letrozole Versus Clomiphene Citrate

Letrozole has been widely used for OI since 2001[43]. It suppresses estrogen synthesis, leading to compensatory increases in FSH, without exerting anti-estrogenic effects on the endometrium or the cervical mucus. Its short half-life (~48 hours) ensures rapid clearance letrozole also has proven reversible effects in postmenopausal breast cancer therapy[44]. Clomiphene citrate (CC), a selective ER modulator introduced in 1961, has long been used for OI in polycystic ovary syndrome (PCOS) and in intrauterine insemination (IUI) and IVF treatments[49]. By competitively binding to ERs, CC removes estrogen's negative feedback, thereby increasing gonadotropin secretion and follicular growth. However, CC exerts anti-estrogenic effects on endometrial development and cervical mucus, contributing to lower pregnancy rates despite adequate ovulation[50]. ER depletion in the endometrium leads to endometrial thinning in 15-50% of patients on CC treatment[51,52].

Many studies—including meta-analyses—show higher pregnancy and live-birth rates with letrozole. Fixed-dose study designs, however, limit some analyses. Letrozole has also been evaluated in normo-ovulatory women, showing favorable outcomes[53,54].

Letrozole's advantages include rapid elimination, the absence of endometrial ER depletion, and lower estradiol levels, despite similar numbers of preovulatory follicles. Letrozole-stimulated cycles typically avoid the supraphysiological E2 levels seen with CC[55]. Mitwally et al.[56] reported that pregnancies conceived after letrozole had miscarriage and ectopic rates similar to those in other stimulation groups, and that patients treated with letrozole had lower multiple gestation rates. Formun AltıMultifollicular development is common during CC treatment, and the risk of multiple gestation is increased to approximately 10-20% overall, compared with natural cycles.

Letrozole also appears to preserve endometrial receptivity better than CC. Experimental studies show that CC—but not letrozole—reduces key implantation markers, such as HOXA10 and integrin αvβ3[57]. Molecular studies further suggest that letrozole improves endometrial gene expression in PCOS, thereby making letrozole an alternative to CC[58].

Some evidence suggests increased aromatase activity in PCOS, potentially enhancing responsiveness to letrozole[59,60]. In unexplained infertility, letrozole improves endometrial thickness compared with CC, but results in similar pregnancy and miscarriage rates[61]. Additional studies indicate superior endometrial receptivity markers in PCOS treated with letrozole[62,63]. Letrozole is consistently associated with higher pregnancy rates, shorter time to conception, and a lower risk of multiple pregnancy due to monofollicular development.

Letrozole is also recommended for CC-resistant PCOS[64]. and may offer an effective alternative to CC-gonadotropin combinations in controlled ovarian hyperstimulation[65]. Mejia et al.[66] showed that the combination of letrozole and CC was associated with a higher ovulation rate than letrozole alone in women with infertility and PCOS. This therapy may be an alternative low-risk, low-cost infertility treatment that improves ovulation rates.

For unexplained infertility, heterogeneity across studies and patient populations limits the ability to draw firm conclusions; meta-analyses show no consistent difference between letrozole and CC[67].

Letrozole Use in Ovulation Induction

Letrozole has been widely used as an OI agent for over two decades. As an aromatase inhibitor, it blocks the conversion of androgens to estrogens, thereby relieving the hypothalamic-pituitary axis of estrogen-mediated negative feedback. This mechanism increases endogenous gonadotropin secretion while preserving endometrial receptivity, thereby distinguishing letrozole from traditional agents such as CC. The ability of letrozole to avoid antiestrogenic effects on the endometrium confers a significant clinical advantage over CC.

Its efficacy has been demonstrated in multiple randomized controlled trials and meta-analyses, which report superiority, or at least non-inferiority, to CC with respect to ovulation and pregnancy outcomes, as well as reduced multiple pregnancy rates and improved live birth rates[66].

Letrozole is now considered the first-line OI agent for women with PCOS, following the pivotal multicenter randomized controlled trial by Eskew et al.[67], which demonstrated significantly higher live birth rates than CC. In unexplained infertility, the combination of letrozole with IUI yields pregnancy rates comparable to CC but with fewer adverse effects.

Letrozole has also shown benefit in women with minimal-to-mild endometriosis by reducing estrogen-driven endometriotic activity and enhancing ovarian response[68]. In addition, recent evidence suggests potential utility in women with diminished ovarian reserve, in whom its ability to stimulate follicular recruitment without excessive estrogen exposure may offer a more physiological and tailored approach[69,70].

Letrozole Use in In Vitro Fertilization

Modified natural IVF (Mona-IVF) is a form of natural IVF in which follicle growth is augmented either with oral agents alone or together with parenteral drugs. Spontaneous ovulation can be suppressed or serum LH monitored without suppression, then final oocyte maturation is usually triggered by human chorionic gonadotropins.

CC and letrozole can only be used in a modified natural manner or as an adjunct to gonadotropin therapy for OI as a co-treatment in ovulatory and anovulatory patients in IVF protocols when ovarian function is present[71]. Advantages of Mona-IVF include fewer injections, reduced treatment burden, fewer side effects, reduced stress, and substantially decreased OHSS risk[13].

Letrozole promotes follicular development via aromatase inhibition, increasing intraovarian androgens that may upregulate FSH receptors and improve ovarian responsiveness-an effect particularly relevant for poor responders[72-74]. Its ability to maintain physiologic estradiol levels also makes it suitable for breast cancer patients who require controlled estrogen exposure during the IVF process.

Letrozole has also been used for endometrial preparation, resulting in physiologic serum estradiol levels and favorable endometrial morphology[75,76]. As proposed in a recent publication of Aydin et al.[77], letrozole may, due to its mechanism of action and its ability to enable formation of a corpus luteum, even be considered a first choice compared with natural and programmed cycles in various clinical scenarios. These features make letrozole useful for assisted reproductive techniques (ART).

Letrozole can be effectively used for OI in IVF cycles across different infertile populations, including patients with a poor ovarian response[71,78-80], patients with PCOS[81,82], patients with unexplained infertility[83], and women with contraindications to stimulation drugs. A recently published meta-analysis reported no difference in the number of oocytes retrieved [p=0.72, 95% confidence interval (CI): -0.41 to 0.60] or in the clinical pregnancy rate (CPR) (p=0.39, 95% CI: -0.02 to 0.06) between letrozole co-treatment and conventional IVF. However, subgroup analysis of five studies (n=526) involving patients with poor ovarian reserve revealed significantly higher live birth rates favoring letrozole, with a risk difference of 0.07 (p=0.03, 95% CI: 0.01 to 0.13)[84].

Letrozole can also be added to gonadotropins continuously throughout the ovarian stimulation period, with the aim of normalizing the disrupted endocrine milieu and reducing excessive estradiol levels resulting from multiple follicular development, particularly in patients with hormone-dependent breast cancer[85].

Letrozole Use in Modified Natural Fet Cycles (Mona-FET)

Freeze-all strategies are beneficial for patients at high-risk of OHSS, particularly patients with PCOS, and permit optimization of embryo transfer timing while maximizing cumulative live birth rates[86]. Endometrial preparation for FET can be performed via full natural cycle, modified natural cycle, or artificial cycle with hormone-replacement therapy (HRT)[87,88].

Although HRT cycles were previously dominant, natural[89] and modified natural approaches have gained preference due to more physiological hormonal profiles and reduced thromboembolic and hypertensive risks[90].

Full natural cycles require detection of the LH peak and have limited scheduling flexibility. Modified natural cycles address this by triggering ovulation with human chorionic gonadotropin (hCG), thereby providing improved timing control and a reduced monitoring burden.

Letrozole may be used alone or with gonadotropins in Mona-FET cycles, achieving adequate endometrial thickness (>7 mm) and preserving endometrial receptivity[75,76]. Letrozole-induced cycles have shown improved clinical pregnancy rates and live-birth rates compared with artificial cycles and gonadotropin-based preparations[82]. Several studies report that letrozole priming achieves outcomes comparable to natural cycles without adverse maternal or perinatal effects[91]. Tatsumi et al.[92] reported improved CPR and live birth rate (LBR) following frozen blastocyst transfers using letrozole compared with natural cycles.

In patients with PCOS, observational and propensity-score-matched analyses show that letrozole-FET improves CPR and LBR, reduces miscarriage rates, and lowers the incidence of hypertensive disorders and gestational diabetes compared with HRT. Endometrial thickness and morphology appear comparable to those in natural cycles, with potentially increased integrin expression[93].

Letrozole Use for Fertility Preservation

Letrozole is widely used in cancer patients undergoing oocyte cryopreservation due to its ability to suppress estradiol levels during controlled ovarian stimulation (COS). Studies have shown that adding letrozole to COS protocols reduces luteal-phase progesterone and estradiol levels, which is desirable in ER-positive breast cancer[94,95].

A French study reported comparable numbers of cryopreserved oocytes in COS with and without letrozole, and significantly lower luteal progesterone and estradiol levels in the letrozole group[96].

The letrozole-triggered decrease in the post-ovulatory peak serum concentration of estradiol is the desired effect in

women with breast cancer undergoing fertility preservation to diminish the risk of cancer recurrence. Whether to choose a COS protocol with letrozole in such patients depends on the growing evidence regarding the long-term safety of estrogen modulation and its benefits for cancer patients in terms of cancer recurrence rates[97].

An Italian study showed that letrozole significantly altered follicular steroid profiles; however, insufficient pregnancy outcome data prevented definitive conclusions regarding oocyte competence[98].

Use of letrozole for cryopreservation does not limit the risk of OHSS, and caution should be exercised, especially in cancer patients, to avoid delaying chemotherapy. The role of letrozole in fertility preservation in patients with gynecological malignancies remains unknown, but its efficacy for ovarian stimulation in patients with ovarian cancer has been described in case reports[99,100].

Letrozole Use in In Vitro Maturation

Compared to other uses mentioned above, the use of letrozole in IVM is a relatively recent approach, and the results of letrozole-primed IVM are promising. Rose[101] published the first paper on the use of letrozole-primed IVM. In their retrospective non-inferiority study, they compared letrozole-primed IVM with FSH-hCG-primed IVM and reported that letrozole-primed IVM can be used for IVM cycles in a more patient-friendly manner.

Hatırnaz et al.[102] reported a second paper on letrozole priming in IVM; in their study, they used letrozole-primed IVM in women with PCOS cancer phobia, and oocyte maturation abnormalities (OMAS). Their work led to the first live births following letrozole-primed IVM in patients with OMAS[103]. In the review by Rose and Brown[13] in 2020, the authors questioned whether letrozole use is optimal. In that paper, the benefits of letrozole use were extended.

Emerging observations suggest that IVM may serve as a dynamic platform for exploring maturation competence in women with OMAS-related mutations. These insights have driven the development of two innovative therapeutic concepts. The first involves letrozole-primed IVM combined with growth hormone supplementation, which is applied both *in vivo* and in the culture environment to support maturation in individuals with empty follicle syndrome, reactive oxygen species, mixed ovarian endometrioma (OMA), or poor embryo development. The second approach is designed for patients who demonstrate maturation only under stimulated conditions: a stimulated IVF cycle with adjunctive growth hormone is followed by an IVM-based laboratory protocol, where the addition of growth hormone to the culture medium appears essential. This letrozole-growth hormone strategy aims to recapitulate physiologic follicular signaling. Early experience indicates that the strategy is potentially applicable even to PCOS patients and yields high-quality blastocysts suitable for cryopreservation.

Letrozole Use for OHSS Prevention

OHSS is a potentially serious iatrogenic complication in ART cycles[104].

It typically arises after hCG administration for final oocyte maturation and is associated with substantial morbidity[105]. The clinical manifestations of OHSS, regardless of trigger type[106], include ascites, pleural effusion, electrolyte imbalance, venous thromboembolism, and significantly enlarged ovaries driven by cytokine-mediated vascular permeability changes, primarily mediated by vascular endothelial growth factor (VEGF)[107].

Based on symptom severity, the American Society for Reproductive Medicine classifies OHSS as mild, moderate, or severe[108]. Although treatment strategies exist, prevention remains the cornerstone of clinical management[109].

Elevated estradiol levels correlate strongly with OHSS risk; when E2 exceeds 6.000 pg/mL, the OHSS rate may reach 38%[110,111]. Because letrozole lowers circulating estrogen by inhibiting aromatase, it has been explored as a prophylactic agent in high-risk cycles.

Multiple studies evaluated letrozole at varying doses during the luteal phase. Fatemi et al.[112] demonstrated significant suppression of estrogen levels with 5 mg daily, whereas others observed similar reductions with 2.5 mg daily[113]. He et al.[114] found that higher doses (7.5 mg) more effectively reduced E2 and VEGF levels and lowered the incidence of early-onset OHSS compared with lower doses. However, contradictory findings exist: Haas et al.[115] reported elevated intrafollicular VEGF in letrozole cycles.

A systematic review concluded that letrozole reduces total and moderate-to-severe but does not significantly prevent individual categories of OHSS[116]. A recent Cochrane review found OHSS rates similar between letrozole and selective ER modulators[54].

While promising, letrozole has not yet been incorporated into major guidelines and is not considered first-line for OHSS prevention[117].

Letrozole Use for Ectopic Pregnancy

Laganà et al.[118] conducted a nonrandomized trial in 42 women with tubal ectopic pregnancies, comparing letrozole, methotrexate (MTX), and salpingectomy. Letrozole (5 mg/day for 10 days) demonstrated a success rate of 86%, equivalent to that of MTX. The decline in β-hCG appeared faster with letrozole, but the difference was not statistically significant. Unlike MTX, letrozole did not affect hematologic parameters and had minimal systemic adverse effects.

Additional small studies have similarly reported that β-hCG decline with letrozole is comparable to, or faster than, that with MTX, with no significant pre-treatment differences in β-hCG among groups[118-120].

Alabiad et al.[121] compared 5 mg for 5 days, 10 mg for 10 days, and laparoscopic salpingectomy. The 10 mg/10-day

regimen was significantly more effective in resolving ectopic pregnancy.

In a randomized controlled study, MTX plus letrozole for 5 days was compared with letrozole for 10 days. It was observed that 10-day use resulted in a greater reduction in β-hCG levels, but no difference in treatment success was observed between MTX and letrozole[122].

A systematic review and meta-analysis by Tarafdari et al.[123] concluded that letrozole is an effective and potentially safer alternative to MTX in the medical management of ectopic pregnancy.

Letrozole Use for Endometriosis

Endometriosis is a chronic, neuro-inflammatory disorder affecting approximately 10% of reproductive-aged women and is associated with dysmenorrhea, chronic pelvic pain, dyspareunia, irregular bleeding, and infertility[124]. Despite a variety of medical and surgical treatment options, recurrence rates remain high[125]. Because the disease is estrogen-dependent, aromatase inhibitors such as letrozole have emerged as potential therapeutic alternatives capable of reducing both systemic and lesion-derived estrogen production[126]. This approach offers an additional therapeutic avenue for patients who do not achieve adequate symptom control with standard hormonal regimens.

Clinical evidence indicates that letrozole substantially reduces endometriosis-associated pain, particularly when combined with progestins. Early work demonstrated that the combination of letrozole and norethindrone acetate produced meaningful reductions in pelvic pain and regression of visible lesions[127]. Subsequent data confirmed that letrozole combined with norethisterone acetate is superior to norethisterone acetate alone in alleviating pain[128], and a systematic review found that administering 2.5 mg of letrozole daily for six months effectively reduced pain severity in most patients[129]. While the overall impact on lesion volume has been variable across studies[129], more focused investigations suggest benefits in particular subgroups. For instance, a randomized trial reported that letrozole, administered in combination with either GnRH agonists or progestogens, significantly reduced the size of rectovaginal nodules[130]. Additional biological support for lesion modulation was provided by studies demonstrating that the combination of letrozole and dydrogesterone decreases expression of angiogenic and growth factors[131].

In the context of endometriosis-associated infertility, letrozole is a well-established OI agent and, alongside clomiphene citrate, is considered a first-line option in patients with minimal-to-mild disease prior to IVF[132,133]. Multiple studies suggest that letrozole may offer superior reproductive outcomes compared with clomiphene in this population, contributing to a growing expert consensus in its favor. Letrozole-based ovarian stimulation protocols have also demonstrated advantages in IVF cycles. Kim et al.[134] showed that letrozole combined with gonadotropins maintained lower estradiol levels while producing similar oocyte and embryo yields compared with conventional stimulation, and a double-blind randomized trial reported that adding letrozole reduced gonadotropin requirements and estradiol levels without compromising pregnancy rates[135]. Further, combining letrozole with GnRH agonists may provide enhanced reproductive outcomes in more advanced disease stages. For example, co-treatment with letrozole and leuprolide acetate improved clinical pregnancy and live-birth rates in women with OMAs[23]; similar benefits were observed in stage I-II endometriosis[136]. Collectively, these findings suggest that integrating peripheral aromatase inhibition with central ovarian suppression may offer a synergistic benefit for selected patients undergoing fertility treatment.

Complications Related to the Use of Letrozole

Letrozole is generally considered a well-tolerated and patient-friendly medication. Commonly reported adverse effects include mild headaches, fatigue, cramps, and dizziness, which are typically less severe than those associated with clomiphene citrate[2].

Like other OI agents, letrozole remains associated with multiple pregnancy, a major complication in OI cycles. Although twin pregnancies are the most common, triplet and higher-order gestations are also reported[137]. Close cycle monitoring and cycle cancellations to avoid extreme gestations would be mandatory, especially for patients with a history of multifollicular development or unresponsiveness to the standard dosage (5 mg/day)[138]. Supporting this, reports indicate that letrozole dosage correlates with complications. The Best results are obtained with 5 mg/day. When the dosage is 2.5 mg/day, fewer complications and no cyst formation are reported. When the dose is 7.5 mg/day (administered because of no response to lower doses), it helps induce ovulation and conception but is associated with increased cyst formation in 3.7% of cycles[139].

Letrozole is not associated with an increased risk of OHSS compared with CC[140]. Estradiol >3.500 pg/mL indicates elevated OHSS risk[141]; however, high estradiol alone does not induce OHSS[142,143]. Meta-analysis shows no significant OHSS reduction with letrozole alone, therefore, it should not be considered as the first-line treatment for prevention[116]. Letrozole promises benefits in combination regimens[144].

Another issue to be taken in to consideration for drug safety is teratogenicity Although aromatase inhibitors—particularly letrozole—are approved for breast cancer treatment and prevention, they are widely used off-label for OI. In 2005, a study comparing 150 infants conceived with letrozole to 36,005 controls reported methodological limitations, yet suggested increased cardiac and skeletal anomalies[145], prompting the manufacturer to advise against letrozole use in premenopausal women. However, a 2006 Canadian study of 911 newborns conceived after letrozole or CC found

no difference in the rates of major or minor congenital malformations[146]. More recent data evaluating infertility drugs similarly found no association between letrozole and teratogenicity[147]. Thus, despite its oncological origin, letrozole continues to be considered safe for use in infertile patients.

Conclusion

Letrozole has evolved from a breast cancer therapy into a versatile agent with broad applications in reproductive medicine. Its unique ability to selectively inhibit aromatase and modulate estrogen-dependent pathways provides therapeutic advantages in diverse clinical scenarios, ranging from OI and COS to endometrial preparation, fertility preservation, and the management of complex reproductive conditions. Evidence supports its efficacy as a first-line OI agent, particularly in women with polycystic ovary syndrome, and a growing body of evidence demonstrates its usefulness in IVF protocols by reducing gonadotropin requirements, maintaining physiologic estradiol levels, and improving outcomes in selected patient populations. Its estrogen-suppressive capacity also offers potential benefits for reducing the risk of OHSS, treating ectopic pregnancy, and managing endometriosis-related pain and infertility, especially in combination regimens.

Across indications, letrozole is generally well tolerated, with a favorable side-effect profile compared with other hypoestrogenic therapies. However, optimal dosing strategies, ideal treatment combinations, and the long-term consequences of extended aromatase inhibition remain areas of active investigation. Future research should aim to refine individualized treatment algorithms, identify patient subgroups most likely to benefit from letrozole-based approaches, and clarify long-term safety, particularly regarding bone health and metabolic effects.

In summary, letrozole represents a safe, adaptable, and clinically valuable tool within reproductive medicine. As mechanistic insights deepen and evidence from large-scale randomized trials continues to accumulate, letrozole is poised to become an increasingly integral component of personalized treatment strategies, ultimately improving reproductive outcomes and quality of life for a wide range of patients.

Footnotes

Authorship Contributions

Concept: G.A., Ş.H., M.D., Design: G.A., Ş.H., M.D., Data Collection or Processing: G.A., Ş.H., E.S.H., M.B.Ç., M.C., S.L.T., Analysis or Interpretation: Ş.H., M.B.Ç., M.C., S.L.T., A.U., M.D., Literature Search: G.A., Ş.H., E.S.H., M.B.Ç., M.A., N.D.G., O.G., M.A.M., A.U., S.E., Ö.T., A.B., E.Y., B.K., H.G., N.G., P.K., Z.Y., G.M.B., A.İ.T., R.S., N.T., A.T., M.C., S.L.T., O.H., M.D., Writing: G.A., Ş.H., E.S.H., M.B.Ç., M.A., N.D.G., O.G., M.A.M., A.U., S.E., Ö.T., A.B., E.Y., B.K., H.G., N.G., P.K., Z.Y., G.M.B., A.İ.T., R.S., N.T., A.T., M.C., S.L.T., O.H., M.D.

Conflict of Interest: No conflict of interest was declared by the authors.

Financial Disclosure: The authors declared that this study received no financial support.

References

1. Goss PE, Ingle JN, Martino S, Robert NJ, Muss HB, Piccart MJ, et al. A randomized trial of letrozole in postmenopausal women after five years of tamoxifen therapy for early-stage breast cancer. N Engl J Med. 2003;349:1793-802.
2. Legro RS, Brzyski RG, Diamond MP, Coutifaris C, Schlaff WD, Casson P, et al. Letrozole versus clomiphene for infertility in the polycystic ovary syndrome. N Engl J Med. 2014;371:119-29.
3. Rajan RK, M SSK, Balaji B. Soy isoflavones exert beneficial effects on letrozole-induced rat polycystic ovary syndrome (PCOS) model through anti-androgenic mechanism. Pharm Biol. 2017;55:242-51.
4. Falck B. Site of production of oestrogen in rat ovary as studied in micro-transplants. Acta Physiol Scand Suppl. 1959;47:1-101.
5. Short RV. Steroids in the follicular fluid and the corpus luteum of the mare. A "two-cell type" theory of ovarian steroid synthesis. J Endocrinol. 1962;24:59-63.
6. Ryan KJ, Petro Z, Kaiser J. Steroid formation by isolated and recombined ovarian granulosa and tehcal cells. J Clin Endocrinol Metab. 1968;28:355-8.
7. Sasano H, Okamoto M, Mason JI, Simpson ER, Mendelson CR, Sasano N, et al. Immunolocalization of aromatase, 17 alpha-hydroxylase and side-chain-cleavage cytochromes P-450 in the human ovary. J Reprod Fertil. 1989;85:163-9.
8. Sasano H. Functional pathology of human ovarian steroidogenesis: normal cycling ovary and steroid-producing neoplasms. Endocr Pathol. 1994;5:81-9.
9. Recombinant human luteinizing hormone (LH) to support recombinant human follicle-stimulating hormone (FSH)-induced follicular development in LH- and FSH-deficient anovulatory women: a dose-finding study. The European Recombinant Human LH Study Group. J Clin Endocrinol Metab. 1998;83:1507-14.
10. Simpson ER, Davis SR. Minireview: aromatase and the regulation of estrogen biosynthesis--some new perspectives. Endocrinology. 2001;142:4589-94.
11. Kristensen SG, Mamsen LS, Jeppesen J V, Bøtkjær JA, Pors SE, Borgbo T, et al. Hallmarks of human small antral follicle development: implications for regulation of ovarian steroidogenesis and selection of the dominant follicle. Front Endocrinol (Lausanne). 2017;8:376.
12. Bulun SE, Lin Z, Imir G, Amin S, Demura M, Yilmaz B, et al. Regulation of aromatase expression in estrogen-responsive breast and uterine disease: from bench to treatment. Pharmacol Rev. 2005;57:359-83.
13. Rose BI, Brown SE. A review of the physiology behind letrozole applications in infertility: are current protocols optimal? J Assist Reprod Genet. 2020;37:2093-104.
14. Holzer H, Casper R, Tulandi T. A new era in ovulation induction. Fertil Steril. 2006;85:277-84.
15. Yang A-M, Cui N, Sun Y-F, Hao G-M. Letrozole for female infertility. Front Endocrinol (Lausanne). 2021;12:676133.

16. Franks S, Hardy K. Androgen action in the ovary. Front Endocrinol (Lausanne). 2018;9:452.
17. Hsueh AJ, Billig H, Tsafriri A. Ovarian follicle atresia: a hormonally controlled apoptotic process. Endocr Rev. 1994;15:707-24.
18. Simpson ER. Aromatization of androgens in women: current concepts and findings. Fertil Steril. 2002;77(Suppl 4):S6-10.
19. Buzdar AU, Robertson JFR, Eiermann W, Nabholtz J-M. An overview of the pharmacology and pharmacokinetics of the newer generation aromatase inhibitors anastrozole, letrozole, and exemestane. Cancer. 2002;95:2006-16.
20. Smith IE, Dowsett M. Aromatase inhibitors in breast cancer. N Engl J Med. 2003;348:2431-42.
21. Cuzick J, Sestak I, Baum M, Buzdar A, Howell A, Dowsett M, et al. Effect of anastrozole and tamoxifen as adjuvant treatment for early-stage breast cancer: 10-year analysis of the ATAC trial. Lancet Oncol. 2010;11:1135-41.
22. Leone Roberti Maggiore U, Scala C, Venturini PL, Remorgida V, Ferrero S. Endometriotic ovarian cysts do not negatively affect the rate of spontaneous ovulation. Hum Reprod. 2015;30:299-307.
23. Cantor A, Tannus S, Son W-Y, Tan SL, Dahan MH. A comparison of two months pretreatment with GnRH agonists with or without an aromatase inhibitor in women with ultrasound-diagnosed ovarian endometriomas undergoing IVF. Reprod Biomed Online. 2019;38:520-7.
24. Perez EA, Weilbaecher K. Aromatase inhibitors and bone loss. Oncology (Williston Park). 2006;20:1029-39; discussion 1039-40, 1042, 1048.
25. Johnston SRD. Are current drug development programmes realising the full potential of new agents? The scenario. Breast Cancer Res. 2009;11(Suppl 3):S21.
26. Nelson SM, Klein BM, Arce J-C. Comparison of antimüllerian hormone levels and antral follicle count as predictor of ovarian response to controlled ovarian stimulation in good-prognosis patients at individual fertility clinics in two multicenter trials. Fertil Steril. 2015;103:923-930.e1.
27. Khojah M, Khayat S, Dahan MH. Comparison of in vitro fertilization cycles stimulated with 20 mg letrozole daily versus high-dose gonadotropins in Rotterdam consensus ultra-poor responders: a proof of concept. Int J Gynaecol Obstet. 2022;156:102-6.
28. Rasmussen BB, Regan MM, Lykkesfeldt AE, Dell'Orto P, Del Curto B, Henriksen KL, et al. Adjuvant letrozole versus tamoxifen according to centrally-assessed ERBB2 status for postmenopausal women with endocrine-responsive early breast cancer: supplementary results from the BIG 1-98 randomised trial. Lancet Oncol. 2008;9:23-8.
29. Santen RJ, Santner S, Davis B, Veldhuis J, Samojlik E, Ruby E. Aminoglutethimide inhibits extraglandular estrogen production in postmenopausal women with breast carcinoma. J Clin Endocrinol Metab. 1978;47:1257-65.
30. Santen RJ, Langecker P, Santner SJ, Sikka S, Rajfer J, Swerdloff R. Potency and specificity of CGS-16949A as an aromatase inhibitor. Endocr Res. 1990;16:77-91.
31. Stein RC, Dowsett M, Hedley A, Davenport J, Gazet JC, Ford HT, et al. Treatment of advanced breast cancer in postmenopausal women with 4-hydroxyandrostenedione. Cancer Chemother Pharmacol. 1990;26:75-8.
32. Stein RC, Dowsett M, Hedley A, Gazet JC, Ford HT, Coombes RC. The clinical and endocrine effects of 4-hydroxyandrostenedione alone and in combination with goserelin in premenopausal women with advanced breast cancer. Br J Cancer. 1990;62:679-83.
33. Zhou DJ, Pompon D, Chen SA. Stable expression of human aromatase complementary DNA in mammalian cells: a useful system for aromatase inhibitor screening. Cancer Res. 1990;50:6949-54.
34. Yue W, Zhou D, Chen S, Brodie A. A new nude mouse model for postmenopausal breast cancer using MCF-7 cells transfected with the human aromatase gene. Cancer Res. 1994;54:5092-5.
35. Gibson LJ, Dawson CK, Lawrence DH, Bliss JM. Aromatase inhibitors for treatment of advanced breast cancer in postmenopausal women. Cochrane Database Syst Rev. 2007;CD003370.
36. Dhillon S. Everolimus in combination with exemestane: a review of its use in the treatment of patients with postmenopausal hormone receptor-positive, HER2-negative advanced breast cancer. Drugs. 2013;73:475-85.
37. Jones S, Vogel C, Arkhipov A, Fehrenbacher L, Eisenberg P, Cooper B, et al. Multicenter, phase II trial of exemestane as third-line hormonal therapy of postmenopausal women with metastatic breast cancer. Aromasin Study Group. J Clin Oncol. 1999;17:3418-25.
38. Murray J, Young OE, Renshaw L, White S, Williams L, Evans DB, et al. A randomised study of the effects of letrozole and anastrozole on oestrogen receptor positive breast cancers in postmenopausal women. Breast Cancer Res Treat. 2009;114:495-501.
39. Goss PE, Ingle JN, Pritchard KI, Ellis MJ, Sledge GW, Budd GT, et al. Exemestane versus anastrozole in postmenopausal women with early breast cancer: NCIC CTG MA.27--a randomized controlled phase III trial. J Clin Oncol. 2013;31:1398-404.
40. Sayyad NB, Sabale PM UM. Aromatase inhibitors: development and current perspectives. Indian J Pharm Educ Res. 2022;56:311-20.
41. Jamshidifar E, Eshrati Yeganeh F, Shayan M, Tavakkoli Yaraki M, Bourbour M, Moammeri A, et al. Super magnetic niosomal nanocarrier as a new approach for treatment of breast cancer: a case study on SK-BR-3 and MDA-MB-231 cell lines. Int J Mol Sci. 2021;22:7948.
42. Kao YC, Cam LL, Laughton CA, Zhou D, Chen S. Binding characteristics of seven inhibitors of human aromatase: a site-directed mutagenesis study. Cancer Res. 1996;56:3451-60.
43. Dellapasqua S, Colleoni M. Letrozole. Expert Opin Drug Metab Toxicol. 2010;6:251-9.
44. Goss PE. Letrozole in the extended adjuvant setting: MA.17. Breast Cancer Res Treat. 2007;105 (Suppl):45-53.
45. Bhatnagar AS. The discovery and mechanism of action of letrozole. Breast Cancer Res Treat. 2007;105 (Suppl):7-17.
46. Mitwally MF, Casper RF. Aromatase inhibitors in ovulation induction. Semin Reprod Med. 2004;22:61-78.
47. Palomba S. Aromatase inhibitors for ovulation induction. J Clin Endocrinol Metab. 2015;100:1742-7.
48. Ganesh A, Chauhan N, Das S, Chakravarty B, Chaudhury K. Endometrial receptivity markers in infertile women stimulated with letrozole compared with clomiphene citrate and natural cycles. Syst Biol Reprod Med. 2014;60:105-11.
49. Mitwally MF, Casper RF. Use of an aromatase inhibitor for induction of ovulation in patients with an inadequate response to clomiphene citrate. Fertil Steril. 2001;75:305-9.

50. Eden JA, Place J, Carter GD, Jones J, Alaghband-Zadeh J, Pawson ME. The effect of clomiphene citrate on follicular phase increase in endometrial thickness and uterine volume. Obstet Gynecol. 1989;73:187-90.
51. Dickey RP, Olar TT, Taylor SN, Curole DN, Matulich EM. Relationship of endometrial thickness and pattern to fecundity in ovulation induction cycles: effect of clomiphene citrate alone and with human menopausal gonadotropin. Fertil Steril. 1993;59:756-60.
52. Opsahl MS, Robins ED, O'Connor DM, Scott RT, Fritz MA. Characteristics of gonadotropin response, follicular development, and endometrial growth and maturation across consecutive cycles of clomiphene citrate treatment. Fertil Steril. 1996;66:533-9.
53. Fisher SA, Reid RL, Van Vugt DA, Casper RF. A randomized double-blind comparison of the effects of clomiphene citrate and the aromatase inhibitor letrozole on ovulatory function in normal women. Fertil Steril. 2002;78:280-5.
54. Franik S, Eltrop SM, Kremer JA, Kiesel L, Farquhar C. Aromatase inhibitors (letrozole) for subfertile women with polycystic ovary syndrome. Cochrane Database Syst Rev. 2018;5:CD010287.
55. Barroso G, Menocal G, Felix H, Rojas-Ruiz JC, Arslan M, Oehninger S. Comparison of the efficacy of the aromatase inhibitor letrozole and clomiphene citrate as adjuvants to recombinant follicle-stimulating hormone in controlled ovarian hyperstimulation: a prospective, randomized, blinded clinical trial. Fertil Steril. 2006;86:1428-31.
56. Mitwally MF, Biljan MM, Casper RF. Pregnancy outcome after the use of an aromatase inhibitor for ovarian stimulation. Am J Obstet Gynecol. 2005;192:381-6.
57. Bao SH, Sheng S Le, Peng YF, Lin Q De. Effects of letrozole and clomiphene citrate on the expression of HOXA10 and integrin alpha v beta 3 in uterine epithelium of rats. Fertil Steril. 2009;91:244-8.
58. Wallace KL, Johnson V, Sopelak V, Hines R. Clomiphene citrate versus letrozole: molecular analysis of the endometrium in women with polycystic ovary syndrome. Fertil Steril. 2011;96:1051-6.
59. Wang H, Li Q, Wang T, Yang G, Wang Y, Zhang X, et al. A common polymorphism in the human aromatase gene alters the risk for polycystic ovary syndrome and modifies aromatase activity in vitro. Mol Hum Reprod. 2011;17:386-91.
60. Maia H, Casoy J, Valente Filho J. Is aromatase expression in the endometrium the cause of endometriosis and related infertility? Gynecol Endocrinol. 2009;25:253-7.
61. Harira M. Use of Letrozole versus clomiphene-estradiol for treating infertile women with unexplained infertility not responding well to clomiphene alone, comparative study. Middle East Fertil Soc J. 2018;23:384-7.
62. Wang L, Wen X, Lv S, Zhao J, Yang T, Yang X. Comparison of endometrial receptivity of clomiphene citrate versus letrozole in women with polycystic ovary syndrome: a randomized controlled study. Gynecol Endocrinol. 2019;35:862-5.
63. Bansal S, Goyal M, Sharma C, Shekhar S. Letrozole versus clomiphene citrate for ovulation induction in anovulatory women with polycystic ovarian syndrome: a randomized controlled trial. Int J Gynaecol Obstet. 2021;152:345-50.
64. Najafi PZ, Noghabi SP, Afzali N, Mohammadzadeh S. Comparing the effect of clomiphene citrate and letrozole on ovulation induction in infertile women with polycystic ovary syndrome. J Pak Med Assoc. 2020;70:268-71.
65. Sh. Tehrani nejad E, Abediasl Z, Rashidi BH, Azimi nekoo E, Shariat M, Amirchaghmaghi E. Comparison of the efficacy of the aromatase inhibitor letrozole and clomiphen citrate gonadotropins in controlled ovarian hyperstimulation: a prospective, simply randomized, clinical trial. J Assist Reprod Genet. 2008;25:187-90.
66. Mejia RB, Summers KM, Kresowik JD, Van Voorhis BJ. A randomized controlled trial of combination letrozole and clomiphene citrate or letrozole alone for ovulation induction in women with polycystic ovary syndrome. Fertil Steril. 2019;111:571-578.e1.
67. Eskew AM, Bedrick BS, Hardi A, Stoll CRT, Colditz GA, Tuuli MG, et al. Letrozole compared with clomiphene citrate for unexplained infertility. Obstet Gynecol. 2019;133:437-44.
68. Abu Hashim H, El Rakhawy M, Abd Elaal I. Expression of concern: randomized comparison of superovulation with letrozole vs. clomiphene citrate in an IUI program for women with recently surgically treated minimal to mild endometriosis. Acta Obstet Gynecol Scand. 2012;91:338-45.
69. Anderson RA, Nelson SM, Wallace WHB. Measuring anti-Müllerian hormone for the assessment of ovarian reserve: when and for whom is it indicated? Maturitas. 2012;71:28-33.
70. Mitwally MFM, Casper RF. Aromatase inhibition improves ovarian response to follicle-stimulating hormone in poor responders. Fertil Steril. 2002;77:776-80.
71. Jovanovic VP, Kort DH, Guarnaccia MM, Sauer MV LR. Does the addition of clomiphene citrate or letrazole to gonadotropin treatment enhance the oocyte yield in poor responders undergoing IVF? J Assist Reprod Genet. 2011;28:1067-72.
72. Oktay K, Hourvitz A, Sahin G, Oktem O, Safro B, Cil A, et al. Letrozole reduces estrogen and gonadotropin exposure in women with breast cancer undergoing ovarian stimulation before chemotherapy. J Clin Endocrinol Metab. 2006;91:3885-90.
73. Løssl K, Freiesleben N la C, Wissing ML, Birch Petersen K, Holt MD, Mamsen LS, et al. Biological and clinical rationale for androgen priming in ovarian stimulation. Front Endocrinol (Lausanne). 2020;11:627.
74. Weil S, Vendola K, Zhou J, Bondy CA. Androgen and follicle-stimulating hormone interactions in primate ovarian follicle development. J Clin Endocrinol Metab. 1999;84:2951-6.
75. Cort´nez A, De Carvalho I, Vantman D, Gabler F, Iñiguez G, Vega M. Hormonal profile and endometrial morphology in letrozole-controlled ovarian hyperstimulation in ovulatory infertile patients. Fertil Steril. 2005;83:110-5.
76. Miller PB, Parnell BA, Bushnell G, Tallman N, Forstein DA, Higdon HL, et al. Endometrial receptivity defects during IVF cycles with and without letrozole. Hum Reprod. 2012;27:881-8.
77. Aydin G, Aslan K, Arac M, Ergin E, Kasapoglu I, Uncu G. Considering its mechanism of action it may be logical to choose letrozole as an initial option for endometrium preparation before vitrified-warmed embryo transfer. J Obstet Gynaecol Res. 2025;51:e70048.
78. Garcia-Velasco JA, Moreno L, Pacheco A, Guillén A, Duque L, Requena A, et al. The aromatase inhibitor letrozole increases the concentration of intraovarian androgens and improves in vitro fertilization outcome in low responder patients: a pilot study. Fertil Steril. 2005;84:82-7.
79. Yarali H, Esinler İ, Polat M, Bozdag G, Tiras B. Antagonist/letrozole protocol in poor ovarian responders for intracytoplasmic sperm injection: a comparative study with the microdose flare-up protocol. Fertil Steril. 2009;92:231-5.

80. Goswami SK. A randomized single-blind controlled trial of letrozole as a low-cost IVF protocol in women with poor ovarian response: a preliminary report. Hum Reprod. 2004;19:2031-5.
81. Begum MR, Ferdous J, Begum A, Quadir E. Comparison of efficacy of aromatase inhibitor and clomiphene citrate in induction of ovulation in polycystic ovarian syndrome. Fertil Steril. 2009;92:853-7.
82. Zhang J, Wei M, Bian X, Wu L, Zhang S, Mao X, et al. Letrozole-induced frozen embryo transfer cycles are associated with a lower risk of hypertensive disorders of pregnancy among women with polycystic ovary syndrome. Am J Obstet Gynecol. 2021;225:59.e1-59.e9.
83. Coughlan C, Ata B, Gallego R Del, Lawrenz B, Melado L, Samir S, et al. Interindividual variation of progesterone elevation post LH rise: implications for natural cycle frozen embryo transfers in the individualized medicine era. Reprod Biol Endocrinol. 2023;21:47.
84. Chen Z-J, Shi Y, Sun Y, Zhang B, Liang X, Cao Y, et al. Fresh versus frozen embryos for infertility in the polycystic ovary syndrome. N Engl J Med. 2016;375:523-33.
85. Macklon NS, Stouffer RL, Giudice LC, Fauser BCJM. The science behind 25 years of ovarian stimulation for in vitro fertilization. Endocr Rev. 2006;27:170-207.
86. Asserhøj LL, Spangmose AL, Aaris Henningsen A-K, Clausen TD, Ziebe S, Jensen RB, et al. Adverse obstetric and perinatal outcomes in 1,136 singleton pregnancies conceived after programmed frozen embryo transfer (FET) compared with natural cycle FET. Fertil Steril. 2021;115:947-56.
87. Ghobara T, Gelbaya TA, Ayeleke RO. Cycle regimens for frozen-thawed embryo transfer. Cochrane Database Syst Rev. 2017;7:CD003414.
88. Gu F, Wu Y, Tan M, Hu R, Chen Y, Li X, et al. Programmed frozen embryo transfer cycle increased risk of hypertensive disorders of pregnancy: a multicenter cohort study in ovulatory women. Am J Obstet Gynecol MFM. 2023;5:100752.
89. Mackens S, Santos-Ribeiro S, van de Vijver A, Racca A, Van Landuyt L, Tournaye H, et al. Frozen embryo transfer: a review on the optimal endometrial preparation and timing. Hum Reprod. 2017;32:2234-42.
90. Lawrenz B, Coughlan C, Melado L, Fatemi HM. The ART of frozen embryo transfer: back to nature! Gynecol Endocrinol. 2020;36:479-83.
91. Li D, Khor S, Huang J, Chen Q, Lyu Q, Cai R, et al. Frozen embryo transfer in mildly stimulated cycle with letrozole compared to natural cycle in ovulatory women: a large retrospective study. Front Endocrinol (Lausanne). 2021;12:677689.
92. Tatsumi T, Jwa SC, Kuwahara A, Irahara M, Kubota T, Saito H. Pregnancy and neonatal outcomes following letrozole use in frozen–thawed single embryo transfer cycles. Hum Reprod. 2017;32:1244-8.
93. Wang X, Li Y, Tan H, Cai S, Ma S, Peng Y, et al. Letrozole-stimulated endometrial preparation protocol is a superior alternative to hormone replacement treatment for frozen embryo transfer in women with polycystic ovary syndrome, a cohort study. Reprod Biol Endocrinol. 2023;21:101.
94. Oktay K, Buyuk E, Libertella N, Akar M, Rosenwaks Z. Fertility preservation in breast cancer patients: a prospective controlled comparison of ovarian stimulation with tamoxifen and letrozole for embryo cryopreservation. J Clin Oncol. 2005;23:4347-53.
95. Wang A, Letourneau JM, Juarez-Hernandez F, Abel MK, Mok-Lin E, Rosen MP. Hormone concentrations of dominant follicles in the TALES randomized controlled trial comparing letrozole with tamoxifen. J Assist Reprod Genet. 2022;39:2617-24.
96. Lalami I, Labrosse J, Cedrin-Durnerin I, Comtet M, Vinolas C, Krief F, et al. Is letrozole during ovarian stimulation useful in breast cancer patients undergoing fertility preservation to reduce early luteal progesterone levels following GnRH-agonist trigger? Reprod Biol Endocrinol. 2022;20:87.
97. Balkenende EME, Dahhan T, Beerendonk CCM, Fleischer K, Stoop D, Bos AME, et al. Fertility preservation for women with breast cancer: a multicentre randomized controlled trial on various ovarian stimulation protocols. Hum Reprod. 2022;37:1786-94.
98. Dallagiovanna C, Reschini M, Polledri E, Pinna M, Ciaffaglione M, Cuce' V, et al. Effect of letrozole on follicular fluid steroids concentrations in cancer patients undergoing oocyte cryopreservation. J Assist Reprod Genet. 2022;39:1169-76.
99. Iorio GG, Rovetto MY, Conforti A, Carbone L, Vallone R, Cariati F, et al. Severe ovarian hyperstimulation syndrome in a woman with breast cancer under letrozole triggered with GnRH agonist: a case report and review of the literature. Front Reprod Health. 2021;3:704153.
100. Lombardi Fäh V, Del Vento F, Intidhar Labidi-Galy S, Undurraga M. Ovarian stimulation with letrozole in nulliparous young women with relapsing early-stage serous borderline ovarian tumors. Gynecol Oncol Rep. 2024;56:101531.
101. Rose BI. The potential of letrozole use for priming in vitro maturation cycles. Facts Views Vis Obgyn. 2014;6:150-5.
102. Hatırnaz Ş, Hatırnaz ES, Başbuğ A, Kanat Pektaş M, Erol O, Dahan M, et al. In vitro maturation with letrozole priming: can it be a solution for patients with cancerophobia? A pilot study. Turk J Obstet Gynecol. 2020;17:247-52.
103. Hatirnaz S, Hatirnaz E, Dahan M, Ata B, Basbug A, Hatirnaz K, et al. P–709 Dual stimulation in-vitro-maturation (Duostim IVM) for overcoming oocyte maturation arrest, resulting in embryo transfer and livebirth. Hum Reprod. 2021;36.
104. Golan A, Ron-El R, Herman Ar, Soffer Y. Ovarian hyperstimulation syndrome. Obstet Gynecol Surv. 1989;44:430-40.
105. Abbara A, Clarke SA, Dhillo WS. Novel concepts for inducing final oocyte maturation in in vitro fertilization treatment. Endocr Rev. 2018;39:593-628.
106. Abbara A, Islam R, Clarke SA, Jeffers L, Christopoulos G, Comninos AN, et al. Clinical parameters of ovarian hyperstimulation syndrome following different hormonal triggers of oocyte maturation in IVF treatment. Clin Endocrinol (Oxf). 2018;88:920-7.
107. Royal College of Obstetricians & Gynaecologists. The management of ovarian hyperstimulation syndrome (Green-top guideline no. 5). London: Royal College of Obstetricians & Gynaecologists; 2016. Available from: https://www.rcog.org.uk/media/or1jqxbf/gtg_5_ohss.pdf
108. Pfeifer S, Butts S, Dumesic D, Fossum G, Gracia C, La Barbera A, et al. Prevention and treatment of moderate and severe ovarian hyperstimulation syndrome: a guideline. Fertil Steril. 2016;106:1634-47.
109. Sansone P, Aurilio C, Pace MC, Esposito R, Passavanti MB, Pota V, et al. Intensive care treatment of ovarian hyperstimulation syndrome (OHSS). Ann N Y Acad Sci. 2011;1221:109-18.
110. Aboulghar M. Prediction of ovarian hyperstimulation syndrome (OHSS). Estradiol level has an important role in the prediction of OHSS. Hum Reprod. 2003;18:1140-1.
111. Asch RH, Li H-P, Balmaceda JP, Weckstein LN, Stone SC. Severe ovarian hyperstimulation syndrome in assisted reproductive technology: definition of high risk groups. Hum Reprod. 1991;6:1395-9.

112. Fatemi H, Popovic-Todorovic B, Donoso P, Papanikolaou E, Smitz J, Devroey P. Luteal phase oestradiol suppression by letrozole: a pilot study in oocyte donors. Reprod Biomed Online. 2008;17:307-11.

113. Garcia-Velasco JA, Quea G, Piró M, Mayoral M, Ruiz M, Toribio M, et al. Letrozole administration during the luteal phase after ovarian stimulation impacts corpus luteum function: a randomized, placebo-controlled trial. Fertil Steril. 2009;92:222-5.

114. He Q, Liang L, Zhang C, Li H, Ge Z, Wang L, et al. Effects of different doses of letrozole on the incidence of early-onset ovarian hyperstimulation syndrome after oocyte retrieval. Syst Biol Reprod Med. 2014;60:355-60.

115. Haas J, Bassil R, Gonen N, Meriano J, Jurisicova A, Casper RF. The VEGF and PEDF levels in the follicular fluid of patients co- treated with LETROZOLE and gonadotropins during the stimulation cycle. Reprod Biol Endocrinol. 2018;16:54.

116. Zhao J, Xu B, Huang X, Yan Y, Li Y. Whether letrozole could reduce the incidence of early ovary hyperstimulation syndrome after assisted reproductive technology? A systematic review and meta-analysis. Reprod Health. 2020;17:181.

117. Di Guardo F, Lello C, Incognito GG, Bruno MT, Palumbo M. Letrozole and ovarian hyperstimulation syndrome (OHSS): a promising prevention strategy. J Clin Med. 2023;12:614.

118. Laganà AS, Etrusco A, Haydamous J, Semaan S, Agrifoglio V, Chiantera V, et al. Efficacy of letrozole for the treatment of tubal ectopic pregnancy: a meta-analysis. Eur J Obstet Gynecol Reprod Biol. 2024;299:322-8.

119. Medical treatment of ectopic pregnancy: a committee opinion. Fertil Steril. 2013;100:638-44.

120. Auger N, Ayoub A, Wei SQ. Letrozole: future alternative to methotrexate for treatment of ectopic pregnancy? Fertil Steril. 2020;114:273-4.

121. Alabiad MA, Said WMM, Gad AH, Sharaf ElDin MTA, Khairy DA, Gobran MA, et al. Evaluation of different doses of the aromatase inhibitor letrozole for the treatment of ectopic pregnancy and its effect on villous trophoblastic tissue. Reprod Sci. 2022;29:2983-94.

122. Tarafdari A, Eslami Khotbesara S, Keikha F, Parsaei M, Poorabdoli M, Chill HH, et al. Comparing the effectiveness of letrozole versus methotrexate for treatment of ectopic pregnancy: a randomized controlled trial. Eur J Obstet Gynecol Reprod Biol. 2024;299:219-24.

123. Tarafdari A, Keikha F, Asadi F, Hantoushzadeh S, Gargari OK, Forouzin M, et al. The effectiveness of letrozole alone or in combination with methotrexate in the management of ectopic pregnancy, a systematic review and meta-analysis. Reprod Sci. 2024;31:3651-9.

124. Saunders PTK, Horne AW. Endometriosis: etiology, pathobiology, and therapeutic prospects. Cell. 2021;184:2807-24.

125. Dunselman GAJ, Vermeulen N, Becker C, Calhaz-Jorge C, D'Hooghe T, De Bie B, et al. ESHRE guideline: management of women with endometriosis. Hum Reprod. 2014;29:400-12.

126. Zeitoun KM, Bulun SE. Aromatase: a key molecule in the pathophysiology of endometriosis and a therapeutic target. Fertil Steril. 1999;72:961-9.

127. Ailawadi RK, Jobanputra S, Kataria M, Gurates B, Bulun SE. Treatment of endometriosis and chronic pelvic pain with letrozole and norethindrone acetate: a pilot study. Fertil Steril. 2004;81:290-6.

128. Ferrero S, Camerini G, Seracchioli R, Ragni N, Venturini PL, Remorgida V. Letrozole combined with norethisterone acetate compared with norethisterone acetate alone in the treatment of pain symptoms caused by endometriosis. Hum Reprod. 2009;24:3033-41.

129. Ferrero S, Gillott DJ, Venturini PL, Remorgida V. Use of aromatase inhibitors to treat endometriosis-related pain symptoms: a systematic review. Reprod Biol Endocrinol. 2011;9:89.

130. Ferrero S, Venturini PL, Gillott DJ, Remorgida V. Letrozole and norethisterone acetate versus letrozole and triptorelin in the treatment of endometriosis related pain symptoms: a randomized controlled trial. Reprod Biol Endocrinol. 2011;9:88.

131. Sun S, Zhang H, Zhong P, Xu Z. The effect of letrozole combined with dydrogesterone for endometriosis in china: a a meta-analysis. Ozgu-Erdinc AS, editor. Biomed Res Int. 2021;2021.

132. Leung AS, Dahan MH. The benefits of other treatments than in vitro fertilization to aid conception in minimal and mild endometriosis. Minerva Ginecol. 2016;68:675-86.

133. Abu Hashim H. Aromatase inhibitors for endometriosis-associated infertility; do we have sufficient evidence? Int J Fertil Steril. 2016;10:270-7.

134. Kim SJ, Choo CW, Kim SK, Lee JR, Jee BC, Suh CS, et al. The effects of letrozole on women with endometriosis undergoing ovarian stimulation for in vitro fertilization. Gynecol Endocrinol. 2020;36:257-60.

135. Ebrahimi M, Akbari Asbagh F, Davari Tanha F, Pakniat H, Feizabad E, Rasouli Y. Co-treatment of gonadotropin and letrozole in infertile women with endometriosis: a double-blind randomized clinical trial. Int J Reprod Biomed. 2022;20:483-90.

136. Piedimonte S, Volodarsky-Perel A, Tannus S, Tan SL, Dahan MH. Pretreatment with a gonadotropin-releasing hormone agonist and an aromatase inhibitor may improve outcomes in in vitro fertilization cycles of women with stage I–II endometriosis. F S Sci. 2020;1:98-103.

137. Dicken CL, Nakhuda GS, Guarnaccia MM, Sauer M V, Lobo RA. Triplet pregnancy after ovulation induction with an aromatase inhibitor. Fertil Steril. 2008;90:1199.e9-11.

138. Warraich G, Vause TDR. First reported case of sextuplets conceived via letrozole for ovulation induction. Fertil Steril. 2015;103:535-6.

139. Rahmani E, Ahmadi S, Motamed N, Maneshi HO. Dosage optimization for letrozole treatment in clomiphene-resistant patients with polycystic ovary syndrome: a prospective interventional study. Obstet Gynecol Int. 2012;2012:758508.

140. Li Y, Hao Z. Severe ovarian hyperstimulation syndrome induced by clomiphene: a case report. Gynecol Endocrinol. 2022;38:1008-13.

141. Practice Committee of the American Society for Reproductive Medicine. Electronic address: ASRM@asrm.org, Practice Committee of the American Society for Reproductive Medicine. Prevention and treatment of moderate and severe ovarian hyperstimulation syndrome: a guideline. Fertil Steril. 2016;106:1634-47.

142. Hendriks DJ, Klinkert ER, Bancsi LFJMM, Looman CWN, Habbema JDF, te Velde ER, et al. Use of stimulated serum estradiol measurements for the prediction of hyperresponse to ovarian stimulation in in vitro fertilization (IVF). J Assist Reprod Genet. 2004;21:65-72.

143. Lee T-H, Liu C-H, Huang C-C, Wu Y-L, Shih Y-T, Ho H-N, et al. Serum anti-Müllerian hormone and estradiol levels as predictors of ovarian hyperstimulation syndrome in assisted reproduction technology cycles. Hum Reprod. 2008;23:160-7.

144. Yanagihara Y, Tanaka A, Nagayoshi M, Tanaka I, Shinohara R, Fukushima F, et al. A modified GnRH antagonist method in combination with letrozole, cabergoline, and GnRH antagonist for PCOS: safe and effective ovarian stimulation to treat PCOS and prevent OHSS. Reprod Med Biol. 2022;21:e12429.

145. Biljan MM, Hemmings R, Brassard N. The outcome of 150 babies following the treatment with letrozole or letrozole and gonadotropins. Fertil Steril. 2005;84(Suppl 1):S95.

146. Tulandi T, Martin J, Al-Fadhli R, Kabli N, Forman R, Hitkari J, et al. Congenital malformations among 911 newborns conceived after infertility treatment with letrozole or clomiphene citrate. Fertil Steril. 2006;85:1761-5.

147. Elizur SE, Tulandi T. Drugs in infertility and fetal safety. Fertil Steril. 2008;89:1595-602.